Biomarkers to predict Tuberculosis treatment response

Itumeleng Boshielo

1144115

A thesis submitted to the Faculty of Health Science, University of the Witwatersrand, Johannesburg, in fulfilment of the requirements for the degree of Doctor of Philosophy in medicine.

Johannesburg, 2023

Declaration

I, Itumeleng Boshielo, am a student registered for the degree of Doctor of Philosophy in Medicine at the University of the Witwatersrand in the academic year 2020.

I hereby declare the following:

- I am aware that the use of someone else's literature and work without their permission and/or without acknowledging the original source is unacceptable.
- I confirm that the work submitted for assessment for the above-mentioned degree is my own unaided work except where explicitly indicated otherwise.
- I have not submitted this work before for any other degree or examination at any other university.
- I have followed the required conventions in referencing the thoughts and ideas of others.
- I understand that the University of the Witwatersrand may take disciplinary action against me if there is a belief that this is not my own unaided work or that I have failed to acknowledge the source of the ideas or words in my writing.

Signature of candidate .....  ..... Date...15/06/2023.....

Dedication

This work is dedicated to myself and the most precious gifts that God has given to me, my beautiful children; **Onthatile Boshielo** and **Nala Boshielo**.

Acknowledgements

- First of all, I'd like to thank the **God of mount Zion** for his protection and mercy.
- **Prof Bavesh Kana**, who undertook to act as my supervisor despite his many other academic and professional commitments; His wisdom, knowledge and commitment to the highest standards inspired and motivated me. You have consistently encouraged me despite my circumstances, not just professionally but also as one person to another.
- **Prof Caroline Tiemessen**, my co-supervisor who took her precious time to assist and provide her input throughout my study.
- **Dr Diana Schramm**, for her patience and the time she took to assist me with the luminex bead array assay step by step from the beginning to end.
- **Dr Julian Peters,** for providing the samples used for this study as well as the time she took to assist me with the project setup**.**
- **Dr Stanford Kwenda,** for providing your expertise in completing this complex statistical analysis.
- My grandmother **Asnath Moloto** for always being the pillar of my strength.
- **Cathrine** and **Nelson Boshielo**, my parents, who have always supported, encouraged and believed in me, in all my endeavours and who so lovingly and unselfishly cared for me.
- My siblings **Thabo**, **Lebogang** and **Tshepo Boshielo** for their constant love and support.
- **Mokete Mokhothu,** for their support and constant encouragement.
- The Centre of Excellence for Biomedical TB Research for providing the environment all these years for me to be able to conduct this research.
- I would also like to express my appreciation to everyone from the **CBTBR** and **NICD HIV/STI** Lab. I am thankful for their aspiring guidance, constructive criticism and friendly advice during the study.
- Lastly, my sincere gratitude goes to the Medical Research Council and National Research Foundation and for funding me in the academic year 2018-2021 and 2022, respectively.

Psalm 136:1

*"O **give thanks unto the Lord**; for he is good: for his mercy endureth for ever"*

Table of Contents

List of Symbols and Abbreviations

µg	Microgram
µL	Microlitre
µm	Micrometre
α	Alpha
β	Beta
A1AG1	Alpha-1-acid glycoprotein 1
A2GL	Alpha-2-glycoprotein
AMACR	α-methylacyl-CoA racemase
AMBP	α-1-microglobulin/bikunin precursor
APRIL	A proliferation-inducing ligand
ART	Antiretroviral treatment
ATP	Adenosine triphosphate
AUC	Area under the Curve
BAFF	B-cell activating factor
BCG	Bacillus Calmette-Guérin
BK	Bradykinin
BLC	B Lymphocyte Chemoattractant
Ca	Circa
CBTBR	Centre of Excellence for Biomedical TB Research
CCL-22	C-C Motif Chemokine Ligand 22
CF	Culture filtrate
CFP-10	Culture filtrate protein-10 kDa

CFU	Colony forming unit
CLR	C-type Lectin Receptors
COVID-19	Coronavirus disease-2019
CRP	C-Reactive Protein
DABK	desArg9-bradykinin
DC	Differentially culturable
DCTB	Differentially Culturable Tubercle Bacilli
DNA	Deoxyribonucleic acid
EGF	Epidermal Growth Factor
ELISA	Enzyme-linked immunosorbent assay
ELISPOT	Enzyme-linked immunospot
EMB	Ethambutol
ENA-78	Epithelial Neutrophil-Activating Peptide-78
FcR	Fc Receptor
FGF-2	Fibroblast Growth Factor 2
G-CSF	Granulocyte colony-stimulating factor
GM-CSF	Granulocyte-macrophage colony-stimulating factor
GROα	Growth-regulated oncogene α
ESAT-6	Early Secreted Antigenic Target 6 kDa
ETH	Ethionamide
HGF	Hepatocyte growth factor
HIV	Human immunodeficiency virus
IFN-α	Interferon-alpha

IFN-γ	Interferon-gamma
IGKC	Immunoglobulin kappa chain C
IGCL2	Immunoglobulin lambda-2 chain C
IGRAs	Interferon-gamma release assays
IL	Interleukin
ILRA	Interleukin-1 receptor antagonist
INH	Isoniazid
iNOS	inducible nitric oxide synthase
IP-10	Interferon γ-induced protein 10
IRIS	Immune reconstitution inflammatory syndrome
I-TAC	Interferon–inducible T Cell Alpha Chemoattractant
ISO	Isoxyl
L	Litre
Lam	Lipoarabinomannan
LAM	Latin American (LAM)
LC–MS/MS	Liquid chromatography with tandem mass spectrometry
LDHB	L-lactate dehydrogenase B chain
LIF	Leukemia inhibitory factor
LJ	Lowenstein-Jensen
LPS	Lipopolysaccharide
LTBI	Latent tuberculosis infection
MCP	Monocyte chemoattractant protein
MDR	Multi drug resistant

MGIT	Mycobacterial Growth Indicator Tube
MET	Metronidazole
MFI	Mean fluorescence intensity
MIF	Macrophage migration inhibitory factor
MHC	Major Histocompatibility Complex
MIG	Monokine induced by gamma interferon
MIP	Macrophage Inflammatory Protein
MiRNAs	MicroRNAs
mL	Millilitre
MMP-1	Matrix metalloproteinase-1
MOI	Multiplicity of infection
MPN	Most probable number
Mtb	*Mycobacterium tuberculosis*
MTBC	*Mycobacterium tuberculosis* complex
MVA85A	Modified vaccinia virus Ankara expressing antigen 85A
NAATs	Nucleic acid amplification tests
NGFβ	Nerve growth factor beta
NGS	Next-generation sequencing
NID1	Nidogen-1
NK	Natural killer cells
NICD	National Institute for Communicable Diseases
NLRs	(NOD)-like receptors
NMR	Nuclear magnetic resonance spectroscopy

NRP	Non-replicating persistence
NO	Nitric Oxide
OADC	Oleic acid, Albumin, Dextrose, Catalase
OD	Optical density
OOR	Out of range
ORM1	α-1-acid glycoprotein 1
PAMP	Pathogen-Associated Molecular Patterns
PBS	Phosphate Buffered Solution
PCR	Polymerase Chain Reaction
PCT	Procalcitonin
PHRU	Perinatal HIV Research Unit
PiRNA	PIWI-interacting RNAs
PRRs	Pattern Recognition Receptors
PSTK	Phosphoseryl-tRNA kinase
PTGDS	Proteins prostaglandin-H2 D-isomerase
PTX-3	Pentraxin-3
PZA	Pyrazinamide
QFT	QuantiFERON® Gold In-Tube assay
RAP1B	Ras-related protein Rap-1b
RIF	Rifampicin
RNA	Ribonucleic acid
RNI	Reactive nitrogen intermediates
ROC	Receiver operating curve

ROI	Reactive oxygen intermediates
Rpf	Resuscitation promoting factor
RPMI	Roswell Park Memorial Institute Medium
RT-MLPA	Reverse transcription multiplex ligation dependent probe amplification assay
RT-PCR	Real-time polymerase chain reaction
SAA1	Serum amyloid A1
SCF	Stem cell factor
SCTM1	Secreted and transmembrane protein 1
SDF-1α	Stromal cell-derived factor-1 alpha
SELDI-TOF MS	Surface enhanced laser desorption/ionization time-of-flight mass spectrometry
SEM	Standard error of the mean
SIV	Simian immunodeficiency virus
SnRNA	Small nuclear RNAs
SnoRNA	Small nucleolar RNAs
SR	Scavenger Receptor
TAC	Thiacetazone
Th1	T helper 1
TLR	Toll-Like Receptor
TNF-α	Tumour Necrosis Factor alpha
TNF-β	Tumour Necrosis Factor beta
TNFR2	Tumour necrosis factor receptor 2

TRAIL	Tumour necrosis factor (TNF)-Related Apoptosis Inducing Ligand
TSLP	Thymic stromal lymphopoietin
TST	Tuberculin Skin Test
TWEAK	Tumor necrosis factor (TNF)-like weak inducer of apoptosis
VBNC	Viable But Non-Culturable
VEGF-A	Vascular Endothelial Growth Factor A
WGS	Whole genome sequencing
WHO	World Health Organization
XDR	Extensively drug-resistant

List of Tables

List of Figures

Abstract

Tuberculosis (TB) is a chronic disease caused by *Mycobacterium tuberculosis* (Mtb). Despite the implementation of multifaceted TB prevention and control efforts, a significant number of people still dee from TB. Consistent with this, an uptick in TB-related mortality was recently noted, which has been ascribed to the negative effects of Coronavirus disease-2019 (COVID-19) on TB programs. The complex life cycle of Mtb is largely due to the use of immune evasion mechanisms to establish initial infection, remain dormant in the host, and reactivate pathogenicity under favourable circumstances. The prolonged TB treatment regimen is necessitated by the slow response of bacterial populations to standard TB chemotherapy, a phenomenon that may be caused by persistent, drug-tolerant bacteria. Scientific literature has provided evidence for these types of bacterial populations in the form of Differentially Culturable Tubercle Bacilli (DCTB). It has been demonstrated that DCTB represent drug tolerant bacteria that appear to be cleared at slower rate than organisms detected by routine culture methods. However, it remains unclear if DCTB populations elicit different immune responses when compared to their conventionally culturable counterparts.

Herein, we address this question by optimizing a laboratory model for the generation of DCTB *in vitro* and test the capacity of clinical isolates of Mtb from Lineage 2 (Beijing) and Lineage 4 (LAM) to adopt the DCTB state. Using the Most probable number (MPN) assay, in the presence of culture filtrate (CF) as a source of growth factors to resuscitate DCTB, and colony forming units, the amount of DCTB in our model was quantified. As demonstrated by the limited growth on agar plates and increased growth in liquid media supplemented with CF from an axenic culture of Mtb, our findings demonstrated that carbon starvation was able to generate DCTB from clinical Mtb strains. After generating these populations, we stimulated whole blood with DCTB and conventionally culturable populations and report on the stimulation of a select set of cytokines (IFN-γ, IL-4, IL-5, IL-6, IL-12p70 and TNF-α) using a Bead Array Multiplex Immunoassay. In comparison to H37Rv-DCTB and LAM-DCTB, Beijing-DCTB induced significantly reduced levels of IL-5 and TNF-α. When comparing cytokine production between culturable and DCTB populations, within a single strain, we noted that LAM-DCTB was delayed in the production of IFN-γ whilst Beijing-DCTB was not able to induce production of this cytokine when compared to conventionally culturable counterparts. These data suggest that shifting to a non-replicating DCTB state does indeed affect the ability of clinical isolates to induce immune responses.

Based on these observations, we next set out to determine if DCTB affects immune responses during treatment of Mtb infected individuals. In prior work, using a prospective observational cohort, we demonstrated a substantive heterogeneity in clearance of DCTB in individuals with drug susceptible TB. We were able to classify these response patterns into three broad groups including (I) participants who were able to clear DCTB within the first two weeks of treatment (treatment-responsive); (II) those with delayed ability to clear these organisms (delayed-responsive) and (III) a group of individuals where DCTB did not change substantively during treatment (non-responders). Given these stark differences in treatment response patterns, we hypothesized that the immune responses associated with these patterns would be substantively different. In the second component of this work, we set out identify immune biomarkers that predict an effective response of DCTB to TB treatment. To quantify cytokines, chemokines and growth factors in plasma from these groups, we used a 65-plex Luminex assay, with a broad selection of targets. Statistically significant differences between these groups were analysed using the Kruskal-Wallis test with Dunn's multiple comparisons, with $p<0.05$ was considered as statistically significant. When compared to patients who had TB and HIV co-infection, the number of cytokines that may possibly be used to report on the effectiveness of TB treatment was significantly higher in Mtb-only infected patients. This suggests that HIV infection significantly reduces the number of cytokines that can be used to report on TB treatment response. The ROC analysis of I-TAC, G-CSF and VEGF-A showed that these cytokines have a significant discriminatory power to distinguish treatment-responsive and non-responsive patients from HCs using DCTB as the measure of treatment response. No unifying cytokine signature that predicted DCTB response in all groups was identified. Together, our results indicate that some inflammatory markers are elevated in individuals with TB that rapidly clear bacteria during treatment. Given that these responses are based on DCTB, which represent drug tolerant populations, these select cytokines may be useful in evaluating the effectiveness of novel shorter TB treatment regimens.

CHAPTER 1

1. TUBERCULOSIS

1.1. Introduction

Tuberculosis (TB) caused by *Mycobacterium tuberculosis* (Mtb) is a disease killing millions of people globally (Lourens et al., 2019). TB infection is established when an individual inhales aerosolized particles carrying Mtb. Primary factors in TB transmission include the host's immunological health status, the amount of inhaled bacteria, the proximity of contacts, and the infectiousness of the primary case (Mathema et al., 2008). Dendritic cells and macrophages, as well as non-phagocytic alveolar endothelial cells such as M cells and type 1 and type 2 epithelial cells (pneumocytes), are susceptible to infection by inhaled Mtb. Before the adaptive immune system sets in, Mtb can replicate within macrophages and spread to pulmonary lymph nodes and to a number of extra pulmonary sites (Teitelbaum et al., 1999, Ryndak et al., 2015). A number of scenarios exist that describe the outcome of infection, including: (I) elimination of infection by host immune activation; (II) bacterial growth leading to primary infection, and (III) bacterial dormancy/lack of replication, which renders the host non-contagious and asymptomatic (Trauner et al., 2012). Given these complex outcomes, the clinical presentation of TB can take one of two major forms including, asymptomatic, previously referred to as latent TB infection (LTBI), where the bacteria can persist for many years in the host without replicating and active disease where the bacteria replicate and cause symptoms (Pai et al., 2016).

LTBI is a term that has been used to describe a state of long-term immunological control of Mtb infection that develops in most infected people. Approximately 2 to 5% of infected people eventually progress to active TB disease, typically within the first six months to two years of infection (Goletti et al., 2018). With the advent of higher resolution imaging techniques for TB disease in humans, LTBI has been reclassified as a spectrum of TB infection (Drain et al., 2018). Within this spectrum, specific states have been described including subclinical TB infection (asymptomatic with radiological or microbiological evidence of TB) and incipient TB (asymptomatic with radiological or microbiological evidence of TB, together with a biomarker signature that predicts progression to active disease.) As further information becomes available on TB immune responses and bacterial viability/replication competence, it

is likely that these definitions will require further revision. In general, here we use the term LTBI to refer to these collective asymptomatic clinical presentations.

Active TB often affects the lungs, but it can also affect any organ outside of the lung, resulting the development of extra pulmonary TB (Behr et al., 2018). In this clinical presentation, tubercle bacilli have colonized the lung to form lesions that impair respiratory sufficiency. This results in symptoms associated with TB such as shortness of breath, night sweats, weight loss and persistent coughing with blood. The pathogenesis of active TB will be discussed later. When this condition is diagnosed, treatment is necessary to achieve clinical cure.

Historically, streptomycin was the first antibiotic used to treat TB however, resistance to this drug developed quickly rendering it of limited use. Subsequently aminoglycosides and rifamycins were discovered as effective tools to treat TB, leading the first combination regimens to achieving durable cure (Rocha et al., 2021). Currently, TB treatment comprises a combination regimen of isoniazid (INH), rifampicin (RIF), pyrazinamide (PZA), and ethambutol (EMB), the four first-line antibiotics that are routinely used (Somasundaram et al., 2014). Resistance to a select set of these drugs results in multidrug-resistant TB (MDR-TB) or extensively drug-resistant TB (XDR-TB) (Pai et al., 2016). MDR-TB is defined as infection with Mtb strains that are genetically resistant to RIF and INH, with XDR being defined as MDR with additional resistance to second line drugs including aminoglycosides and fluoroquinolones (Yang et al., 2018). In addition to chronic infections brought on by the emergence of M/XDR-TB, a sizable reservoir of people harbouring Mtb in asymptomatic state can progress to active disease, thus contributing to the increase in new TB cases globally (Peddireddy et al., 2017). A good strategy to successfully eradicate TB on a global scale is to provide efficient vaccination, better diagnostics, and new, shortened treatment regimens (Abu-Raddad et al., 2009). Owing in part to the absence of effective methods to accurately identify Mtb or its by-products in host samples from asymptomatic individuals, TB biomarkers that predict disease progression are required. In addition, host biomarkers that aid in TB diagnosis as well as to assess the effectiveness of treatment are urgently needed (Walzl et al., 2011).

1.2. Global prevalence of TB

According to World Health Organisation (WHO) global report in 2021, an estimated 10 million people were infected with TB, 5.6 million men, 3.3 million women and 1.1 million children. There was a 18% (7.1 million in 2019 to 5.8 million in 2020) decline in the number of people

newly diagnosed with TB and reported. This decline was attributed to the COVID-19 pandemic.

The global burden of TB disease differs between countries and overall geographies, with incidence ranging from fewer than five to more than 500 new cases per 100 000 population per year. In 2020, the 30 high TB burden countries accounted for 86% of new TB cases. Eight countries account for two thirds of the total, with India leading the count, followed by China, Indonesia, the Philippines, Pakistan, Nigeria, Bangladesh, and South Africa (see **Figure 1.1**).

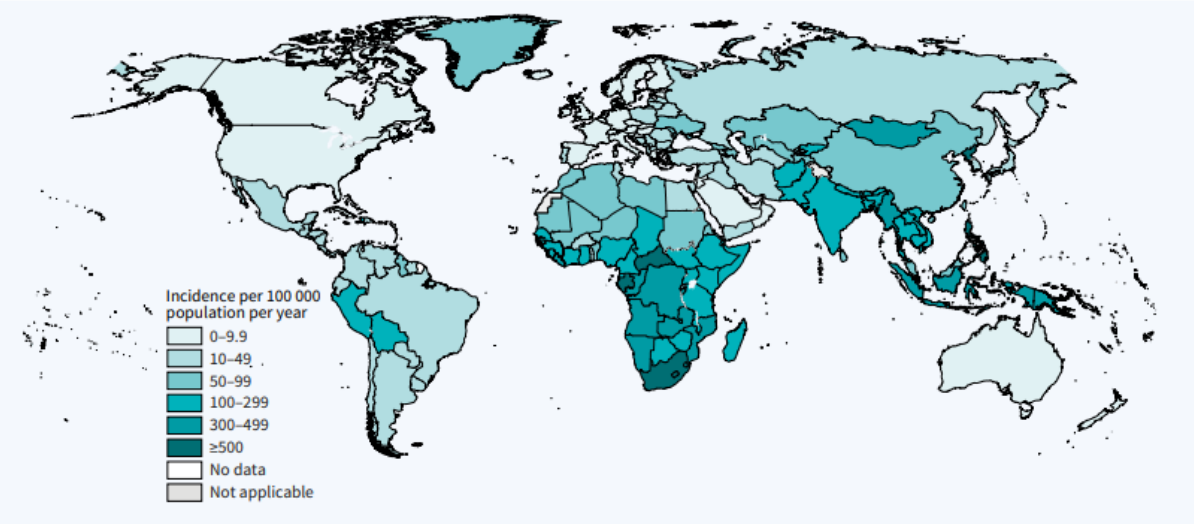

Figure 1.1. Estimated annual tuberculosis incidence (per 100,000 population), by region worldwide (WHO, 2022).

WHO reported that in 2020, 1.3 million TB deaths were among human immunodeficiency virus (HIV)-negative people (up from 1.2 million in 2019) and an additional 214 000 among HIV-positive people (up from 209 000 in 2019), with the combined total giving an incidence equivalent to 2017 rates. HIV is one of the leading risk factors for developing active TB followed by diabetes, malnutrition, smoking and excessive alcohol use (Narasimhan et al., 2013).

1.3. Diagnosis and treatment Mtb infection

New tools, including enhanced diagnostic tests, are urgently needed to curb the spread of TB. Microbiological, radiographic, and immune-based assays can be used to diagnose TB infections (Gill et al., 2022). Smear microscopy, Mtb culture, and nucleic acid amplification assays such as the GeneXpert® MTB/RIF assay are among the most frequently used tests for the diagnosis of active TB (Cudahy and Shenoi, 2016). In areas with limited resources, smear

microscopy is the preferred technique, involving detection of acid-fast mycobacteria in sputum clinical samples using the Ziehl-Neelsen stain. Given the ease of use, molecular diagnostics have become widespread for the detection of TB. However, due to its enhanced sensitivity over smear and excellent specificity, Mtb culture is still regarded as the gold standard for the detection of active TB (Halliday et al., 2019). In general, culture compares well with molecular diagnostics, however, with low numbers of bacteria, both of these methods can miss cases.

Since the discovery of Mtb, the general approach to growing bacteria has been culturing on Lowenstein-Jensen (LJ) media, which can take up to 4-6 weeks to detect colonies. This method has a relatively high specificity and sensitivity, but it also needs a laboratory with BioSafety Level III facilities. It has been shown that at least 10 viable bacilli per mL of sputum is necessary for Mtb culture using the LJ medium to successfully detect Mtb (Munir et al., 2015). Owing to the slow growth of Mtb, improved methods for culture such the BACTEC mycobacterial growth indicator tubes (MGIT) are being used. This method has a better turn-around time by shortening the time required to detect Mtb by 1-3 weeks (Kolibab et al., 2014).

The development of molecular nucleic acid amplification tests (NAATs) tests such as GeneXpert has been considered a major breakthrough in TB diagnosis and most recently, the introduction of an improved GeneXpert Ultra has improved on sensitivity (Nguyen et al., 2019). These tests, use polymerase chain reaction (PCR)-based amplification technique to detect TB and can also be used in drug susceptibility detection for first line drugs such as RIF (MacLean et al., 2020). In developing countries, sputum smear microscopy using Ziehl-Neelsen staining for TB diagnosis is preferred, due to its affordability, high specificity, and reduced requirement for expensive equipment. Results from smear microscopy can be acquired in less than two hours, but this approach is less sensitive as it requires between 5,000 and 10,000 bacilli per milliliter (mL) of sputum to obtain a positive result (Riaz et al., 2016).

Alternative methods for diagnosis of active TB such as antibody-based serological tests have been used but have been shown to have poor accuracy (Pai et al., 2008).The Lipoarabinomannan (Lam) urinary detection method is also gaining interest for use in diagnosing active TB (Zijenah et al., 2015). Lam has proven particularly useful for diagnosis of TB in people living with HIV given the extra pulmonary manifestation of disease, which can manifest more than 50% of cases in some instances (Kerkhoff et al., 2020). In addition, Lam has shown promise for detection of TB in children (Iskandar et al., 2017). However, a

significant limitation of LAM is that it is only useful with extrapulmonary disease and has low sensitivity.

As Mtb infection has a spectrum of clinical outcomes including asymptomatic and active TB disease with chronic symptoms (Lin and Flynn, 2018), there are two primary methods for diagnosis of LTBI. In the health sector, for many years. clinicians have been using tuberculin the skin test (TST) for diagnosis of LTBI, with interferon-gamma release assays (IGRAs) as an alternative (Zellweger et al., 2020, Gooding et al., 2007). This will be discussed later.

1.4. Physiology of Mycobacteria

The phylum of Gram-positive bacteria known as Actinobacteria is incredibly complex and contains several species that have developed distinct symbioses (commensal or parasitic) with a variety of hosts, including various mammals. For instance, whereas certain species of the genera *Mycobacterium* and *Nocardia* are harmful, others from the genus *Bifidobacterium* are recognized to be beneficial members of the normal gut microbial flora and have a significant positive impact on human health (Barka et al., 2016, O'Callaghan and Van Sinderen, 2016). In the phylum Actinobacteria, the genus *Mycobacterium* includes a collection of gram-positive, rod-shaped, acid-fast organisms (Gao and Gupta, 2012). The term "*Mycobacterium tuberculosis* complex" (MTBC) refers to a group of species that have been found to be genetically similar, including *Mycobacterium pinnipedii*, *Mycobacterium canettii*, *Mycobacterium africanum*, *Mycobacterium microti*, *Mycobacterium bovis*, *Mycobacterium microti* and Mtb. The majority of *Mycobacterium* species typically live in a variety of environments, including soil and water, and engineered water systems (Falkinham, 2009). Numerous members are recognized human pathogens, most notably Mtb and *Mycobacterium leprae*, which cause TB and leprosy, respectively (Medjahed et al., 2010). In addition, *Mycobacterium ulcerans* has been attributed as the causative agent of Buruli ulcer (Stinear et al., 2007). This disease manifests as open sores on the skin, required combination treatment and sometimes amputation of limbs (Yotsu et al., 2018).

From the MTBC group, Mtb is one of the most researched species (Pai et al., 2016). One notably distinctive characteristic that sets *Mycobacterium* species apart from other bacteria is the amazing molecular complexity of the mycobacterial cell wall. Despite being categorized as gram-positive organisms, their envelopes have several characteristics in common with gram-negative cell walls, namely an outer permeability barrier that serves as a pseudo-outer membrane (Ratledge and Stanford, 1982, Brennan and Nikaido, 1995, Alderwick et al., 2015).

The extensive structure of the mycobacterial cell envelope is depicted in **Figure 1.2**. Glycolipids that penetrate the periplasmic region are linked to the inner membrane phospholipid bilayer. A cross-linked peptidoglycan polymer, a highly branched arabinogalactan polysaccharide, and long-chain mycolic acids make up the fundamental core cell wall structure. Solvent-extractable lipids, such as non-covalently coupled

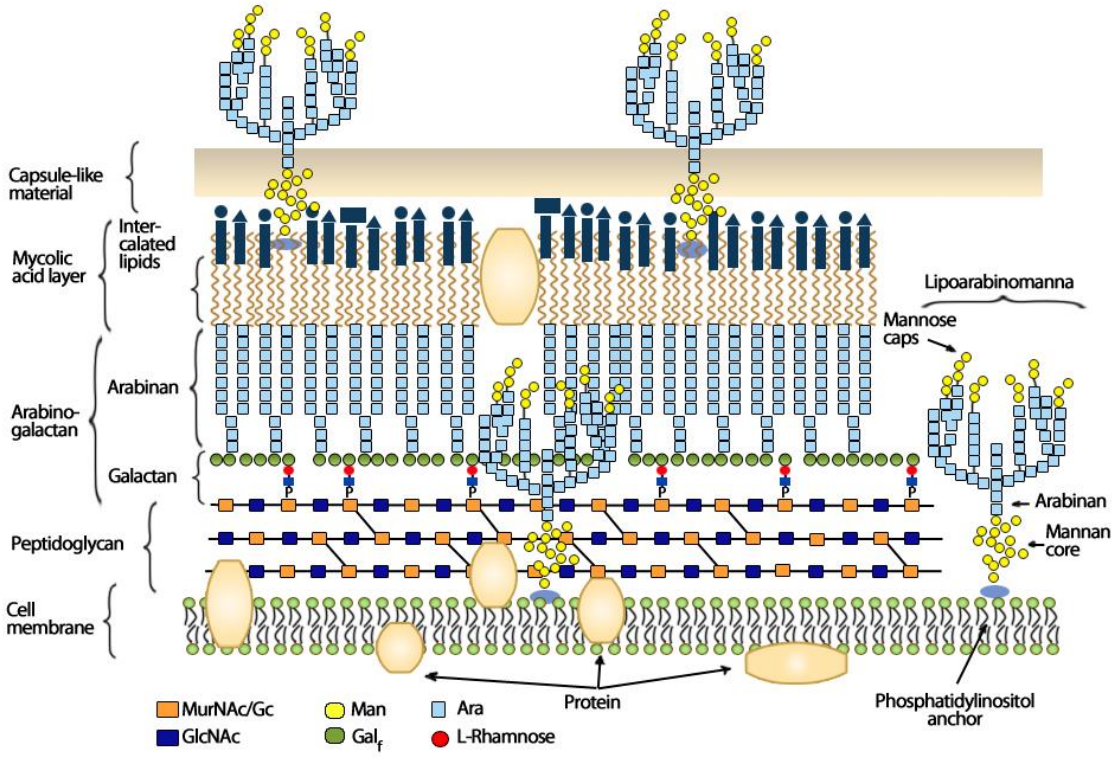

glycophospholipids and inert waxes, are intercalated into the mycolate layer to create the outer membrane. The carbohydrate- and lipid-rich layers of the cell wall are crucial for pathogenesis and survival in addition to acting as a permeability barrier that guards against hydrophilic substances (Daffe and Reyrat, 2008, Forrellad et al., 2013, Abrahams and Besra, 2018).

Figure 1.2. Mycobacterial cell wall. A schematic representation of the mycobacterial cell wall, depicting the prominent features, including the glycolipids (phosphatidyl-myo-inositol mannosides, mannosylated lipoarabinomannan), peptidoglycan, arabinogalactan and mycolic acids. Intercalated into the mycolate layer are the acyl lipids (including trehalose monomycolate, trehalose dimycolate, diacyltrehalose, polyacyltrehalose, phthiocerol dimycocerosate, sulfoglycolipid). This image was taken from (https://2009.igem.org/wiki/index.php?title=Team:SupBiotech-Paris/Concept1&oldid=159486)

Numerous opportunities exist to develop anti-mycobacterial drugs to eradicate Mtb, owing to the complexity of its cell wall. A more effective chemotherapy can be produced by disrupting the structure of the cell wall, which can facilitate the entry of other TB drugs. More significantly, cellular death in mycobacteria can result from suppression of biosynthesis of cell wall components (Vilchèze, 2020). This approach can potentiate the activity of current TB

drugs, increase intracellular concentrations of drugs and also limit the emergence of drug resistance.

1.5. Pathogenesis of M. tuberculosis

1.5.1. Transmission of Mtb

Mtb is spread via the air as droplet nuclei when infectious people with pulmonary TB cough, sneeze, talk, laugh or spit. Recent work suggests that tidal breathing also contributes to TB transmission (Dinkele et al., 2022). Mtb in these tiny droplets of small size (1–2 mm or less) can remain viable as airborne droplets, suspended in the air for several hours depending on the environment. A susceptible host needs substantial exposure to multiple droplet nuclei during interaction with a TB diseased individual to become infected as shown in **Figure 1.3**. The factors that affect transmission are mentioned in **Table 1.1** (Mack et al., 2009). TB predominately affects the lungs but can also spread via the systematic and lymphatic circulation and infect other organs and tissues such as the liver, bones, spleen and the brain (Loddenkemper et al., 2016).

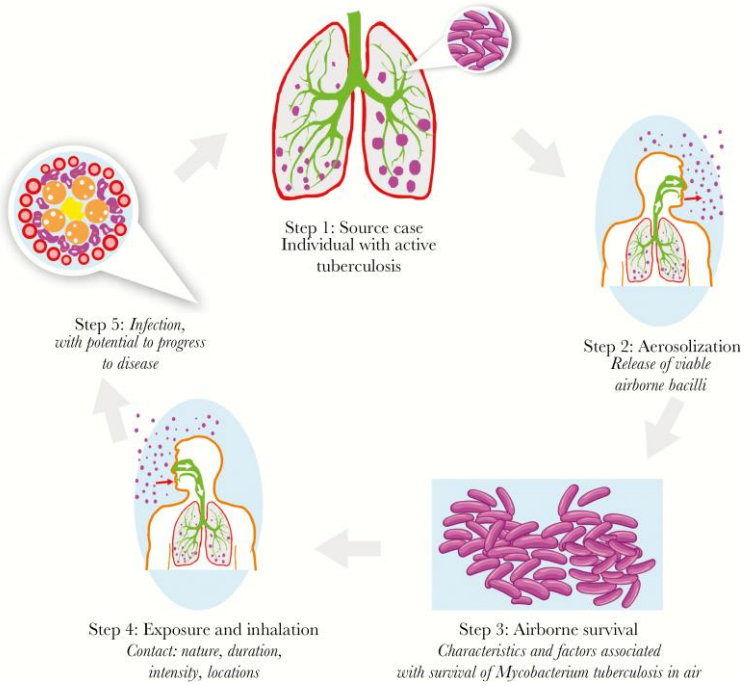

Figure 1.3. A cascade for tuberculosis transmission is proposed in which (1) a source case of TB (2) generates infectious particles (3) that survive in the air and (4) are inhaled by a susceptible individual (5) who may become infected and (6) who then has the potential to develop TB. This picture was extracted from (Churchyard et al., 2017).

1.5.2. Host immunity against Mtb

The human immune system comprises the innate and adaptive immune responses, with innate immunity being the first to act during infection. The immune response that results during the interaction between Mtb and the host is complex, multifaceted and depends on the health and nutrition of the host. The encounter may result in numerous potential outcomes including the development of latent infection, subclinical disease, primary disease or elimination of the

Table 1.1: Factors that determine the transmission of *Mycobacterium tuberculosis*.

Factors	Description
Features of the source case	Culture or smear positivity-high bacterial load results in increased transmission risk. Drug treatment-prolonged treatment reduces transmission potential. Previous history of TB. Ability to generate aerosols, lung capacity and cough frequency. Health seeking behaviour.
Susceptibility of the new host	Immune status of the exposed individual (HIV infection). Prior history of lung damage. Any other comorbidities such as diabetes.
Environment	Environmental factors that affect the concentration of *M. tuberculosis* such as ventilation, room size and movement of individuals. Other factors include number windows, doors etc. Relative humidity, TB bacilli can survive in humid environments. Recirculation of air in closed settings. Environments that promote congregation such as schools, prisons and places of worship.
Exposure	Proximity, frequency, and duration of exposure with source cases.

tubercle bacilli (de Martino et al., 2019). Once the pathogen successfully reaches the alveoli, it encounters immune cells such as alveolar macrophages, dendritic cells, T-lymphocytes, neutrophils, fibroblast, which aggregate and form a structure called the granuloma via cytokine mediation. This results in further containment of the bacterium following the initial engulfment of the bacilli by recruited macrophages (Marakalala et al., 2018).

Due to the lack of oxygen and nutrients within the granulomatous caseous centres, the bacilli can enter a dormant state and stop replicating, thus establishing latent infection (Barry et al., 2009, Lerner et al., 2015). Macrophages and CD4+ T lymphocytes, together with granuloma formation, play an important role in deciding the outcome of the infection which can either favour pathogen survival or kill it (de Martino et al., 2019). Factors such as HIV infection and diabetes cause immune suppression/dysregulation and these individuals have considerably increased risk of Mtb reactivation/disease progression as a result of dissolution of the granuloma leading to replication of the bacilli. This eventually progresses to full-blown disease causing lung cavitation and spread of bacteria into other parts of the lungs, and subsequently into the air during respiratory manoeuvres, which can increase transmission potential (Abrahem et al., 2020).

Granulomas are known to assist in controlling TB infection and are therefore a key feature in the host response to Mtb (Basaraba, 2008, Esmail et al., 2014). Paradoxically, whilst mediating this protective role, they facilitate intracellular survival of bacilli. During asymptomatic infection, Mtb bacilli are able to reside and persist within the granulomas for a long time (Kolloli et al., 2018). The granuloma represents the end result of inflammatory mononuclear cell infiltration that limits the growth of Mtb, while also providing a survival niche for the bacteria to disperse (Orme and Basaraba, 2014, Ehlers and Schaible, 2013). Granulomas are formed by aggregation of immune cells at the onset of infection as shown below in **Figure 1.4**. The granuloma undergoes morphological evolution from early infection to late TB stages, with the bacilli being intracellular at the start of infection and extracellular as the necrotic caseous lesion proceeds (Grosset, 2003). Granulomas can be found in active TB, LTBI, and in cases of recurrent TB. As a result, simply forming a granuloma is insufficient for infection control; rather, the granuloma must operate effectively. In active TB, the host often has several granulomas that are unable to control bacteria, whether extracellular or within macrophages or dendritic cells. The bacteria then migrate throughout the lung or disperse to other organs, resulting in the formation of additional lesions (Flynn et al., 2011). The caseous granuloma is the most advanced granuloma in TB, so named because the centre of the granuloma has a "cheese-like" look. This granuloma is made up of multiple cells, primarily with epithelioid macrophages that surround an acellular necrotic zone, as well as a lymphocytic cuff that includes both B and T cells and fibroblasts (Flynn and Klein, 2011).

1.5.3. Innate immunity

Innate immune responses play a central role in the pathology of infectious and inflammatory diseases, with phagocytes such as macrophages, dendritic cells and neutrophils playing a critical role in host-pathogen interactions. Together with inflammatory mediators like cytokines, chemokines, and proteases, these innate immune cells are essential contributors to the host defence against Mtb infection (Etna et al., 2014, Muefong and Sutherland, 2020, Newson et al., 2014).

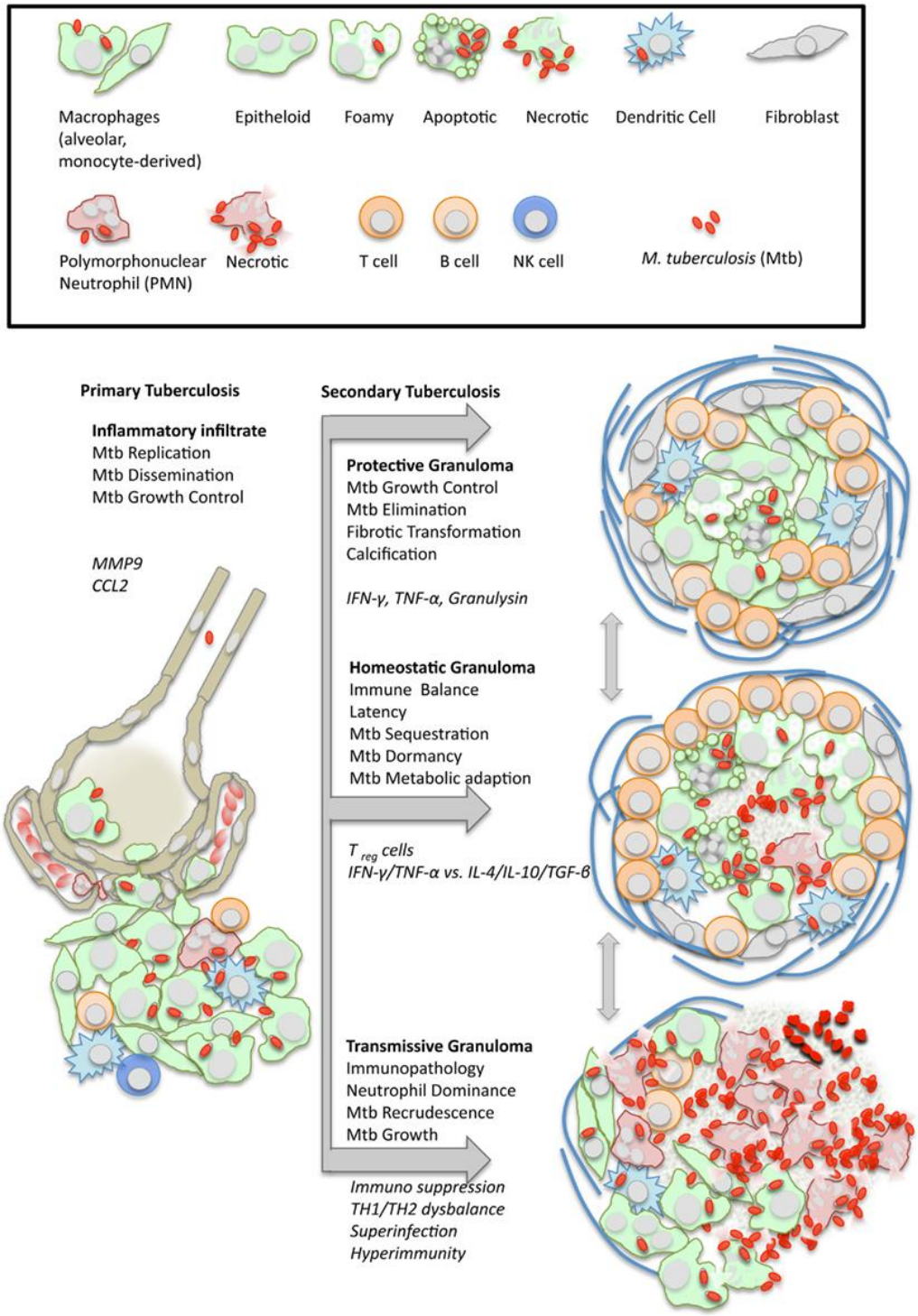

Figure 1.4. Dynamics of granuloma formation and pathology in tuberculosis. Mtb triggers a local inflammatory infiltration which may give rise to (i) protective immunity, (ii) balanced inflammation, or (iii) transmission within the bronchi of the lungs in necrotizing granulomas. The varieties of organized granulomas that are pictured are simplified representations of different points along a pathologic continuum. These represent distinct phases of the Mtb life cycle, including either metabolic adaption or slowed development within the granulomatous lesion, or recrudescence and dissemination to the subsequent host after granuloma breakup. Typical cellular and humoral mediators of granuloma differentiation are indicated in italics. This diagram was taken from (Ehlers and Schaible, 2013).

Macrophages are the first line of defence against pathogen invasion and play an important role in maintaining overall immune protection. Resident alveolar macrophages are phagocytic cells that encounter bacilli as they reach the pulmonary alveolus but usually fail to eliminate mycobacterial invaders (Naeem et al., 2018). Chemokines produced by alveolar macrophages and pneumocytes attract the first wave of inflammatory cells, including neutrophils, monocyte-derived macrophages, natural killer (NK) cells, Gamma Delta (γδ)-T cells and T cells, which drive inflammation and tissue remodelling (Eum et al., 2010, Feng et al., 2006). This further triggers the release of pro-inflammatory cytokines tumour necrosis factor (TNF), IL (interleukin)-6, IL-1α, and IL-1β (Kroon et al., 2018). This interaction is facilitated by the recognition of Pathogen-Associated Molecular Patterns (PAMPs), present on the bacterial surface, by Pattern Recognition Receptors (PRRs) of the host cell such as Toll-Like Receptors (TLRs), C-type Lectin Receptors (CLRs), Fc Receptors (FcRs), NOD-like receptors (NLRs), Scavenger Receptors (SRs), and cytosolic Deoxyribonucleic acid (DNA) sensors (Ponnusamy and Arumugam, 2022). These immune responses also lead to activation of other cellular processes such as apoptosis, antigen presentation, inflammasome activation, phagosome maturation, and autophagy. Macrophages also play a role in initiating adaptive immunity by presenting antigens to T cells to initiate the cellular response (Mortaz et al., 2014, Queval et al., 2017). Activated macrophages employ multiple strategies to eliminate the phagocytosed bacilli and these include restriction of pathogen growth through phagosome-lysosome fusion, apoptosis, nitric oxide (NO) release, generation of reactive oxygen intermediates (ROI), and the respiratory burst (Khan et al., 2016, Mihret, 2012).

1.5.4. Adaptive immunity

The adaptive immune response is initiated early and matures over a period 3-8 weeks post infection. Antibody and cell mediated immunity effector systems, make up the adaptive immune response and their production or effects are initiated by B and T cells, respectively. T cell mediated immunity plays a crucial role in managing TB infection (Bandaru et al., 2020).

The presentation of antigens to other cells in host immune response against pathogens is done most efficiently by dendritic cells. This activity, together with antigens presented by macrophages as their secondary role, links the innate and adaptive immune response during TB infection. Dendritic cells exist either in an immature or mature form. Bacterial pathogens trigger immature dendritic cells to develop into mature dendritic cells, which are more efficient in antigen-presenting activity to T cells (Mbongue et al., 2014). DCs transport bacterial

antigens from the infection site to the thoracic lymph nodes, where naïve T cells reside. As naïve T cells are not able to recognise antigens, mature dendritic cells are required to breakdown these proteins and present the peptides through Major Histocompatibility Complex (MHC I and II) complexes that can then be recognized by effector CD4+ and CD8 T cells (Mellman and Steinman, 2001). In the lymphatic system, mature dendritic cells can stimulate specific T cell responses by secreting cytokines that induce differentiation of CD4+ T cells into several subtypes which include Th1, Th2, Th17, and regulatory T cells. CD4+ T cells differentiate into Th1 cells when mature dendritic cells secrete IL-12, which in turn causes Th1 cells to secrete interferon-gamma (IFN-γ), causing a positive feedback loop for dendritic cells to further produce IL-12 and produce more Th1 cells. Th2 activation also occurs in a similar fashion, but with IL-6 secretion, allowing these cells to secrete IL-4. IL-6 plays a dual role together with IL-1β and IL-23 in activating Th17 cells (Abrahem et al., 2020, Kim and Kim, 2018).

Th17 cells secrete IL-17 that in turn stimulates the production of Granulocyte colony-stimulating factor (G-CSF), Granulocyte-macrophage colony-stimulating factor (GM-CSF), monocyte chemoattractant protein-1 (MCP-1), macrophage inflammatory protein-2 (MIP-2), IL-6, and IL-8 in both CD4+ and CD8 T cells. This pro-inflammatory cytokine is essential in the process of recruiting neutrophils to the infection site (Scordo et al., 2016). Neutrophils also play an important role in inflammatory responses and are some of the first phagocytes recruited from the pulmonary vasculature to the site of infection (Jenne et al., 2013). In the early TB granuloma, during oxidative killing of Mtb engulfed from infected macrophages, neutrophils were observed to exert a protective role (Yang et al., 2012). These cells can create chemotactic signals that attract recruitment of dendritic cells and other immune cells to the infection site. A neutrophil-driven blood transcriptional signature from patients with TB has linked the involvement of these cells in the control of Mtb infection (Berry et al., 2010). The study identified a specific 86-transcript signature that was dominated by a neutrophil-driven IFN-inducible gene profile, consisting of both IFN- γ and type l IFN-αβ signalling and could also differentiate between active TB and other inflammatory infections. Despite the many important functions played by neutrophils, which include chemotaxis, phagocytosis, generation of reactive oxygen metabolites and activation of other immune cells, their presence can also cause dramatic tissue damage (Kruger et al., 2015). There are limited *in vitro* studies on these cells because they are short-lived and not easy to handle, hence their complete role in the TB immune response requires further investigation. Nevertheless, animal model studies have proven their

significance in early immune responses against Mtb. For example, an increased number of neutrophils was observed during early days of infection in Balb/c mice infected with Mtb H37Rv, with a demonstrated role in the elimination of the Mtb and limiting dissemination (Barrios-Payán et al., 2006). Another study showed how neutrophils are recruited to the lungs using Lipopolysaccharides (LPS) during infection in rats (Sugawara et al., 2004). Although such findings illustrate the importance of this subset of cells, another study demonstrated that neutrophils don't play any role during early control of slow replicating Mtb but are rather crucial in the control of fast-replicating bacteria from other species (Seiler et al., 2000). Neutrophils have higher phagocytosis intensity and oxidative response as compared to macrophages (Nordenfelt and Tapper, 2011). In response to the host and pathogen interaction via PAMPs, neutrophils can express pro- and anti-inflammatory cytokines including IFN-γ, TNF, IL-4, and IL-10 (Lyadova, 2017, Tecchio and Cassatella, 2016). The interaction between neutrophils, macrophages and T cells is tightly regulated and essential in determining the outcome of infection. However, it is still not fully understood as to how neutrophils facilitate cytokine-mediated communication with other cells in the granuloma. In the TB granuloma, activated neutrophils are thought to express cytokines that can dysregulate immune responses and contribute to pathology (Greenlee-Wacker, 2016, Mantovani et al., 2011, Nicolás-Ávila et al., 2017, Tecchio and Cassatella, 2016). Recently, Gideon et al. (2019) showed that in cynomolgus macaques infected with Mtb, neutrophils express pro-and anti-inflammatory cytokines in granulomas which resembled T-cell cytokine expression and thus may play an important immunoregulatory role.

1.6. Latent TB infection

LTBI is defined as immunological sensitization to Mtb antigens without the presence of clinical symptoms of TB. During this period of infection, Mtb is thought to survive in a non-replicating (dormant) state, with bacteria mostly limited to hypoxic granulomatous lesions in the lungs (Via et al., 2008). The health status of an individual determines the duration of latency, while most individuals can remain latently infected for a lifetime, there is a 5-10% chance for reactivation to occur, which can happen within the first 2 years post infection (Achkar and Jenny-Avital, 2011). The risk is increased annually to 10% more in immune compromised individuals, such as those infected with HIV (Lin and Flynn, 2010). As mentioned previously, LTBI diagnosis is done by measuring immune response to specific Mtb antigens using the TST or IGRAs diagnostic tests. The TST measures the sensitivity of intradermally injected purified protein derivative prepared from culture filtrate of Mtb, whereas the IGRAs measure the T-cell

immune response to Mtb by detecting IFN-γ release in blood (Gooding et al., 2007). The majority of infected people (90-95%) are able to clear the infection or to control the initial infection and enter a latent phase (Denholm et al., 2020). The term "latent" TB or phthisis (as TB was then known) was conceived by French and German physicians in the early 19th century, when the field of anatomopathology in medicine began to develop, to describe the pathological changes of TB in necropsied lungs of people who had not yet displayed any symptoms of the disease before they died (Behr et al., 2021). The state of latency was also observed in cultured tissues of healthy individuals with no pathological evidence of active TB, having died from other causes (Opie, 1927). These and other such observation led to the term LTBI becoming firmly entrenched in the literature and in clinical use.

1.7. Progression to Active TB

TB disease is caused by intricate interplay between the immunological state of the infected individual and the bacillary load (Lawn et al., 2011). HIV infection, diabetes, malnutrition, low body weight, smoking, lung illness, drug use, and previous or current use of immunosuppressive drugs have all been recognized as factors that increase the likelihood of developing active TB disease (Horsburgh Jr and Rubin, 2011). Factors related to the bacteria such as strain virulence and inoculum size, also influence the progression of disease (Carranza et al., 2020). Active TB appears to develop within a year of infection, and the rate of progression drops rapidly after the first year and then slowly declines over the following ten years, **Figure 1.5** (Brooks-Pollock et al., 2011).

1.8. HIV/TB co-infection

The most potent risk factor for the development of TB is HIV infection. According to current knowledge, HIV causes an increased chance of rapidly progressive primary TB following exposure, as well as an increased likelihood of progression to active TB disease from asymptomatic infection (Lawn et al., 2011). TB is the most prevalent disease in immune-suppressed individuals and the primary cause of death in people living with HIV (Swaminathan and Narendran, 2008). WHO reports that there were an estimated 37.7 million people living with HIV at the end of 2020, over two thirds of whom (25.4 million) are in the WHO African region and a total of 214 000 people with HIV and TB died in 2020. According to WHO, HIV-infected people are 18 times more likely than healthy people to get TB (WHO, 2021).

In their interactions with the host, HIV and Mtb both seek to achieve the same goal: efficient replication without killing the host for as long as is feasible in order to increase the possibilities of transmission to a new host (Sharan et al., 2020). HIV infection makes the patient more susceptible to TB by weakening the immune system, primarily by killing and changing CD4+ T-cell activity. The CD4+ T cell loss in lymphoid organs and peripheral blood is the most well-known effect of HIV (Ahmed et al., 2016). A study by (Foreman et al., 2016) showed that Mtb/simian immunodeficiency virus (SIV) co-infection in non-human resulted in rapid reactivation of TB disease, although there were a subset of animals that were still able to contain TB infection.

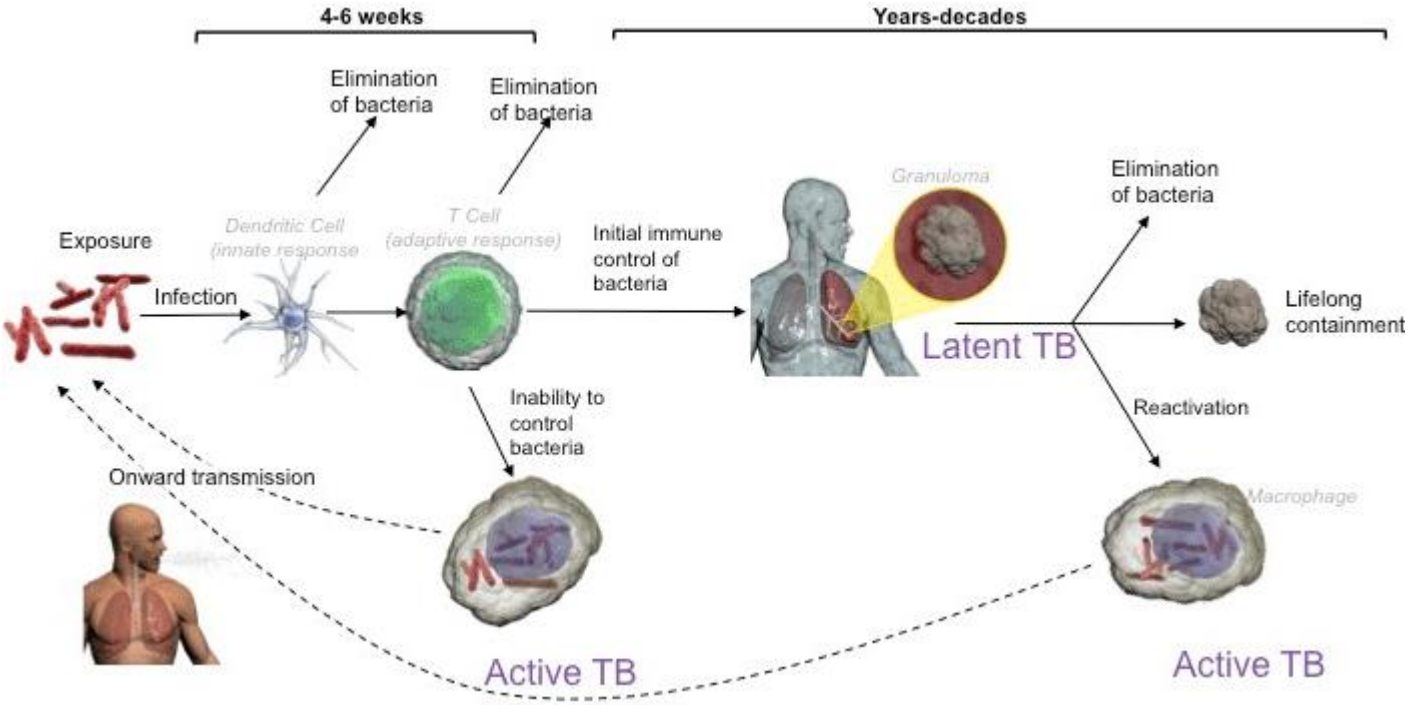

Figure 1.5. Transmission of tuberculosis and progression from latent Infection to reactivated Disease. Mtb is transmitted by inhalation of aerosolized microdroplets that are released by the coughing of infected individuals. The initial stages of infection are characterized by innate immune responses that involve the recruitment of inflammatory cells to the lung. Following bacterial dissemination to the draining lymph node, dendritic cell presentation of bacterial antigens leads to T cell priming and triggers an expansion of antigen-specific T cells, which are recruited to the lung. The recruitment of T cells, B cells, activated macrophages and other leukocytes leads to the establishment of granulomas, which can contain Mtb. Most infected individuals will remain in a 'latent' state of infection, in which no clinical symptoms are present. A small percentage of these people will eventually progress and develop active disease, which can lead to the release of Mtb from granulomas that have eroded into the airways. When individuals with active TB cough, they can generate infectious droplets that transmit the infection. This image was taken from the https://scienceandsamosa.com/killer-disease-on-loose-india-grappling-with-tuberculosis/

Granuloma formation allows the host to contain tubercle bacilli the lung. As people with HIV/TB co-infection have impaired immunity, particularly in the case of low CD4 T cell counts, the ability to form granulomas is impaired. As a result, bacilli readily traffic out of the lung and take up residence in other parts of the body, leading to the development of extra-pulmonary TB independently (Schutz et al., 2010, Marakalala et al., 2016). HIV co-infection may increase the rate of progression to active TB and subsequent transmission by disrupting any granulomas that have formed (Sharan et al., 2020). This also impairs Mtb-induced systemic pro-inflammatory cytokine/chemokine responses (Kassa et al., 2016, Devalraju et al., 2019). Interestingly, co-infection with Mtb results in enhanced HIV replication, suggesting that the two pathogens work synergistically (Bell and Noursadeghi, 2017, Kwan and Ernst, 2011).

The initiation of antiretroviral treatment (ART) in people living with chronic HIV can lead to immunological activation, which can result in a paradoxical worsening of TB in what is known as immune-reconstituted inflammatory syndrome (TB-IRIS) (Silveira-Mattos et al., 2019). IRIS occurs in up to 40% of people who are co-infected with pulmonary TB and HIV, usually after starting ART (Narendran et al., 2013). The mechanism of IRIS pathogenesis is poorly understood, however it appears to be caused by two factors: (i) failure of the immune system to eradicate the pathogen(s), resulting in a prolonged and high burden of infection, as well as (ii) a rapid immunological recovery in response to ART. There are no specific treatments available for IRIS (Barber et al., 2014). The activation of pathogen-specific T-lymphocytes is heightened and dysregulated in IRIS. When compared to people who do not develop IRIS, previous investigations have demonstrated that the frequency of Mtb-specific circulating CD4+ T lymphocytes against Mtb is directly connected with the initiation and prevalence of IRIS (Antonelli et al., 2010, Silveira-Mattos et al., 2019, Vignesh et al., 2017).

HIV infection provides a good guide of how biomarkers can be used for both initial diagnosis and monitoring disease development. Viral Ribonucleic acid (RNA) and p24 antigen detection are utilized to establish an early diagnosis after HIV infection and are detectable prior to the formation of HIV antibodies (Pilcher et al., 2005, Kfutwah et al., 2013). Following that, viral load in plasma is detected using viral RNA quantification, and disease progression is assessed using whole blood CD4+ T cell counts (Tucci et al., 2014). Developing similar approaches for TB will enhance clinical management and improve treatment outcomes.

1.9. Rationale for the current study

The last decade has witnessed a ground swell of research in the discovery and validation of novel biomarkers to monitor risk of disease progression and diagnosis of active TB versus asymptomatic infection (Wykowski et al., 2021). There is however, a huge paucity in the knowledge regarding bacterial biomarkers for reporting on these effects and for reporting on the risk of disease recurrence. In the case of asymptomatic infection, the challenge has been meaningfully sampling bacterial populations from asymptomatic individuals, hence the reliance on host biomarkers. There is a growing body of evidence suggesting that tubercle bacilli can exist in various states of culturability that limit their detection with standard laboratory methods. It is unclear if these phenomena manifest in early TB infection however, the presence of these organisms has also been noted in cases of active TB (Mukamolova et al., 2010, Chengalroyen et al., 2016, McAulay et al., 2018, Peters et al., 2023). It has been demonstrated that these DCTB represent those drug tolerant organisms that resist clearance during early treatment (Zainabadi et al., 2021, Peters et al., 2023). As such, DCTB represent a potential bacterial biomarker to monitor treatment response and also to evaluate the risk of recurrent disease. It also remains unclear if DCTB elicit differential immune responses. The hypothesis in this case being that non-replicating bacteria possibly express a diverse set of antigens compared to their conventionally culturable counterparts, leading to consequent effects of immune responses. This dissertation aimed to address this scientific question through two primary approaches. The first involved the generation of DCTB *in vitro*, using clinical isolates followed by an assessment of their ability to induce immune responses, when compared to replicating bacteria from the same genetic background. The second approach involved the use of a prospective cohort of individuals with drug susceptible TB who were placed on standard TB chemotherapy. During the early phase of treatment, and upon treatment completion, plasma samples were collected to assess immune responses. Concurrently, sputum specimens were assessed for the presence of DCTB. As such, this cohort provided a unique opportunity to measure immune responses that prevail during TB treatment and to correlate these with bacterial clearance. The experimental components of the dissertation are divided into two broad chapters, the first addressing the question of immune responses to DCTB and the second detailing the results from the cohort study. Individual hypotheses and aims are detailed in these respective chapters.

CHAPTER 2

Differential culturable tubercle bacteria: Implications for immune responses during tuberculosis infection

2.1. Introduction

Microorganisms are threatened by a range of stresses in the natural habitat and as a result, they use a variety of species-specific tactics to provide tolerance against factors that are hostile for growth and survival. One well described adaptive mechanism is the ability of bacteria to enter into a viable but non-culturable (VBNC) state where bacteria cease to replicate and not recoverable on conventional media (Li et al., 2014). The VBNC state is beneficial for the long-term survival of bacteria as without it, environmental pressures might wipe out the entire population (Pinto et al., 2015). When the stressors are removed, or when the cells get signals indicating favourable, environmental conditions prevail, these seemingly inactive cells emerge again (Oliver, 2016). Similarly, bacterial dormancy, which can or cannot be associated with the VBNC state – depending on the species, is generally referred to as a functional state that is reversible in bacteria and is characterised by decreased metabolic activity such as transcription, translation as well as improved tolerance to harmful factors and a halt to cell division (Chao and Rubin, 2010). The ability to adopt these non-replicative metabolically quiescent states enable entire bacterial populations to control their overall biomass and adapt to antibiotic stress (Stolpovsky et al., 2011). Dormant bacterial states have historically been linked to the development of spores or cysts, which represent substantive morphological changes when compared to vegetative or rapidly replicating states. Nevertheless, the potential for non-spore forming bacteria, such as mycobacteria, to enter a dormant stage has been experimentally proven; it resulted in the development of less distinct, cyst-like forms that are distinct from spores observed in bacillus species (Shleeva et al., 2010). The production of the dormant state by non-spore forming mycobacteria, including Mtb, is of particular interest for this work.

2.2. Viable but non-culturable state

The term "VBNC " refers to a dormant state brought on by severe environmental factors, such as nutrient deprivation, extreme temperatures, abrupt changes in pH or salinity, osmotic stress, limited oxygen availability and related conditions. (Fakruddin et al., 2013). The ability to culture bacteria in the laboratory using standard media and growth conditions is an essential feature for the general study of bacteriology (Buck, 1979). However, over a century ago, it emerged that bacteria have different propensities to grow on laboratory media. This is best

described by the “Great Plate Count Anomaly”, where the number of organisms that are recoverable on agar plates and are significantly lower than those recovered in liquid media for the same organism. This suggested that bacteria display differential culturability, depending on the growth conditions and prior stress exerted on the bacterial population as a whole. Whilst intimately related to the VBNC state, this differential culturability can also occur in populations that have mixtures of dormant and actively replicating bacteria (Staley and Konopka, 1985).

The existence of the VBNC state was first identified in 1982 in *Escherichia coli* and *Vibrio cholerae* cells. The use of integrated culture techniques including indirect enumeration by most probable number (MPN) calculation and direct plating with immunofluorescent microscopy, acridine orange direct counting, and direct viable counting demonstrated that *E. coli* and *V. cholerae* both go through a "nonrecoverable" state whilst maintaining viability (Xu et al., 1982). Contrary to conventionally culturable cells, which can be cultured on suitable media and form colonies, VBNC cells have lost the capacity to grow on the select media and as they are not replicating, they display tolerance to those antibiotics that target actively replicating processes in bacteria (Oliver, 2000).

Mtb can survive after infection and subvert host immune responses to manifest a spectrum of clinical outcomes. Key to this is its ability to reprogram macrophage function to enable survival in the phagosome, induce the careful orchestration of cellular recruitment to the site of infection for the formation of granulomas, and to modulate its own metabolism for the establishment of non-replicating states that display drug tolerance (Gengenbacher and Kaufmann, 2012). In the literature, this non-replicating state has been associated with the term dormancy. For the purpose of this thesis, we will use this term when describing the literature but will use the term Differentially Culturable Tubercle Bacteria (DCTB) in the description of our work, and related literature.

In the host, it has been hypothesized that the dormant state in mycobacteria is brought on in response to immune system-imposed stresses during colonization of the lung (Chengalroyen et al., 2016). This state assumed by Mtb is characterized by the absence of growth during stressful conditions, with the ability to spontaneously transition between replicating and non-replicating phenotypes (Caño-Muñiz et al., 2018). Given the important role of environmental conditions for establishment of non-replicating persistence, the ability to adopt this is influenced by both the genetics of the host, which determine the strength of the immune response and specific genetic features of the pathogen (Russell, 2011). An investigation of these genetic features is

central to developing a broader understanding of how Mtb adapts to the host and for the development of interventions to combat persisting bacteria. The latter is important for the development of shorter treatment regimens. As an example, in the murine model of TB infection, several host genes such as *Nramp1* and loci on chromosomes 1 and 11 affect organ bacillary loads in a strain-specific manner (Di Pietrantonio et al., 2010). With respect to the pathogen, several genetic factors have been implicated in the establishment of heterogeneity or non-replicating persistence. Particularly, a group of 47 genes, known as the DosR regulon, which is tightly regulated by the dormancy survival regulator transcription factor (DosR), regulates bacterial metabolism in response to oxygen deprivation and nitrogen stress (Park et al., 2003, Roberts et al., 2004). This response, collectively serves the purpose of helping Mtb adapt to anaerobic environment and survive in the host granuloma (Bartek et al., 2009). As expression of the DosR regulon is increased during hypoxia, several genes that play an important role in adaptation to these conditions are induced. For example, the DosR regulon comprises genes involved in nitrogen metabolism with the possible use of nitrate as an alternative electron acceptor during energy metabolism (Voskuil et al., 2003, Galagan et al., 2013, Park et al., 2003, Singh et al., 2020). Similarly, there appears to be overlap between the DosR regulon and those genes required for survival in macrophages (Schnappinger et al., 2003) and in mice and guinea pigs (Karakousis et al., 2004, Sharma et al., 2006).

2.3. Resuscitation of non-culturable bacteria

It is essential to keep in mind that bacteria that enter the VBNC stage may revert to the culturable state. Roszak et al. (1984) coined the term "resuscitation" to characterize the recovery of *Salmonella enteritidis* non-culturable cells, following the addition of Heart Infusion broth. Two decades later, Baffone et al. (2006) described resuscitation as the reversal of the physiological and metabolic changes that distinguish VBNC cells from their conventionally culturable counterparts. They demonstrated that cell division, which indicated recovery of *Campylobacter jejuni* VBNC to culturability, can be achieved via passage in the mouse colon depending on how long the *Campylobacter jejuni* VBNC cells remained in this state. Mtb was found to be among human pathogens that can enter the VBNC state (Shleeva et al., 2002). Numerous factors, including an increase in temperature, an increase in the concentration of nutrients, and the presence of host cells, led to the resuscitation of these species as summarised by (Li et al., 2014). The first obstacle that scientists came across when conducting resuscitation studies was the inability to distinguish between the normal proliferation of remaining culturable cells in a sample and the resuscitation of VBNC cells.

Thus far, there are no simple ways to differentiate culturable cells from those that grow normally as a result of exposure to the stimuli from those that do so after resuscitation. This limitation is important as many laboratory models (including those tested and used in this study) generate VBNC cells, create these in mixtures with conventionally culturable populations. Whilst this limits the study of molecular factors that underpin the DCTB state, it does allow for the best rendition of clinical specimens, which usually harbour these populations in mixtures.

The aforementioned environmental pressures lead to the VBNC state and removing them may aid in the return to cultivability. However, this approach is not always successful to revive some species and further growth stimulants are required. Distinct bacterial taxa have different resuscitation processes that can be induced by a variety of triggers (Zhang et al., 2021b). A few resuscitation stimuli have been employed successfully in recent years to rescue bacteria from their native environments. As an example, secreted cell wall hydrolases have been identified in mycobacteria as potent stimulators of growth, this will be discussed in next section.

2.4. Differentially culturable tubercle bacteria

Whilst adaption of Mtb during infection in macrophage and animal models of TB has been well described, similar data from human TB is lacking. Consequently, the presence of non-replicating mycobacteria during TB infection in humans has only been inferred through clinical presentation where these inferences have been made primarily based on the presence or absence of symptoms. As mentioned previously, the lack of symptoms has been associated with LTBI whilst symptomatic infection implies the presence actively replicating bacteria. For over a century this dogmatic view has not been challenged.

In the last decade several research groups have identified the presence of heterogeneous bacterial populations in various clinical specimens. These bacteria have been characterized by the lack of culturability under routine laboratory conditions. A study by Mukamolova et al. (2010) assessed the number of cells recovered in the sputum of TB patients before and during treatment using the colony-forming unit (CFU) assay and liquid growth in the form of the most probably number (MPN) assay, supplemented with culture filtrate (CF) from an axenic culture of Mtb. They demonstrated that 80-99.99% of the cells recovered by the MPN assay were not detectable on conventional agar plates and these differentially culturable populations increased during chemotherapy (Mukamolova et al., 2010). In this study, the ability to recover these occult organisms was dependent on a group of growth stimulatory proteins termed resuscitation

promoting factors (Rpfs). Rpf was initially identified in *Micrococcus luteus* as a single essential protein that able to stimulate the recovery of dormant bacterial cells (Mukamolova et al., 1998). Subsequently, five homologues (termed RpfA-E) were identified in Mtb. Combinatorial deletion studies demonstrated that these genes were dispensable for growth *in vitro* (Downing et al., 2004, Downing et al., 2005, Tufariello et al., 2004, Kana et al., 2008) but were required for resuscitation in an *in vitro* model of mycobacterial dormancy (Downing et al., 2005, Kana et al., 2008). Furthermore, *rpf* double, triple, quadruple and quintuple deletion mutants displayed attenuation in the murine model of TB, and also displayed defects in reactivation from chronic infection (Kana et al., 2008, Russell-Goldman et al., 2008). Rpfs hydrolyse bacterial peptidoglycan and how this biochemical activity results in growth stimulation has been the subject of much speculation. It has been hypothesized that one or more of several mechanisms prevail, these include: (I) the direct hydrolysis of the cell wall results in metabolic reprogramming within the cytoplasm to restart growth; (II) hydrolysis of the cell wall results in the formation of cell wall breakdown products that serve as signalling molecules to modulate growth; (III) the binding of Rpfs directly to the cell surface triggers initiation of growth and (IV) Rpfs exert their activity through partnering (direct interactions or indirect, combinatorial effects) with other proteins/cofactors/metabolites to either hydrolyse the cell wall and/or directly initiate growth (Kana and Mizrahi, 2010). Prevailing evidence suggests that Rpfs partner with an NplC-P60 endopeptidase RipA (Rpf Interacting Protein A) and this interaction results in synergistic peptidoglycan degradation to yield muropeptides that can stimulate the growth of dormant cells (Hett et al., 2008, Nikitushkin et al., 2015).

Given these collective observations, combined with the fact that Rpfs are secreted proteins (Mukamolova et al., 2002), it was tempting to speculate that the growth stimulation observed (Mukamolova et al., 2010) in CF supplemented sputum cultures could be attributed to Rpfs. To further investigate this, a subsequent study assessed growth stimulation of these bacterial populations using CF that was derived from a quintuple *Rpf*-deletion mutant. In a pretreatment cohort of South African TB patients, bacteria that were unable to grow on agar plates, but were recoverable in MPN assays supplemented with CF were noted in the majority of clinical specimens assessed (Chengalroyen et al., 2016). For the remainder of this dissertation, these differentially culturable bacterial populations will be referred to as Differentially Culturable Tubercle Bacteria (DCTB). In addition to finding CF-dependent DCTB, a substantiative number of sputum specimens haboured Rpf-independent DCTB in addition to CF-dependent DCTB (Chengalroyen et al., 2016). These data provide the first evidence that growth of DCTB

could be dependent on other factors. Consistent with this notion, it has been demonstrated, in another distinct cohort of South African TB patients prior to TB treatment, that removal of Rpfs from CF did not significantly reduce recovery of DCTB. In this study the effect of using cyclic-AMP and a combination of structurally diverse fatty acids was also tested, with the observations pointing to the fact that recovery of DCTB is most likely dependent on a combination of factors present in CF (Gordhan et al., 2021).

Comparatively greater CF-supplemented MPN counts were seen in the sputum of those without HIV co-infection when compared to HIV infected counterparts leading to the speculation that host immunity was an important driver for the establishment of DCTB populations (Chengalroyen et al., 2016, Peters et al., 2023). In support of this, CD4+ T cell levels also influenced the relative proportions of DCTB (Chengalroyen et al., 2016). These collective data pointed to a complexity in bacterial heterogeneity that prevails in sputum specimens with important implications for TB diagnosis (Dartois et al., 2016). Another study by Júnior et al. (2020) analysed the dynamics of Mtb subpopulations that are CF-dependent in patients throughout a standard 6-months TB treatment. They found that CF supplementation increases the bacillary load by 30% in samples taken before treatment and in patients treated for one month, it increased the bacillary load by 35%. In addition, their findings support the use of CF to maximise the detection of DCTB in liquid media. This aspect was investigated further in another study aimed at enhancing detection of TB in people living with HIV. HIV infection results in reduced granuloma formation, with a consequent reduction in cavities, leading to low numbers of bacteria in sputum that are difficult to detect using conventional culture. To address this, CF was supplemented into standard Mycobacterial Growth Indicator Tubes (MGIT) in a 1:1 ratio and sputum specimens from individuals with HIV-TB coinfection, prior to TB treatment, were cultured in these modified MGIT tubes. It was demonstrated that supplementation of MGIT cultures with CF enabled enhanced detection of TB in people living with HIV who had low bacterial burdens in sputum and low CD4 counts (McIvor et al., 2021). In addition to sputum, DCTB populations have been identified in specimens from various extrapulmonary sites suggesting that this phenomenon is inherent to tubercle bacilli (Rosser et al., 2018).

These non-replicating Mtb cells are widely thought to contribute to the protracted treatment period required to achieve durable cure (Dhar and McKinney, 2007). This transient, reversible drug tolerance profile develops when genetically vulnerable bacteria are not eradicated by inhibitory drug levels and can emerge again when antibiotic treatment is stopped (Wallis et al.,

1999). Even though RIF and PZA have a potent sterilizing capacity, TB treatment is still protracted, suggesting that drug tolerant populations likely prevail thus necessitating 6 months of chemotherapy (Hu et al., 2006). To investigate the role of DCTB in treatment response a prospective cohort study, with individuals presenting with drug susceptible TB was conducted using a combination of methods to quantify bacteria during treatment. It was demonstrated that DCTB levels do not change significantly during early treatment (2 weeks – 1 month), with a substantive number of individuals (ca two thirds) habouring DCTB upon treatment completion (Peters et al., 2023). In another study, based in Haiti, it was demonstrated that during the first two weeks of TB treatment DCTB populations are not eliminated and in fact, accumulate in some patients (McAulay et al., 2018). These data suggest that DCTB comprise a novel biomarker that potentially report on the responsiveness of drug tolerant bacteria to TB treatment.

In addition to drug susceptible TB, DCTB populations have also been detected in participants with drug resistant TB. In a prospective cohort aimed at using whole genome sequencing to direct treatment of drug resistant TB, it was demonstrated that substantive quanta DCTB could be recovered from participants with RIF resistant TB (Gordhan et al., 2022). Interestingly, in this study it was demonstrated that CF without Rpfs enabled greater recovery of DCTB from participants with multi-drug resistant TB when compared to those with rifampicin monoresistant TB. As with drug susceptible TB, DCTB populations were slow to clear during treatment and were detected up to 16 weeks post treatment initiation, a time point when conventionally culturable bacteria were completely eliminated (Gordhan et al., 2022). In this cohort, HIV status and CD4 count did not affect the prevalence of DCTB populations. These data were further corroborated in another study aimed at assessing levels of DCTB in drug susceptible and drug resistant TB patients in Haiti, during treatment. However, in the case drug resistant TB, DCTB were cleared during treatment in this cohort (Zainabadi et al., 2021) .

2.5 DCTB and the immune response

The differential clearance of DCTB, when compared to their conventionally culturable counterparts, during standard TB treatment raises the possibility that these organisms could substantively contribute to the immune response. Whilst this hypothesis is attractive, there are challenges in investigating these phenomena given that DCTB prevail in combination with conventionally culturable bacteria in the lung. It is possible that as bacteria enter the non-replicative state, certain antigens are no longer expressed whilst others that were not expressed

during growth, become prevalent. There is no substantive evidence in the literature for this and the work in this chapter was aimed at addressing this knowledge gap. Critical to this, is availability of laboratory model to mimic DCTB, as it is found in clinical specimens. Once generated in the lab, these DCTB populations can then be used in *ex vivo* models to study immune responses. Below, we provide a synthesis of various models used in the TB field to generate non-replicating bacteria, with the outlook to providing the framework for the model used in this study.

2.6. *In-vitro* modelling of Mtb dormancy

In TB, the non-replicating or dormant state will be dependent on conditions present within the granuloma, and by precisely simulating these conditions *in vitro*, innovative models have been created, providing a depth of new information on adaptive responses in tubercle bacteria. The *in vitro* experimental models of Mtb dormancy include not only pure mycobacterial cultures, but also infected cultures of macrophages or other immunocompetent cells as well as 3D granuloma-like structures, simulating actual granulomas *in vivo* (Batyrshina and Schwartz, 2019). A summary of the different models developed for Mtb is given in **Figure 2.1**, a select few are discussed below.

Distinctive environmental characteristics of the granuloma include hypoxia, deficiency of nutrients, a lack of carbon and nitrogen sources, acidic environment, and a high level of nitric oxide (NO) (Kaur et al., 2016). The most basic and affordable Mtb dormancy models are those that use pure bacterial cultures. These models, in general, comprise culturing techniques that allow a mycobacterial population to enter dormancy in response to external stimuli, followed by characterization of this state (Batyrshina and Schwartz, 2019). However, the majority of these models concentrate on a single condition alone and fail to produce an Mtb population that is completely inactive (Deb et al., 2009). Nevertheless, a few studies include two or more conditions in the mode to create a combination of stresses that mimic the granulomatous environment. As an example, by applying a combination of stressors, or by subjecting Mtb to antibiotics, Saito et al. (2017) and (Loraine et al., 2016) respectively, were able to generate DCTB *in vitro*. This will be discussed in detail later in the context of conditions that mimic nutrient deprivation and stress, detailed further next.

2.6.1. Hypoxia

One of the main components of the granuloma is hypoxia, or the steady reduction of oxygen (Guirado and Schlesinger, 2013). The caseous regions inside granulomas, non-destructive

infiltrative foci and macrophages, where Mtb lives is characterized by low oxygen concentrations (Via et al., 2008). There have been several *in vitro* models that attempt to mimicking hypoxia.

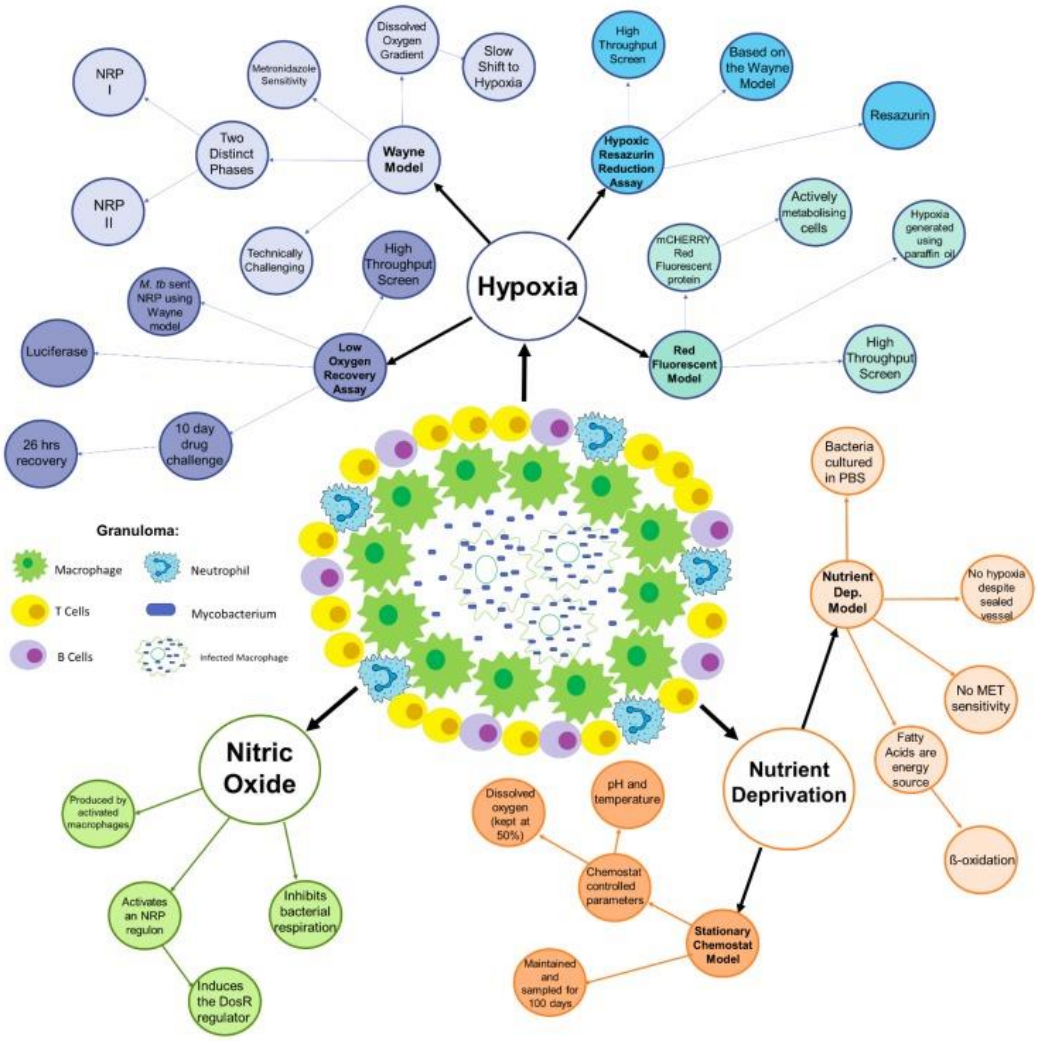

Figure 2.1. A summary diagram of the *in vitro* models of Non-Replicating Persistent or dormant Mtb categorised by the granuloma condition it models. There are various hostile conditions encountered by Mtb *in-vivo* in the host. Mtb enters the host via inhalation, the first encounter *in-vivo* is with the immune cells: the macrophages which phagocytose and attack Mtb with their ammunition like low pH, hydrolases, and free-radicals. Further, it progresses into a larger immune structure: the granuloma. During the process, the other stresses in the granuloma, especially in the caseating/ necrotizing lesions are the gradually decreasing levels of O_2, Nitrogen, Carbon, representing hypoxia, the arrest of various biosynthesis processes and poor nutrition nearly close to starvation. This image was taken from (Gibson et al., 2018).

The Wayne model is widely recognized as a turning point for the field with respect to *in vitro* models of non-replicating persistence that are based on hypoxia. It entails culturing Mtb in sealed tubes while gradually depriving bacteria of oxygen, resulting in a two-step transition to non-replicating persistence (NRP), referred to as NRP1 and NRP2 (Wayne, 1976). When oxygen saturation in the medium reaches 1%, the first stage—which the authors refer to as the

microaerophilic stage—begins. It is characterized by a delay in Mtb replication, as well as a slowing in the replication of nucleic acids and an increase in the amount of adenosine triphosphate (ATP) in bacterial cells. Anaerobic stage begins when oxygen saturation levels drop below 0.06%. Under these circumstances, Mtb replication stops, and glycine dehydrogenase concentration drops considerably (Wayne and Hayes, 1996). Additionally, there is a considerable increase in the Mtb nitrate reductase activity at the microaerophilic stage (Wayne and Hayes, 1998). As a result, non-replicating bacilli are created, which are intended to resemble those present in the hypoxic environment of the granuloma. Some adaptations of the Wayne model showed how hypoxia plays a part in the formation of Mtb dormancy *in vitro* in other studies (Rustad et al., 2008). A rapid anaerobic dormancy model was created by (Leistikow et al., 2010). An Mtb mutant that was unable to express the DosR regulon genes was one of the experimental strains that was used. By days 10 and 20 of anaerobic incubation on agar media, the capacity of the mutant strain to regain its growth was diminished by 58 and 88% respectively in comparison to the wild-type strain. Based on these and other studies, the importance hypoxia has been investigated in several studies. Hypoxia is also included in certain combination models of stress (Leistikow et al., 2010).

2.6.2. Nutrient Deprivation

Mtb encounters a shortage in the supply of nutrients necessary for its metabolism and proliferation when inside macrophages in the relatively secluded phagosomes (Batyrshina and Schwartz, 2019). Granuloma-derived Mtb differs in terms of morphology from those developed *in vitro* using standard culture, whereas nutrient-starved Mtb resembles the *in vivo* phenotype (Nyka, 1974). This would imply that nutrient deprivation is a crucial environmental factor in the granuloma, that results in substantive metabolic reprogramming in bacteria *in vivo*, which could be further compounded with hypoxia triggered gene expression/reprograming to produce the clinical phenotype (Li et al., 2002, Griffin et al., 2012). As a result, several microbiological models mimic Mtb nutrient deprivation.

In 1933, Loebel et al. (1933a), (Loebel et al., 1933b) demonstrated that Mtb consumed less oxygen when grown for a prolonged period of time in nutrient-free medium or in the presence of high hydrogen ion concentrations. It was also shown that mycobacterial cultures lose their ability to grow after being exposed to anaerobic conditions for 3 to 15 days in both culture medium and phosphate buffered saline (PBS). As a result of the capacity of bacteria to reduce oxygen consumption and continue to survive off nutrients that were stored from previous

rounds of replication, Loebel and colleagues concluded that Mtb was capable of withstanding prolonged nutrient deprivation which contributes to virulence. Subsequent models later provided evidence that this hypothesis was accurate. Based on Loebel's prior study, Betts and her colleagues developed a model that would inhibit respiration and proliferation, yet leave the bacteria alive (Betts et al., 2002). In their model, bacteria are harvested and re-suspended in PBS after growing for 7 days in nutrient-rich media. They are kept in airtight containers and incubated at 37 °C. CFU counts at successive points were used to estimate viability. This approach demonstrated that CFU counts remained constant throughout these conditions, despite no growth at any stage, demonstrating that the non-replicating state had been reached. Moreover, they showed that methylene blue does not decolorize while Mtb was cultured in sealed containers, similar to the Wayne model. Methylene blue in this case served as an indicator for oxygen availability and the fact that it did not decolorize confirmed that oxygen was still available in the cultures. This gave rise to the theory that the bacilli entered the non-replicating state by slowing their respiration rates, thus consuming less oxygen in contrast to the Wayne model (Wayne and Hayes, 1996). According to this non-replicating model, Mtb develop resistance to INH and RIF but they do not become more sensitive to Metronidazole (MET). Additionally, variation in gene expression related to nutrient deprivation was also noted. Whilst these models have proven to be useful to probe mycobacterial biology, they share the same shortcoming in that they only include one stress, without considering all the physiological circumstances within the granuloma. Subsequent models have attempted to address this using combinations of stressors.

As an example, an *in vitro* model for generating DCTB was established, which consists of two sequential stresses: Mtb starvation in PBS for at least two weeks and antibiotic exposure to RIF for at least 2 days (Saito et al., 2017). Longer periods of starvation did not affect recovery of DCTB and exposure to RIF resulted in an increase in the fraction of DCTB. RIF could be utilized at lower dosages for longer periods of time. Based on these findings, the authors hypothesized that RIF induces the DC phenotype by selectively affecting the transcription of certain genes, as opposed to completely stopping transcription in starving Mtb. This model formed the basis of the work conducted in this chapter.

Recently, Batyrshina and Schwartz (2020) analysed the impact of nutrient depletion on Mtb culture as a potential dormant phenotypic inducer. They grew the Mtb laboratory strain for 30 days in Middlebrook 7H9 medium without albumin, dextrose, sodium chloride, or catalase. They assessed Mtb's growth capacity daily by optical density (OD) and CFU. The propensity

of bacilli to resuscitate was assessed upon reintroduction of nutrients into 7H9 medium. Reduction in growth in nutrient-deficient medium was observed as early as the second day of Mtb incubation. After 2-3 days of incubation, CFU numbers was also reduced. The capacity of Mtb to proliferate was completely abrogated after 4 days of starvation. Following this, Mtb was able to resuscitate on liquid and solid media. This model for generating the dormant Mtb phenotype can be utilized as a novel *in vitro* method to explore dormancy and its molecular factors, including examining the sensitivity of dormant Mtb to antibiotics.

2.6.3. Nitric Oxide

It is known that the host's capacity to create NO through an inducible nitric oxide synthase (iNOS) affects immunity to TB (Mishra et al., 2013) and microbial physiology (Voskuil et al., 2003), regulating a variety of illnesses (Nathan and Shiloh, 2000), such as TB (MacMicking et al., 1997). TB infected Macrophages residing within TB lesions in humans and macaques produce functional iNOS, confirming the importance of nitric oxide in controlling mycobacteria growth (Nicholson et al., 1996, Mattila et al., 2013). Furthermore, exhaled breath from TB-infected individuals carries detectable amounts of NO (Wang et al., 1998). NO is produced by activated macrophages as a signalling molecule and an effective antimicrobial agent (Nathan and Ehrt, 2004). Additionally, the suppression of bacterial and mitochondrial respiration has also been linked to NO (Brown, 2001). According to earlier studies, Mtb uses the DosR/S/T system to produce transcriptional alterations, stop growth, and a transition from aerobic to anaerobic respiration in response to NO stress (Sardiwal et al., 2005, Kumar et al., 2007). Although other gases, such as carbon monoxide and oxygen limitation, similarly activate the DosR pathway (Park et al., 2003, Shiloh et al., 2008), the NO-mediated activation of the DosR regulon is temporary (Cortes et al., 2017).

In murine studies, it was shown that Mtb-infected iNOS knockout and immunodeficient mice have a markedly increased risk of death as compared to the control mice. In the spleen, Mtb growth was noticeably increased, but less pronounced in the lungs until later in the infection. When activated, iNOS knockout mice macrophages produced reactive oxygen intermediates (ROI) but did not produce reactive nitrogen intermediates (RNI) and were unable to control Mtb infection (Adams et al., 1997). Contrary to the murine TB model, there has been debate concerning the role NO plays in killing and inhibiting Mtb in humans (Nathan and Shiloh, 2000). It has been demonstrated that human alveolar macrophages can limit mycobacterial growth at an early stage without the need for NO. In particular, human alveolar macrophages

exposed to exogenous IFN-γ failed to exhibit mycobactericidal activity in after infection with H37Ra associated with that of BCG. (Aston et al., 1998).

Regardless of NO detected in exhaled breath, there appears to be difference in people living with HIV where reduced exhaled NO levels have been linked to HIV infection. Whilst HIV-TB coinfected individuals had lower levels of NO, they had significantly higher urinary NO metabolites levels (Idh et al., 2008). More recently, a cross sectional study by Sovershaeva et al. (2019) looked at the connections between exhaled nitric oxide, HIV status, and abnormalities of the airways in perinatally HIV-infected children aged 6 to 19 years. They found that exhaled NO levels decreased in correlation with HIV status. Additionally, it was demonstrated that history of prior TB was linked to lower exhaled NO levels in the HIV-infected group. Together, these findings confirm that NO plays a critical role in the human host response to Mtb infection.

2.7. Other *in vitro* models of dormancy

There are other models of dormancy that have been developed and summarised in **Table 2.1**. The model that most closely resembles Mtb during chronic infection in humans is difficult to predict, and these multiple models may represent distinct metabolic states at different phases of infection.

In this work, we set out to investigate whether DCTB induce distinct immune responses when compared to conventionally culturable bacteria. For this, our first task was to select the best model to generate DCTB. In considering all the previously described models, we opted to use the model developed by (Saito et al., 2017) with modifications, discussed later. Our hypothesis and aims are described in the next section.

Table.2.1: *Mycobacterium tuberculosis* dormancy models frequently used *in vitro*.

Model	Description	Reference
Hundred-day static culture	Extended stationary phase culture without agitation and development of rifampicin tolerance.	**(Hu et al., 2006)**
Chemostat culture system	Adaptation to stationary phase by carbon deprivation and growth under specified condition.	**(James et al., 2002)**
In vitro granuloma model	Lung myofibroblasts and a fresh peripheral blood mononuclear cell mixture were combined with a *Mycobacterium bovis* BCG strain containing the luciferase gene to create a granuloma.	**(Puissegur et al., 2004)**
Hypoxic resazurin reduction assay	Culture dilutions are placed in vacutainer tubes, and then they are examined visually after a redox indicator is added.	**(Taneja and Tyagi, 2007)**
Low-oxygen recovery assay (LORA)	H37Rv that has been modified to express the dormancy luciferase gene from *Vibrio harveyii.*	**(Cho et al., 2007)**
Nitrate reductase assay (NRA)	The basis of NRA is the idea that *Mycobacterium tuberculosis* has the ability to convert nitrate to nitrite. Griess reagent is used to detect the presence of nitrite which changes the colour of the culture medium when nitrite is available.	**(Montoro et al., 2005)**
Biofilm model	*Mycobacterium tuberculosis* develops biofilms that have unique environmental and genetic requirements from those for planktonic growth and contain a significant drug-tolerant population that endures despite being exposed to high levels of antibiotics.	**(Ojha et al., 2008)**
Potassium depletion model	*Mycobacterium tuberculosis* growth in potassium-deficient medium under aerobic circumstances produced bacilli that were non-culturable on solid media but detectable in liquid media.	**(Salina et al., 2014)**

2.8. Hypothesis, Aim and Objectives of the study

2.8.1. Hypothesis

We hypothesized that nutrition deprivation-induced non-replicating Mtb promotes a bacterial form that differs from exponentially growing Mtb, which will have a distinct effect on the immune response, when measured by a select set of cytokines.

2.8.2. Aim

To determine the *in vitro* cytokine response to DCTB created from different clinical strains used to infect whole blood from healthy donors.

2.8.3. Objectives

Specific objectives were to:

- Assess the growth properties of clinical isolates from Lineage 2 (Beijing) and Lineage 4 (LAM).
- Generate DCTB from five representatives of these selected clinical strains.
- Recruit healthy donors to obtain blood for the whole blood assay.
- Use the DCTB generated above to infect blood from healthy donors.
- Design the bead array of selected cytokines based on the profile of cytokines associated with TB infection.
- Determine whether there are differences in the cytokine response induced by DCTB when compared to culturable bacteria.

2.9. Preliminary data supporting our approach

In prior work from our lab, the DCTB model developed by (Saito et al., 2017) was evaluated for its suitability to generate DCTB populations that mimic sputum specimens [work done by MSc Student Kiyasha Padarath – (Padarath, 2020)]. In this work, it was demonstrated that addition of RIF to starved cultures resulted in a substantive reduction in bacterial viability when using *Mycobacterium smegmatis* as a model system, **Figure 2.2B and C**.

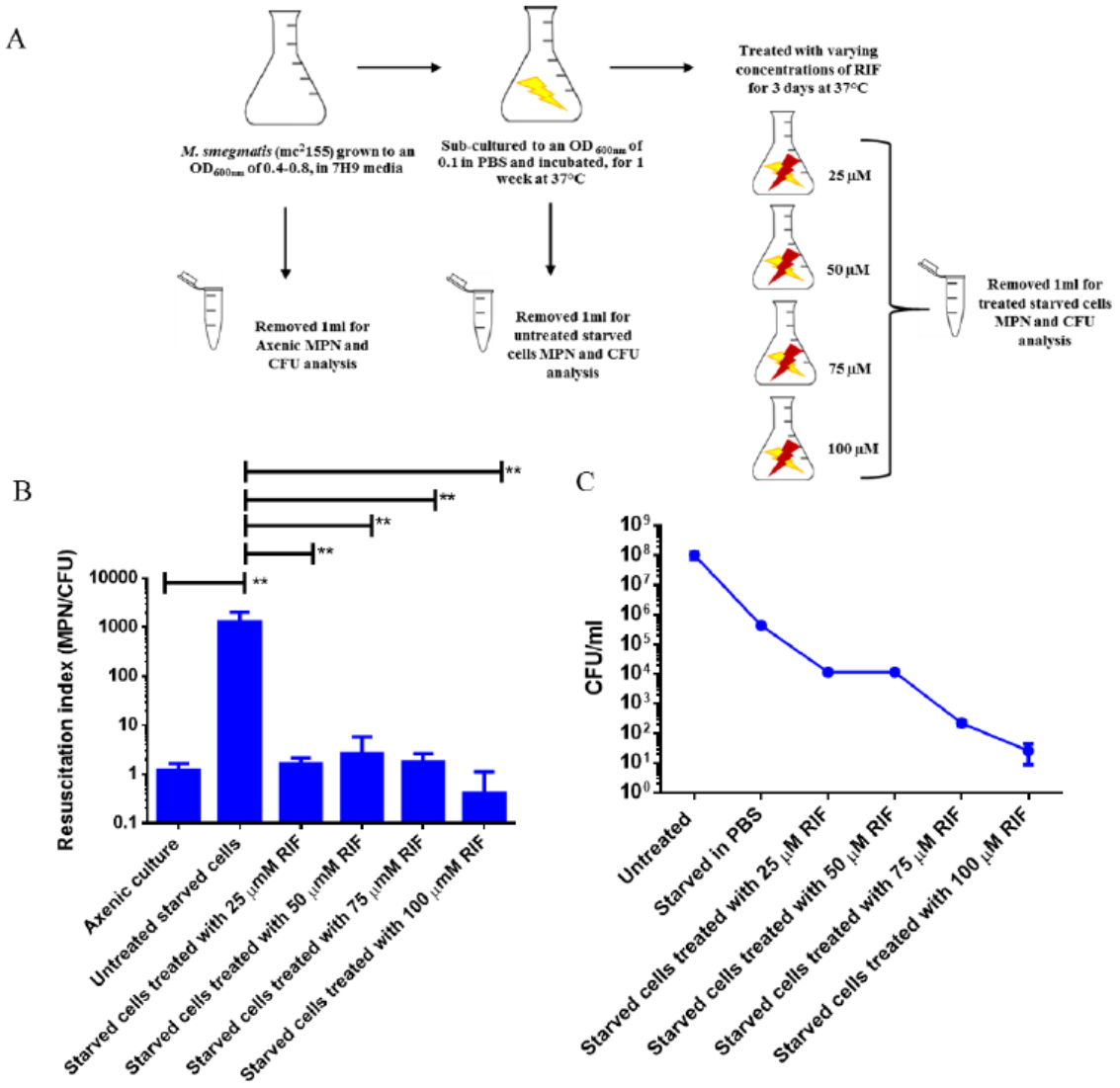

Figure 2.2. The effect of Rifampicin (RIF) on survival of DCTB in an *in vitro* model of starvation. (A) Shown is the schematic workflow for generation of DCTB involving carbon starvation, followed by treatment with different concentrations of RIF. (B) Resuscitation of DCTB, as measured by the MPN (most probably number), normalized by CFU. (C) Survival of bacteria during treatment with RIF. Figure taken from (Padarath, 2020).

Based on these findings, an Mtb model of nutrient starvation was used to generate DCTB. This approach led to generation of significant levels of DCTB when Mtb H37Rv was passaged through a similar system.

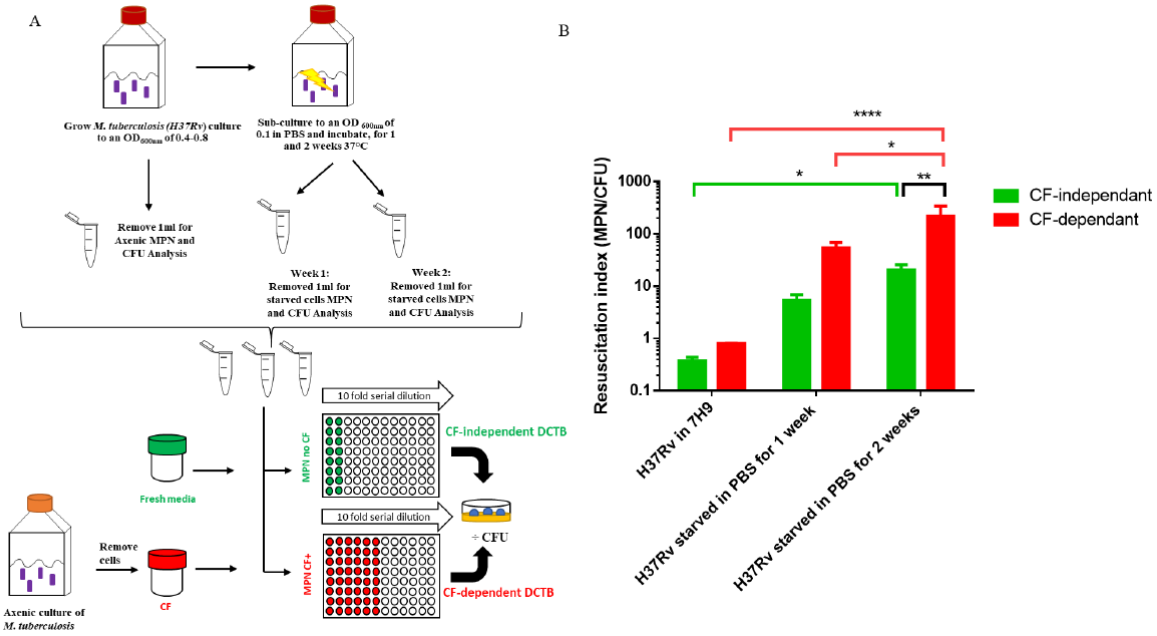

Figure 2.3. Generation of DCTB in Mtb using nutrient starvation. (A) Schematic workflow for generation of DCTB which involve culturing bacteria in carbon replete media (7H9), followed transfer to Phosphate buffered saline (PBS) and incubation for 1 and 2 weeks. After this, bacteria were subjected to resuscitation using the MPN (most probable number) limiting dilution assay with culture filtrate (CF) as a source of growth stimulatory factors. Resuscitation of DCTB was measured by normalising the (MPN) value by the CFU count. Culture in carbon replete media was used a control for the measure of DCTB. Ideally, under these conditions no, or minimal, DCTB populations should be detected. (B) Quantification of DCTB from MPN and CFU assays. Taken from (Padarath, 2020).

Incubation of Mtb under starvation conditions for two weeks yielded the greatest quantum of DCTB, **Figure 2.3B**. Based on this, we opted to use a two-week incubation period. We also tested a variation of this model where instead of using PBS, strains were incubated in 10% 7H9 routine media (to stimulate nutrient deprivation). This diluted media was also adjusted to a pH=5, to stimulate acid stress.

The effect of strain type was also examined. The global TB epidemic is driven by a diverse collection of strains that have phylogeographically evolved with human populations. There is evidence for certain strains appearing to have better success in the human host (summarized in (Peters et al., 2020). In particular the Beijing lineage (which is located in the broader Lineage 2 classification) has been associated with increased transmissibility, increased mortality, induction of drug resistance and increased pro/anti-inflammatory cytokines (summarized in (Peters et al., 2020). Similarly, Latin American (LAM) strains (which are located in the broader Lineage 4 classification) have been associated with increased apoptosis, an elevated oxidative burst, increased expression of pro-inflammatory cytokines and increased transmissibility (summarized in (Peters et al., 2020). Based on these findings, we selected five Beijing and five

LAM strains have were collected in prior studies (Chengalroyen et al., 2016, Peters et al., 2023). Preliminary data from our lab confirmed that other representative strains from these lineages were able to adopt the DCTB state (Padarath, 2020).

Collectively, these preliminary data provided the framework for work done in this chapter. In addition to the clinical isolates, the laboratory strain H37Rv was used as a control.

2.10. Methods for DCTB assay

2.10.1. Bacterial strains cell culture

To prepare pre-cultures, 1 mL of frozen stock culture (OD_{600nm}=0.6 to 0.9) of the different bacterial lineages (H37Rv, Beijing and LAM) were added to 8 mL of 7H9 Middlebrook media containing 0.2% glycerol, 0.02% tyloxapol and 10% OADC (oleic acid, bovine albumin, dextrose, catalase) in 50 mL tissue culture flasks. The cultures were then incubated at 37 °C for 3 days, then transferred to a 550 mL culture flask, where they reached an OD_{600nm} of 0.6 to 0.9.

2.10.2. Starvation model assay for DCTB generation

The population of DCTB of laboratory (H37Rv) and clinical strains was generated using the carbon starvation stress model as described by (Saito et al., 2017) with some modifications. H37Rv laboratory strain was included as an appropriate control. Bacterial cells grown to an OD_{600nm} of 0.4– 0.8 were washed twice with phosphate buffered saline (PBS) (pH 7.4, modified without calcium chloride and magnesium chloride (Sigma)) supplemented with 0.02% Tyloxapol (PBS-Tx) and centrifuged at 4000 x g for 8 minutes. To create single cell suspensions, the cultures were centrifuged at 200 x g for 8 minutes with no brake. The suspension was then diluted to an OD_{600nm} of 0.1 and incubated in PBS-Tx at 37 °C and 5% CO_2 without shaking for 2 weeks. A volume of 1 mL starved cultures after 2 weeks was removed for MPN and CFU assays. As a control, bacterial grown in standard 7H9 were used to detect DCTB, in all cases, no DCTB were detected (data not shown, the value is 0 on graphs). To further evaluate the propensity of strains to adopt the DCTB state, a variation of the carbon starvation model was used. This involved the use of diluted 7H9 media (to stimulate nutrient deprivation), adjusted to pH=5 (to stimulate acid stress). 7H9 media was diluted with distilled water at a ratio of 1:10.

2.10.3. Culture filtrate preparation

CF is a mixture of growth stimulatory factors released into the media by bacteria during growth and is used to aid in the resuscitation of DCTB (Mukamolova et al., 2010). H37Rv axenic cultures were made by inoculating a 1 mL freezer stock into 8 mL of 7H9 Middlebrook media and growing to an OD_{600nm} of 0.5. The culture was sub-cultured to 50 mL of 7H9 Middlebrook media to an OD600nm of 0.6-0.8. The culture was centrifuged for 10 minutes at 4000 x g.

Before use, the supernatant was filtered through a 0.2-m filter and diluted in a 1:1 ratio with 7H9 medium. Mycobacterial contamination was tested by spreading 100 µL of CF onto 7H11 and incubated at 37 °C and 5% CO_2 for 3 weeks. All CF preparations were freshly made on the day required.

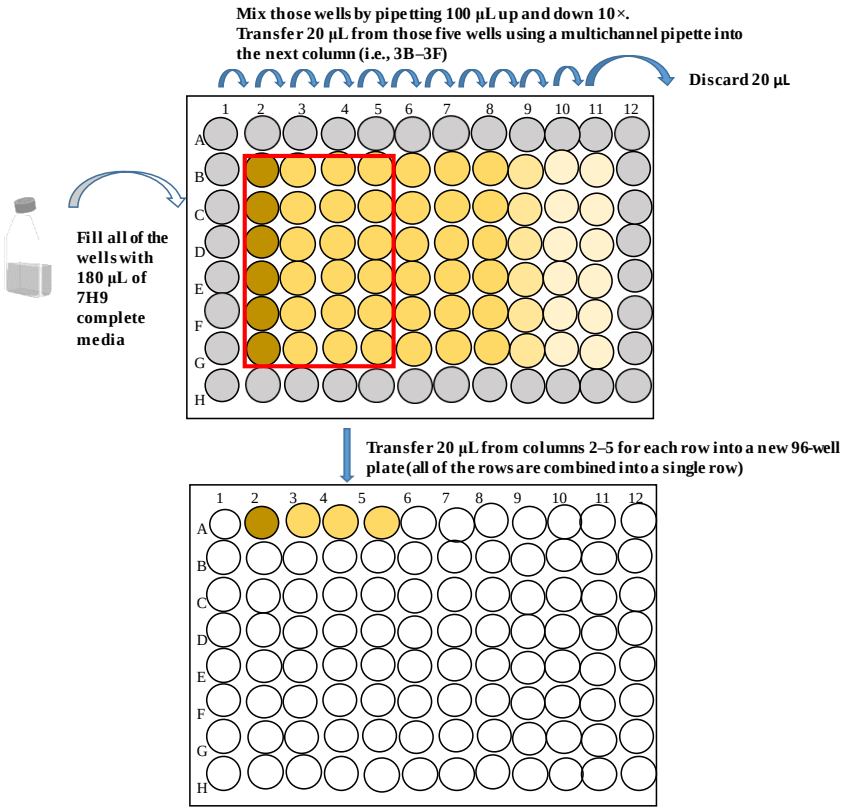

Figure 2.4. Schematic diagram for the serial dilution during generation of DCTB. Mtb is grown to log phase, stressed in PBS-Tyloxapol (PBS-Tx), and then serially diluted in complete 7H9 media until no growth is observed at the higher dilutions. For CFU counts, samples from the same dilution series (10^{-1} to 10^{-4}) are spread on 7H11 nutrient-rich agar plates.

2.10.4. MPN assay

The MPN assay was conducted in a 96-well plate. This assay measures the recovery of bacteria in liquid, using a limiting dilution to enumerate the organisms. All the wells were filled with 180 µL of 7H9 media. To this, 20 µL of starved (or control) bacteria were added to the wells labelled 2B-2G (shown in **Figure 2.4**). After mixing by pipetting 100 µL 10 times up/ down, 20 µL from these wells were transferred into the next column using a multichannel pipette. The same procedure was repeated until column 11 and after mixing in this column, the remaining 20 µL was discarded. These wells comprised the limiting dilution series to determine the MPN.

The next step after all dilutions were complete involved setting up the CFU assay. For this, 20 µL from columns 2-11 (**Figure 2.4**) for each row was transferred into a new 96-well plate for CFU plating. The dilutions plated for the control and starved samples were 10^{-5} -10^{-8} and

10^{-1}- 10^{-4}, respectively. The plates were incubated at 37 °C and 5% CO_2 without shaking for 5 weeks. After incubation, the MPN plates were scored for growth using an inverted mirror. Growth-containing wells were marked as positive. Using software (www.wiwiss.fu-berlin.de/fachbereich/vwl/iso/ehemalige/wilrich/index.html), the total number of bacteria collected from the MPN experiment was calculated. The algorithm uses the Poisson distribution of positive and negative growth incidence to determine the MPN.

2.10.5. Colony forming units (CFU) Assay

The CFU analysis was done according to a protocol described by (Saito et al., 2017) . The above-mentioned 20µl was taken from the MPN plate and transferred to a new 96 well microtiter plate. Thereafter 25µl of each dilution were then spotted and dispersed on 7H11 quarter plates in duplicates. Three biological replicates were used in the experiments.

2.10.6. Donor recruitment criteria

For collection of whole blood, a total of three healthy donors were recruited, two males and one female between the ages of 20–45 years. Ethics Approval was provided by the Wits Human Research Ethics Committee (Protocol number: M190995). The donors declared no history of latent TB infection and were not vaccinated within the last 4 weeks with live or attenuated vaccine. There were no cases of active TB. Volunteer donors gave informed written consent to collect 10 mL of blood.

2.10.7. Whole blood assay

A volume of 10 mL whole blood was collected from consenting healthy donors using heparin-coated tubes and were diluted five-fold with serum-free complete synthetic cell culture medium Roswell Park Memorial Institute Medium (RPMI 1640) and used within 2 hours. To prepare for whole blood infection with Mtb, bacterial cultures were grown and DCTB were generated as described in section 2.10.1 and 2.10.2, respectively.

2.10.8. Whole blood infection with Mtb

Mycobacterial cells previously grown in 7H9 and starved in PBS-tx were used to infect whole blood at a multiplicity of infection (MOI) of 10 (the number of bacteria were based on the OD).

Based on literature, an OD reading of 0.5 is equivalent to 1 x 10^8 cells/mL. From this culture, it was possible to calculate how much is needed to dilute to get the required number of cells for an MOI of 10. After incubation, 1 mL of the culture was added into a 1.5 mL eppendorf tube and centrifuged at 4000 x g for 15 minutes. Both control and starved culture pellets were then re-suspended in 1 mL PBS and centrifuged again at 4000 x g for 15 minutes. The pellets were then re-suspended in 1 mL RPMI for infections. To measure OD_{600nm}, bacterial cultures were diluted to a ratio of 1:10 (100 µL of the washed bacteria + 900 µL RPMI). Aliquots of 200 µL (diluted blood + bacteria at MOI of 10) were added to the designated well of 96-well flat bottom plates and for positive controls, whole blood was stimulated with 1 µg/mL of lipopolysaccharide (LPS) diluted in RPMI. Plates were incubated at 37 °C and 5% CO_2 for 12, 24, and 48 hours.

2.10.9. Harvesting plasma from whole blood

After blood infections and incubation as described above, samples were centrifuged for 5 minutes at 16 000 × g to recover plasma. Thereafter, 150 µL of plasma was carefully removed and added into 1.5 mL eppendorf tubes. To remove any remaining bacteria from plasma, samples were centrifuged again for another 3 minutes at 10 000 × g and filtered through a 0.22 µm pore size filter units. Aliquots were then pooled into 2 mL clearly labelled cryotubes and stored at –80°C.

2.10.10. Cytokines determination using Luminex multiplex immunoassay

Frozen plasma samples from whole blood infections were thawed on ice for multiplex cytokine array analysis using a Th1/Th2 panel 6-plex Luminex Bead Array Multiplex Immunoassay (ProcartaPlex™, Invitrogen, ThermoFisher Scientific), according to the manufacturer's instructions. The targets from the ProcartaPlex Hu Essential Th1/Th2 panel 6-plex are mentioned in **Table 2.2**. This assay allows for the simultaneous quantification of multiple cytokines. The kit was allowed to warm to room temperature. To prepare the antigen standards, universal assay buffer (1x) was added to lyophilized standard mix containing all 6 proteins. The standard vial was centrifuged at 2,000 xg for 30 seconds then vortexed for 10 seconds and stored on ice for 10 minutes to reconstitute. Serial dilutions (1:4) were performed for a 7 point standard curve for each target and a blank tube containing just the universal assay buffer. The magnetic bead solution was added to a 96-well plate using a multichannel pipette. The plate was securely inserted into the hand-held magnetic washer and the beads were allowed to accumulate at the bottom of the plate. After 2 minutes, the liquid was removed by inverting the

hand-held magnetic plate washer and wash buffer (1x) was added into each well to wash the beads. The 96-well plate was removed after the washing step and universal buffer was added to each well, followed by prepared standards and plasma samples into their dedicated wells. The plate was then covered with a plate seal and black lid and incubated for 120 minutes in a shaker at 500 rpm. After incubation, the plate was washed twice with wash buffer (1x), followed by addition of detection antibody mixture and incubated for 30 minutes at 500 rpm shaking. This was followed by another wash with wash buffer (1x) then Streptavidin-PE was added and the plate was incubated for 30 minutes at 500 rpm shaking. The plate was then washed twice with wash buffer (1x) then reading buffer was added and incubated at 500 rpm shaking for 5 minutes. The plate was the read on a Bio-Rad™ Luminex instrument. One biological sample was used for each patient at different time points as this assay is highly sensitive and reliable.

Table 2.2: Standard curve concentration for each target (lot-specific) in the ProcartaPlex Immune Monitoring Th1/Th2 panel 6-plex.

Analyte (Bead region)	Standard 1 (pg/mL)
IFN-gamma (43)	41400
IL-12p70 (34)	33500
IL-4 (20)	54800
IL-5 (21)	37900
IL-6 (25)	41700
TNF-alpha (45)	28900

2.10.11. Data analysis

The concentration of each cytokine was determined by the Bio-Plex analysis software on the Luminex instrument. This was done by plotting the expected concentration of the standards against the Mean fluorescence intensity (MFI) generated by each standard. A 5PL algorithm was chosen for the best curve fit. For each analyte, calculated concentration values are reported and data were recorded as "<" for out of range (OOR) values. These were assigned zero for statistical analysis as they were below the limit of detection. The concentration for IL-4 was undetectable in all conditions at all the time points.

2.10.12. Statistical analysis

Statistically significant differences among the groups were determined using two-way ANOVA and Tukey Post-hoc tests. The data in the graphs are expressed as the mean ±SEM (Standard error of the mean). Values were considered significantly different when $p<0.05$.

2.11. Quantification of DCTB between different bacterial strains

2.11.1. Growth kinetics of Mtb laboratory (H37Rv) and clinical strains

To generate DCTB, prior culture in standard 7H9 media was required. To ensure that bacteria were able to grow under these conditions, the growth rates of LAM and Beijing clinical isolates in 7H9 media were compared to the laboratory strain H37Rv. As shown in **Figure 2.5A**, LAM strains grew at a similar rate as H37Rv, except for L3816, which grew at a slower

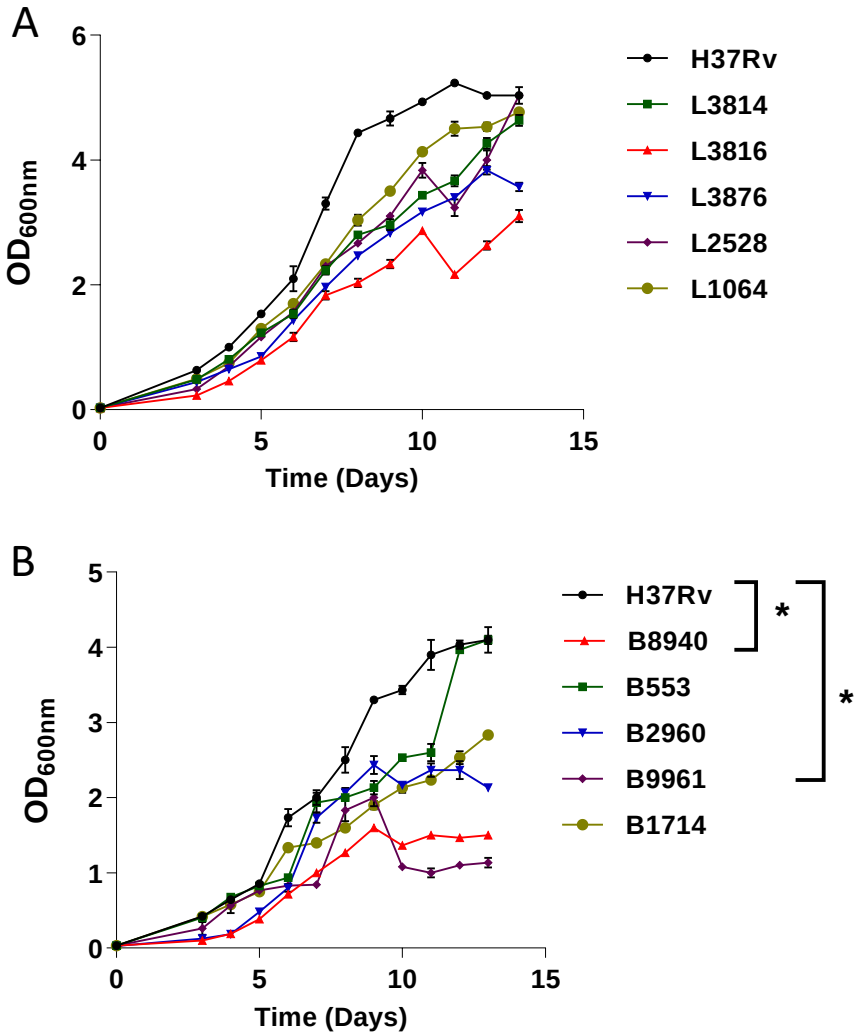

Figure 2.5. Growth kinetics of H37Rv, Beijing and Lam strains. Growth kinetics of the 5 Beijing and LAM strains compared to H37Rv, showing that most of Beijing strains have a much slower growth rate to H37Rv. Data are representative of three independent experiments *P <0.01; **P < 0.001.

than H37Rv, **Figure 2.5A**. Beijing strains (B8940 and B9961) grew at a significantly slower rate compared to H37Rv, **Figure 2.5B**.

The differences noted in growth of clinical strains would not affect the generation of DCTB as in our model, bacteria are harvested at an OD of ca. 0.5. At this cell density, there was no difference in the growth of all isolates used.

2.11.2 The propensity of clinical isolates to adopt the DCTB state

The schematic workflow for generating DCTB is shown in **Figure 2.6**.

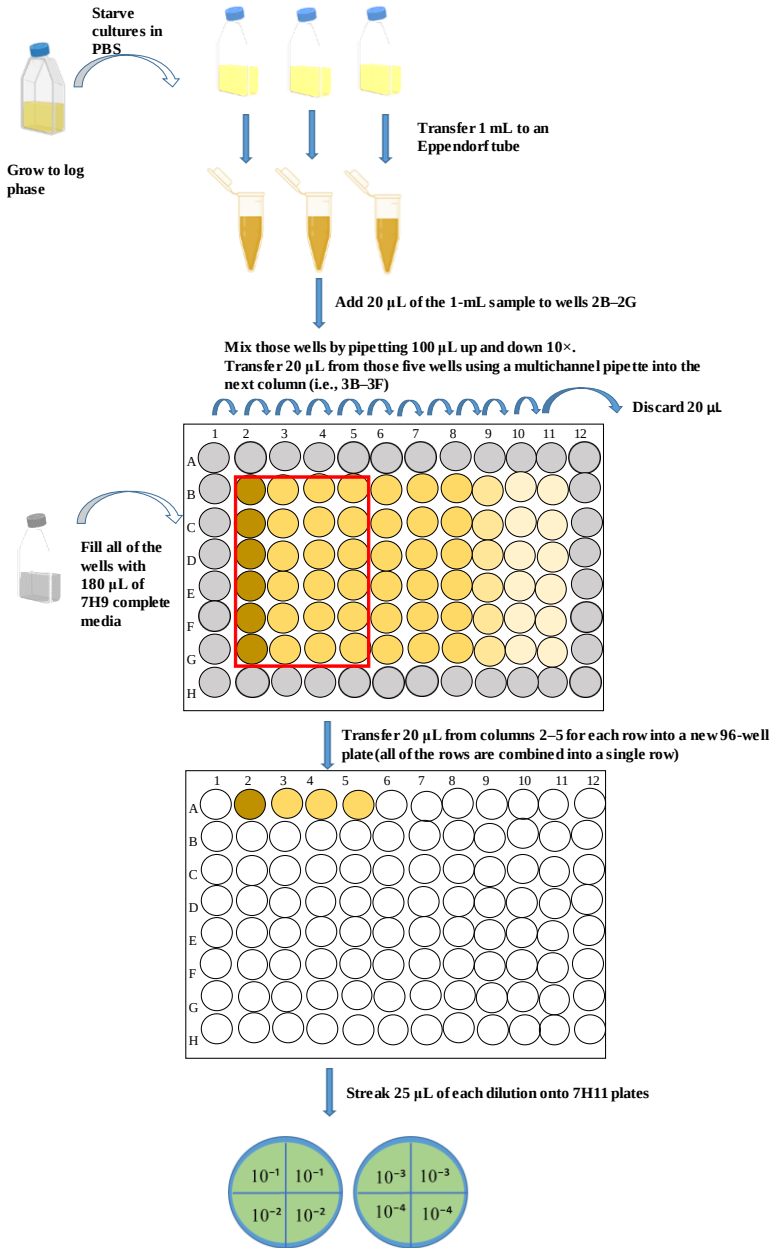

Figure 2.6. Schematic diagram for the generation of DCTB. Mtb is grown to log phase, stressed in PBS-Tyloxapol (PBS-Tx), and then serially diluted in complete 7H9 media until no growth is observed at the higher dilutions. To count CFU's, samples from the same dilution series (10^{-1} to 10^{-4}) are spread on 7H11 nutrient-rich agar plates.

Similar to how it was done (Padarath, 2020), we first looked into the effect of RIF on starving *Mycobacterium smegmatis*. The PBS-starved cells were treated with 100 µM RIF and 1% DMSO. We observed, a 4-log difference in the number of cells in the MPN as compared to the CFU in PBS-starvation, DMSO treatment also affected cell survival but there was still a 2 log difference between MPNs and CFUs. There were no colonies on plates of RIF-treated cells, but some cells showed phenotypic resistance as growth was seen in the MPN wells, shown in **Figure A1** in appendix A.

Success with generating DCTB was measured by the presence of a significant difference in bacterial viability between MPNs (with or without CF) and CFUs. Based on this criterion, there were no DCTB detected with the H37Rv laboratory strain, **Figure 2.8** panels A and B. With respect to LAM strains, L3814 and L3876 yielded significant differences between MPN and CFUs, confirming the presence of DCTB. There was no difference in recovery of DCTB without CF. With respect to Beijing isolates, B2960 and B9961 were able to generate DCTB. In the case of B 9961, no CFUs were detected indicating that the entire bacterial population had shifted to the DCTB state. For B2960, there was reduction in recovery of DCTB without CF, but this difference was not statistically different. By comparing bacterial recovery in the DCTB assay with or without CF, in Beijing strains, B2960 yielded the most DCTB, without CF (**Figure 2.7C**). There was no significant difference in DCTB recovery between LAM strains.

To further evaluate the ability to generate DCTB, a variation of the carbon starvation model was used, involving the use of 10% 7H9 media (diluted in distilled water, adjusted to a pH=5). We tested this to evaluate whether variations in the model would yield significantly different profiles between the clinical isolates. In this model, the control H37Rv strain yielded DCTB counts, **Figure 2.8A** and **B**. With respect to LAM isolates, L3814 and L3876 were able to generate DCTB, as measured by significant differences between MPNs and CFUs. The remaining isolates did not generate appreciable amounts on DCTB. Regarding Beijing strains, B1714 generated DCTB, whereas the other strains did not generate DCTB. B553 is not represented in these experiments as the strain was not able to grow in this instance. It is unclear why this occurred, but repeated attempts did not improve growth.

After generating DCTB using these two approaches, we set about selecting strains for use in the whole blood assay for measuring the ability of DCTB to stimulate immune responses. For LAM strains, the standard carbon starvation experimental approach yielded DCTB for

L3814 and L3876. The modified assay, with acidified media yielded the same effect. Hence, for LAM strains, between L3814 and L3876, L3814 was arbitrarily selected. For Beijing strains, the standard assay yielded DCTB for B2960 and B9961. With the modified

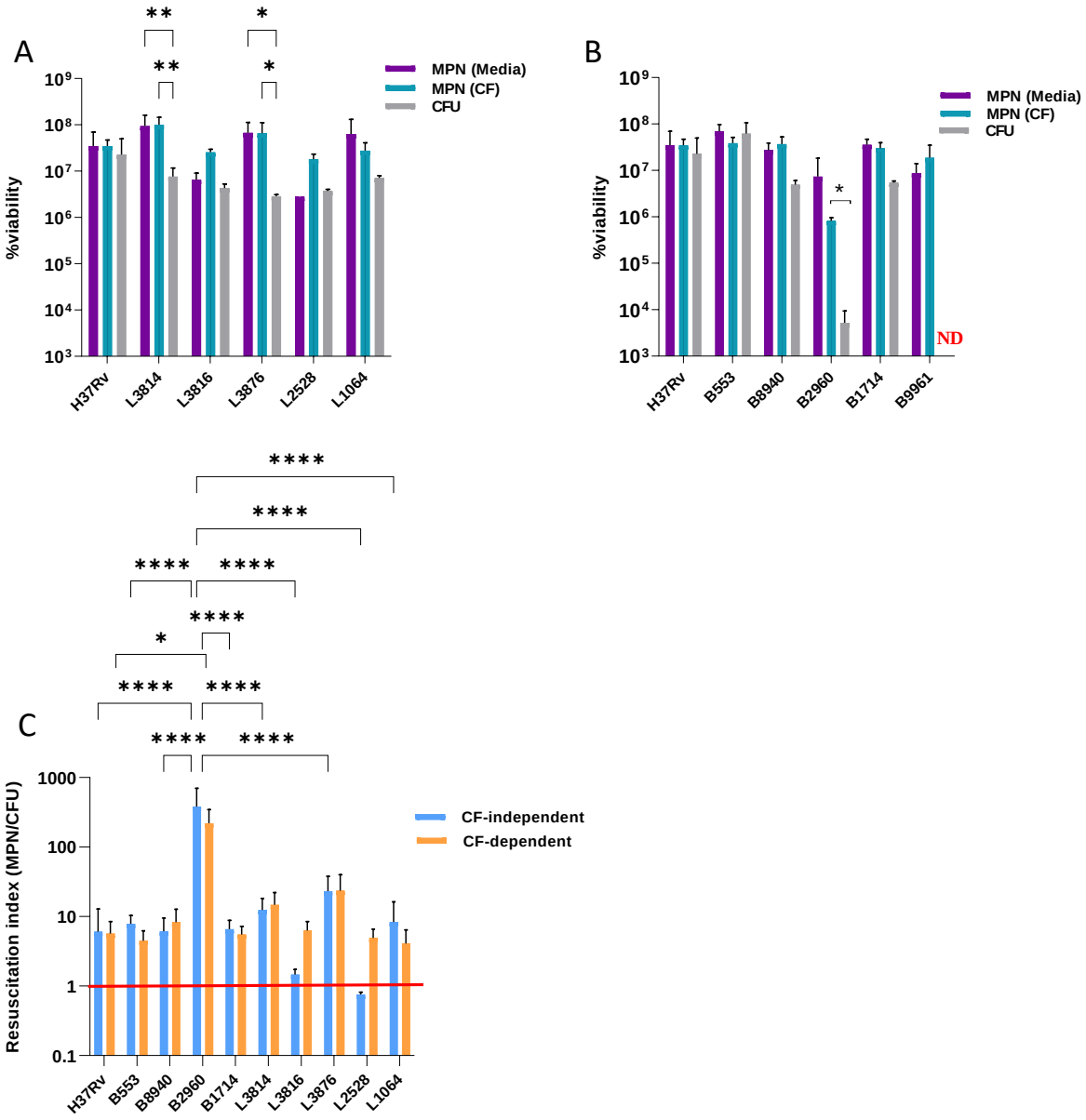

Figure 2.7. The susceptibility of carbon starved clinical strains to assume the DC state. H37Rv, Beijing and LAM strains starved in PBS for 2 weeks were compared to each other. The bacteria were resuscitated with media and media supplemented with Culture filtrate (CF), in a 96 well plate. (A) Percentage viability of LAM strains were compared between the different growth conditions [Most probable number (MPN) and Colony forming units (CFU)] using two-way ANOVA. (B) Percentage viability of Beijing strains were compared between the different growth conditions (MPN and CFU) using two-way ANOVA. (C) Resuscitation index was calculated using MPN/CFU ratio. The effect of CF in all strains was compared using a two-way ANOVA. Data are means for three replicates *P <0.01; ****P < 0.0001.

assay, DCTB were recovered for B1714. We also noted some differences in the ability of Beijing and LAM strains to adopt CF-dependent/independent DCTB, **Figure 2.8C**. We opted to select a strain from the original carbon starvation model, as this is most widely used in the field. Within this model, we opted for B2960, as the complete lack of recovery of B9961 on CFUs was concerning and could be related to some inherent defect in the strain. As we had no explanation for this, and considering that the complete loss of CFUs was not seen with this strain in the acidified media, the selection of B2960 seemed the most rational course of action.

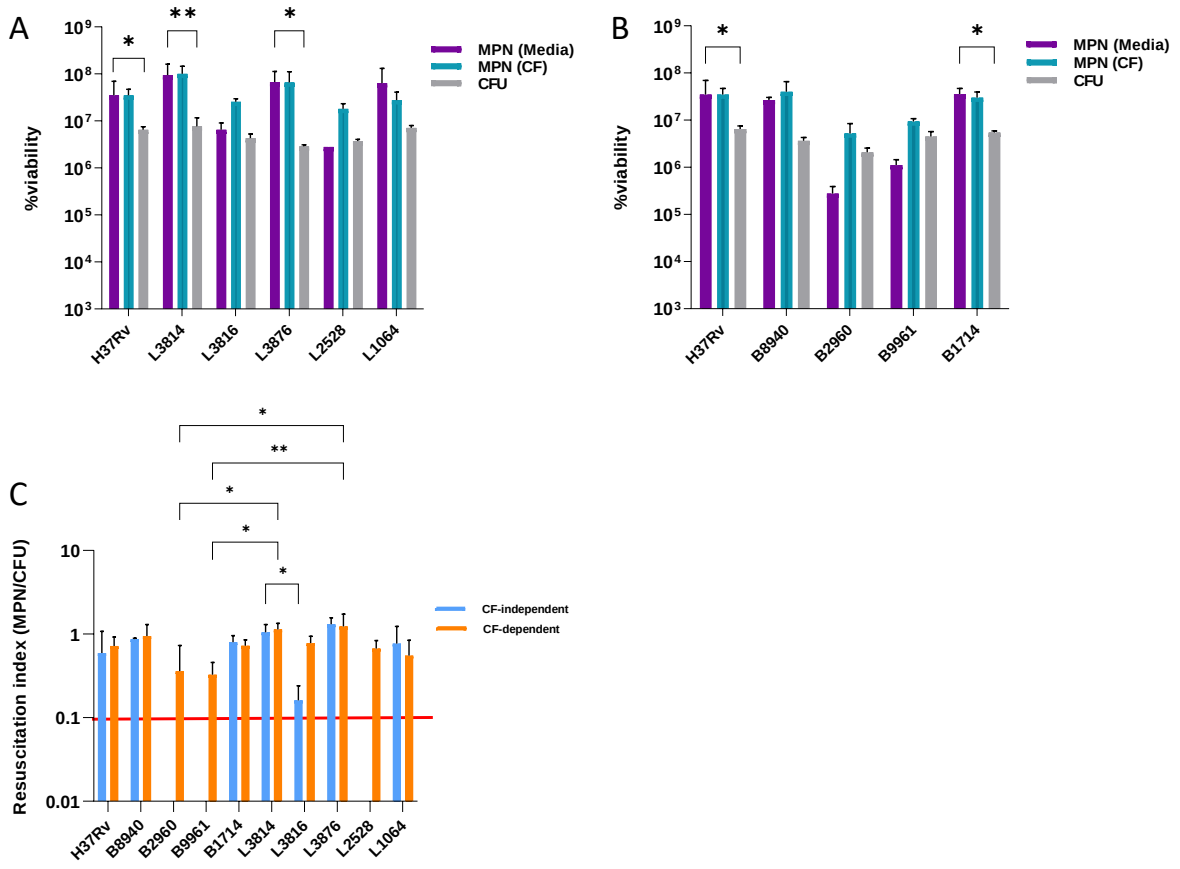

Figure 2.8. The susceptibility of starved clinical strains in nutrient-limited acidic conditions to assume the DC state. H37Rv, Beijing and LAM strains starved in 10% 7H9 a pH 5 for 2 weeks were compared to each other. The bacteria were resuscitated with media and media supplemented with CF, in a 96 well plate. (A) Percentage viability of LAM strains were compared between the different growth conditions (MPN and CFU) using two-way ANOVA. (B) Percentage viability of Beijing strains were compared between the different growth conditions (MPN and CFU) using two-way ANOVA. (C) Resuscitation index was calculated using MPN/CFU ratio. The effect of CF in all strains was compared using a two-way ANOVA. Data are means for three replicates *P <0.01; ****P < 0.0001.

2.12. Production of Th1/Th2 cytokines in blood samples infected with actively growing and starved DCTB

2.12.1. Effect of actively growing Mtb infection on pro-inflammatory cytokine production

We compared the capacities for cytokine production in whole blood between three strains of bacteria (H37Rv, LAM [L3814] and Beijing [B2960]) grown to log-phase. The concentrations of cytokines (IFN-γ, IL-4, IL-5, IL-6, IL-12p70 and TNF-α) in plasma were measured for 0, 12, 24, and 48 hours post-infection and shown in **Figure 2.9**. Beijing infection at 12 hrs did not induce any IFN-γ production (**Figure 2.9A**). At later time points, IFN-γ was detected but there was no significant difference between the clinical isolates and when compared to the laboratory strain.

The Th2 cytokine IL-5, was detected at all the time points but found to be significantly higher at 12 hrs in LAM [(116.79±10.94 pg/ml) compared to Beijing (63.43±26.15 pg/ml), p= 0.0242] and also at 48 hrs LAM [(106.46±10.17 pg/ml) compared to Beijing (59.28±12.15 pg/ml), p= 0.0482], **Figure 2.9B**. For IL-6, the mean concentration this Th1 cytokine was significantly increased only at 12 hrs in the LAM strain (4677.31±1461.94 pg/ml) compared to the mean values observed in the Beijing strain (1747.64±867.91 pg/ml, p=0.0296), **Figure 2.9C**. Whilst being detected at the other time points, no difference in the abundance of this cytokine was noted between strains. None of the strains were able to induce the production of IL-12p70, as seen in **Figure 2.9D**.

TNF-α concentrations were significantly higher at 12 hrs in H37Rv [(2294.63±785.54 pg/ml) compared to Beijing strains (1073.74±161.35 pg/ml), p=0.0486]. The concentrations of TNF-α were significantly higher in LAM infected group at 24 hrs (3447.69±457.82 pg/ml) compared to H37Rv infected group [(1819.42±1068.18 pg/ml), p= 0.0081] and 48 hrs in LAM [(2586.96±581.02 pg/ml) compared to H37Rv (1092.08±728.62 pg/ml), p= 0.0148]. There was an increase in the concentrations of TNF-α in the LAM infected cells at 24 hrs (3447.69±457.82 pg/ml) compared to the Beijing infection [(1207.48±18.69 pg/ml), p= 0.0005] and 48 hrs in LAM [(2586.96±581.02 pg/ml) compared to Beijing (836.99±168.92 pg/ml), p= 0.0047]. This was also true for LAM at 12 hours. Unstimulated blood showed an expression of IL-5 (34.96±60.55 pg/ml), IL-6 (1716.70±2973.41 pg/ml), IL-12p70 (3.83±6.63 pg/ml) and TNF-α (875.57± 1516.53 pg/ml) before infection. LPS stimulation demonstrated the capacity to promote the production of all cytokines.

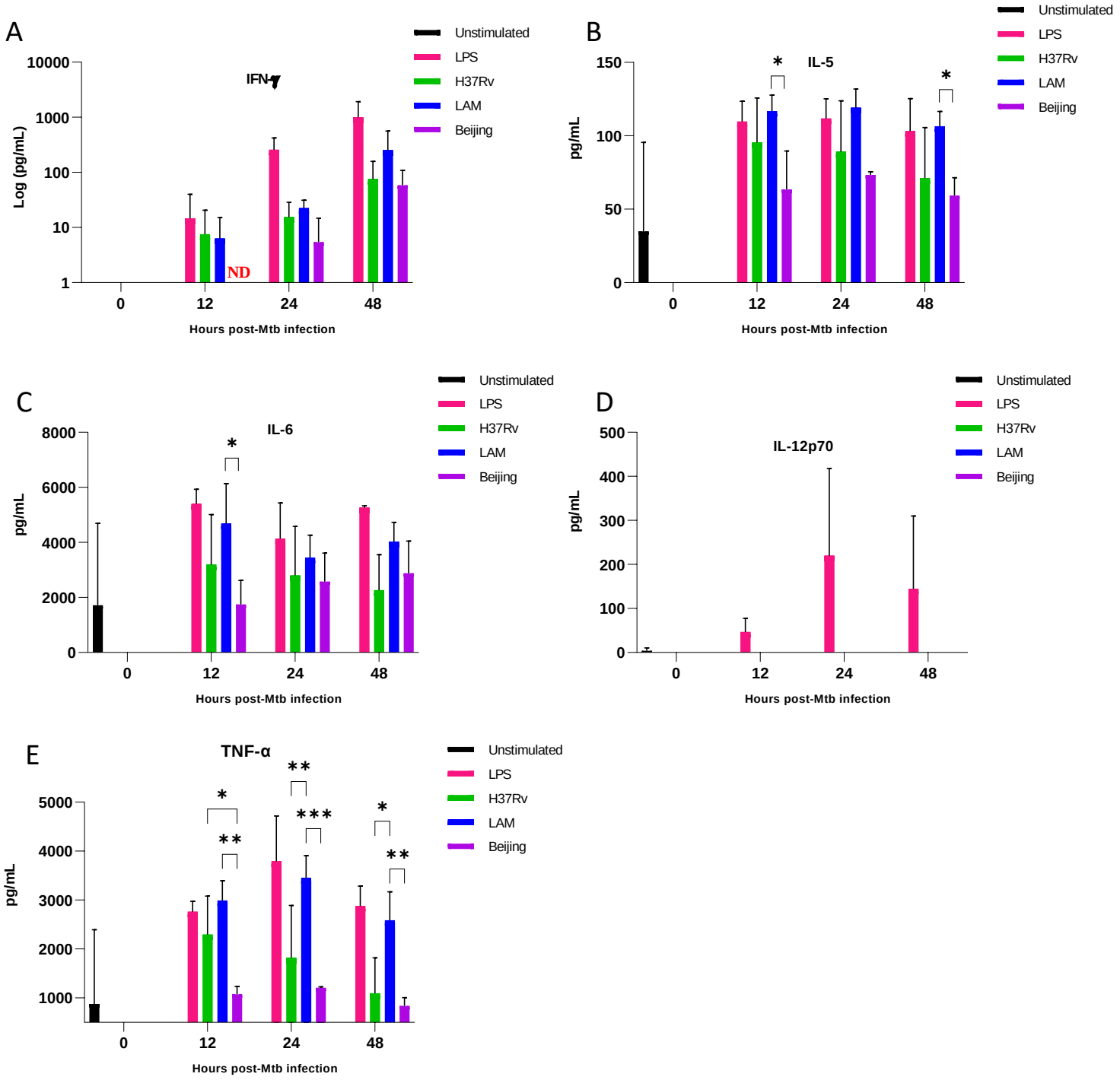

Figure 2.9. Pro-inflammatory cytokine production in whole blood with replicating Mtb infection at a MOI of 10 for 12, 24 and 24 hours. Plasma samples were collected and the levels of IFN-γ, IL-5, IL-6, IL-12p70 and TNF-α were determined by Luminex multiplex assay. Data were plotted as mean ± SD and represent 3 samples per group. A $p<0.05$ value was considered statistically significant. *P <0.01; **P < 0.001; ***P < 0.001; ****P < 0.001.

2.12.2. Effect of non-replicating DCTB infection on pro-inflammatory cytokine production

To determine whether cytokine production in DCTB differed between the strains, we compared the levels of pro-inflammatory cytokines at different time points post-infection. Between strains, no significant increase in the production of IFN-γ, IL-6 and IL-12p70 was detected after infection at the different time-points, **Figure 2.10A-C**. Starved-Beijing infection at 12, 24 and 48 hrs did not induce any IFN-γ production, **Figure 2.10A**. Starved-LAM infection at 12 and 24 hrs and starved-H37Rv at 12 hrs did not induce any IFN-γ production, **Figure 2.10A**.

The mean levels of IL-5 production at 12 and 24 hrs were significantly different in H37Rv [(125.20±34.47 pg/ml) compared to starved-Beijing (64.05±10.94 pg/ml), p= 0.0011] and also at 48 hrs starved-H37Rv [(94.10±14.14 pg/ml) compared to starved-Beijing (54.41±8.88 pg/ml), p= 0.0300] as shown in **Figure 2.10D**. A significant increase in the concentration of IL-5 was also observed in the starved LAM infected cells compared to starved-Beijing at 12 hrs [LAM (95.90±20.78 pg/ml) compared to starved-Beijing (64.05±10.94 pg/ml), p= 0.0025] and at 48 hrs [LAM (91.62±14.55 pg/ml) compared starved-Beijing (54.41±8.88 pg/ml), p= 0.0428].

At 12, 24 and 48 hrs, the starved-H37Rv infected cells and the starved-LAM infected cells had significantly higher mean TNF-α concentrations than the starved-Beijing group. The values were starved-H37Rv [(2484.10±151.92 pg/ml) compared to starved-Beijing (549.48±288.45 pg/ml), p= 0.0002] at 12 hrs, 24 hrs H37Rv [(2520.28±414.01 pg/ml) compared to starved-Beijing (980.08±353.84 pg/ml), p= 0.0019] and also at 48 hrs starved-H37Rv [(2049.26±310.93 pg/ml) compared to starved-Beijing (731.18±267.41 pg/ml), p= 0.0069]. In starved-LAM [(2151.76±647.22 pg/ml) compared to starved-Beijing (549.48±288.45 pg/ml), p= 0.0013] at 12 hrs, 24 hrs starved-LAM [(2262.15±738.70 pg/ml) compared to starved-Beijing (980.08±353.84 pg/ml), p= 0.0085] and also at 48 hrs starved-LAM [(2124±620.60 pg/ml) compared to starved-Beijing (731.18±267.41 pg/ml), p= 0.0044], **Figure 2.10E**.

Mean levels of IL-5 were shown to be significantly increased at 12 hrs in starved-H37Rv [(105.21±5.17 pg/ml) compared to starved-Beijing (39.86±17.41 pg/ml), p= 0.0006], at 24 hrs

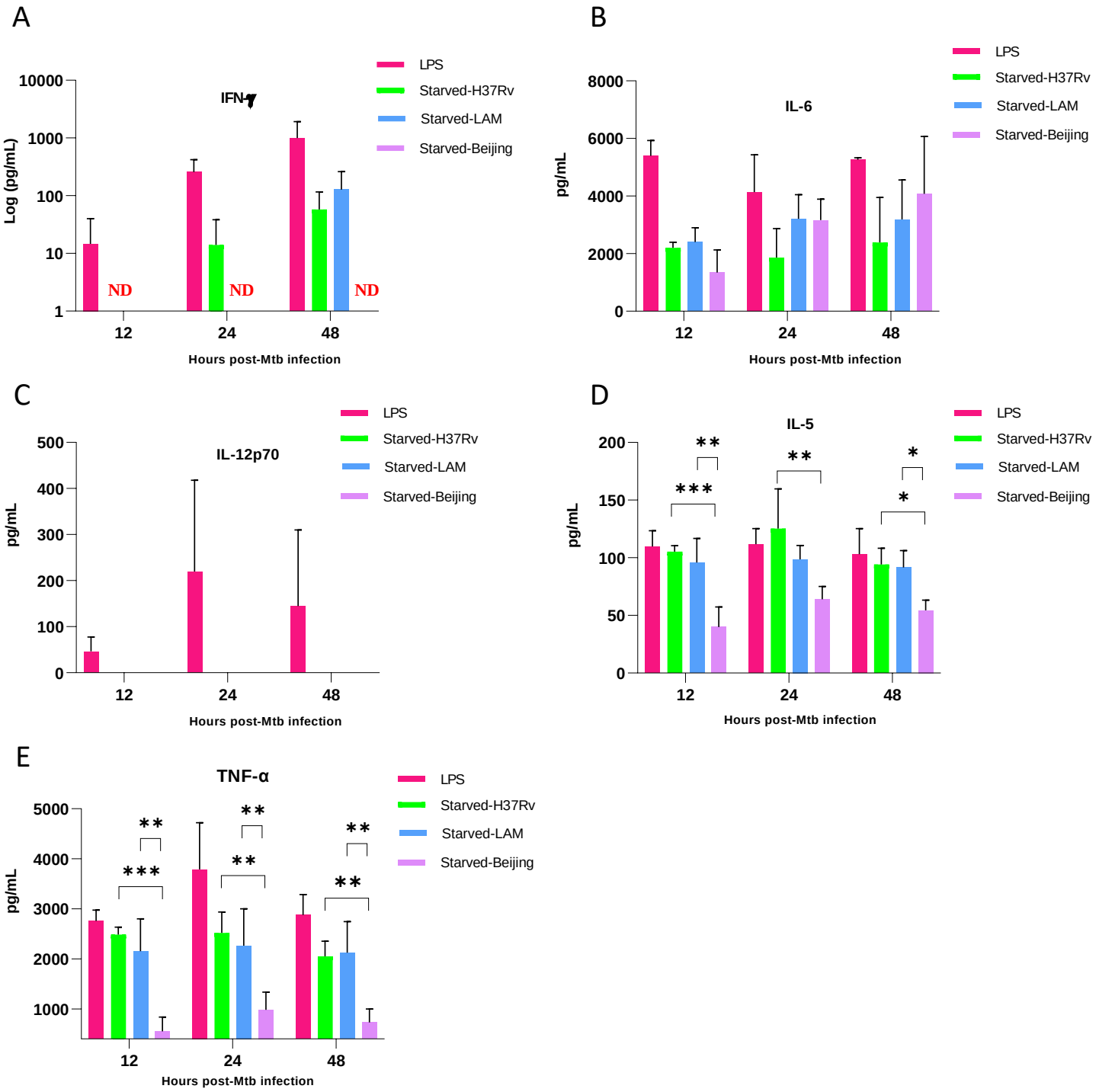

Figure 2.10. **Pro-inflammatory cytokine production in whole blood with starved Mtb infection** at a MOI of 10 for 12, 24 and 24 hours. Plasma samples were then collected and the levels of IFN-γ, IL-5, IL-6, IL-12p70 and TNF-α were determined by Luminex multiplex assay. Data were plotted as mean ± SD and represent 3 samples per group. A $p<0.05$ value was considered statistically significant. *P <0.01; **P < 0.001; ***P < 0.001; ****P < 0.001.

2.12.3. Comparison of cytokine production by DCTB (starved cells) compared to replicating bacteria

The cytokine response to starved and replicating bacteria was investigated to assess how Mtb in the DCTB state influences the host immune response during infection. For this, pairwise comparisons were conducted between replicating bacilli and DCTB for each cytokine. These comparisons were done within each strain type and not between strains, as this was done in the prior sections. Replicating Beijing and all the starved isolates did not induce IFN-γ production at 12 hrs, but after 24 hrs starved-H37Rv induced detectable levels. At this time point, starved-LAM and starved-Beijing infections were still not able to induce detectable amount of IFN-γ. At 48 hrs, Starved-LAM induce IFN-γ production, but starved-Beijing infection was still not able to induce any detectable levels of IFN-γ, **Figure 2.11A**. By putting these strains into a DCTB state, the induction of IFN-γ is delayed. No significant increase in the production of IL-5, IL-6 and TNF-α were detected after infection at all time-points. IL-12p70 was not detected at any time point.

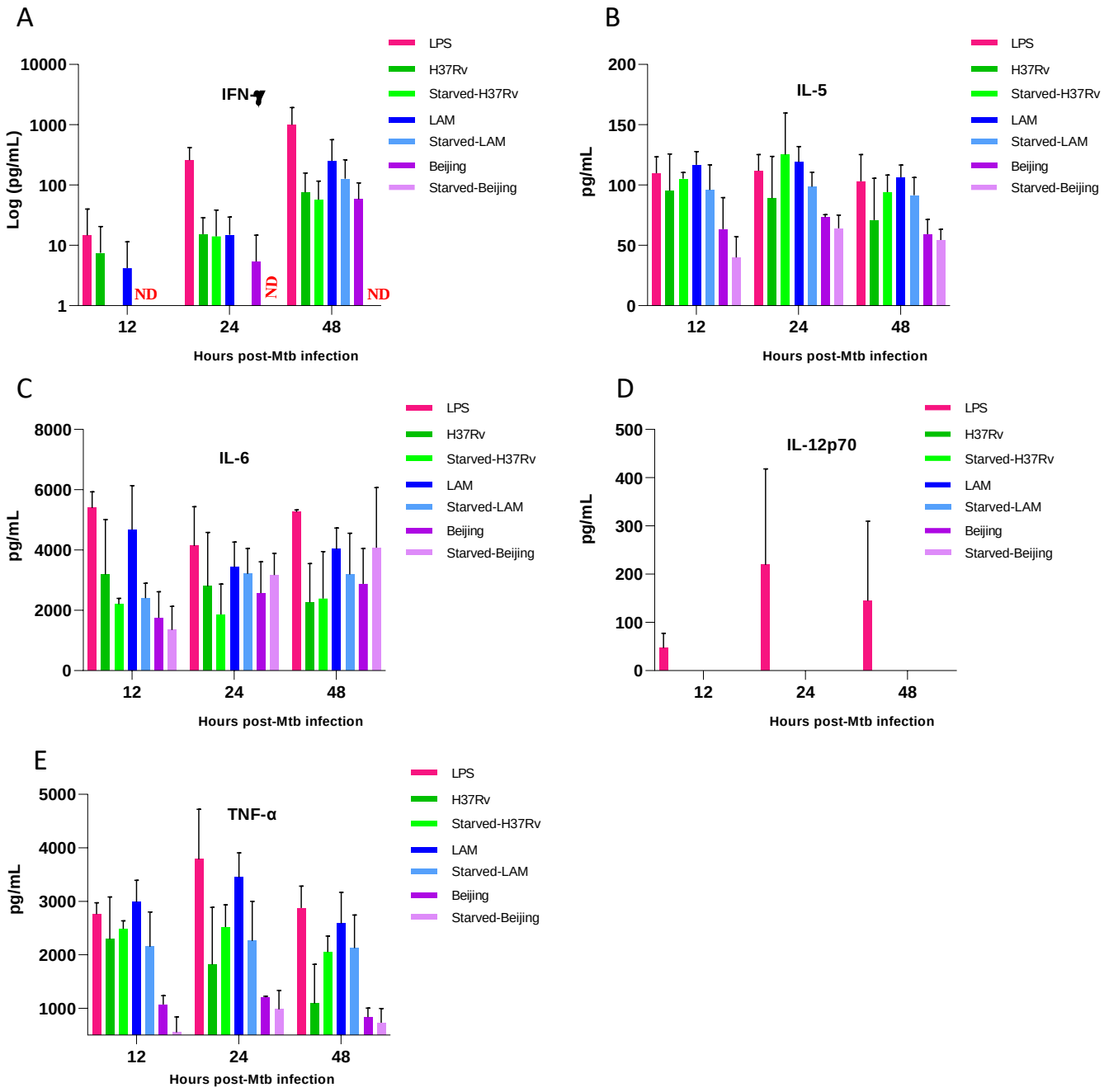

Figure 2.11. Pro-inflammatory cytokine production in whole blood with replicating and starved Mtb infection at a MOI of 10 for 12, 24 and 24 hours. Plasma samples were then collected and the levels of IFN-γ, IL-5, IL-6, IL-12p70 and TNF-α were determined by Luminex multiplex assay. Data were plotted as mean ± SD and represent 3 samples per group. A $p<0.05$ value was considered statistically significant.

2.13. A summary of the analysis and key observations

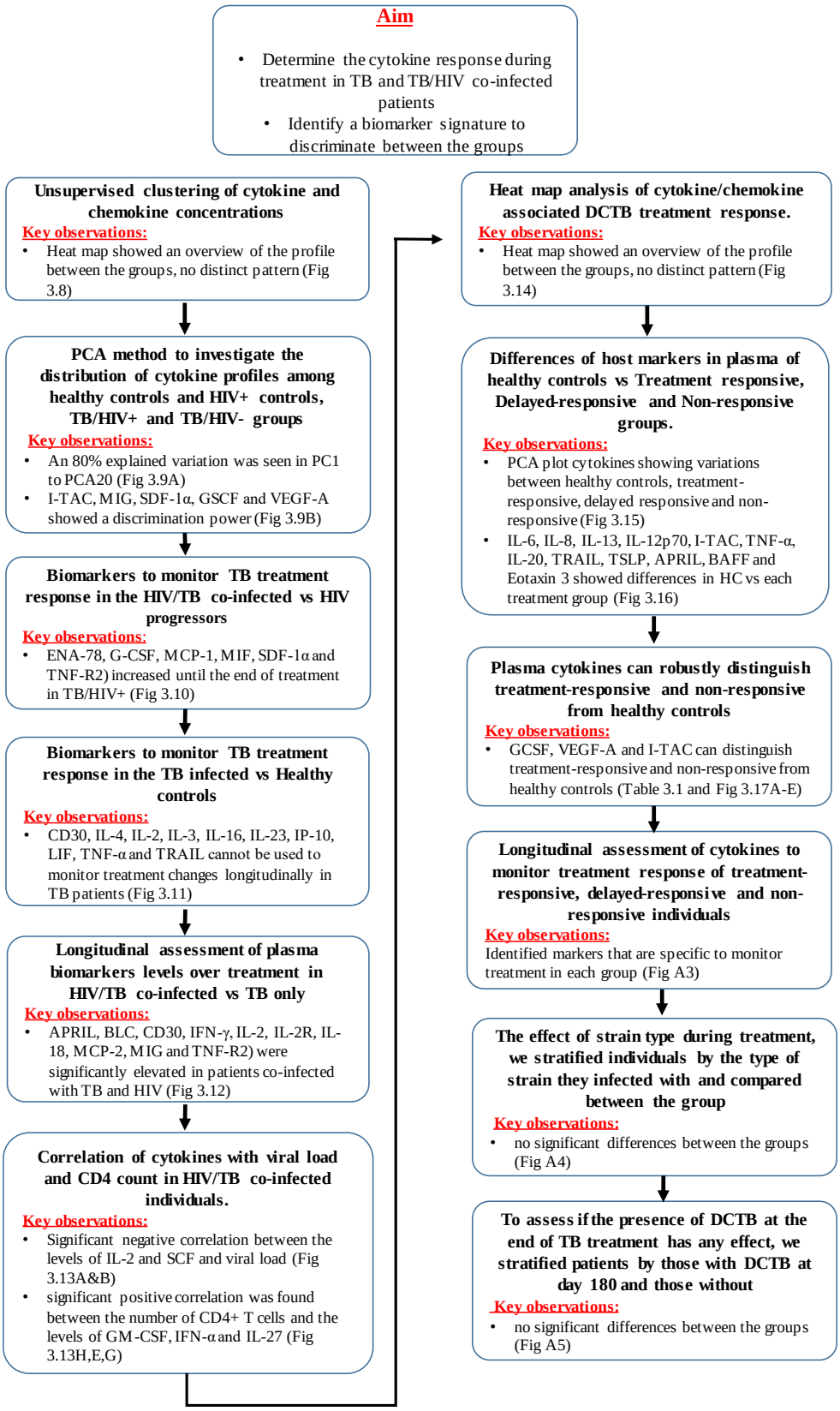

Figure 2.12. A Flow diagram summarising the results observed in whole blood assay infection with the different strains in distinct growth phases.

DISCUSSION

Mycobacteria are known to regulate their metabolism, protein expression, and replication to adapt to adverse environments. Among other characteristics, Mtb can persist for an extended period of time in host granulomas via dormancy (Lipworth et al., 2016). Reduced metabolic activity, increased lipid metabolism, tolerance to antibiotics and non-culturability are the characteristics associated with dormant bacteria (Arbués et al., 2021). Understanding the microenvironment within the granuloma and accurately mimicking these conditions is critical for creating the a non-replicative state in Mtb for experimental purposes (Belton et al., 2016). Well studied stress factors in the granuloma include hypoxia, nutritional restriction, a lack of carbon sources, and a high concentration of nitric oxide (Campaniço et al., 2020). Whilst these factors induce the non-replicative state in mycobacteria, the ability of these model systems to establish the DCTB state has not been investigated.

To ultimately create improved TB diagnostic tests, it is crucial to examine the physiology and metabolism of the DCTB bacteria using *in vitro* conditions that elicit this differentially culturable state (Dusthackeer et al., 2019). Systematic analyses of various *in vitro* models to generate DCTB indicated that the combination of carbon starvation and RIF treatment was able to generate robust DCTB populations (Saito et al., 2017). Here, the authors also attempted to generate DCTB using a clinical isolate of Mtb that was resistant to RIF and were unable to generate any non-culturable populations. They concluded that addition of RIF to the model system was essential for DCTB production and that the emergence of DCTB in experimental systems, and possibly even in the human host, was dependent on the engagement of RIF with its molecular target, which would induce intracellular stress in bacteria. In this regard, prior work demonstrated that changes in the immune response, as measured by HIV infection and CD4 counts above 200 cells/ml, was a key factor in the prevalence of DCTB in sputum and consequently, the human lung. Individuals who were HIV infected with low CD4 counts established lower levels of DCTB when compared to HIV uninfected counterparts (Chengalroyen et al., 2016, Peters et al., 2023).

We first examined the induction of the differentially culturable state using an *in vitro* model with carbon nutrient limitation and RIF treatment. Similar to previous work done in our lab (Padarath, 2020), we noted that RIF treatment resulted in significant loss of viability, in contrast to the observations of Saito et al. (2017). As this stage, we have no clear explanation for this. It is possible that strain background has an important effect on the establishment of DCTB in

laboratory systems. Our isolates, and the laboratory control strain, were different to that used by Saito and colleagues, possibility explaining the discrepancy. Saito et al., 2017 also reported that RIF resistant isolates were unable to form DCTB populations, which is contrast to a recent study from our lab confirming the presence of DCTB populations in individuals with RIF-monoresistant TB, multidrug resistant TB and extensively drug resistant TB (Gordhan et al., 2022).

Despite these differences, we were able to successfully generate DCTB in our laboratory using H37Rv, LAM and Beijing strains, these DCTB populations were able to be resuscitated in media and media supplemented with CF (**Figure 2.7 and 2.8**). This effect was not seen for all strains tested. For LAM strains, carbon starvation yielded DCTB populations for two (L3814 and L3876) of the five strains tests and for Beijing strains, only B2690 generated DCTB. For Beijing, we also noted that B9961 lost the ability to form colonies after carbon starvation, whilst still retaining the ability to be resuscitated in MPN assays. Whilst this could potentially suggest that the entire population of bacteria had shifted to the DCTB state, we had not seen this phenomenon before with any clinical isolate. Saito et al. (2017) had also not reported seeing this effect with the strains used in their study. Based on this, we opted not to use B9961 for the whole blood assay. Rather, we sought to test a different model for the generation of DCTB in the form of using a model that mimicked acid stress.

During colonization of macrophages, Mtb is resident in phagocytic vacuoles. Whilst tubercle bacilli are able to prevent acidification of the vacuole, this phenomenon does occur as part of the overall response to control infection (Choudhary et al., 2022). As such, tubercle bacilli experience acid stress during infection and this component can be modelled into experimental systems. We opted to use a media made up of 10% 7H9 mycobacterial culture media that was acidified to pH=7 in an attempt to mimic nutrient limitation, together with acid stress. With this model we found that LAM strains L3814 and L3876 still retained the ability to adopt the DCTB state. The consistency between LAM isolates was encouraging and based on this, we arbitrarily chose L3814. In contrast, we saw some inconsistency with Beijing isolates where B2960, which induced formation of DCTB in the standard carbon starvation model, yielded no DCTB in the acid stress model. B1714 formed DCTB in the acid stress model whilst yielding no DCTB in the standard model. It is possible that Beijing isolates have specific responses to acid stress that are not seen in LAM strains and that this response is highly variable in Beijing isolates.

When comparing within strains, it was curious that select strains within a particular lineage were able to form DCTB whilst others did not. This points to possible genetic differences that confer differential inherent ability to shift to non-replicating states. Further work is needed in this regard.

There are number of studies that have demonstrated that DCTB can be detected in TB sputa when supplemented with CF. During early treatment, this subpopulation seems to be more prevalent (Beltran et al., 2020, Chengalroyen et al., 2016, Gordhan et al., 2021, Gordhan et al., 2022, Mukamolova et al., 2010, Peters et al., 2023). In preclinical TB models, Beijing strains appear more virulent than strains from other lineages and result in larger mycobacterial burdens, more lung damage, and early mortality (Mourik et al., 2019). Their capacity to generate DCTB, however, is little understood. In this regard, it is interesting to note that members of the DosR regulon are all constitutively overexpressed in the Beijing strains (Domenech et al. (2017), which could possibly explain the ability of the one Beijing strain to produce more DCTB. In prior work from our lab, we investigated the inherent propensity of Beijing versus LAM isolates to adopt the DCTB state in sputum. Here the quantum of DCTB detected directly in sputum was assessed and compared between lineages. It was noted that within sputum, Beijing isolates had a greater propensity to adopt the DCTB state when compared to LAM strains. In addition, when comparing the quantum of DCTB, Beijing isolates formed more DCTB than LAM strains (Padarath, 2020). In a separate MSc study, our lab demonstrated that this observation holds true for drug resistant isolates of Mtb (Nonkula, 2022). Based on these differences we hypothesized that variations in the ratio of culturable to DCTB could possibly affect the immune response, given that shifting to the DCTB state requires remodelling of metabolism that could affect the expression of select antigens.

A robust *in vitro* technique for evaluating the cellular immune responses of humans to Mtb is whole blood infection assays. Compared to peripheral blood mononuclear cells (PBMCs), they have been found to more accurately simulate the variety of cellular interactions that occur during the immune response to infection, possessing higher cell viability and encompassing all immune cell types, as well as non-cellular components of the human blood (Silva et al., 2013). We used this model to test the capacity to induce select cytokines in response to our DCTB populations that were generated in the laboratory. It is well-known that during infection, Mtb substantially promotes the production of cytokines (Flynn and Chan, 2001). Anti-mycobacterial defensive mechanisms come into play when the bacteria alters host cytokine production during infection (Liu et al., 2017). It has been previously shown that in TB

granulomas, the mRNA expression of IFN-γ, TNF-, IL-6, IL-8, and IL-12 were elevated and secretion of cytokines IL-1β, TNF-α, and IL-6 in bronchoalveolar lavage fluid from implicated areas of pulmonary TB have also been observed (Kim et al., 2011). Along with IL-1β and TNF-α, IL-6 plays an important role in the immune response to Mtb infection. Mtb, however, has the ability to influence the production of this cytokine and by decreasing it, thus promoting the disease progression (Boni et al., 2022). In our experimental system, we observed the production of IFN-γ, TNFα, IL-5, IL-6 and IL-12p70. The LAM strain, when in a conventionally culturable state, induced a significant increase in the plasma concentrations of TNFα, IL-5 and IL-6 compared to the Beijing strain in the culturable state. As a result, our *in vitro* model did accurately mimic some *in vivo* observations in terms of release of Th1/Th2 cytokines in response to Mtb infection.

When comparing cytokine production of strains that shifted to the DCTB state, we noted that there was a significant decrease in the levels of IL-5 and TNF-α induced by Beijing-DCTB in comparison to H37Rv-DCTB and LAM-DCTB. This is not surprising given that in order to reduce host immunity, hyper virulent Beijing strains increase the synthesis of anti-inflammatory cytokines while decreasing the production of pro-inflammatory cytokines (Sohn et al., 2009). Beijing strains are notable for a number of reasons, including the prevalence of these strains in individuals with active TB, treatment failure, and drug resistance, as well as their ability to efficiently proliferate in lung macrophages (Keikha and Majidzadeh, 2021). They appear to be more transmissible and to produce more severe disease than strains from other sublineages, however the underlying pathogenic mechanisms are still unknown (Tong et al., 2020). The decreased production of these cytokines in starved-Beijing may be an immune escape mechanism for the suppression of Th-1 responses. It is also possible that starving Mtb to produce the DCTB state affect the emergence of an immune response with functional impairment, resulting in T cells unable to fight infection. Further in vivo studies in animal models are needed to investigate such effects. We observed no significant differences in the mean concentrations of IL-5, IL-6 and TNF-α between DCTB and conventionally grown strains. Thus, these cytokines are not affected by metabolic shifts affecting replication competency in Mtb.

When comparing the effect of culturability to alter immune responses within particular lineages, it was found that when the LAM strain shifted to the DCTB state, it was impaired in the ability to induce IFN-γ in the whole blood assay. This was evidenced by no IFN-γ production at early time points. An exacerbation of this effect was noted with the Beijing

isolate, which failed to induce any IFN-γ when it shifted to the DCTB state. Whilst only seen with one cytokine, these data provide compelling preliminary evidence that shifting to the DCTB may affect the ability of tubercle bacilli to induce immune responses.

Collectively our data indicate that clinical isolates of Mtb have differing inherent capacities to adopt the DCTB state. Those LAM strains that can form DCTB in laboratory models, displayed a consistent ability to do this in two distinct models mimicking carbon starvation with or without acid stress. In contrast, Beijing strains displayed greater variability in their ability to form DCTB. Shifting to the DCTB state resulted in impaired IFN-γ production in the whole blood assay with clinical Mtb isolates, suggesting that DCTB may differentially affect immunity in individuals with TB when compared to conventionally culturable bacteria. These and related effects were explored in the next chapter.

CHAPTER 3:

Tuberculosis treatment biomarkers using clearance of differentially culturable tubercle bacteria as a measure of therapeutic success

3.1. Introduction

Biomarkers are used in medicine for screening, diagnosis, prognosis, and treatment. They come in a variety of forms, some of which may overlap, like those based on genes or proteins are such example (Flepisi et al., 2014, Justice et al., 2018). A biomarker is a trait that may be measured and examined objectively as a sign of normal biological processes, pathogenic processes, or pharmacological reactions to a therapeutic intervention (McNerney et al., 2012). Biomarkers are necessary for providing more information about the pathogenic process involving health status and future illness risk. They can either be host- or pathogen-specific in an infectious disease. For TB, a pathogen or host marker particular to the underlying disease process would be appropriate for use as a diagnostic biomarker or combined with other biomarkers to report on treatment response, risk of disease progression/recurrence (Wallis et al., 2013). Usually, TB diagnostic biomarkers aim to categorize individuals as having active TB, LTBI, or no infection (Wallis et al., 2010, McNerney and Daley, 2011). For TB biomarkers to exert maximum benefit, they should be applied to readily obtainable samples like blood, urine, or breath and be instrument-free or achievable with minimal apparatus (MacLean et al., 2019). The following categories can be used to categorize TB biomarkers: (I) Mtb components, (II) antibody responses, (III) cellular immune responses (derived from transcriptional signatures or cytokine/chemokine abundance), or (IV) metabolites that are modulated by disease processes (Yong et al., 2019).

The last decade has witnessed substantive advances in TB biomarker signatures. Initially, these were driven by monitoring the changes in blood transcriptional responses as individuals progressed from asymptomatic disease to full-blown active TB. These efforts yielded numerous biomarker signatures that report on risk of disease progression with the outlook of targeting TB preventative therapies with greater precision. The search for a unified biomarker signature that yielded similar benefits in genetically diverse populations resulted in substantive effort to analyse transcriptional signatures using innovative bioinformatics and computational biology approaches. Unified signatures are emerging and being incorporated into diagnostic devices, as an example, Cepheid has formulated a 3-gene signature into a GeneXpert cartridge that is currently being evaluated. In addition, these and other studies have also focused on using

transcriptional and proteomics biomarkers to monitor response to TB treatment, here with the outlook to developing approaches to bolster treatment shortening efforts (Thompson et al., 2017, Kaewseekhao et al., 2020). There are fewer efforts focused on developing biomarkers for monitoring risk of disease recurrence, as these require long follow up time frames to quantify recurrence. Also, given that recurrences occur at a lower frequency than primary disease, large sample sizes are required to achieve statistical significance. The use of pathogen-specific biomarkers has been largely neglected. There has been a recent focus on Lipoarabinomannan (Lam), but this also has not yielded maximum clinical benefit (Lawn, 2012).

In this chapter, we set out to develop a novel biomarker that unifies a pathogen treatment pattern, together with appending immune response. To create the appropriate context, TB biomarker research has focused on host and pathogen aspects using various approaches, summarized below. The general approach to search for biomarkers, together with the technique used is described in **Figure 3.1**.

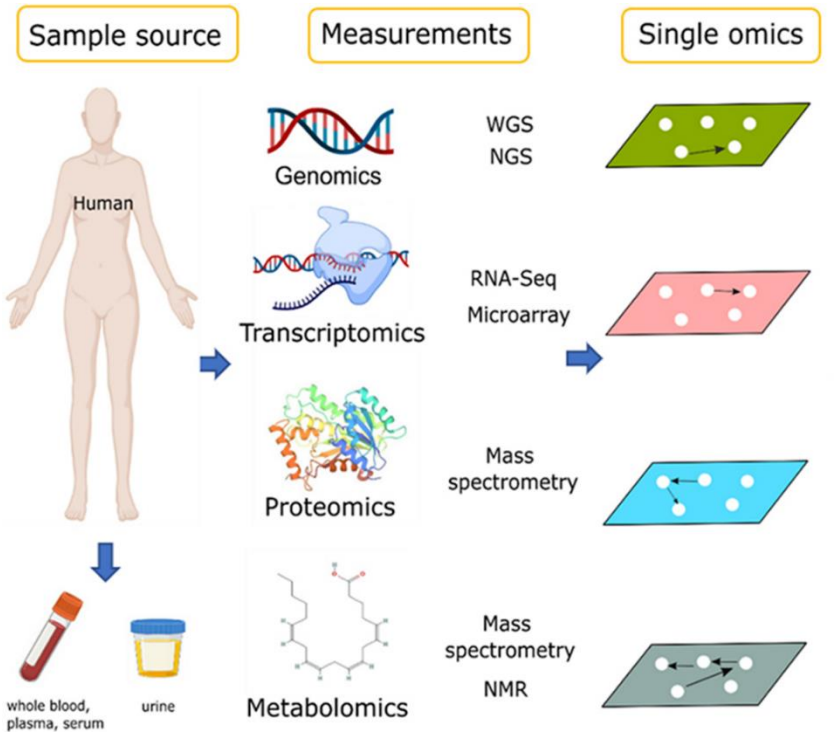

Figure 3.1. Schematic representation of 'omics' approach. These methods are used in the discovery TB diagnosis and monitoring of TB treatment biomarkers. Whole genome sequencing (WGS); Next-generation sequencing (NGS), RNA sequencing; Microarray; Nuclear magnetic resonance (Pitaloka et al., 2022).

3.2. Pathogen-specific TB biomarkers

When Mtb replicates in the human host, it secretes a variety of proteins and by-products. Pathogen-derived compounds must reach detectable amounts in clinical specimens such as sputum, urine, plasma, saliva, cerebrospinal fluid, and pleural fluid of infected patients to be regarded targets for antigen detection tests, so they can be beneficial as diagnostic biomarkers (Bekmurzayeva et al., 2013). A rapid biomarker-based, non-sputum test for diagnosing active TB with the aim of commencing treatment is one of the highest priority in TB diagnosis (WHO, 2020). Low bacterial load in sputum is often seen in active TB patients, including HIV co-infected people and children, with blood and urine being the more practical samples for diagnosis in these vulnerable populations (Acharya et al., 2020). Urine is easier to collect from both adults and children, and it is safer to handle and less inconsistent than sputum (Tucci et al., 2014). Sputum also requires respiratory manoeuvres that generate aerosols and create the risk of infection for clinical staff and healthcare workers.

The measurement of Lam, a pathogen component that is shed from the complex mycobacterial cell wall, illustrated in section 1.4 (**Figure 1.2**), has been extensively investigated, despite low sensitivity (Vaezipour et al., 2022). Several lipid-based compounds that form a thick "waxy" surface make up an outer cell wall of all mycobacteria (Bulterys et al., 2019). Lam, which accounts for up to 15% of the bacterial mass, is a key component of the cell membrane and its immunomodulatory characteristics are significant and unique (Correia-Neves et al., 2019). A study done by Hamasur et al. (2001), was the first published report on the potential use of Lam in urine as a diagnostic test and demonstrated that individuals infected with active TB, as well as mice injected with sonicated Mtb, have Lam in their urine. Some studies have shown that the level of Lam in urine is strongly correlated with mycobacterial density in sputum samples and other markers of high mycobacterial burden in smear-positive than smear-negative TB patients (Kerkhoff et al., 2014, Hamasur et al., 2015, Nakiyingi et al., 2015). The WHO recommends the use of Lam in HIV-positive patients who have (I) TB symptoms, (II) advanced HIV disease, (III) no TB symptoms when CD4 count is less than 200 cells/mL, or (IV) individuals who are seriously ill (WHO, 2019). There are also consideration for in-and out-patients. Rollout of these recommendations are facilitated by the availability of lateral flow assays (strip tests) for Lam from several commercial suppliers, Alere Determine™, FujiLAM and Abbott.

Lipids account for roughly 60% of the dry mass of the mycobacterial cell wall. These combine to form a permeability barrier, which serves as the first line of defence against the host's immune system. Mycolic acids, which are long-chain fatty acids esterified to arabinogalactan, are one of the fundamental lipid components of mycobacterial cell walls (Jeffrey North et al., 2014, Korb et al., 2016). The most common form of mycolic acid found in Mtb is alpha-mycolates, which have no oxygen substitutions in their chains (Jeffrey North et al., 2014). Interestingly, structural changes and variations in the chemical composition of mycolates have a significant impact on bacilli virulence and physiology. It was shown that removing the cyclopropane molecule inhibits the growth of mycobacteria (Glickman et al., 2000, Barkan et al., 2012). Some studies have shown the presence of mycobacterial mycolic acids in both modern and ancient TB, implying that mycolates could be used as sensitive disease biomarkers (Gernaey et al., 2001, Borowska-Strugińska et al., 2014).

For a variety of reasons, mycolic acids appear to be appropriate diagnostic indicators of mycobacterial infections. First, regardless of growth conditions, the compounds are present in high concentrations in the bacterial cell wall. Second, these are specific to mycobacteria and are not produced in the human body. Third, because mycolic acids are chemically stable and relatively easy to extract, they can be studied using state-of-the-art chemical analysis techniques (Ndlandla et al., 2016). The mycolic acid biosynthetic pathway is a well-established and effective therapeutic target for chemical intervention, as the approved drugs INH, ethionamide (ETH), isoxyl (ISO), and thiacetazone (TAC) all act against it through different mechanisms (Schroeder et al., 2002, Alahari et al., 2007, Barry et al., 2007). Using a lipidomics approach, a subclass of mycolic acids, obtained directly from sputum of TB patients and mouse lungs was identified for potential use as a diagnostic marker for acute TB infection in humans and mice. This mycolic acid signal was able to clearly distinguish active TB samples from non-active or cured TB, as no mycolic acid was detected in the non-TB control group or in RIF-treated mice (Shui et al., 2012).

Mtb employs a variety of strategies to help surviving bacteria enter cells; the most important of these tools are secreted proteins such as Mpt64, the 6-kDa early secreted antigenic target (ESAT6), the 10-kDa culture filtrate protein (CFP10), and the antigen 85 (Ag85) complex, which plays an important role in Mtb virulence. The main secretory antigen is the Ag85 complex, which plays an important role in Mtb pathogenicity (Babaki et al., 2017). The Mtb antigen 85 complex (Ag85) complex is a family of three proteins [(Ag85A (31 kD), Ag85B (30 kD) and Ag85C (31.5 kD)] that have enzymatic mycolyl transferase activity and are

involved in the coupling of mycolic acids to the cell wall arabinogalactan and the biogenesis of cord factor (Ronning et al., 2000, Armitige et al., 2000). Although it has been found in the mycobacterial cell wall, Ag85 is a major mycobacterial secreted antigen. The A, B, and C proteins are generally expressed in a 2:3:1 ratio by all mycobacteria species, regardless of pathogenicity; however, the ratio may vary depending on environmental conditions (Tang et al., 2012, Świerzko et al., 2016). The Ag85C is far more biologically active (Ronning et al., 2000). In addition, all three Ag85 proteins have the ability to bind human fibronectin, an extracellular matrix glycoprotein that reduces macrophage phagocytosis of Mtb and facilitates pathogen adherence and dissemination into other tissues (Armitige et al., 2000).

The Ag85 complex has been found in a variety of biological samples from Mtb patients, including blood, urine, sputum, and cerebrospinal fluid (Kashyap et al., 2005). A study (Kumar et al., 2010) assessed the diagnostic capability of Ag85 complex-associated proteins together with, other Mtb-specific secreted components (ESAT-6 and CFP-10) from the RD1 region (a 9.5-kb segment of DNA known as region of difference 1). Higher sensitivity was observed with the Ag85 complex compared to ESAT-6 and CFP-10, with nearly comparable specificity.

As the BCG vaccine is able to effectively protect children against TB (al-Kassimi et al., 1995), but not adults, with variable efficacy ranging from 0% to 80% (Brewer, 2000), there have been several attempts to improve it. It was discovered that recombinant modified vaccinia virus Ankara expressing antigen 85A (MVA85A) induces high levels of antigen-specific IFN-γ-secreting T cells when compared to BCG alone in healthy BCG-naive volunteers. Previously BCG vaccinated individuals (with two doses) aged 0.5-38 years had significantly higher levels of antigen-specific IFN-γ-secreting T cells, and these levels were 5-30 times higher at 24 weeks after vaccination than in those who had only received a single BCG vaccination (McShane et al., 2004).

In general, cell wall components have formed the basis of pathogen-specific biomarker research. The high abundance of these molecules, combined with their antigenic nature has facilitated progression to clinical evaluation. Regrettably, not much work has been done on their components of the tubercle bacillus.

3.3. Host-derived TB diagnostic biomarkers

The majority of these biomarkers are associated with host immunity and include proteins, metabolites, cell markers, and transcriptional signals (La Manna et al., 2018). Host

immunological responses to Mtb infection leave traceable signals within the host, which may be useful for accurate TB diagnosis and/or prognosis (Dey and Bishai, 2014, Parida and Kaufmann, 2010). In terms of ease, feasibility, and the amount of sample that can be obtained, human blood and derivative samples are appropriate for TB diagnosis based on biomarkers (Guo et al., 2022).

3.3.1. Transcriptomic TB biomarkers

A useful technique for biomarker discovery is transcriptomics, which is the study of the transcriptome, or the genes that are transcribed from an organism's genomic DNA (Fryer et al., 2002). Several high-throughput techniques can be used to obtain gene expression profiles, which provide information on biological processes and regulatory mechanisms (Laub et al., 2000). Such high-throughput techniques include quantitative RT-PCR, microarray analysis, reverse transcription multiplex ligation dependent probe amplification assay (RT-MLPA), nanostring and RNA sequencing are used to analyse gene and MicroRNA expression (Van Rensburg and Loxton, 2015). Transcriptional profiling has greatly aided numerous research studies aimed at understanding diseases, including the investigation of various tissue-specific and blood-based responses. When investigating diseases, biomarkers or bio-signatures (a group of transcripts or genes) are usually discovered; these are then evaluated in clinical specimens or other studies (Pankla et al., 2009, Flanagan et al., 2009). Host gene expression has been used extensively to discover TB biomarkers and is useful in identifying various infection states (Gupta et al., 2020). Furthermore, by analysing the expression of specific genes during the course of treatment, TB biomarkers can be used to track the effectiveness of the treatment (Van Rensburg and Loxton, 2015).

To distinguish patients with pulmonary TB from healthy controls, or those suffering from other infectious or respiratory disorders, numerous host blood transcriptional signatures have been proposed (MacLean et al., 2019). A study (Kaforou et al., 2013) and colleagues looked at African patients with and without HIV from Malawi and South Africa to determine if blood RNA expression could identify TB from other illnesses that are common in African populations and serve as the foundation for a TB diagnostic test using microarray analysis. They discovered a group of 44 transcripts and a group of 27 transcripts that could identify TB from other diseases and LTBI, respectively. For separating TB from LTBI, the disease risk score demonstrated good sensitivity of 95% CI (87–100) and specificity of 90% CI (80–97). In another study involving fewer patients from Brazil, the authors identified a smaller set of transcriptional

biomarkers of Fc gamma receptor 1A, granzyme A, and guanylate-binding protein 5 using real-time PCR on whole blood samples. The three genes combined offered a potent bio-signature to distinguish TB from other pulmonary diseases, with 95% specificity and 93% sensitivity and AUC of 0.955 (0.885–1.000) (da Costa et al., 2015). A similar set of biomarkers was seen earlier in a study by (Maertzdorf et al., 2011), where they analysed whole-blood microarray gene expression in both latently and actively infected TB patients as well as healthy individuals. Granzyme A, guanylate-binding protein 5, Fc gamma receptor 1A, Fc gamma receptor 1B, and lactotransferrin bio-signature were able to distinguish active TB and LTBI. In a much larger study including 1417 participants, the authors aimed to test and confirm the capacity of a select set of host genes using RT-PCR assays to distinguish between active TB and other disorders and healthy individuals in whole blood and peripheral blood mononuclear cells. They demonstrated a minimum of two genes (Guanylate Binding Protein 5 and Krüppel-like Factor 2) that provide great sensitivity and specificity in distinguishing active TB from other diseases and healthy controls. The two-gene set had the highest predictive power for separating active TB from healthy controls in whole blood, with an AUC of 0.86, a sensitivity of 77.8%, and a specificity of 87.1%. Additionally, with an AUC of 0.89, sensitivity of 96.1%, and specificity of 85.2%, this combination also had the strongest predictive capacity in differentiating active TB from other diseases (Francisco et al., 2017).

With the development of RNA sequencing technology, the transcriptome of a bio-sample could be measured and profiled simultaneously while avoiding biases usually produced during microarray hybridization (Zhao et al., 2014). Through the use of RNA sequencing technology, De Araujo et al. (2016) discovered that the levels of the genes DOCK9, EPHA4, and NPC2 were significantly altered in the blood of TB patients in Brazil. Independent validations were carried out in cohorts from various places to support these results. Quantitative RT-PCR was used to assess the gene expression levels in blood in Brazil, with reanalysis of publicly available microarray data from United Kingdom, South Africa, Germany, and France. When TB cases were compared to healthy recent close TB contacts, substantial modification of all target genes was found in the Brazilian population. NPC2 mRNA high expression had a 92% specificity and the highest sensitivity 85% [CI (65-96); AUROC = 0.88)]. The potential of NPC2 as a biomarker for TB was confirmed by all the other reanalysed cohorts (sensitivity: 82-100%; specificity: 94-97%). In a recent study, the same researchers did a thorough assessment of NPC2, EPHA4, and DOCK9 mRNA levels as diagnostic biomarkers in accordance with WHO TB target product profile criteria for a referral examination to find those

who are thought to have TB. In addition, possible biomarkers for projecting the development of TB disease from LTBI and correlates of the clinical response to anti-TB therapy were also investigated. All three genes had significantly different expression when compared between TB and healthy controls or LTBI. NPC2 exhibited the highest mean AUROC curve for TB vs. healthy controls (0.95) and LTBI (0.94). Intriguingly, people who progressed from LTBI to TB had consistently higher NPC2 expression throughout compared to people who didn't, with a substantial change occurring around the time of the onset of active disease. In addition, NPC2 expression returned to normal when the anti-TB therapy was completed (de Araujo et al., 2021). In a predictive model, the best bio-signature was found to be a three-gene signature made up of BAFT2, ETV7, and CD1C with a AUC of 0.86 (95% CI, 0.69-1.00), sensitivity of 76.92% (95% CI, 46.19-94.96), and specificity of 94.12% (95% CI, 71.31-99.85) for TB diagnosis (Chendi et al., 2023).

MicroRNAs (miRNAs) are important posttranscriptional regulators of gene expression; they are known to affect the pathophysiology and immunological responses in infectious illnesses and may have diagnostic applications (Mehta and Baltimore, 2016). Small nuclear RNAs (snRNA), PIWI-interacting RNAs (piRNA), and small nucleolar RNAs (snoRNA) are three more significant groups of small noncoding RNAs that also have a role in the regulation of gene expression (Esteller, 2011). miRNAs are also believed to be more stable biomarkers than mRNA because of their compact size and chemical structure (Liu et al., 2009, Samir and Pessler, 2016). They are now acknowledged for their significant contribution to the complex interplay between hosts and bacterial pathogens, whether as a component of the host immune response to combat infection or as a bacterial molecular strategy to divert host pathways for their own purposes (Aguilar et al., 2019). In fact, a number of studies have revealed that variations in host miRNA expression are a distinctive feature of bacterial infections in people and animals at the cellular and organismal levels (Aguilar et al., 2019), including infections with Mtb (Latorre et al., 2015, Sabir et al., 2018). In a study using serum, the authors discovered a miRNA signature for the detection of TB in healthy, active pulmonary TB (PTB), HIV/TB co-infected, LTBI, other pulmonary infections, and active extra-pulmonary (EPTB) (Miotto et al., 2013). They demonstrated that 15 miRNAs on individual serum samples serve as signatures for the healthy and PTB categories, with diagnostic accuracy of 82% (CI 70.2-90.0) and 77% (CI 64.2-85.9), respectively. By using the specific signature for the European group (10 miRNAs), in consideration of the various ethnic groups, the diagnosis accuracy rose further to 83% (CI 68.1-92.1) and 81% (65.0-90.3), respectively. The diagnostic accuracy was raised to

95% (CI 76.4-99.1) and 100% (83.9-100.0), respectively when the African-specific signature (12 miRNAs) was used. They concluded that a new fascinating source of biomarkers for TB infection is serum miRNA profiles, which have the ability to distinguish not only between PTB and LTBI but also between the other groups (Miotto et al., 2013). Another study investigated the expression of miRNA, piRNA, snoRNA, and snRNA in whole blood of individuals with TB, LTBI, and treated LTBI and in uninfected exposed individuals using RNA sequencing. They were able to demonstrate that snRNA reprogramming is more pronounced in TB than in LTBI, with miRNA populations exhibiting the most significant modifications, as per their prediction. However, the populations of piRNA and snoRNA also showed significant dynamic changes. One miRNA, two piRNAs were shown to be fairly accurate (AUC = 0.70 to 0.74) biomarkers for LTBI, as well as one miRNA, one piRNA, and two snoRNAs (AUC = 0.79 to 0.91) as biomarkers for successful LTBI treatment. Together, their findings demonstrated that, in addition to miRNA, snoRNA and piRNA should also be taken into account as markers and pathogenesis components in the different phases of TB infection (de Araujo et al., 2019).

3.3.2. Proteomic TB biomarkers

The study of proteins in their entirety in a cell, tissue, or organism is known as proteomics (Bisht et al., 2019). Proteomics has continued to provide a robust approach for examining the changes in protein diversity that accompany health and disease processes by comparing different patterns within the proteome, allowing for clinical diagnosis, prognosis, and even treatment of many diseases (Kavallaris and Marshall, 2005). Proteomic biomarkers are biomarkers discovered using technologies capable of analysing many proteins at the same time, such as protein microarray and mass spectrometry (Jacquier et al., 2014).

The host response to Mtb infection is to generate and secrete particular effectors to combat the invading pathogen (Brites and Gagneux, 2015). Molecules released during host immune responses, such as cytokines, are mostly transported through the bloodstream and blood is regularly taken for clinical testing. Blood samples are used in the majority of proteomic biomarker studies for TB detection (Guo et al., 2022).

A study by Agranoff et al. (2006) used Surface enhanced laser desorption/ionization time-of-flight mass spectrometry (SELDI-TOF MS) to search for proteomic biomarkers in serum samples to distinguish between TB infected and control patients. The proteomic profile of patients with active TB was distinguished from that of controls with a diagnostic accuracy of 94% using their support vector machine classifier, which is based on a supervised machine

learning approach. Another study conducted a comprehensive and thorough proteomic analysis of 1,470 serum samples from seven countries where TB is prevalent: South Africa, Peru, Zimbabwe, Uganda, Vietnam, Colombia, and Bangladesh using the 4,000-plex SOMAscan assay. SYWC, kallistatin, complement C9, gelsolin, testican-2, and aldolase C were included in the 6 host response markers, which was tested with a blinded verification set of 204 samples and yielded an AUC of 0.87 (95% CI, 0.81–0.91) (De Groote et al., 2017). More recently, Singer et al. (2022) investigated and compared plasma host proteins from people living with HIV in South Africa (a high-TB-incidence region), and the United State (a low-TB-incidence region), demonstrating that soluble CD14, Alpha-2-glycoprotein (A2GL), Nidogen-1 (NID1), secreted and transmembrane protein 1 (SCTM1), and Alpha-1-acid glycoprotein 1 (A1AG1) were overlapping in both cohorts. Additionally, cross-validation was used to examine the diagnostic performance of these host proteins and found that panels of 5–12 proteins were also able to predict TB up to two years before diagnosis. Another study in China used data-independent acquisition MS-based proteomics to examine 200 HIV positive plasma samples. In the HIV/TB group, data-independent acquisition-MS found 13 upregulated and 33 downregulated proteins. They discovered that the protein markers, α-methylacyl-CoA racemase (AMACR), L-lactate dehydrogenase B chain (LDHB), and Ras-related protein Rap-1b (RAP1B), when used together, might be essential TB markers in people with HIV (Shen et al., 2020).

Small protein molecules known as cytokines and chemokines modulate immune responses at the cellular level (Domingo-Gonzalez et al., 2016). They activate and attract a variety of immune and inflammation-related cells. A cytokine effect can be pleiotropic, meaning that one cytokine can affect several cell types, or redundant, meaning that multiple cytokines perform the same function. Some cytokines cause a cascade effect, where one cytokine can influence the production and activity of others. They can also have antagonistic effects, where one effect opposes that of others, or synergistic effects, in which two different cytokines act together (Mihret and Abebe, 2013). Chemokines may work in a homeostatic manner, guiding cells during immunological surveillance for infections by interacting with antigen-presenting cells in specific organs. Some chemokines play a role in stimulating angiogenesis or directing cells to organs that give crucial signals for cellular maturation. Other chemokines are inflammatory, and their primary purpose is to recruit leukocytes from the bloodstream, to infection or tissue damaged areas (Kaufmann, 2002, Cooper and Khader, 2008).

The protective response to Mtb is complicated and varied, including numerous immune system components, and relying primarily on productive collaboration between macrophages and T-cell populations. Several animal and human studies conclusively demonstrated that cytokines and chemokines have a significant impact in the outcome of Mtb infection (Salam et al., 2008, Redford et al., 2010, Domingo-Gonzalez et al., 2016). Cytokines in blood can be related to TB disease state, thus serving as effective biomarkers (Mensah et al., 2021). Enzyme-linked immunosorbent assay (ELISA), Luminex, enzyme-linked immunospot (ELISPOT), and real-time polymerase chain reaction (RT-PCR) are among the techniques used to detect cytokines. In many studies, IL-2, IP-10, IL-5, and IL-10 all demonstrated good diagnostic performance for both active TB and LTBI. A study (Won et al., 2017) evaluated the ability of multiplex cytokine responses to distinguish Mtb disease states in active TB patients, LTBI, and healthy controls using the Luminex assay in supernatants collected from the QuantiFERON® Gold In-Tube assay (QFT). They found that eight Mtb antigen-specific biomarkers (GM-CSF, IFN-γ, IL-1RA, IL-2, IL-3, IL-13, IP-10, and MIP-1β), out of the 29 cytokines, were substantially different from those of the healthy controls in the Mtb-infected group. There were significant changes between active TB and LTBI in five Mtb-specific biomarkers (EGF, GM-CSF, IL-5, IL-10, and VEGF) and one Mtb-specific biomarker ratio (IL-2/IFN-γ). Three cytokine biomarker combinations enabled the precise prediction of 92.1–93.7% of Mtb-infected patients and 92.3–100% of healthy controls, respectively. Additionally, combinations of five biomarkers successfully predicted 80–100% of LTBI participants and 90.9–100% of active TB cases. A much earlier study conducted the QFT test on 23 pulmonary TB patients and 34 household contacts from Cape Town, South Africa. Using a Luminex multiplex cytokine assay, the levels of 29 biomarkers in QFT supernatants were measured to study the potential of new host markers to distinguish between LTBI and active TB. Eight out of 29 biomarkers discriminated active TB from LTBI. EGF and MIP-1β together were able to predict 92% of LTBIs and 96% of active TB cases (Chegou et al., 2009). A meta-analysis study by Wei et al. (2020), assessed the ability of cytokines to discriminate between LTBI and active TB. They included 14 studies with 982 participants (456 LTBI and 526 active TB patients) and examined the overall sensitivity and specificity. The AUC and confidence intervals respectively (shown in parenthesis) for differentiating between active and LTBI were as follows: IL-2 (0.87, 0.61 and 0.9093), IP-10 (0.77, 0.73 and 0.8609), IL-5 (0.64, 0.75 and 0.8533), IL-13 (0.75, 71 and 0.8491), IFN-γ (0.67, 0.75 and 0.8031), IL-10 (0.68, 0.74 and 0.7957), and TNF-α (0.67, 0.64 and 0.7783). According to the meta-analysis, the production of cytokines can help distinguish between active TB and LTBI, with IL-2 having the highest accuracy level. Due to their low

sensitivity and specificity, single biomarkers are unlikely to demonstrate sufficient diagnostic performance. Despite the fact that various markers have been proposed for the diagnosis of TB infection as well as the distinction between active TB and LTBI, the specificity and sensitivity of each marker varied across different studies (Wei et al., 2020). To determine the ideal combination of biomarkers to improve diagnostic capability in clinical practice, further prospective studies are required.

Urine samples, in addition to blood samples, are a common alternative for discovering proteomic biomarkers for TB diagnosis, and some relevant studies have been published. Recently, Liu et al. (2021) examined and evaluated the urine proteome profiles of TB patients and healthy controls. They used the liquid chromatography coupled with tandem mass spectrometry (LC–MS/MS) to test for putative biomarkers in 20 TB and 20 healthy control individuals, then confirmed the biomarkers in another 52 TB, 52 LTBI, and 52 healthy individuals. Based on the findings, they concluded that together, glutathione peroxidase 3, neurotrimin, poliovirus receptor, signaling lymphocytic activation molecule family 1, and hemicentin-2 could potentially be used to diagnose TB, with an 82.7 percent sensitivity and 92.3 percent specificity for TB diagnosis in the LTBI group. In a much earlier study, (Young et al., 2014) discovered seven immune-related human proteins immunoglobulin kappa chain C (IGKC), retinol binding protein 4 (RBP4), proteins prostaglandin-H2 D-isomerase (PTGDS), α-1-microglobulin/bikunin precursor (AMBP), α-1-acid glycoprotein 1 (ORM1), immunoglobulin lambda-2 chain C (IGCL2), and secreted and transmembrane protein 1 (SECTM1) as possible biomarkers for distinguishing TB from LTBI or healthy controls using LC–MS/MS. This was based on analyzing urine samples from 21 active TB, 24 LTBI, and 18 healthy controls. They did not, however, validate the biomarker group in a second cohort or elucidate the diagnostic sensitivity or specificity.

Saliva and sputum, which contain thousands of proteins, mRNA, and bacteria, have long been utilized in biomarker research and as samples for diagnosis and assessment of numerous diseases (Ruhl, 2012, Carpenter, 2013, Kaczor-Urbanowicz et al., 2017, Sun et al., 2017). Proteomics methods have been used to reveal several protein biomarkers for the detection of TB in saliva. More recently, a novel salivary 5-protein bio-signature Alpha-1-antichymotrypsin, NAD(P)H-hydrate epimerase, Proteasome subunit beta type 6, Immunoglobulin kappa variable 1-33, and Neuroserpin was discovered using a QExactive Orbitrap Mass Spectrometer. After leave-one-out cross validation, this bio-signature was able to diagnose TB with an AUC of ≥ 0.80 (Mutavhatsindi et al., 2021). With an AUC of 0.75, a

signature in sputum consisting of β-integrin, vitamin D-binding protein, uteroglobin, profilin, and cathelicidin antimicrobial peptide was validated to discriminate active TB patients from non-TB patients using MS (Bishwal et al., 2019). According to a study by (Mateos et al., 2019), TB patients have a distinct concentration of proteins associated with complement activation, inflammation, and immune response regulation, as well as a decrease in proteins related to glucose and lipid metabolism in their saliva. Additionally, proteins linked to the innate immune response were shown to be significantly overrepresented in the sputum of uninfected people who previously had close contact with an active TB patient. Using an ultrafast sample-preparation approach, (HaileMariam et al., 2018) studied the sputum proteome of patients with active TB and LTBI, as well as healthy controls. They successfully identified a 49-protein signature to distinguish TB from control participants; however, this group of proteins was unable to distinguish LTBI from healthy controls.

3.3.3. Metabolomic TB biomarkers

Metabolomics offers the opportunity to obtain extraordinary insights into the biology of a host and pathogen during various disease processes. More so than alterations in gene expression, metabolites in particular can be seen as the final manifestation of the clinical phenotype in the host (Illig et al., 2010). As a result, untargeted methods, such as metabolomics, are a better approach for a broad search and assessment of significant biomarkers. This strategy also helps to address one of the key challenges in developing a reliable TB diagnosis test, whilst also addressing the inadequate understanding of host-pathogen interactions in TB (Preez et al., 2017). Compared to transcriptomics and proteomics, fewer studies have addressed the metabolomics changes that take place during infectious diseases, despite the fact that metabolic profiling has been effectively used to discover biomarkers in a variety of non-communicable diseases such as Alzheimer's disease (Han et al., 2002), sepsis (Langley et al., 2013), leprosy (Amaral et al., 2013) and diabetes (Salek et al., 2007). In order to identify large numbers of small-molecule metabolites in biological fluids or tissues, metabolomics approaches usually integrate nuclear magnetic resonance (NMR) spectroscopy-based or MS-based techniques with advanced biostatistics and bioinformatics methods to find potential regulated biological markers and metabolic processes related to a particular disease (Yu et al., 2013, Feng et al., 2015, Conde et al., 2021). Due to the high sensitivity of these techniques, it is possible to simultaneously identify and analyse a variety of low-abundance metabolites, such as those that may be generated from pathogens like Mtb (Frediani et al., 2014, Collins et al., 2016). In cell culture experiments, targeted metabolomics techniques have been utilized to

study certain metabolites and associated pathways in Mtb (Marrero et al., 2010) and Mtb-specific metabolites which may be associated with drug resistance (Loots, 2014).

A study by Weiner 3rd et al. (2012) assessed the viability of discovering serum small molecule biochemical profiles to get new biological understanding of TB processes with the aim to clarify the function of host metabolites during TB pathogenesis. They identified a number of notable variations between the metabolic profiles of healthy individuals and patients with TB, including comparatively lower abundances of amino acids, medium-chain fatty acids, and lysophosphatidylcholines. In individuals with active TB, comparatively higher abundances of fibrinopeptides and adenosine degradation products inosine, hypoxanthine, and ribose, as well as other substances, such as bile acids and uremic toxins were also noted. Metabolic characteristics of active disease showed increased indoleamine 2, 3 dioxygenase 1 activity, reduced phospholipase activity, elevated amount of adenosine metabolism products, and markers of fibrotic lesions. Additionally, they showed a connection between cytokine signaling and metabolic characteristics and that 20 metabolites are sufficient to distinguish TB patients from healthy people with a high degree of certainty (Weiner 3rd et al., 2012). Another metabolomics study used machine learning techniques to identify metabolite signatures that associate with risk of progression to TB across sub-Saharan Africa. Longitudinal variations in metabolic profiles were monitored in plasma and serum from HIV negative adults with TB, who either stayed heathy or developed TB. With the aid of external data sets and blinded test samples, the authors were able to create a trans-African metabolic bio-signature for TB that can detect future progressors, with a 69% sensitivity and 75% specificity in samples taken within five months after a diagnosis (Weiner et al., 2018). Conde et al. (2021) used untargeted NMR-based metabolomics to identify a biomarker profile for TB diagnosis in an effort to provide better diagnostic tools. In this study, blood serum samples from groups of healthy individuals, people with LTBI, and patients with pulmonary and extra pulmonary TB were analysed using ^{1}H NMR spectra. Based on their results, they proposed a signature for TB diagnosis consisting of inosine, hypoxanthine, mannose, asparagine, aspartate, and glutamate.

Despite paediatric TB being a significant contributor to the global TB burden, it is still difficult to diagnose due to inadequate detection techniques and a scarcity of childhood-specific TB biomarkers. A more recent study evaluated the potential of 30 small metabolites as biomarkers of childhood TB, using targeted LC–MS/MS to compare the levels of these metabolites in serum and Mtb antigen-stimulated whole blood cultures from children with active TB, LTBI, nonmycobacterial pneumonia, and healthy individuals. In serum and blood cultures from the

TB and LTBI groups, increased levels of leucine and kynurenine, together with decreased levels of citrulline and glutamine, were noted. Additionally, a drop in valine levels in blood cultures was linked to LTBI status. Citrulline and glutamine concentrations increased whereas leucine, kynurenine, and valine quantities decreased, thus defining the nonmycobacterial pneumonia metabolite profile. Leucine observed in serum and kynurenine found in stimulated blood cultures were found to have the strongest discriminatory capacity for diagnosing Mtb infection (Magdalena et al., 2022).

3.4. TB treatment associated biomarkers

Biomarkers can be utilized to improve treatment outcomes by informing therapy decisions for patients in clinical trials as surrogate endpoints (Wallis and Peppard, 2015). Patients with TB are typically placed on a four-drug treatment regimen (INH, RIF, PZA, and EMB), known as the intensive phase, for two months before beginning a four-month INH and RIF maintenance phase. Despite receiving anti-TB treatment for six long months, some individuals still relapse and have a higher risk of developing MDR or XDR-TB (Yong et al., 2019). Anti-TB therapy may have adverse effects during treatment, which further compound unfavourable outcomes such as treatment failure or disease relapse after treatment withdrawal (Linh et al., 2021). Therefore, new methods to monitor effectiveness of treatment response are urgently needed.

Sputum conversion by culture or microscopy is advised by current recommendations from WHO Global tuberculosis report 2021 (https://www.who.int/teams/global-tuberculosis-programme/tb-reports/global-tuberculosis-report-2021), along with radiographic examination, to monitor therapy response. Sputum culture conversion using solid medium, which has been explored in several studies either as a basic measure (for example, month 2 culture status) or in more intricate versions requiring sequential negative cultures (for example, stable culture conversion), is the best-characterized TB biomarker for effective therapy (Goletti et al., 2016). Sputum-based testing for therapy monitoring does have drawbacks. One of these is the significant decrease in sputum secretion that occurs following therapy, making the tests less accurate to predict outcomes. However, the likelihood of TB relapse can be correlated with considerable bacterial load at diagnosis as determined by a rapid time-to-positivity in bacterial culture (Rockwood et al., 2016, Magombedze et al., 2021). Omics-based methods are better able to accurately predict the development of TB disease and can provide a more complete view of disease processes (Kohonen et al., 2017). Recent improvements in omics technology have resulted in impressive efforts to characterize the molecular changes that direct the onset

and progression of a wide variety of complicated human diseases. In order to fully understand the molecular dynamics behind TB treatment, analyses of numerous datasets from various omics approaches are critical (Subramanian et al., 2020).

3.4.1. Transcriptomic biomarkers in TB treatment

Numerous transcriptome profiling studies have investigated the function of various inflammatory mediators as biomarkers during TB treatment. Some are linked to the severity of the illness and how well patients respond to TB therapy. Cliff et al. (2013) performed an *ex vivo* transcriptome analysis on peripheral blood samples taken from individuals with pulmonary TB, with a focus on monitoring changes following the start of treatment using microarray analysis. Their results showed that throughout the first week following TB therapy, the expression of 1261 genes were downregulated, including immune markers such as complement subunits C1q C2, which were initially upregulated. Later, the expression of B-cell markers, transcription factors, and signalling molecules increased. This was preceded by slower modulation in expression of other networks of genes. According to another study that focused on gene signatures in TB relapse, the expression of a 668-gene signature at diagnosis was significantly different in samples from the relapse group compared to the group that was cured, with 356 genes more upregulated in the cured group. The 18-gene differentially regulated signature contained eight genes that were expressed at higher levels in the group of patients who remained successfully treated. These included Pragmin, a Src family kinase regulator that helps immune cells by retaining the C-terminal Src kinase, a negative regulator, in the cytoplasm. Additionally, downregulated in relapse individuals was the transcription factor RUNX2, which might be preventing PI3K/AKT cell signalling (Cliff et al., 2016).

A possible transcriptomic biomarker for TB treatment that was previously evaluated in blood miRNA was also reported by Wang et al. (2018). They discovered that TB patient, who had successful treatment, harboured considerably lower levels of miR-21-5p, miR-92a-3p, and miR-148b-3p expression than TB infected patients. The level of miR-125a-5p was found to be considerably higher in patients with 2 months of treatment, compared to those who were not treated. The authors hypothesized that these three miRNAs contribute to the reduced frequency of mycobacteria-host associations during anti-TB therapy, which may be brought about by the downregulation of innate host defences. Additionally, the ongoing antibacterial activity of the host was likely the reason for the greater miR-125a-5p level observed in TB patients following a 2-month course of treatment. Many other studies of blood-based transcriptome and gene

expression profiles were investigated for treatment response, including the three-gene Sweeney3 signature (Francisco et al., 2017, Warsinske et al., 2018), the RISK11 signature (Darboe et al., 2019), and more recently the RISK6 signature (Penn-Nicholson et al., 2020).

3.4.2. Proteomic biomarkers in TB treatment

Due to the difficulty in validating Mtb clearance from patient tissues, the identification of proteomic Mtb cleared markers that can be employed for TB treatment monitoring is challenging. The common presumption regarding the eradication of Mtb from TB patients is based on clinical and radiological progress, in addition to sputum microscopy and/or Mtb culture. Acid-fast bacilli labelling and nucleic acid analysis, are still not sensitive enough to show complete removal of Mtb from the host during therapy (Horne et al., 2010). The IL2/IFN-γ ratio in serum of TB patients (Leem et al., 2018), MMP-8 levels (Sigal et al., 2017), and select cytokine profiles (Wanchu et al., 2009, Yong et al., 2019) are among some of the markers suggested to indicate a decrease in Mtb load in a host. Leem et al. (2018) examined how anti-TB drug therapy affects the various cytokines and inflammatory markers (IFN-γ, IL-2, IL-12, IL-10, IL-13 and TNF-α) in supernatants, as well as neutrophil count and neutrophil to lymphocyte ratio in whole blood of patients with active TB. They reported that, neutrophil, and platelet counts were considerably lower after therapy compared to baseline levels. Additionally, the IL-2/IFN-γ ratio was increased following therapy while the neutrophil to lymphocyte ratio considerably declined compared to baseline. They also concluded that the IL-2/IFN-γ ratio in the supernatant and the neutrophil to lymphocyte ratio could potentially serve as valuable biomarkers to determine the success of treatment in active TB patients.

Using a multiplexed electrochemiluminescence assay, seven proteins, Serum amyloid A1 (SAA1), Procalcitonin (PCT), IL-1, IL-6, C - reactive protein (CRP), Pentraxin-3 (PTX-3), and MMP-8, repeatedly demonstrated direct correlations with markers of baseline disease severity, smear grade, and cavitation; they were also significantly regulated by anti-TB therapy (Sigal et al., 2017). None of the above-mentioned studies was robust enough to demonstrate total removal of Mtb infection from the tissues. Another study looked for clearance biomarkers from *in vitro* Mtb-infected leucocytes treated with INH/RIF using LC-MS/MS, and subsequently verified using clinical samples from TB patients receiving treatment for active TB and LTBI. Then authors found that four Mtb lineages shared the clearance markers phosphophoseryl-tRNA kinase (PSTK), FKBP8, and MGMT. Additionally, PSTK was identified as a possible clearance signal during anti-TB therapy. After Mtb infection and clearance, PSTK was

inhibited and then re-expressed. Furthermore, the PSTK biomarker was verified using western blot analysis. Throughout the duration of anti-TB drug treatment, time-dependent increases of PSTK were observed in both active TB and LTBI individuals, but not in healthy people (Kaewseekhao et al., 2020).

Recently, a systematic review by Zimmer et al. (2022), summarised biomarkers that are associated with treatment monitoring and response in pulmonary TB. A meta-analysis of all available studies showed significant heterogeneity in terms of study design and data representation for TB therapy monitoring. But CRP, IL-6, IP-10 and TNF-α have enough information to evaluate fold changes among the selected biomarkers. Within the first eight weeks of treatment, all four of these biomarker levels fell in comparison to both baseline and earlier time points when data were gathered. With 11 studies evaluating longitudinal changes in marker level, IP-10 was the most often examined biomarker for treatment monitoring out of all biomarkers. The authors also suggested that CRP, IL-6, IP-10, and TNF-α biomarkers should be further investigated in the context of anti-TB therapy monitoring based on the minimal evidence that is currently available.

3.4.3. Metabolomic biomarkers in TB treatment

Multiple host metabolic pathways, including the metabolism of nitric oxide, amino acids such as tryptophan, glucose, and lipids like sphingomyelins, ceramides, eicosanoids, and phosphotidylcholines can all be affected by TB (Dutta et al., 2020). A pharmaco-metabolomics study discovered a drug-induced host-metabolomic variation before, and at various time points after treatment, in samples of individuals receiving intensive phase TB therapy for 4 weeks. These variations included: (I) a general decrease in oxidative stress levels throughout the TB treatment; (II) a time-dependent induction and inhibition of several enzymes in response to the drugs (CYP2E1, CYP3A4, alcohol dehydrogenase, and aminocarboxymuconate-semialdehyde decarboxylase) and altered oxidative stress levels (aconitase, formylglycine-generating enzyme, α-ketoglutarate dehydrogenase, and succinate-semialdehyde dehydrogenase); (III) an elevated urea cycle; and (IV) altered insulin synthesis. Their findings provided valuable insights into the mechanisms of TB drug metabolism, action, and side effects related to TB drugs (Combrink et al., 2019).

Bradykinin (BK) and its metabolite desArg9-bradykinin (DABK) were discovered (Qian et al., 2016) to be potential markers for anti-TB therapy. They reported that over the course of prolonged therapy, and beyond therapy completion, serum BK levels stayed relatively below

baseline levels and had decreased from their pre-treatment levels. The DABK levels, on the other hand, increased during therapy and fell at the post-therapy time point. BK levels were congruent with sputum culture conversions during prolonged therapy, indicating reduced Mtb load and positive treatment outcomes. However, following the end of treatment, elevated BK and DABK levels in one patient may have contributed to the development of recurrent TB infection. Yi et al. (2019) detected heparin anticoagulant in the plasma of TB patients who had not received treatment, those who had received treatment for two months, those who had recovered from TB, and healthy individuals using LC-MS. Following six months of TB therapy, analysis for differently expressed metabolites led to the discovery of four such metabolites, including L-histidine, arachidonic acid, biliverdin, and L-cysteine-glutathione disulfide. After two months of TB treatment, L-cysteine-glutathione disulfide and arachidonic acid could be found in all the patients. The study suggested that potential biomarkers for treated TB can be derived from the use of four metabolites L-histidine, arachidonic acid, biliverdin, and L-cysteine-glutathione disulphide in combination.

3.5 Rationale for this study

As the literature review has illustrated, quantum leaps have been made in the development of host biomarkers for monitoring risk of TB disease progression, diagnosis of active TB and for reporting on effectiveness of TB treatment and risk of disease recurrence. In contrast, much work is still needed to identify pathogen-specific biomarkers, with the greatest limitation being the low abundance of pathogen biomarkers compared to host. Furthermore, in cases where the pathogen is present in low numbers such as with subclinical or incipient disease, sampling the pathogen or its components directly is not possible with current techniques. A similar situation would prevail in cases of individuals who have completed treatment. In this context, using a pathogen-specific biomarker, which can be directly correlated with host responses, allows for the development of a host biomarker signature that is more attuned to the metabolic state and rate of clearance of the pathogen.

In chapter 2, we described the approach taken to assess prevalence of differentially culturable tubercle bacteria (DCTB) in clinical specimens. Given that DCTB display drug tolerance, they likely underpin the need for prolonged TB treatment. As such, monitoring the rates of clearance of DCTB provides a novel bacteriologic measure of treatment effectiveness. This sentiment is further substantiated given that DCTB provide a more accurate reflection of total bacillary load, when compared to conventional culture techniques and thus give a better sense of treatment

response. However, given that quantification of DCTB, which requires limiting dilutions and growth factors (as illustrated in chapter 2), is complex, associating host response patterns with levels of DCTB provides a framework to use immunological biomarkers to report on the response of DCTB to treatment. For such an analysis, a prospective cohort of individuals within whom levels of DCTB have been quantified during treatment, together with collection of plasma at the same time points, is required.

In prior work, our group established such a cohort to evaluate the use of DCTB to monitor treatment response (Peters et al., 2023). As a result, DCTB treatment response patterns were available together with plasma specimens with which biomarker studies could be conducted. The DCTB treatment response patterns in this cohort could be divided into three broad categories for immunological analysis including: (I) treatment responsive, (II) delayed responsive and (III) non-responsive. These different response patterns provided the ideal opportunity to investigate how varying clearance rates of differentially culturable organisms affects the immune response. Based on this, we propose a hypothesis and aims in the next section.

3.6. Hypothesis, aims and objectives

3.6.1. Hypothesis

We hypothesize that differences in the rates of DCTB clearance will be associated with unique cytokine responses that can be used to build predictive biomarkers to monitor treatment response.

3.6.2. Aim

To determine the cytokine response during treatment in TB patients and identify a biomarker signature (Chengalroyen et al., 2016) to discriminate between treatment-responsive, delayed-responsive and non-responsive individuals, based on DCTB levels as a measure of treatment effectiveness.

3.6.3. Objectives

Specific objectives were to:

- Optimize techniques for the Luminex multiplex bead array quantitation of 65 cytokines/chemokines.
- Test plasma samples of selected patients using Luminex multiplex bead array.

- Monitor changes in the concentration of the evaluated cytokines.
- Analyse and identify a biomarker signature to discriminate between treatment-responsive, delayed-responsive and non-responsive individuals.

3.7 Preliminary data to support the approach

In prior work, our laboratory demonstrated the presence of DCTB in the sputum of treatment naïve individuals where the prevalence of these organisms was significantly affected by the host immune response (Chengalroyen et al., 2016). Whilst these data suggested that limited detection of DCTB using current TB diagnostics likely affects diagnostic pickup, particularly in cases with paucibacillary TB, the implications on monitoring treatment outcome were not clear. To address this, our laboratory established a second prospective observational cohort of drug susceptible TB patients on standard chemotherapy. These individuals were intensively sampled during the first two weeks of treatment, followed by intermittent sampling during the remaining six months of TB chemotherapy. The sampling schedule (and specimens collected) is given in **Figure 3.2**.

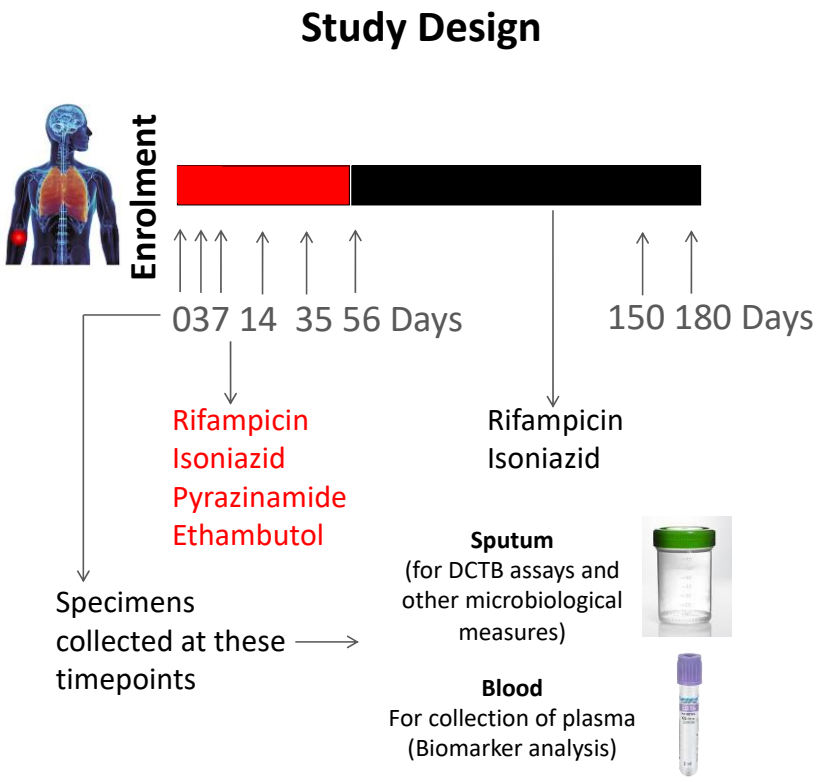

Figure 3.2. Study design for monitoring treatment response using DCTB. Shown is the sampling schedule for this study, with intensive sampling during early treatment and intermittent sampling towards the end of TB treatment. At all time points samples were collected as shown however at baseline, there was no blood collection. As a result, there was no baseline specimen for biomarker work.

Using the specimens collected from this cohort, limiting dilution assays were applied to determine DCTB levels at baseline, prior to TB treatment. The MPN assays was used with and without culture filtrate (CF) to recover DCTB (**Figure 3.3A**). In addition, the CF devoid of resuscitation promoting factors (Rpfs) was used to determine the effect of Rpfs on recovery of DCTB (**Figure 3.3A**). That data, shown in **Figure 3.3**, confirmed the presence of DCTB in these pretreatment sputum specimens and confirmed the substantive benefit in adding CF to MPN assays. Moreover, as noted in previous work, the presence of HIV infection significantly impacted on the recovery of the DCTB, particularly those DCTB populations that were recovered from MPN assays that were supplemented with CF (**Figure 3.3B**).

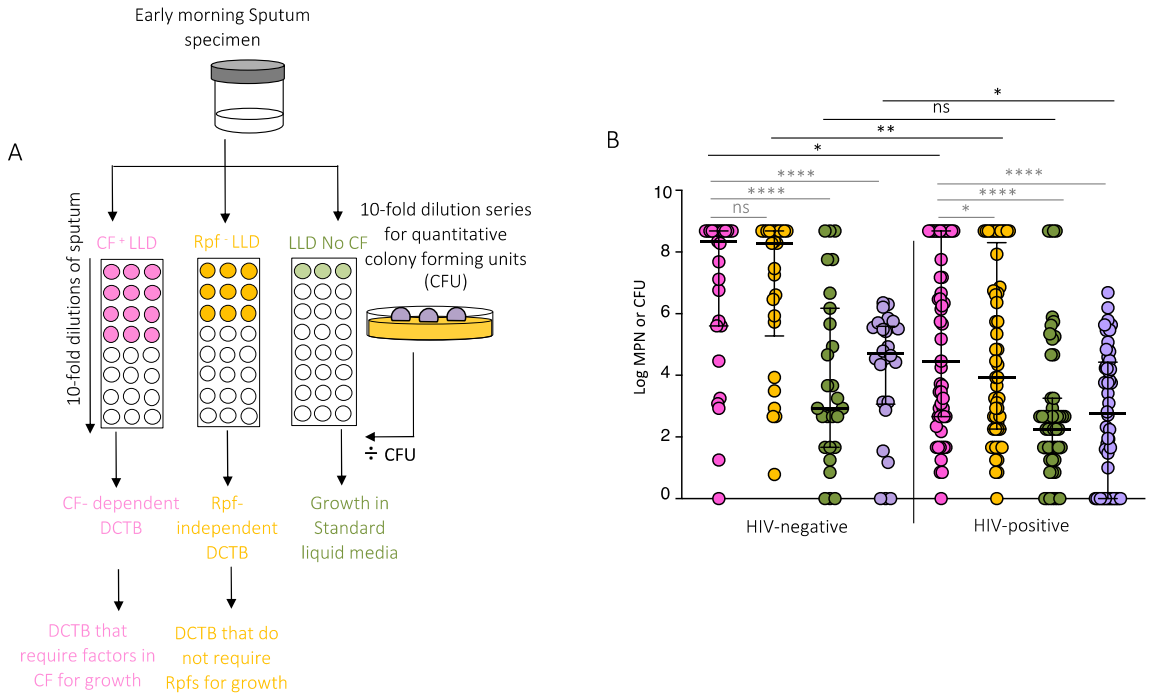

Figure 3.3. The use DCTB assays to detect bacteria in sputum specimens prior to TB treatment. (A) Format of Most probable number (MPN) assays to detect DCTB using different CF preparations and media only as a control. (B) Bacterial yield using Culture filtrate (CF)-supplemented (MPN) assays (pink), Rpf⁻CF-supplemented MPN assays (orange), un-supplemented MPN assays (green) and colony forming units (purple) in enrollment sputum from TB and TB-HIV infected individuals. *p<0.05, **p<0.01, ****p<0.0001. Data are from 80 participants at enrolment. Taken directly from Peters et al., 2023.

During treatment, we serially quantified DCTB levels, together with conventionally culturable CFUs and MGIT assays over the course of treatment. Overall, using data from 73 individuals available for analysis it was noted that DCTB cleared at a rate that was slower than that reported by CFUs and MGIT culture (**Figure 3.4A**, labelled as entire cohort). This treatment response pattern was underpinned by four response patterns: (I) Classic bi-phasic bacterial clearance; (II) early non-responders with slower clearance of DCTB; (III) paradoxical worsening with an

increase in bacterial count upon treatment initiation; and (IV) non-responders with no change in bacterial load, **Figure 3.4B-E**, respectively.

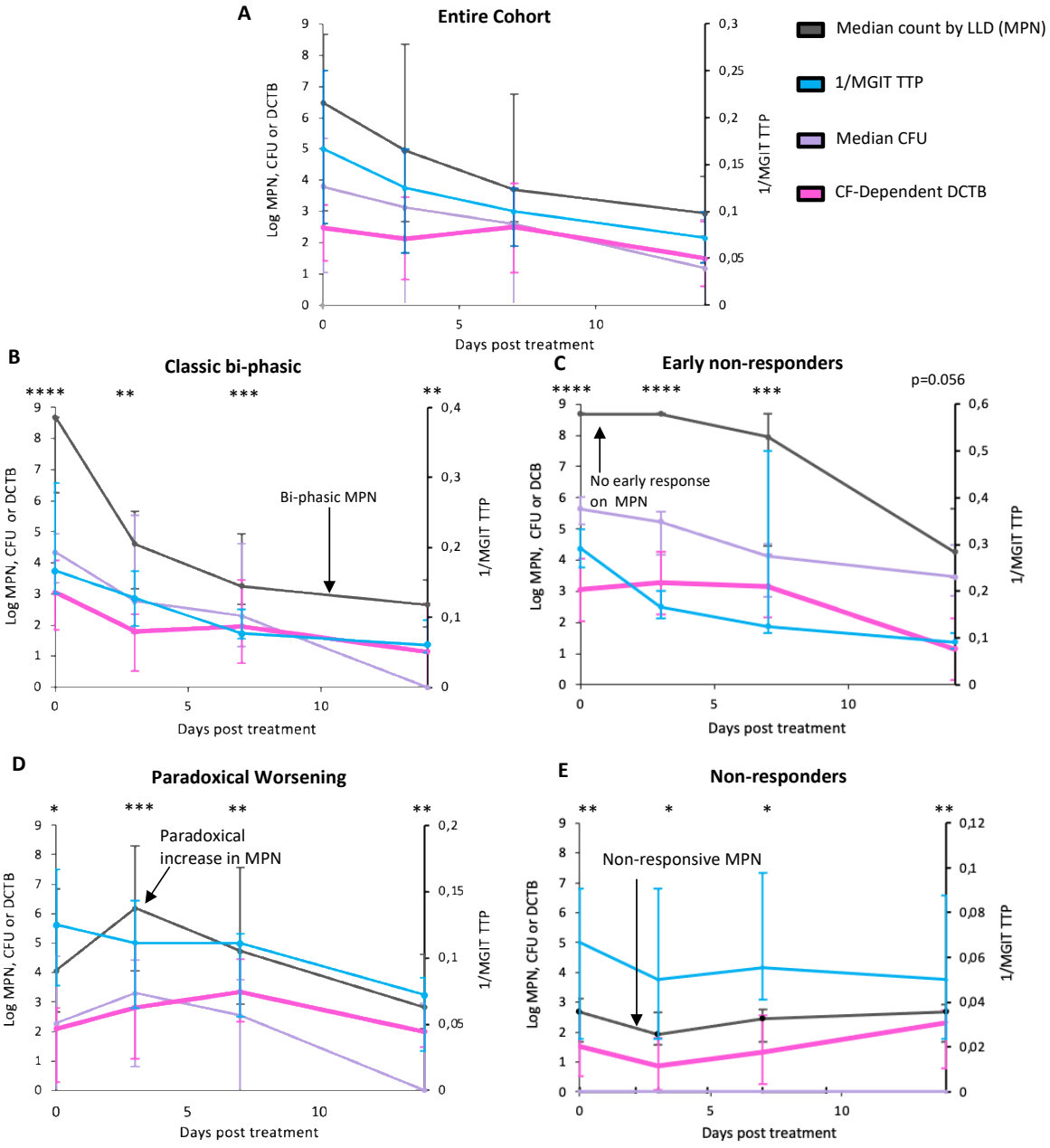

Figure 3.4. Bacterial clearance as reported by DCTB assays and routine measure of TB treatment response. (A) Trendlines for bacterial clearance in the entire cohort of 73 individuals available for analysis. (B-E) Bacterial clearance patterns divided into further subcategories including Classic bi-phasic, Early non-responders, Paradoxical worsening, and Non–responsive groups, based on the median trend line of the Most probable number (MPN) assay. Error bars represent the interquartile range. Taken directly from Peters et al., 2023.

Limitations of using this cohort: The availability of carefully collected sputum specimens and blood tubes for monitoring treatment response was useful for developing a framework for biomarker studies. The added benefit of DCTB assays being conducted on these specimens allowed for the ability to correlate treatment response patterns with immunological signatures. However, a blood tube was not collected at baseline, an unfortunate omission in protocol used by the clinical sites. Given that day 3 post treatment was the first time point used, and where the first blood sample was collected, we opted to use 3-days as our first sample. This was based on hypothesis that immunological signatures will not have substantively changed within the first two days of treatment.

To increase the available specimens, we also included additional specimens that were collected in this cohort but were not included in the Peters et al., 2023 publication. These specimens were collected according to the same protocol. The relative contributions of specimens from the published paper and unpublished data set (referred to as Phase 2) is given in the results section.

Controls: As controls, we opted to include healthy controls (with no TB disease) to compare treatment response in individuals with TB only and HIV progressors as controls to compare treatment response in individuals with TB-HIV co-infection.

Nomenclature: In Peters et al. (2023), treatment response patterns were labelled as Classic bi-phasic, Early non-responders, Paradoxical worsening, and Non–responsive groups. In this study, we simplified this nomenclature as follows:

Classic bi-phasic – referred to as treatment responsive in this study.

Paradoxical worsening – referred to as delayed responsive in this study.

Non–responsive - referred to as non-responsive in this study.

Early non-responders were not selected as these yielded minor changes in DCTB when compared to the paradoxical worsening group. As our selection was guided by those groups that appeared very different, possibly yielding distinct immune biomarker signatures, we opted to exclude the early non-responders from this study.

MATERIALS AND METHODS

3.7. Study Population

Participants (n=57; and further described in the results section) included those that were able to clear DCTB within the first two weeks of treatment (treatment-responsive), those with delayed ability to clear these organisms (delayed-responsive) and those whose TB bacterial counts persisted during treatment (non-responsive). As mentioned before, these groups of patients were classified, from a study done by Peters et al. (2023) in our lab (Human Research Ethics Protocol number: M140265, subsequently revised to the SNT study, Human Research Ethics Protocol number: M200164, PI: Bavesh Kana). Additional uninfected healthy controls as well HIV+ progressors were obtained from the National Institute for Communicable Diseases (NICD), Human Research Ethics Protocol number: M190995, PI Caroline Tiemessen.

3.8. Sample preparation

Plasma samples were allowed to thaw on ice and were then centrifuged at 4000 x g for 15 minutes. Ten separate aliquots were carefully removed with using a 200 µL pipette and added into 1.5 mL cryotubes. The cyrotubes tubes were clearly labelled and stored at –80°C until use.

3.9. Luminex multiplex immunoassay

We used a 65-plex Luminex Bead Array Multiplex Immunoassay (ProcartaPlex^{TM}, Invitrogen, ThermoFisher Scientific, to quantify cytokines, growth factors, chemokines and soluble receptors (see **Table 3.1**) in plasma samples. Blood plasma previously stored was incubated with bead array of specific cytokines following the manufacturer's protocol with minor modifications. The details for this assay and how it was conducted have been provided in Chapter 2 section 2.10.10. The only difference was the use of a 6-plex in chapter 2 versus a 65-plex here. The functional categorization of the analytes into cytokines, chemokines, growth factors and soluble receptors is shown as a shading of a different colour in **Table 3.1**.

Table 3.1: Standard curve assay ranges for each target (lot-specific) in the ProcartaPlex Immune Monitoring 65-plex Panel.

Analyte (Bead region)	Standard Curve Range (pg/mL)	Analyte (Bead region)	Standard Curve Range (pg/mL)
APRIL (88)	82.37–337400	IL-17A (36)	24.34–99700
BAFF (86)	8.35–34200	IL-18 (66)	9.72–39800
BLC (CXCL13) (29)	12.23–50100	IL-20 (81)	9.06–37100
CD30 (84)	10.35–42400	IL-21 (72)	9.08–37200
CD40L (74)	4.76–19500	IL-22 (76)	17.82–73000
ENA-78 (CXCL5) (82)	4.61–18900	IL-23 (63)	14.79–60600
Eotaxin (CCL11) (33)	1.65–6750	IL-27 (14)	17.36–71100
Eotaxin-2 (CCL24) (30)	4.39–18000	IL-2R (9)	84.03–344200
Eotaxin-3 (CCL26) (49)	2.23–9150	IL-31 (37)	19.14–78400
FGF-2 (75)	5.1–20900	IP-10 (CXCL10) (22)	3.08–12600
Fractalkine (CX3CL1) (59)	2.47–10100	I-TAC (CXCL11) (57)	11.06–45300
G-CSF (42)	9.86–40400	LIF (15)	3.83–15700
GM-CSF (44)	15.97–65400	MCP-1 (CCL2) (51)	3.83–15700
Gro-α (CXCL1) (61)	3.1–12700	MCP-2 (CCL8) (8)	0.82–3350
HGF (46)	3.44–14100	MCP-3 (CCL7) (68)	4.83–19800
IFN-α (48)	4.69–19200	M-CSF (67)	65.45–268100
IFN-ɣ (43)	13.13–53800	MDC (CCL22) (87)	13.43–55000
IL-1α (62)	1.61–6600	MIF (53)	0.78–3200
IL-1β (18)	3.74–15300	MIG (CXCL9) (69)	8.64–35400
IL-2 (19)	21.97–90000	MIP-1α (CCL3) (12)	3.05–12500
IL-3 (73)	22.97–94100	MIP-1β (CCL4) (47)	4.57–18700
IL-4 (20)	19.82–81200	MIP-3α (CCL20 (56)	21.04–86200
IL-5 (21)	6.74–27600	MMP-1 (64)	5.13–21000
IL-6 (25)	7.98–32700	NGF-β (55)	5–20500
IL-7 (26)	0.45–1850	SCF (39)	3.39–13900
IL-8 (27)	2.78–11400	SDF-1α (CXCL12) (13)	56.86–232900
IL-9 (52)	9.89–40500	TNF-α (45)	5.52–22600
IL-10 (28)	2.21–9050	TNF-β (54)	6.42–26300
IL-12p70 (34)	7.4–30300	TNF-R2 (85)	2.91–11900
IL-13 (35)	3.61–14800	TRAIL (58)	11.01–45100
IL-15 (65)	3.34–13700	TSLP (80)	4.71–19300
IL-16 (70)	17.26–70700	TWEAK (97) & VEGF-A (78)	709.72–2907000 6.84–28000

3.9.1. Data analysis

The concentration of each cytokine was automatically determined by the Bio-Plex analysis software on the Luminex instrument. This was done by plotting the expected concentration of the standards against the Mean fluorescence intensity (MFI) generated by each standard. A 4PL or 5PL algorithm was chosen for the best curve fit. For each analyte, the calculated concentration values are reported, and data recorded as out of range (OOR) were assigned zero, as they were below the limit of detection.

3.9.2. Statistical analysis

Statistically significant differences between these groups were analysed using the non-parametic Kruskal-Wallis test in conjunction with Dunn's multiple comparisons on GraphPad Prism v9.0.2 software. A p value of <0.05 was considered statistically significant.

3.9.3. Heat map, principle component and ROC analysis

Assistance was obtained from Stanford Kwenda with these statistical approaches. Heatmaps were generated using the Complex-Heatmap package in R (Gu et al., 2016). PCA plots were generated using the bioplot function of the PCA tools package, run in R (Blighe et al., 2019).

RESULTS

3.10. Stratification of participants and study definitions

Our lab has previously investigated changes in DCTB during standard TB treatment with the outlook of identifying new bacterial biomarkers for assessing TB treatment response (Peters et al., 2023). A total of 175 individuals were recruited to this study through the Perinatal HIV Research Unit (PHRU) from TB diagnostic clinics in the Soweto and Klerksdorp areas in South Africa. Patients with a positive GeneXpert MTB/RIF result, before initiation of TB treatment were recruited into the study and those with a RIF resistant GeneXpert were excluded. Other inclusion criteria were: participants had to be at least 18 years of age, able to produce a sputum sample of ≥ 3 ml, have either evidence of HIV infection (using laboratory tests or rapid tests) or a recent hard copy HIV test result, and should have no prior history of treatment for TB. Following informed consent, spot and overnight (collected early in the morning) sputum samples were collected, together with blood for all timepoints shown in **Figure 3.2**, except for baseline (prior to start of treatment) where blood was not collected. Sample collection timepoints whilst patients were taking TB treatment (acceptable visit windows enclosed in parentheses) were: 3 (2 – 4), 7 (5 – 10), 14 (12 – 19), 35 (30 – 40), 56 (50 – 65) and 180 days (170-190) after treatment initiation.

As mentioned in section 3.7, participants were classified into different treatment response patterns including individuals who were either rapidly able to clear DCTB by the 7th day of treatment (treatment-responsive), those who had accumulation of DCTB on day 3 of treatment, followed by a rapid decline (delayed responsive) or those whose TB bacterial counts persisted during treatment (non-responders).

The specimens were collected from the same cohort, but at different times. First collection of plasma came from specimens outlined in the Peters et al., 2023 publication (further detailed in section 3.7). Upon compilation of the manuscript, recruitment and sputum specimen collection still continued, and were subjected to the same analysis, yielding DCTB response patterns. Specimens collected after publication are referred as Phase 2 specimens, this is further detailed in **Figure 3.5**. Specimens from before publication (Peters et al., 2023) and after (Phase 2) were combined to give a total of 57 participants who were included in this work (**Figure 3.5**).

The demographic details of these selected participants and controls are given in **Table 3.2**.

Table 3.2: Patient demographics.

	Healthy controls (n=25)	HIV+ progressors (n=17)	HIV/TB co-infected patients (n=41)	TB patients (n=16)
Age (years) (IQR)	33 (27-37)	36 (32-42)	38 (33-48)	38 (25-51)
Male/ Female	8/17	8/9	24/17	12/4
Body mass Index (BMI)	ND	ND	19.9 (18.2-22.3)	19.4 (18.0-22.5)
CD4 count [cells/dl, IQR]	ND	109 (90-167)	153 (93-239)	ND
>500		2	4	
200-500		1	11	
50-200		11	20	
<50		2	6	
Viral Load[#] (copies/ml, IQR)	ND	87069 (23264-278566)	188682 (78537-343804)	ND
No. of patients on ART	Not relevant	17	5*	Not relevant

* Data from only 5 participants was available in the database
Values are shown as median (The range given represents the first and third quartiles)
ND- not done
[#] No significant difference in viral loads between HIV progressors and TB/HIV co-infected individuals

3.11. Luminex bead array for cytokine concentrations

The ProcartaPlex Human Immune Monitoring 65-plex Panel was chosen for the diversity and quantity of cytokines, chemokines, and growth factors. The panel enables the identification of several inflammatory markers that report on the immune response to TB infection.

Prior to using all our specimens, we first aimed to check the technical aspects of the Luminex technique in our hands. We randomly selected 3 patient samples at four time points (3, 7, 14 and 180 days of treatment), to capture the concentration range between early days of treatment and at the end of treatment. The aspects we wanted to test, included determining the best quantity of beads in each well, assessing the presence of cytokines at low concentrations, and evaluating the sensitivity and assay range of the Luminex kit. The manufacturer's specified

standard curves were used as directed. The kit performed well within the manufacturer-recommended standard curve parameters. The lower limit of quantification (LLOQ) and upper

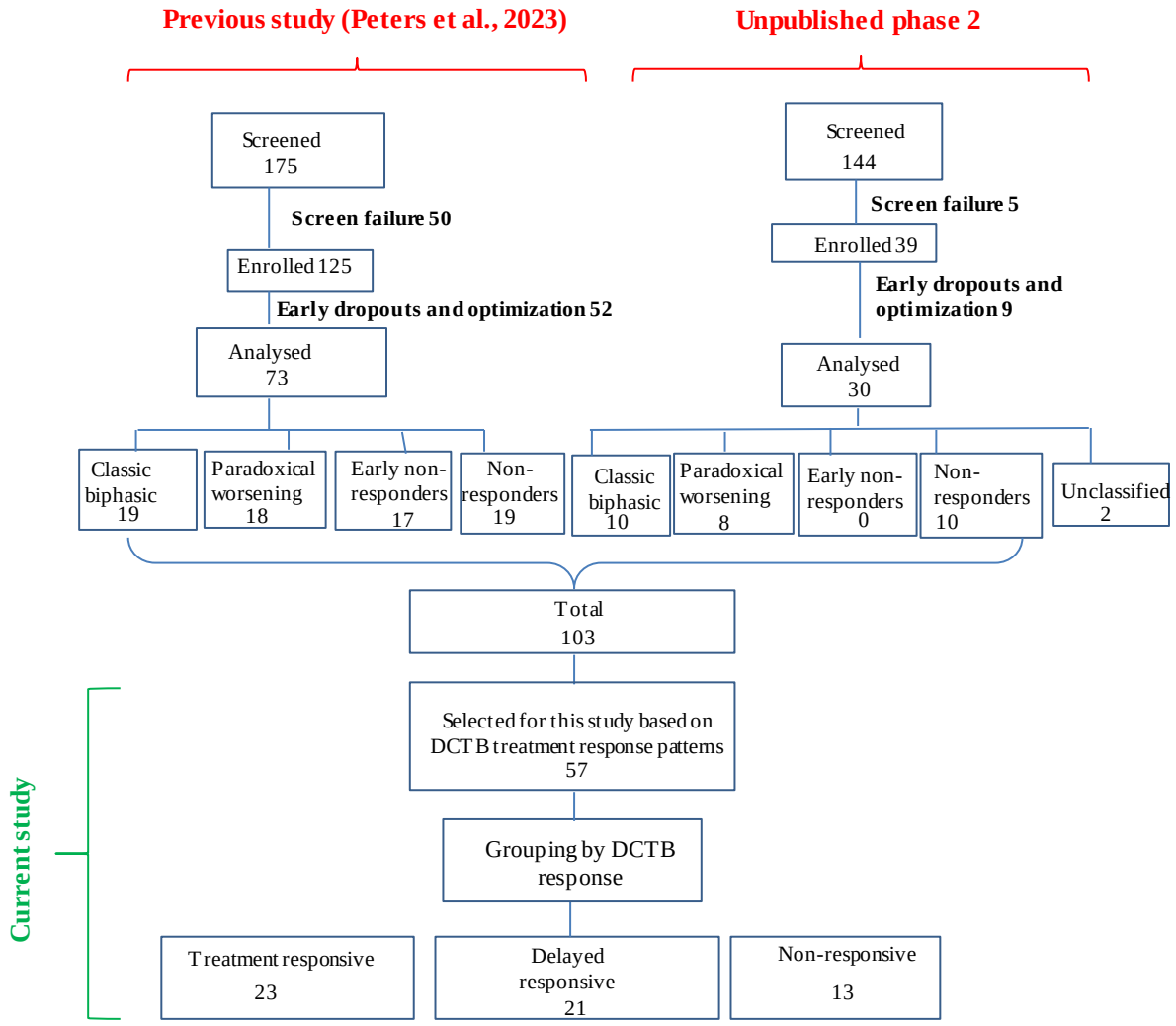

Figure 3.5. A Flow diagram outlining the categorisation of study participants. This study examined 319 potential volunteers from primary health care clinics in the Soweto and Klerksdorp districts. The bold text represents patients who were removed from the study for various clinical and laboratory reasons from each cohort. Potential participants who were initially recruited for the study and subsequently found to not meet the standards requirements (50 from phase 1 and 5 from phase 2) are referred to as screen failures. Some participants dropped out during the study and were then removed from the final analysis. The analysis revealed four patterns (Classic bi-phasic, Early non-responders, Paradoxical worsening, and Non–responsive group) based on the DCTB amount in patients' sputum during treatment. For our study we selected 57 patients from the Peters et al., 2023 publication and phase 2, and simplified the nomenclature to treatment responsive (Classic biphasic), delayed responsive (Paradoxical worsening) and non-responsive (non-responsive).

limit of quantification (ULOQ) performance was most similar to the manufacturer-provided product information for each of the analytes, **Figure 3.6A-J**, shown for a select set of analytes. We displayed 10 plots each for the standard curves and the analyte concentrations in our

samples, **Figure 3.6A-J** and **Figure 3.7A-J**, respectively. The graphs in **Figure 3.7A-J**, are shown to prove that this assay was able to detect readable amounts of different concentrations in our plasma samples. Furthermore, this approach allowed us to establish that no dilution of the plasma would be required when scaling the experiment up. Similar data were obtained for all 65 analytes, the remainder are not shown for brevity. Statistical analysis was done to

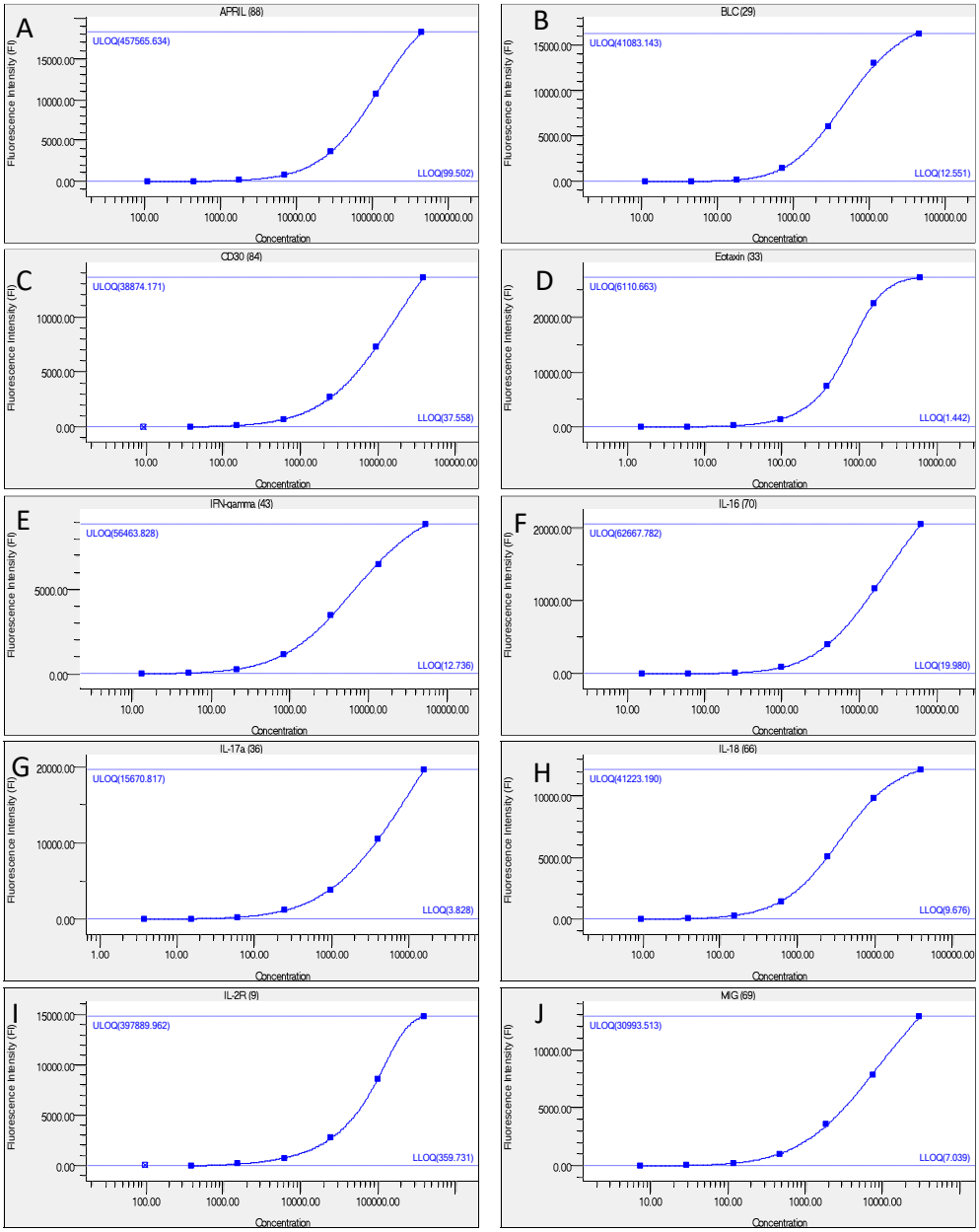

compare differences in the cytokine concentrations during treatment, but no significance was observed and this was mainly due to the small sample size used for assessing technical aspects.

Figure 3.6. Reproducibility of standard curve relative to manufacturer standard. Standard curves were run for all 65 analytes on three patient samples at day 3, 7, 14 and 180, to determine if they matched the profile provided by the manufacturer and if they yielded a quantitative increase that was proportionate to the increase in analyte concentration. Each analyte is shown in a separate plot with the Lower limit of quantification (LLOQ) and

the upper limits of quantification (ULOQ). Panels A-J represent APRIL, BLC, CD30, EOTAXIN, IFN-γ, IL-16, IL-17A, IL-18, IL-2R and MIG, respectively.

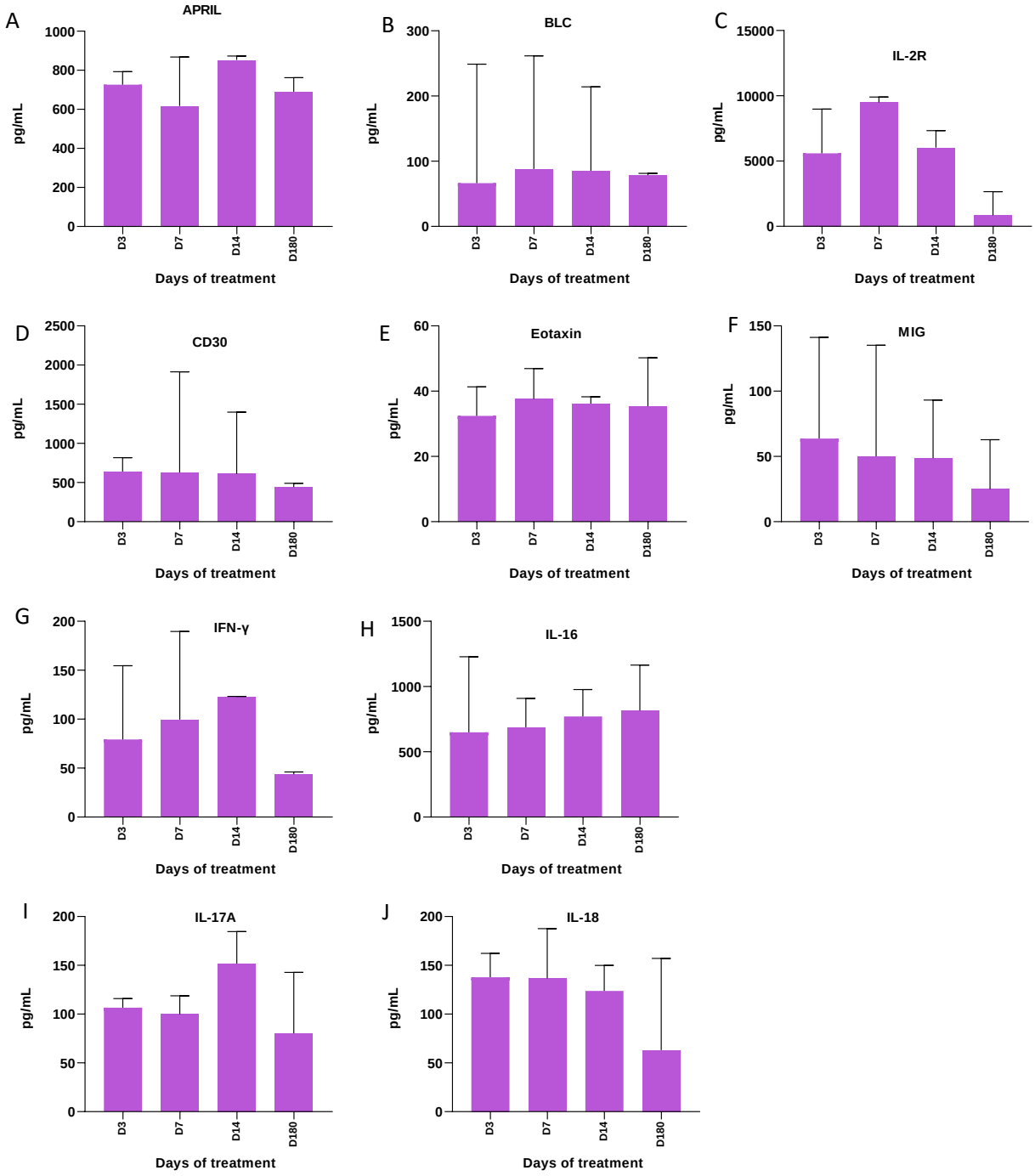

Figure 3.7. Cytokine profiles in specimens selected for technical assessment. The concentration of APRIL, BLC, CD30, Eotaxin, IFN-γ, IL-16, IL-17A, IL-18, IL-2R, and MIG in the plasma of TB patients during treatment is given in panels A-J. The concentrations are expressed in pg/mL and were analysed by the non-parametric Kruskal-wallis test, with significance $P < 0.05$ (Post hoc Dunn's multiple comparisons). No significant differences were observed.

After obtaining reliable results to a selected panel of the cytokines, we then decided to use this approach on the entire specimen collection selected. In the next sections, a summary of our findings is given, followed by a detailed exposition of the results.
The analysis plan for profiling cytokine abundance in all specimens from TB cases and controls was as follows:

1. First, cytokine levels were compared between groups (TB, TB/HIV, healthy controls and HIV+ progressors) at the day 3 time point, which was taken as the baseline for this study, as detailed previously.
2. Next, cytokine levels from HIV+ progressors were compared to HIV/TB individuals at all the time points (days 7, 14, 35, 56 and 180 post treatment) to assess changes in cytokine profiles during treatment and upon treatment completion. As TB treatment takes 6 months, day 180 was considered as the time point for treatment completion.
3. Following this, cytokine levels from healthy controls were compared to individuals with TB at all the time points (days 7, 14, 35, 56 and 180 post treatment) using the same approach outlined in point 2 above.
4. To assess the effect of HIV within the cohort, cytokine levels were also compared between individuals with TB and TB/HIV at all the time points.
5. We attempted to correlate CD4 counts and viral loads with cytokine concentrations, within TB/HIV infected individuals.
6. We use a series of analyses - hierarchical clustering and Principal Component Analysis (PCA) - to determine if patterns of cytokine responses emerge, based on DCTB response patterns.
7. Following this, cytokine profiles were compared between DCTB response patterns.
8. Finally, Receiver Operator Curves (ROC) were plotted for select cytokines to assess their potential to predict treatment response.
9. We also conducted two additional analyses, aimed at investigating (I) whether TB strain type has an effect, and (II) whether residual DCTB at the end of treatment affected cytokine levels. In these two cases, no significant differences were noted, and the data are presented in the Appendix A.

In the next sections, the data are presented in the same order as indicated above.

3.12. Cytokine/chemokine clustering among healthy controls, HIV+ controls, TB/HIV+ and TB/HIV- at day 3 of TB treatment.

Heat map analysis was done for the 65 cytokines, chemokines and growth factors to differentiate the TB and TB/HIV co-infected groups from the control groups and from one another in order to determine if Mtb infected individuals are clearly identified by global patterns of cytokine expression. An overview of the profile between the four groups (TB, TB/HIV and Healthy Controls as well as HIV+ progressors) can be seen in **Figure 3.8**, where the concentrations of the 65 immune mediators are presented as a colour-coded heat map, created using unsupervised hierarchical clustering. Although there was no global trend between the groups that emerged, which was unexpected, we could immediately identify select cytokines that appeared to be differentially modulated.

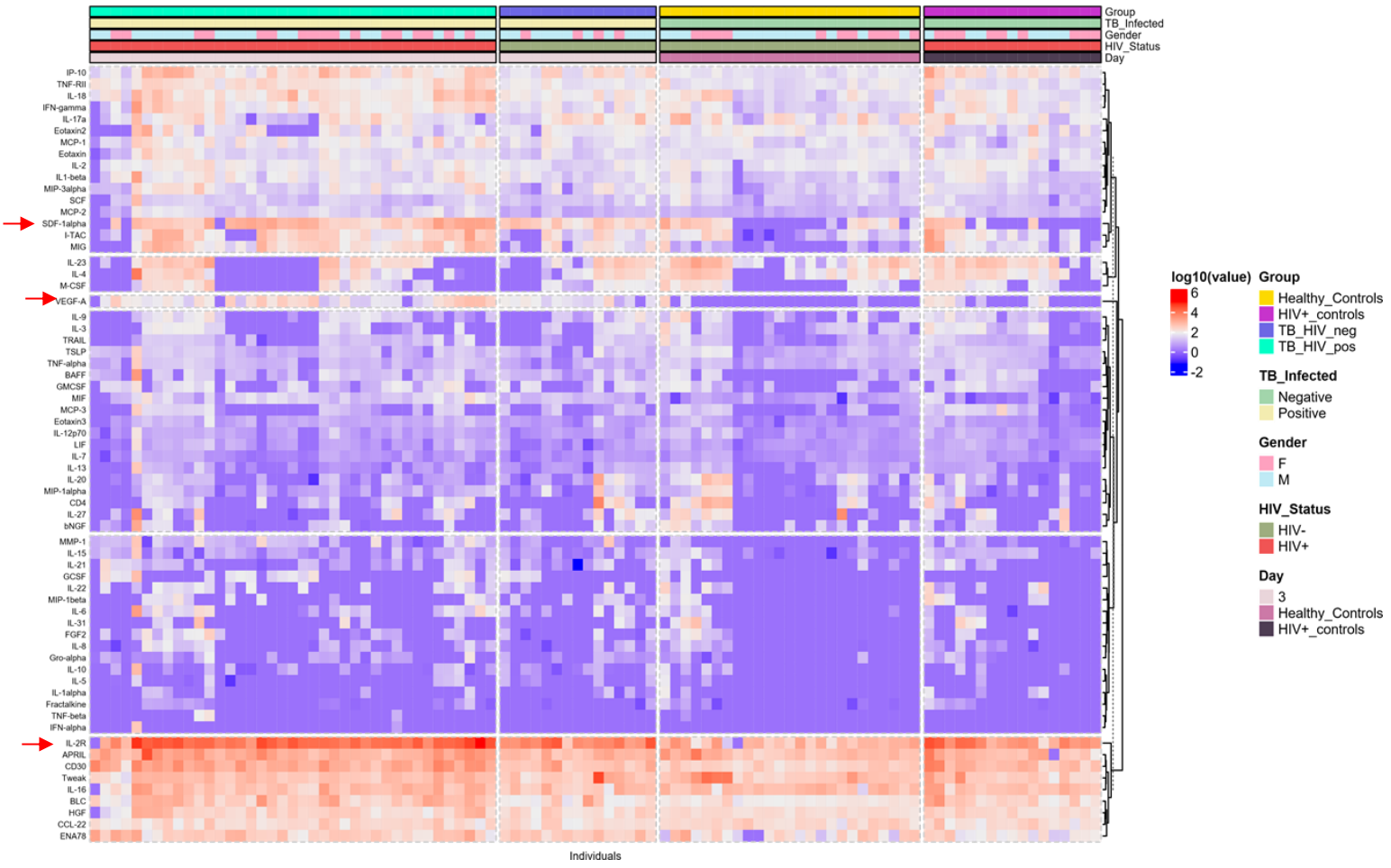

Figure 3.8. Heat map of cytokine and chemokine concentrations among the Healthy and HIV+ controls and different groups of individuals (TB only and TB/HIV co-infected). The heat map represents an unsupervised clustering of cytokine and chemokine concentrations in the inflammatory immune response of 99 individuals (every column indicates one patient) and cytokines/chemokines abundance (rows). Heat map colour corresponds to the Log-transformed concentrations (pg/mL). The spectrum of red to blue corresponds to increasing gradient of chemokine/cytokine concentrations. Red arrows depict examples of differentially regulated cytokines.

As an example, IL-2R is highly expressed in the TB/HIV+ group relative healthy controls. As another example VEGF-A is differentially expressed in TB-infected individuals (with and without HIV) relative to controls. In addition, SDF1-α is also differentially expressed between the different groups.

3.13. Distinguishing cytokine distribution among healthy controls, HIV+ controls, TB/HIV+ and TB/HIV- at day 3 of TB treatment.

Following the clustering analysis, we conducted PCA analyses to investigate the distribution of cytokine profiles among the four groups. An 80% explained variation was seen in PC1 to PC20, as shown in the scree plot in Figure **3.9A**. A clear distinction appeared between healthy controls, HIV+ progressor, TB/HIV+ and TB/HIV- from the PCA analysis (**Figure 3.9B**). This analysis revealed that I-TAC, MIG, SDF-1α, GSCF and VEGF-A were the most important factors determining the discrimination power of the PCA model between healthy controls and HIV+ progressors, TB/HIV+ and TB/HIV- groups.

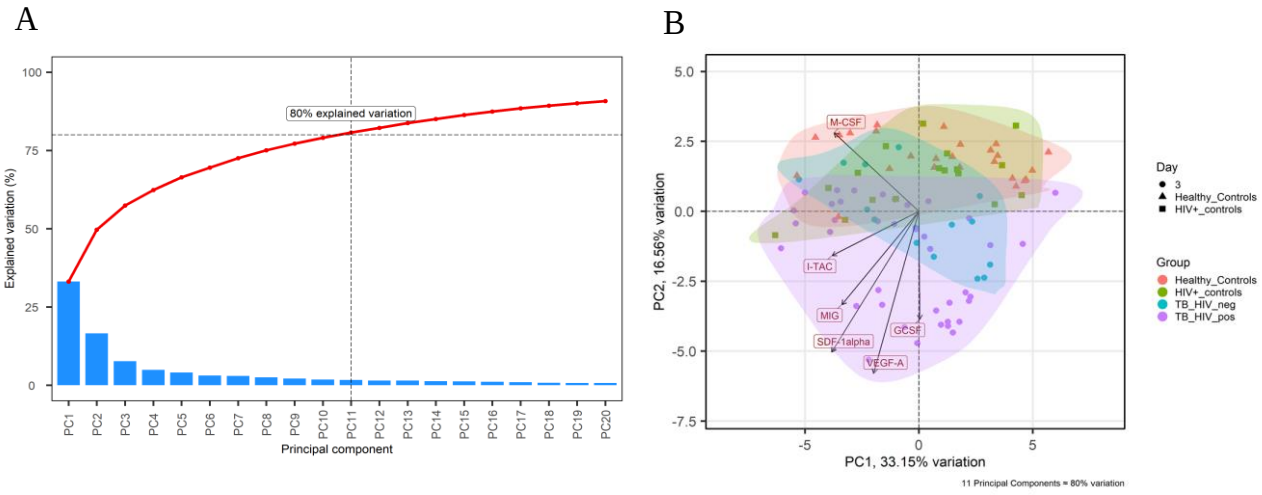

Figure 3.9. Principal Component Analysis (PCA) of cytokines and chemokines among the controls and different groups of patients at day 3. The cytokines and chemokines from plasma were measured using a 65-plex luminex kit. (A) Scree plot showing the cumulative percentage of variation in each of the first 20 principal components. (B) PCA plot highlighting the variations between healthy controls, HIV+ controls, TB/HIV+ and TB/HIV- at day 3 of TB treatment, based on variability captured in PC1 and PC2, both of which represent the bulk of the variation observed.

To further delve into these data, individual cytokines were analysed and represented as scatter plots. These are shown **Figure 3.10,** where cytokine profiles at day 3 and the other time points during treatment are compared with controls, which will be discussed below.

3.14. HIV-Associated TB biomarkers.

To investigate whether any of the analysed host markers captured in PCA1 to PCA20 could potentially be used as markers to monitor TB treatment response, we evaluated the concentrations of the cytokines in plasma at different days post treatment in HIV/TB co-infected individuals compared to HIV progressors. The data for select cytokines that displayed significant differences are given in **Figure 3.10**. Where no difference was observed (either between controls and then TB/HIV infected group, or within different time points in the TB/HIV group), the data are not shown. The plasma concentrations of eight host markers (IL-3, IL-4, IL-7, IL-9, IL-23, IP-10, MCP-3 and M-CSF) were lower at the end of treatment when compared to HIV progressors (**Figure 3.10A, B, C, D, E, F, G and H**, respectively and **Table 3.3**, highlighted in green). In contrast, ENA-78, G-CSF, MCP-1, MIF and SDF-1α were significantly higher at treatment completion when compared HIV progressors (**Figure 3.10I, J, K, L** and **M, Table 3.3**, highlighted in orange). There were thirteen cytokines (APRIL, CD30, Eotaxin, Eotaxin-3, IL-2R, IL-10, IL-17A, IL-18, LIF, MIG, MMP-1, TNF-R2 and VEGF-A) that returned to similar levels at treatment completion when compared to HIV progressors **(Figure 3.10N, O, P, Q, R, S, T, U, V, W, X, Y** and **Z, Table 3.3**, highlighted in yellow). Together, the cytokines that reduced substantively (green in **Table 3.3**) and the ones that yielded levels comparable to HIV progressors (yellow in **Table 3.3**) could potentially be used to monitor treatment response. The concentrations of I-TAC, BLC, IL-6, IL-8, IFN-γ, IL-15, IL-22, MCP-2, and MIP-3α were not significantly different between HIV progressors and HIV/TB co-infected patients at any of the treatment days, but there were differences in abundance of these cytokines within the TB/HIV group as treatment progressed, shown in **Figure 3.10AA, BB,CC, DD, EE, FF, GG, HH, II, JJ, KK and LL** respectively.

We next investigated the changes in the concentrations of all the 65 markers over the treatment period in the TB/HIV+ patients and noted that the cytokines IL-4, LIF, ENA-78, GCSF, MCP-1, IL-9 and Eotaxin-3 cannot be used to monitor treatment changes longitudinally in this group of patients (**Figure 3.10 B, D, I,J,K,Q, and V** – in this case there are no significant differences between the treatment time points and as a result, no significance bars are given in the figures). In contrast, I-TAC, BLC, IL-6, IL-8, Gro-α, MIP-1α, IFN-γ, IL-15, IL-22, MCP-2, MIP-3α and TRAIL showed significant differences at distinct time points during TB treatment (**Figure 3.10AA, BB, CC, DD, EE, FF, GG, HH, II, JJ, KK and LL**).

Table 3.3: Cytokine changes during TB treatment in TB/HIV co-infected individuals.[Ψ]

Cytokine	HIV progressors# (pg/mL)	Day 3 (pg/mL)	Day 7 (pg/mL)	Day 14 (pg/mL)	Day 35 (pg/mL)	Day 56 (pg/mL)	Day 180 (pg/mL)
IL-3	40.69	19.41	15.57 *	19.24	9.658****	24.10 ***	6.680 ***
IL-4	141.6	76.40 **	73.07 **	79.92 *	7.624****	17.75****	47.14 ***
IL-7	4.508	3.943	3.440	3.956	2.505 **	1.989 ***	2.464*
IL-9	22.19	22.35	15.10	24.66	2.998 **	4.946 *	8.523 *
IL-23	243.9	128.3 *	113.3 *	108.7 *	24.95****	29.07****	74.51 **
IP-10	256.1	277.7	215.5	292.5	142.0	108.7	67.71 **
MCP-3	15.49	10.74	8.084	8.494	7.863	8.770 **	5.183 *
M-CSF	59.73	40.74	30.40	39.06	4.854 ***	8.871****	14.72 **
ENA-78	129.2	427.4 **	461.2***	544.2****	614.7****	713.3****	520.7****
G-CSF	0.000	28.31 *	17.69	25.04 *	37.59 ***	50.00****	21.85 *
MCP-1	37.77	87.57 *	93.23 **	111.6****	111.9 ***	106.9 **	97.08 ***
MIF	6.825	25.14***	27.96****	26.57****	31.56****	26.39****	18.97*
SDF-1α	138.5	653.5***	604.2**	692.2***	928.4****	818.5****	603.0**
APRIL	672.2	1457 **	1241 *	1468 *	1403 **	1285 *	782.1
CD30	1281	1752	1853	1912 *	1909 **	2029 **	1026
Eotaxin	76.96	56.36	56.96	59.87	30.52 *	27.52 **	41.69
Eotaxin-3	4.854	9.731 *	7.581	8.352 *	7.719	8.760	6.503
IL-2R	6459	17163 **	13856 *	16104 *	14354	13094	5180
IL-10	2.312	3.561	3.270	4.946	6.521 ***	6.651 **	3.882
IL-17A	108.8	91.94	103.6	125.5	28.79 ***	54.19 **	67.38
IL-18	117.7	260.6 **	225.2 **	249.2 **	235.4 **	211.6 *	124.8
LIF	5.794	6.252	4.715	6.081	3.939	3.405 *	3.492
MIG	241.7	273.9	284.8	304.6*	219.9	169.7	48.54
MMP-1	4.515	32.03*	29.83	26.40	11.06	19.98	9.908
TNF-R2	71.72	142.6***	146.0***	141.9***	169.1****	154.4****	94.02
VEGF-A	36.18	143.0**	141.1**	118.6*	182.6****	176.6****	43.09

[Ψ]Green colour represents cytokines that were significantly lower upon TB treatment completion when compared to HIV progressor controls, Orange colour represents cytokines that were significantly higher upon TB treatment completion when compared to HIV progressor controls, Yellow colour represents cytokines where the levels obtained after TB treatment completion were comparable to HIV progressor controls.

[#]HIV progressors are used as controls for assessing TB cure in TB/HIV co-infected individuals

Concentrations (pg/mL) are shown as mean

*P <0.01; **P < 0.001; ***P < 0.001; ****P < 0.001

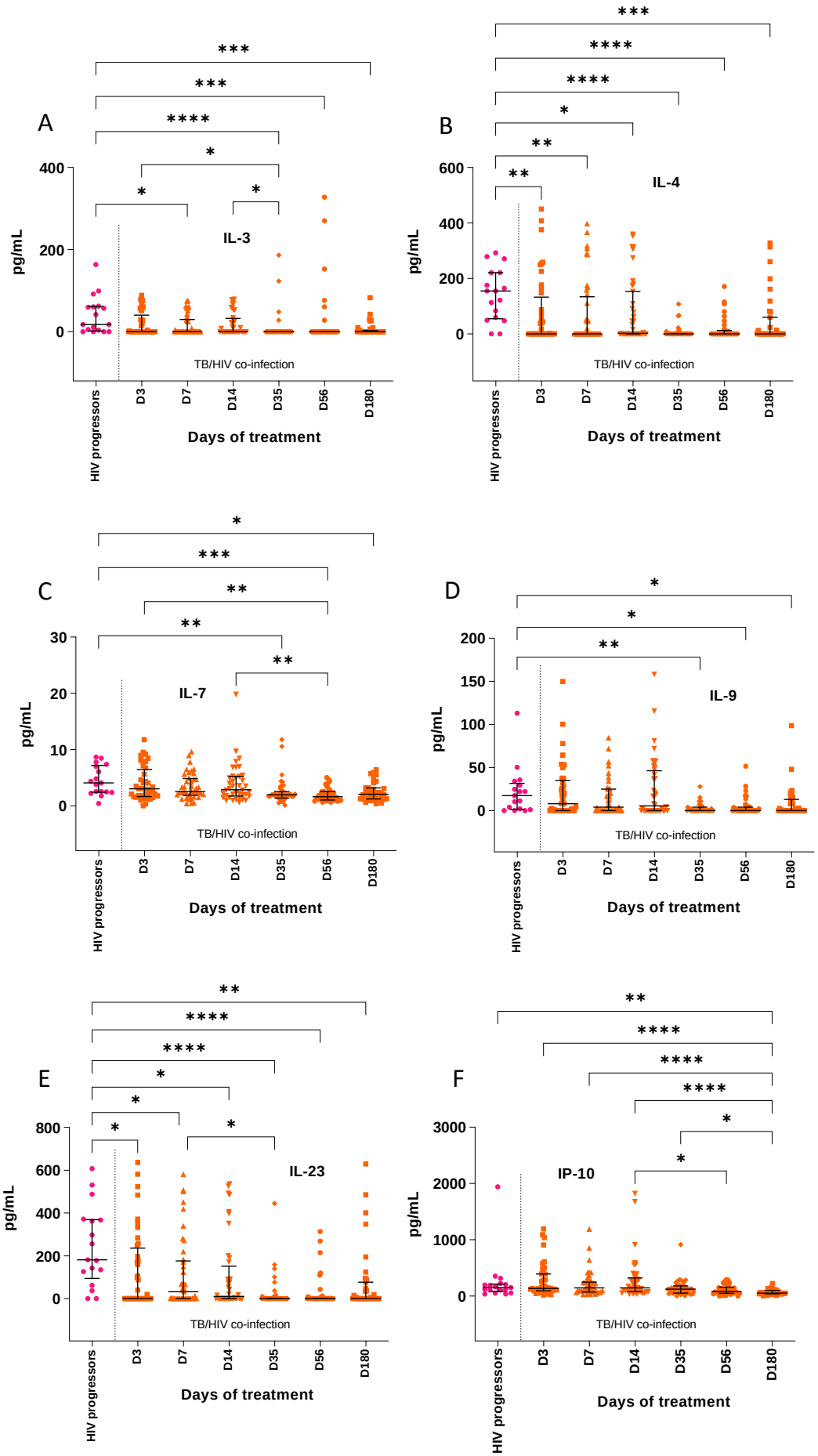
A
IL-3
pg/mL
400
200
0
TB/HIV co-infection
HIV progressors
D3
D7
D14
D35
D56
D180
Days of treatment
B
IL-4
600
400
200
0
C
IL-7
30
20
10
0
D
IL-9
200
150
100
50
0
E
IL-23
800
600
400
200
0
F
IP-10
3000
2000
1000
0

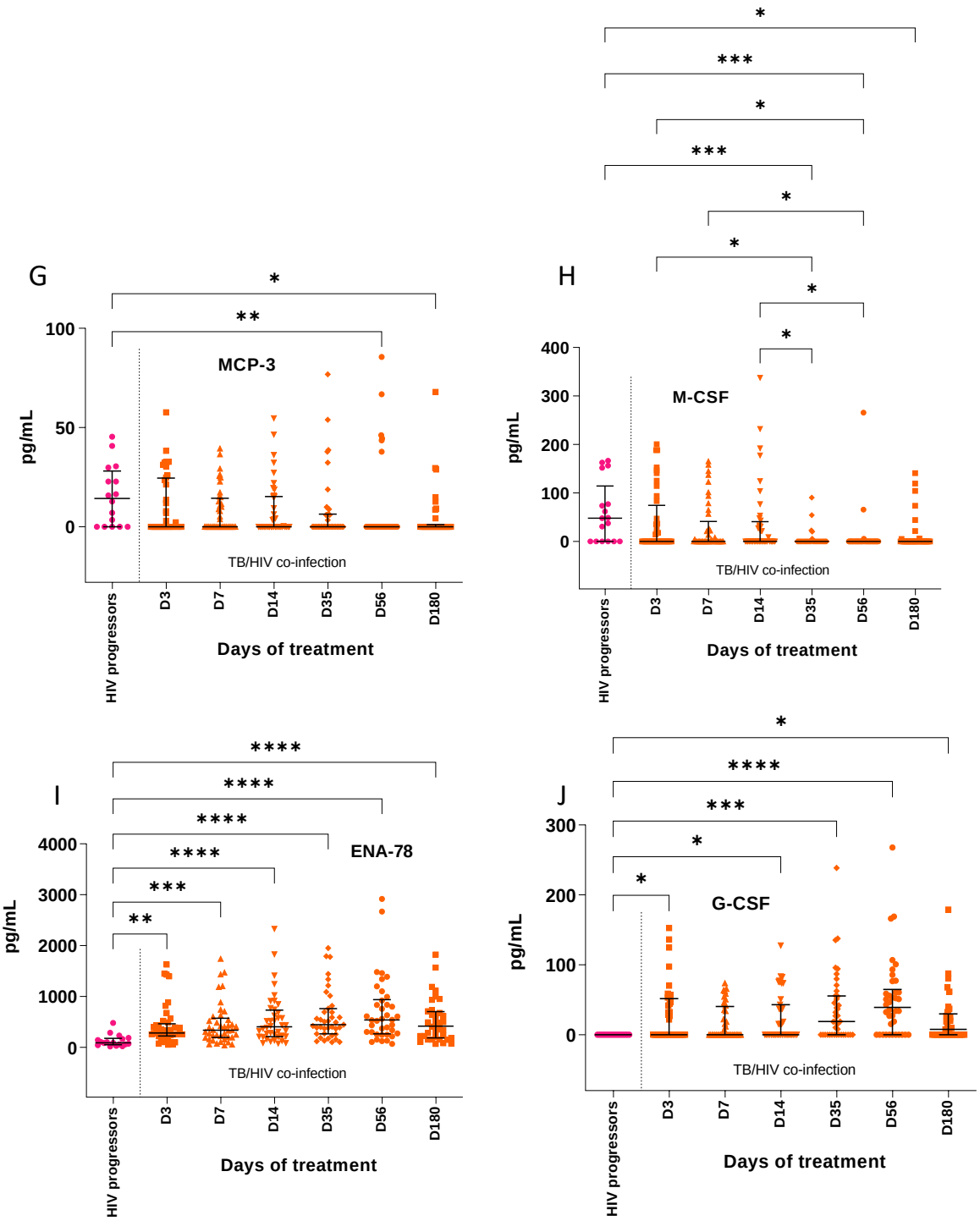
G
MCP-3
pg/mL
100
50
0
TB/HIV co-infection
HIV progressors
D3
D7
D14
D35
D56
D180
Days of treatment
H
M-CSF
pg/mL
400
300
200
100
0
TB/HIV co-infection
HIV progressors
D3
D7
D14
D35
D56
D180
Days of treatment
I
ENA-78
pg/mL
4000
3000
2000
1000
0
TB/HIV co-infection
HIV progressors
D3
D7
D14
D35
D56
D180
Days of treatment
J
G-CSF
pg/mL
300
200
100
0
TB/HIV co-infection
HIV progressors
D3
D7
D14
D35
D56
D180
Days of treatment

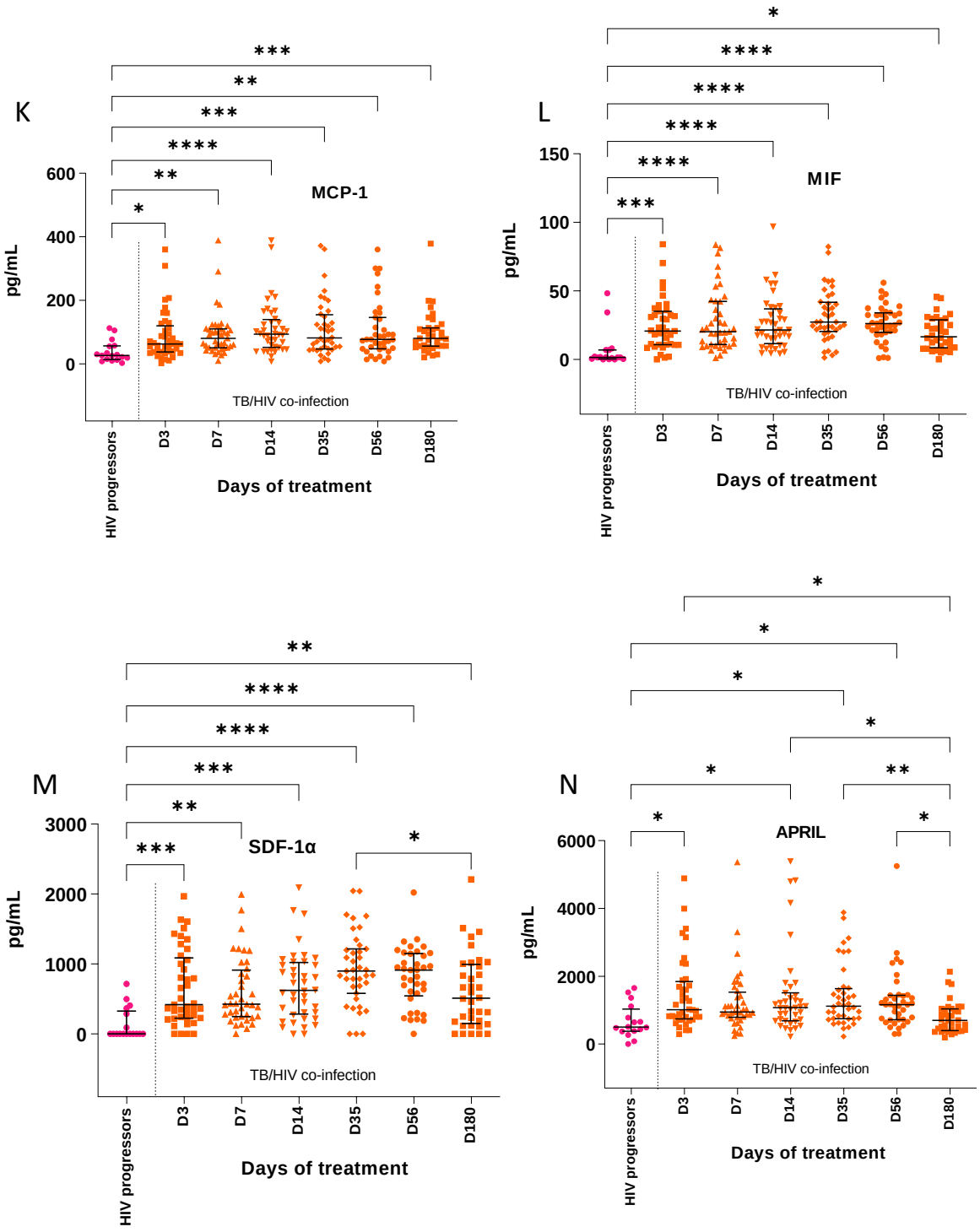
K
MCP-1
pg/mL
600
400
200
0
TB/HIV co-infection
HIV progressors
D3
D7
D14
D35
D56
D180
Days of treatment
L
MIF
pg/mL
150
100
50
0
TB/HIV co-infection
HIV progressors
D3
D7
D14
D35
D56
D180
Days of treatment
M
SDF-1α
pg/mL
3000
2000
1000
0
TB/HIV co-infection
HIV progressors
D3
D7
D14
D35
D56
D180
Days of treatment
N
APRIL
pg/mL
6000
4000
2000
0
TB/HIV co-infection
HIV progressors
D3
D7
D14
D35
D56
D180
Days of treatment

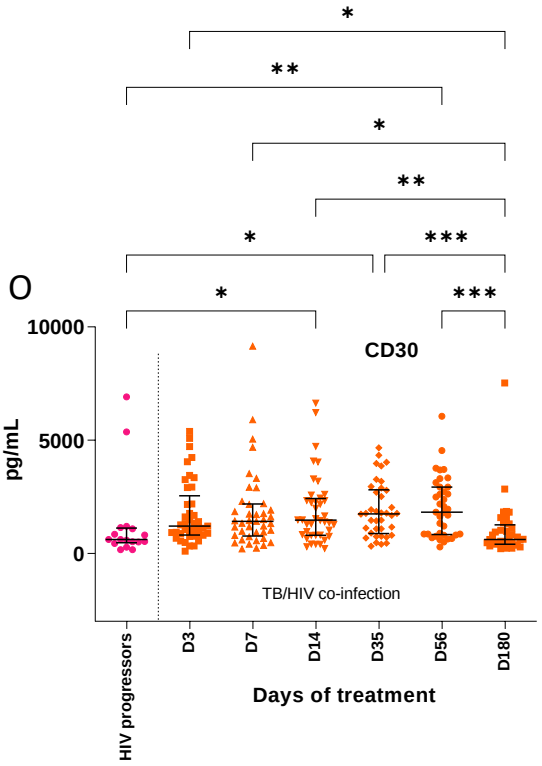
O
CD30
pg/mL
10000
5000
0
TB/HIV co-infection
HIV progressors
D3
D7
D14
D35
D56
D180
Days of treatment

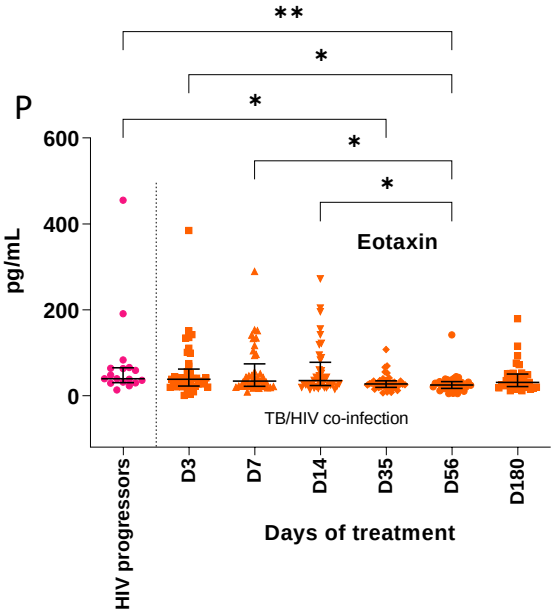
P
Eotaxin
pg/mL
600
400
200
0
TB/HIV co-infection
HIV progressors
D3
D7
D14
D35
D56
D180
Days of treatment

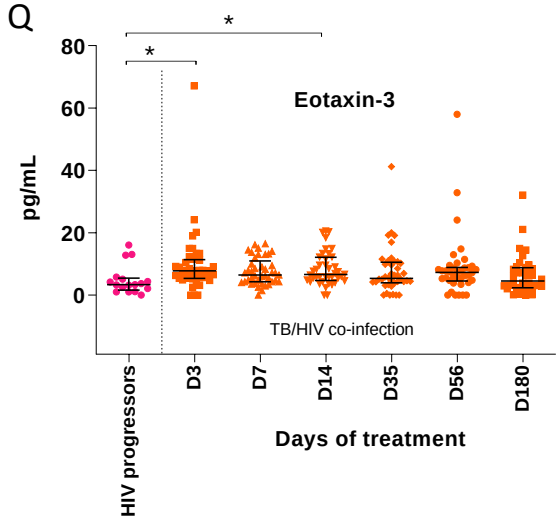
Q
Eotaxin-3
pg/mL
80
60
40
20
0
TB/HIV co-infection
HIV progressors
D3
D7
D14
D35
D56
D180
Days of treatment

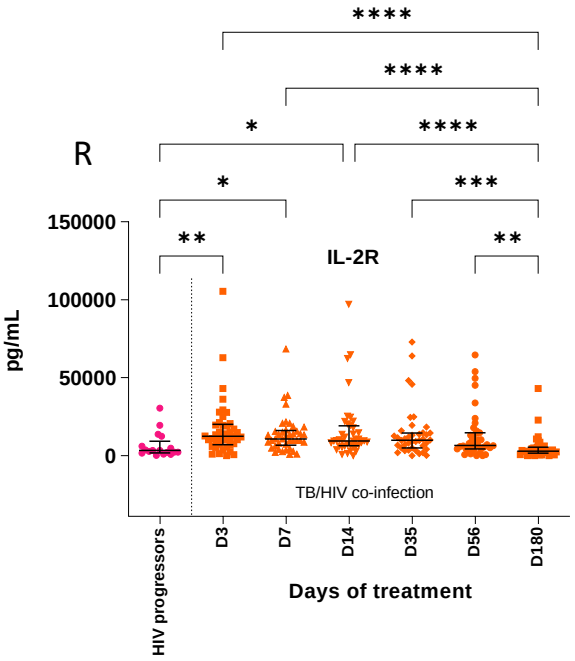
R
IL-2R
pg/mL
150000
100000
50000
0
TB/HIV co-infection
HIV progressors
D3
D7
D14
D35
D56
D180
Days of treatment

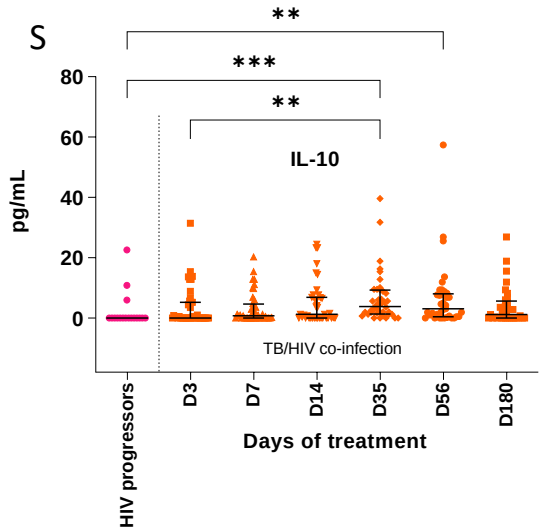
S
**
***
**
IL-10
pg/mL
80
60
40
20
0
TB/HIV co-infection
HIV progressors
D3
D7
D14
D35
D56
D180
Days of treatment

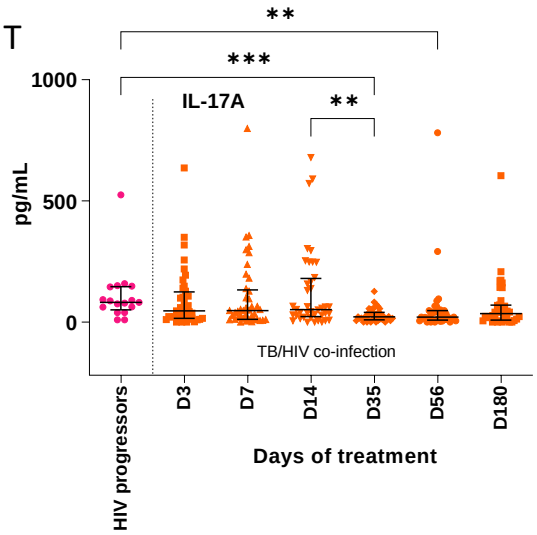
T
**
***
IL-17A
**
pg/mL
1000
500
0
TB/HIV co-infection
HIV progressors
D3
D7
D14
D35
D56
D180
Days of treatment

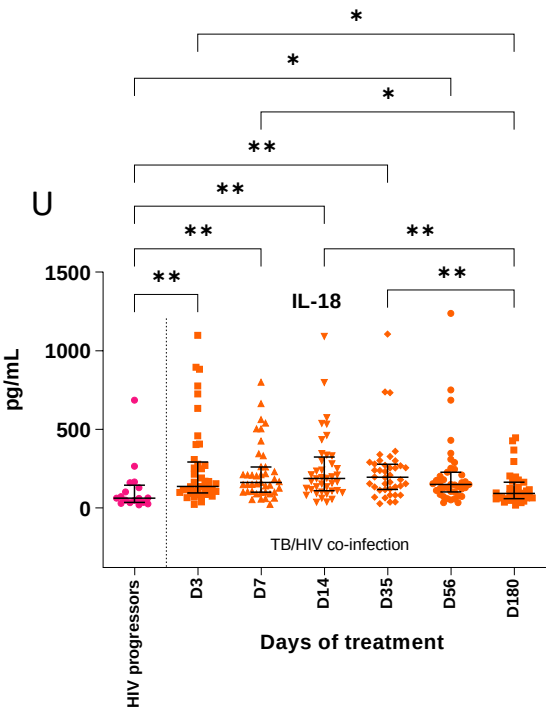
U
*
*
*
**
**
**
**
**
IL-18
pg/mL
1500
1000
500
0
TB/HIV co-infection
HIV progressors
D3
D7
D14
D35
D56
D180
Days of treatment

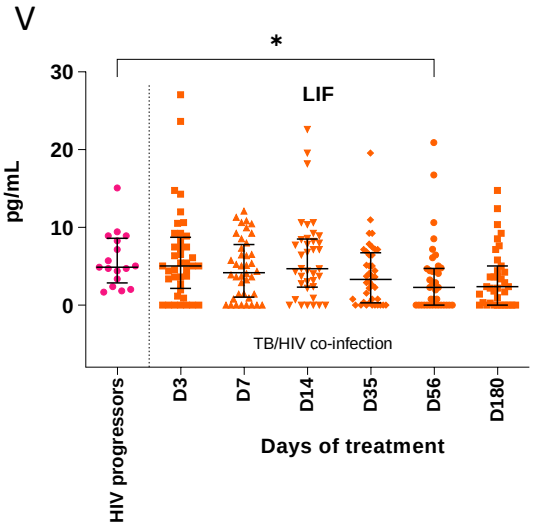
V
*
LIF
pg/mL
30
20
10
0
TB/HIV co-infection
HIV progressors
D3
D7
D14
D35
D56
D180
Days of treatment

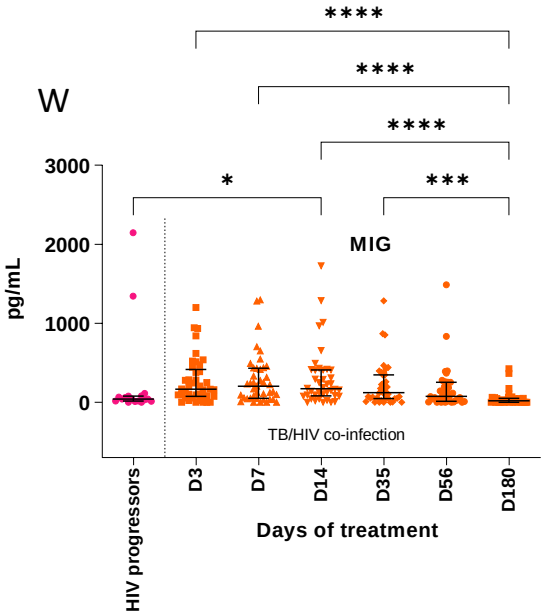
W
MIG
pg/mL
3000
2000
1000
0
****
****
****
*
***
TB/HIV co-infection
HIV progressors
D3
D7
D14
D35
D56
D180
Days of treatment

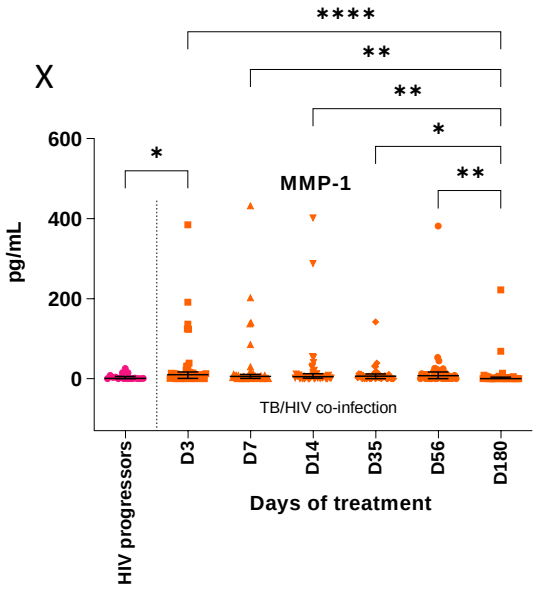
X
MMP-1
pg/mL
600
400
200
0
****
**
**
*
**
*
TB/HIV co-infection
HIV progressors
D3
D7
D14
D35
D56
D180
Days of treatment

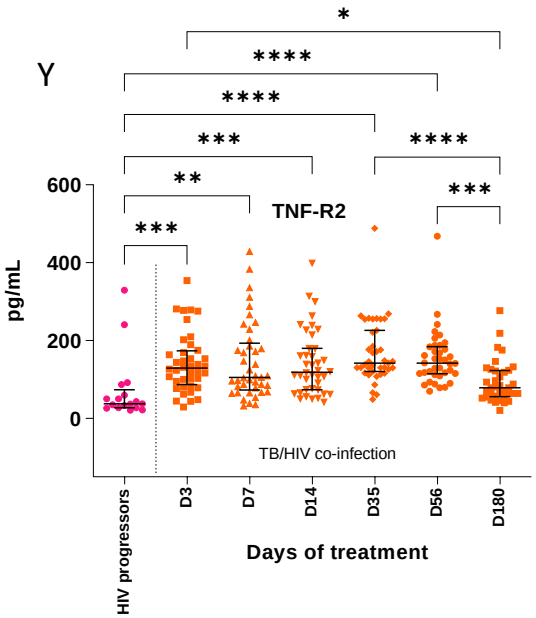
Y
TNF-R2
pg/mL
600
400
200
0
*
****
****
***
****
**
***
***
TB/HIV co-infection
HIV progressors
D3
D7
D14
D35
D56
D180
Days of treatment

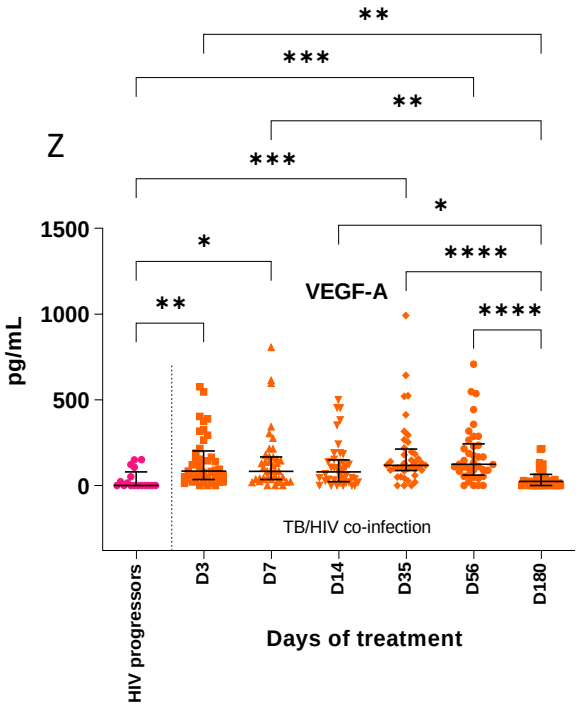
Z
VEGF-A
pg/mL
1500
1000
500
0
**
***
**
***
*
*
**
****
****
TB/HIV co-infection
HIV progressors
D3
D7
D14
D35
D56
D180
Days of treatment

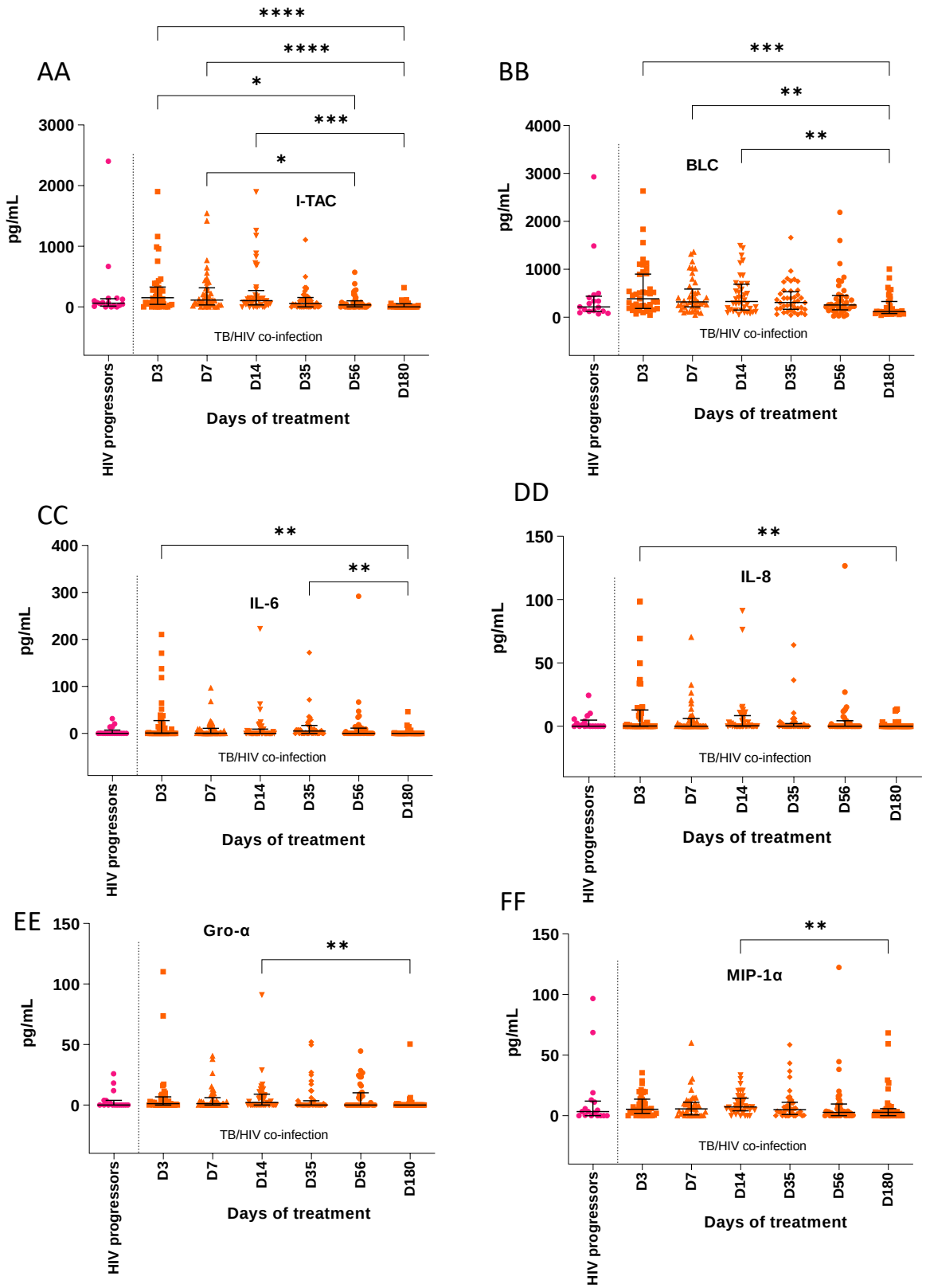
AA
****
****
*
***
*
I-TAC
pg/mL
3000
2000
1000
0
TB/HIV co-infection
HIV progressors
D3
D7
D14
D35
D56
D180
Days of treatment
BB
***
**
**
BLC
pg/mL
4000
3000
2000
1000
0
TB/HIV co-infection
HIV progressors
D3
D7
D14
D35
D56
D180
Days of treatment
CC
**
**
IL-6
pg/mL
400
300
200
100
0
TB/HIV co-infection
HIV progressors
D3
D7
D14
D35
D56
D180
Days of treatment
DD
**
IL-8
pg/mL
150
100
50
0
TB/HIV co-infection
HIV progressors
D3
D7
D14
D35
D56
D180
Days of treatment
EE
Gro-α
**
pg/mL
150
100
50
0
TB/HIV co-infection
HIV progressors
D3
D7
D14
D35
D56
D180
Days of treatment
FF
**
MIP-1α
pg/mL
150
100
50
0
TB/HIV co-infection
HIV progressors
D3
D7
D14
D35
D56
D180
Days of treatment

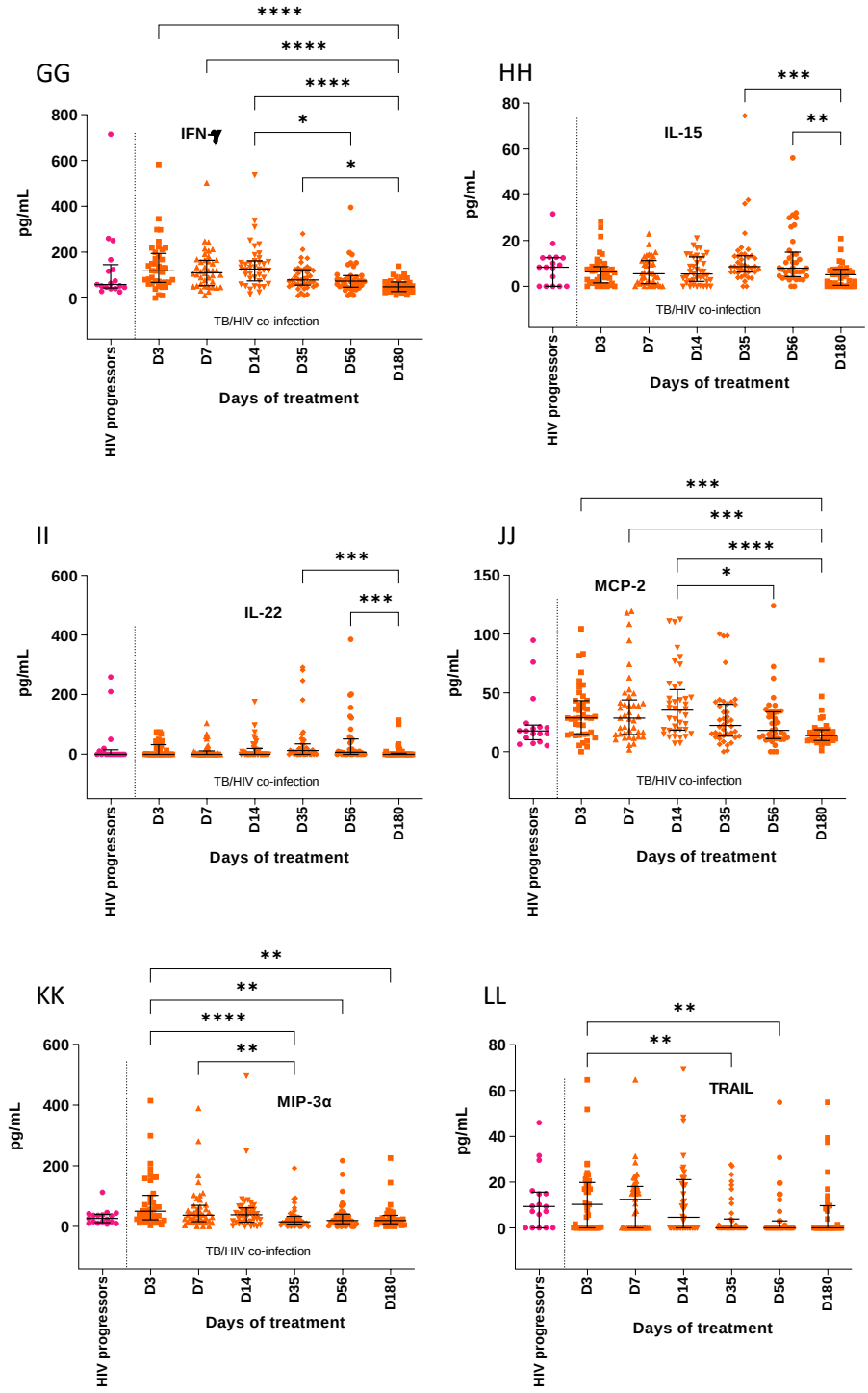

Figure 3.10. **Comparison of cytokines in HIV progressors (controls) with TB/HIV co-infected individuals and longitudinal assessment of cytokines to monitor TB treatment response**. Scatter plots of cytokines/chemokines that were significantly different between the groups during treatment are shown. Magenta dots represent HIV+ controls, orange dots are TB/HIV co-infected patients on TB treatment. The cytokine concentrations are expressed in pg/mL and were analysed by the non-parametric Kruskal-Wallis test, with significance *P <0.01; **P < 0.001; ***P < 0.001; ****P < 0.001 (post hoc corrected by Dunn's multiple comparisons). Controls were compared to TB/HIV infected individuals at all time points. Only significant differences are shown, the lack of statistical bars between groups indicated that no significant difference was observed.

As the majority of participants in our cohort were HIV/TB co-infected, we first presented the data analysis of this group. Next, we present a similar analysis between healthy controls and individuals infected with TB only.

3.15. Biomarkers associated with TB infection.

To evaluate whether any of the biomarkers have the potential to be used for TB treatment monitoring, in TB mono-infected individuals only, longitudinally collected plasma was analysed as before. Out of the 65 cytokines, the concentration of 26 cytokines were significantly different at the different time points of treatment between healthy controls (HCs) and TB patients. When comparing HCs to individuals completing TB treatment, we noted that Eotaxin, IL-2, IL-7, LIF and TNF-α were significantly lower whilst MIF was significantly higher (**Table 3.4**, highlighted in green and orange respectively and **Figure 3.11A, B, C, D, E** and **F** respectively). In addition, we noted that twenty cytokines (**Table 3.4**, highlighted in yellow, **Figure 3.11G, H, I, J, K, L, M, N, O, P, Q, R, S, T, U, V,W, X, Y, Z**) returned to similar levels as that of HCs.

Next, we investigated the changes in cytokine profile at specific time points during TB treatment. We noted that the cytokines IL-2, LIF, TNF-α, CD30, IL-3, IL-4,IL-16, IL-23, IP-10, and TRAIL could not be used to monitor treatment response in this group as there were no significant differences between time points during treatment, **Figure 3.11B, D, E, H, M, N, Q, T, U,** and **Y**). In contrast, IL-7, MIF, APRIL, Eotaxin-3, G-CSF, IL-2R, IL-12p70, IL-15, IL-17A, IL-22, SDF-1α, TNF-R2 and VEGF-A showed significant differences at distinct time points during TB treatment (**Figure 3.11C, F, G, J, K, L, O, P, R, S, W, X** and **Z**).

Table 3.4: Cytokines changes during TB treatment in TB infected individuals.[Ψ]

Cytokine	Healthy controls (pg/mL)	Day 3 (pg/mL)	Day 7 (pg/mL)	Day 14 (pg/mL)	Day 35 (pg/mL)	Day 56 (pg/mL)	Day 180 (pg/mL)
Eotaxin	44.70	28.44 *	28.99 *	27.16 **	22.65 ***	26.77 **	28.16 *
IL-2	59.05	48.05	44.69	42.57	49.57	50.80	26.64 **
IL-7	4.109	3.288	3.103	2.974	1.661 ***	1.507 ***	2.040 **
LIF	4.445	3.391	2.745	2.606	2.512 **	1.181 **	0.9479***
TNF-α	12.22	8.277	7.308	6.955	9.093	6.149	4.399**
MIF	5.265	14.59**	13.08*	14.01**	20.26**	31.47****	13.46**
APRIL	664.3	760.5	709.8	705.2	1220*	852.8	539.3
CD30	255.7	623.0 **	533.6	518.5 **	602.8	683.4	400.2
ENA-78	227.5	374.9	392.3	420.9 *	435.4 *	579.1 *	413.4
Eotaxin-3	5.056	6.971	5.821	6.598	5.347	8.575 **	5.017
G-CSF	3.909	13.78	5.607	12.10	38.64 ***	26.84 *	5.929
IL-2R	798.6	7111****	5415****	4472	3244	4742	2669
IL-3	15.44	17.59	12.59	15.00	8.201	4.760 *	13.68
IL-4	167.1	85.08	66.52	82.10	17.52 **	10.88 ***	45.32
IL-12p70	8.307	5.276	4.406	4.216	2.679*	1.652*	3.253
IL-15	6.411	5.618	5.666	4.577	14.82 ***	7.409	3.357
IL-16	580.7	474.1	372.2	399.8	322.2 *	542.1	422.7
IL-17A	183.1	144.3	168.5	165.2	25.26 **	18.91 ***	84.55
IL-22	17.40	10.80	7.849	12.67	52.51 **	16.79	2.807
IL-23	231.8	138.1	95.83	115.0	25.56 **	7.726 ***	77.31
IP-10	46.62	139.9 *	96.86	85.85	62.90	70.18	44.11
MMP-1	1.716	3.033	2.316	2.448	6.517*	8.685	1.581
SDF-1α	153.9	321.9	285.4	310.3	505.2**	851.4****	324.4
TNF-R2	57.52	64.75	54.86	59.81	86.02	114.8****	53.16
TRAIL	10.21	9.277	9.521	9.906	3.535*	3.525	6.685
VEGF-A	15.01	63.79***	54.11**	45.09*	126.9****	109.4****	22.85

[Ψ]Green colour represents cytokines that were significantly lower upon TB treatment completion when compared to healthy controls, Orange colour represents cytokines that were significantly higher upon TB treatment completion when compared to healthy controls, Yellow colour represents cytokines where the levels obtained after TB treatment completion were comparable to healthy controls.
[#]Healthy controls are used as controls for assessing TB cure in TB infected individuals
Concentrations (pg/mL) are shown as mean
*P <0.01; **P < 0.001; ***P < 0.001; ****P < 0.001

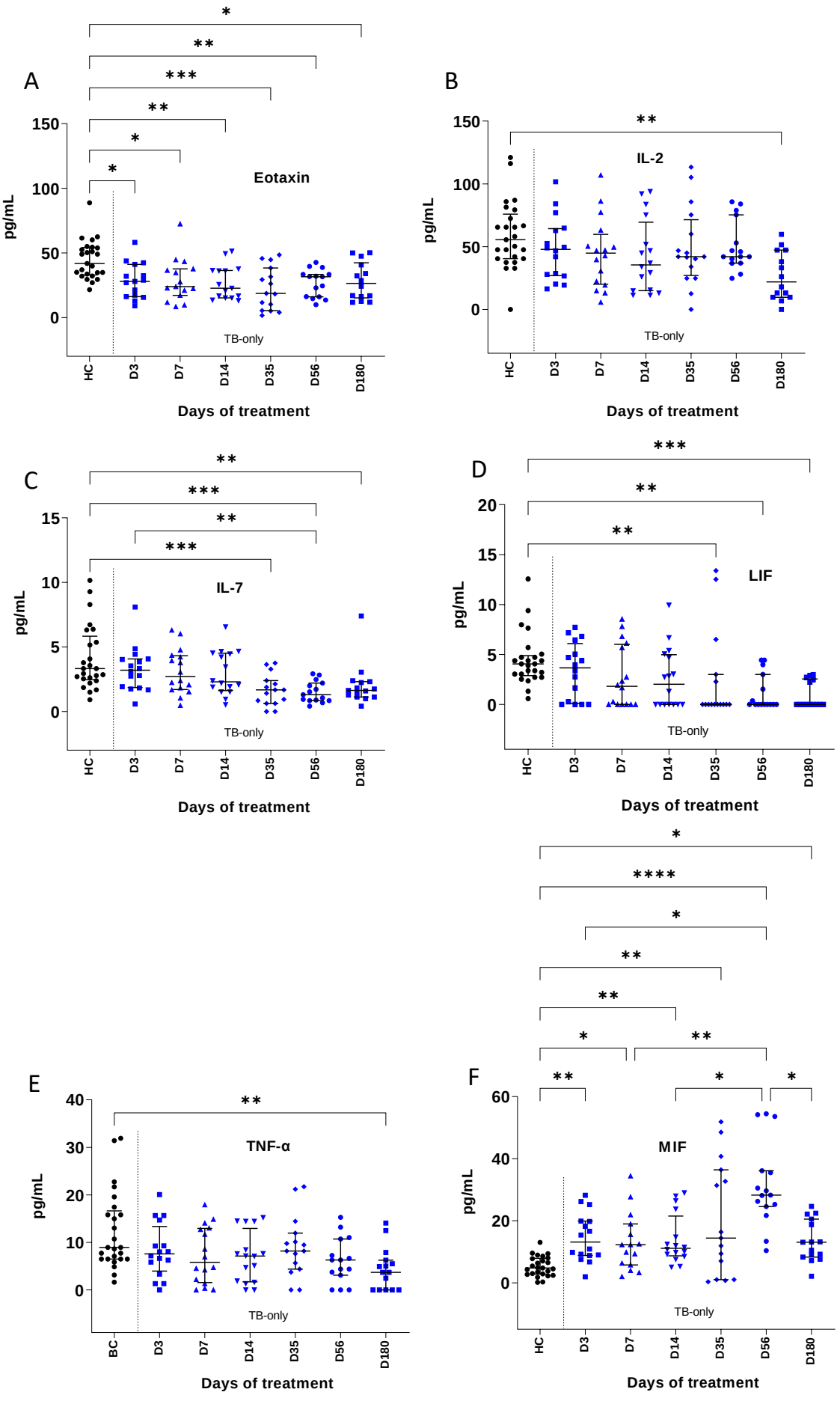
A
Eotaxin
pg/mL
150
100
50
0
TB-only
HC
D3
D7
D14
D35
D56
D180
Days of treatment
*
**
***
**
*
*
B
IL-2
pg/mL
150
100
50
0
**
TB-only
HC
D3
D7
D14
D35
D56
D180
Days of treatment
C
IL-7
pg/mL
15
10
5
0
**
***
**
***
TB-only
HC
D3
D7
D14
D35
D56
D180
Days of treatment
D
LIF
pg/mL
20
15
10
5
0
***
**
**
TB-only
HC
D3
D7
D14
D35
D56
D180
Days of treatment
E
TNF-α
pg/mL
40
30
20
10
0
**
TB-only
BC
D3
D7
D14
D35
D56
D180
Days of treatment
F
MIF
pg/mL
60
40
20
0
*
****
*
**
**
*
**
**
*
*
TB-only
HC
D3
D7
D14
D35
D56
D180
Days of treatment

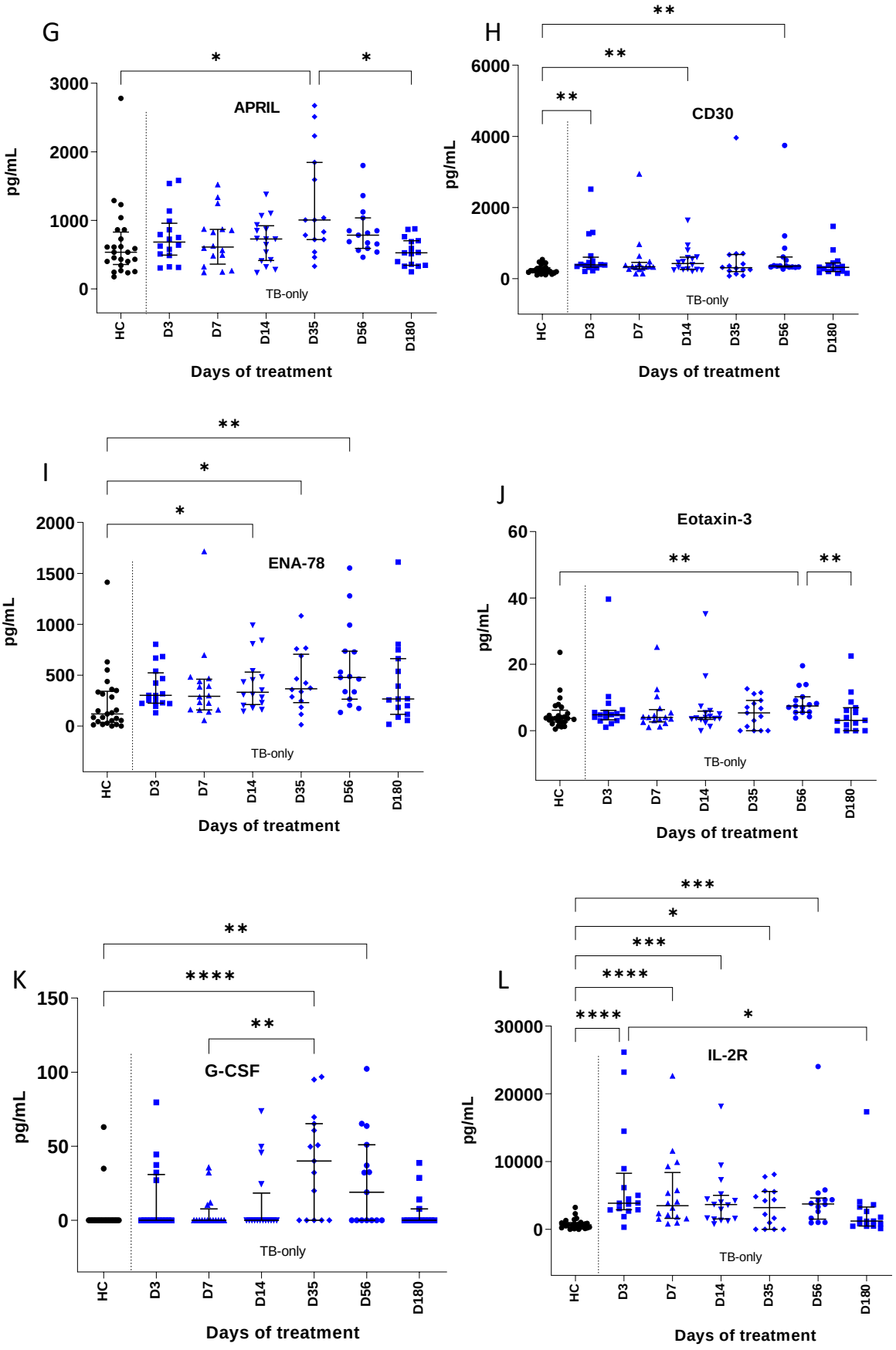
G
APRIL
pg/mL
3000
2000
1000
0
TB-only
HC
D3
D7
D14
D35
D56
D180
Days of treatment
H
CD30
6000
4000
2000
I
ENA-78
1500
500
J
Eotaxin-3
60
40
20
K
G-CSF
150
100
50
L
IL-2R
30000
20000
10000

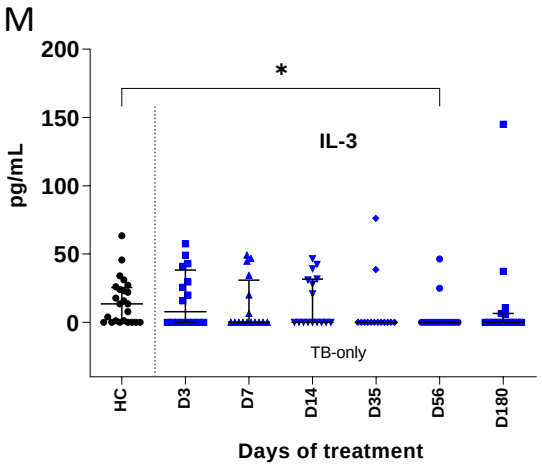
M
200
150
100
50
0
pg/mL
*
IL-3
TB-only
HC
D3
D7
D14
D35
D56
D180
Days of treatment

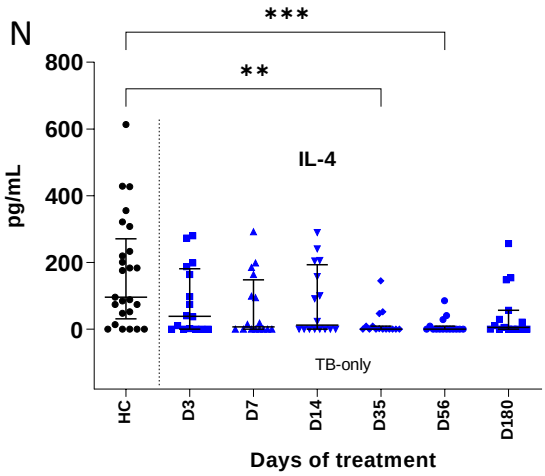
N
800
600
400
200
0
pg/mL
***
**
IL-4
TB-only
HC
D3
D7
D14
D35
D56
D180
Days of treatment

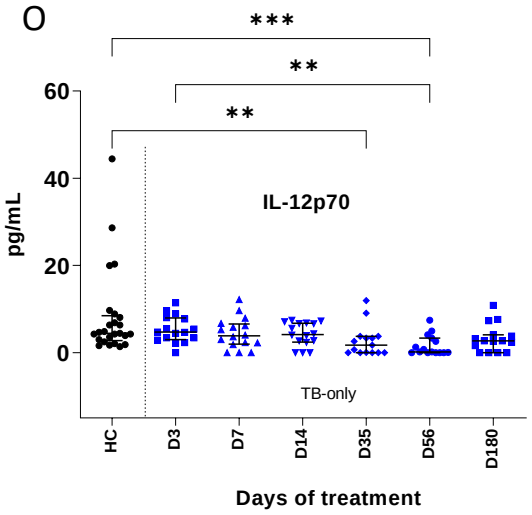
O
60
40
20
0
pg/mL
***
**
**
IL-12p70
TB-only
HC
D3
D7
D14
D35
D56
D180
Days of treatment

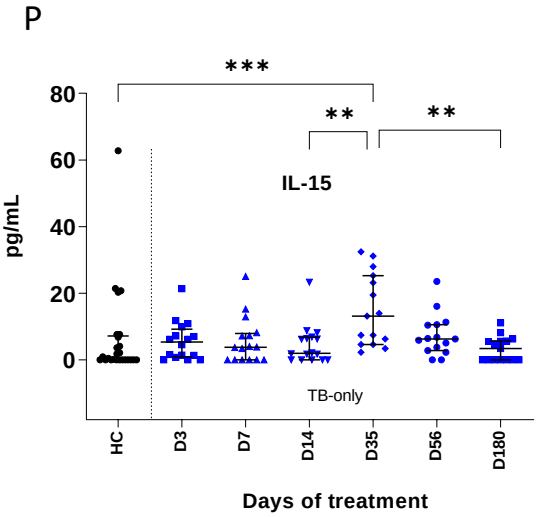
P
80
60
40
20
0
pg/mL
***
**
**
IL-15
TB-only
HC
D3
D7
D14
D35
D56
D180
Days of treatment

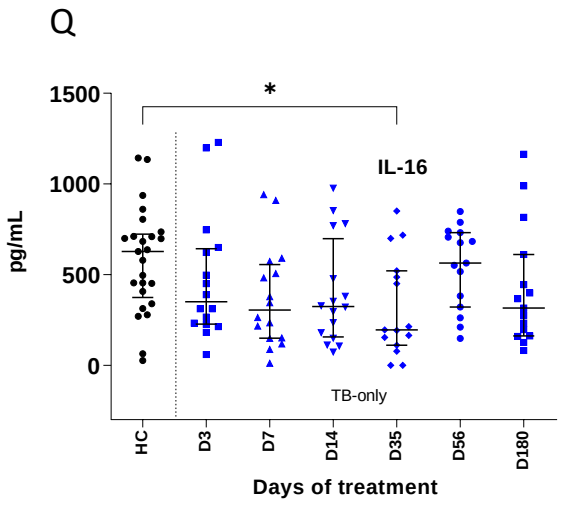
Q
1500
1000
500
0
pg/mL
*
IL-16
TB-only
HC
D3
D7
D14
D35
D56
D180
Days of treatment

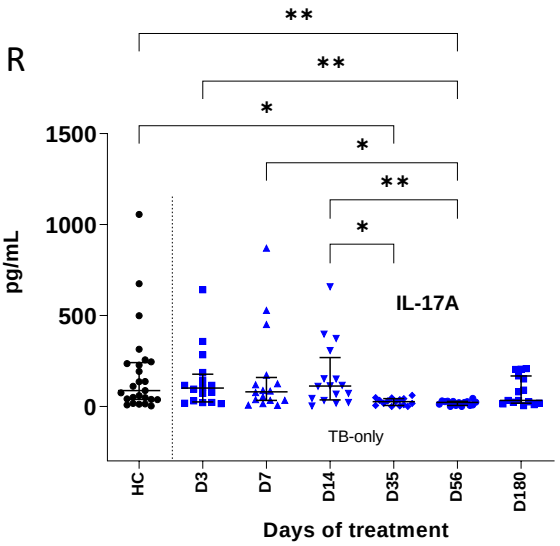
R
1500
1000
500
0
pg/mL
**
**
*
*
**
*
IL-17A
TB-only
HC
D3
D7
D14
D35
D56
D180
Days of treatment

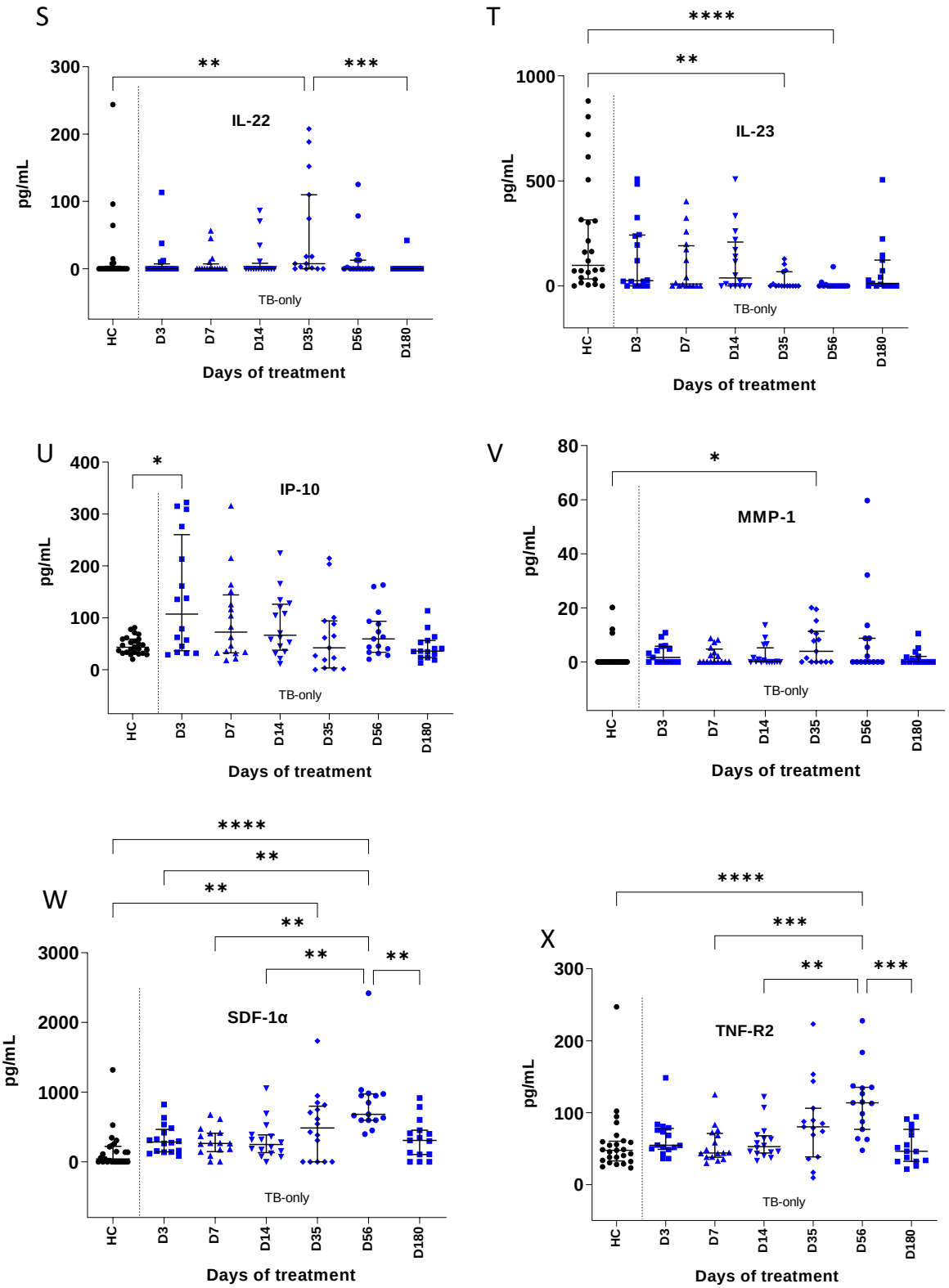
S
IL-22
pg/mL
300
200
100
0
**
***
TB-only
HC
D3
D7
D14
D35
D56
D180
Days of treatment
T
IL-23
pg/mL
1000
500
0
****
**
TB-only
Days of treatment
U
IP-10
pg/mL
400
300
200
100
0
*
TB-only
Days of treatment
V
MMP-1
pg/mL
80
60
40
20
0
*
TB-only
Days of treatment
W
SDF-1α
pg/mL
3000
2000
1000
0
****
**
**
**
**
**
TB-only
Days of treatment
X
TNF-R2
pg/mL
300
200
100
0
****
***
**
***
TB-only
Days of treatment

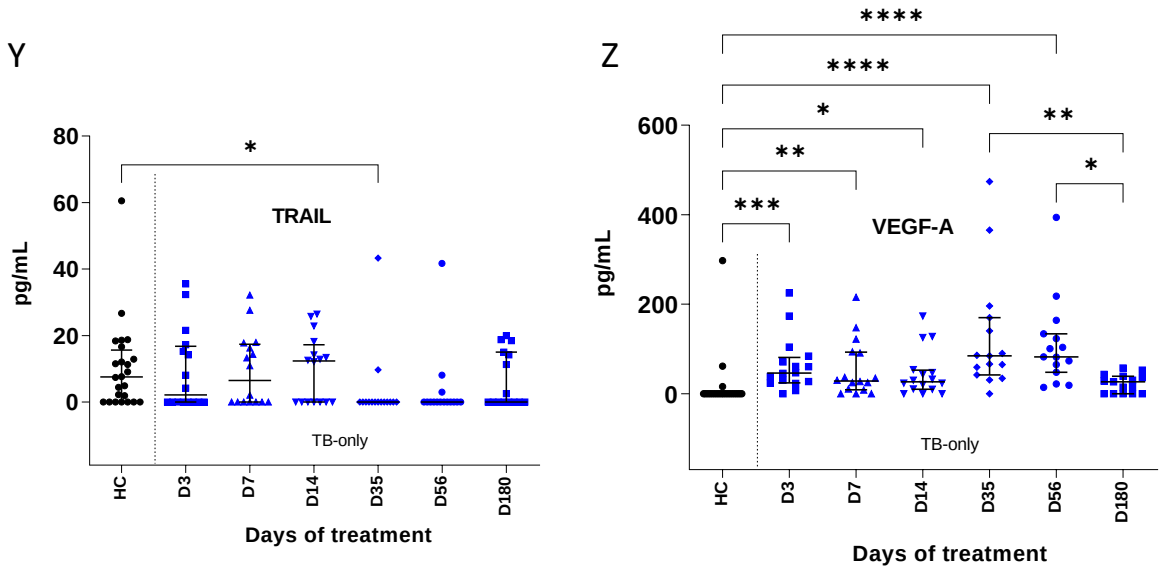

Figure 3.11. Comparison of cytokine levels between healthy controls with TB mono-infected individuals and longitudinal assessment of cytokines to monitor TB treatment response. Scatter plots of cytokines/chemokines that were significantly different between the groups during the course of treatment are shown. Black dots represent healthy controls (HC) and blue dots represent patients on TB treatment. The cytokine concentrations are expressed in pg/mL and were analysed by the non-parametric Kruskal-Wallis test, with significance *P <0.01; **P < 0.001; ***P < 0.001; ****P < 0.0001 (post hoc corrected by Dunn's multiple comparisons). Controls were compared to TB/HIV infected individuals are all time points. Only significant differences are shown, the lack of statistical bars between groups indicated that no significant difference was observed.

After assessing differences in cytokine profiles between TB and TB/HIV co-infected individuals with their respective controls, we next set out to analyse if there are differences in cytokine profiles between TB and TB/HIV co-infected individuals.

3.16. Longitudinal assessment of plasma biomarkers levels over treatment between TB and HIV/TB co-infected individuals.

All patients were then grouped by their HIV status, followed by evaluation of plasma markers. A total of 11 potential host biomarkers (APRIL, BLC, CD30, IFN-γ, IL-18, IP-10, MCP-2, MIG, MMP-1, SDF-1α and TNF-R2) were significantly elevated in patients co-infected with TB and HIV compared to those infected with TB only, **Figure 3.12A-K** respectively.

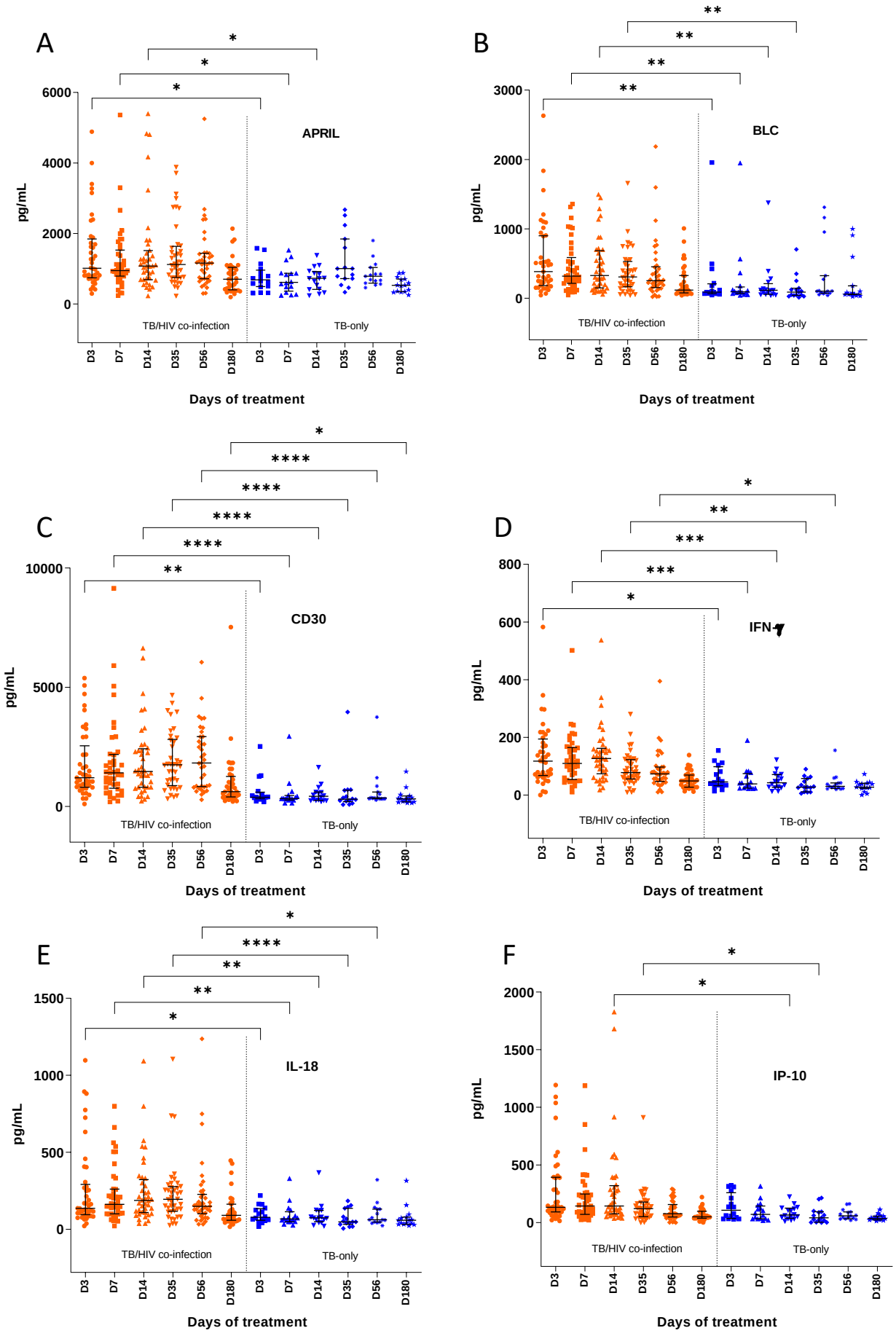
A
APRIL
pg/mL
6000
4000
2000
0
*
*
*
TB/HIV co-infection
TB-only
D3
D7
D14
D35
D56
D180
Days of treatment
B
BLC
3000
2000
1000
**
**
**
**
C
CD30
10000
5000
****
****
****
**
*
D
IFN-γ
800
600
400
200
***
***
**
*
E
IL-18
1500
1000
500
****
**
**
*
F
IP-10
2000
1500
1000
500
*
*

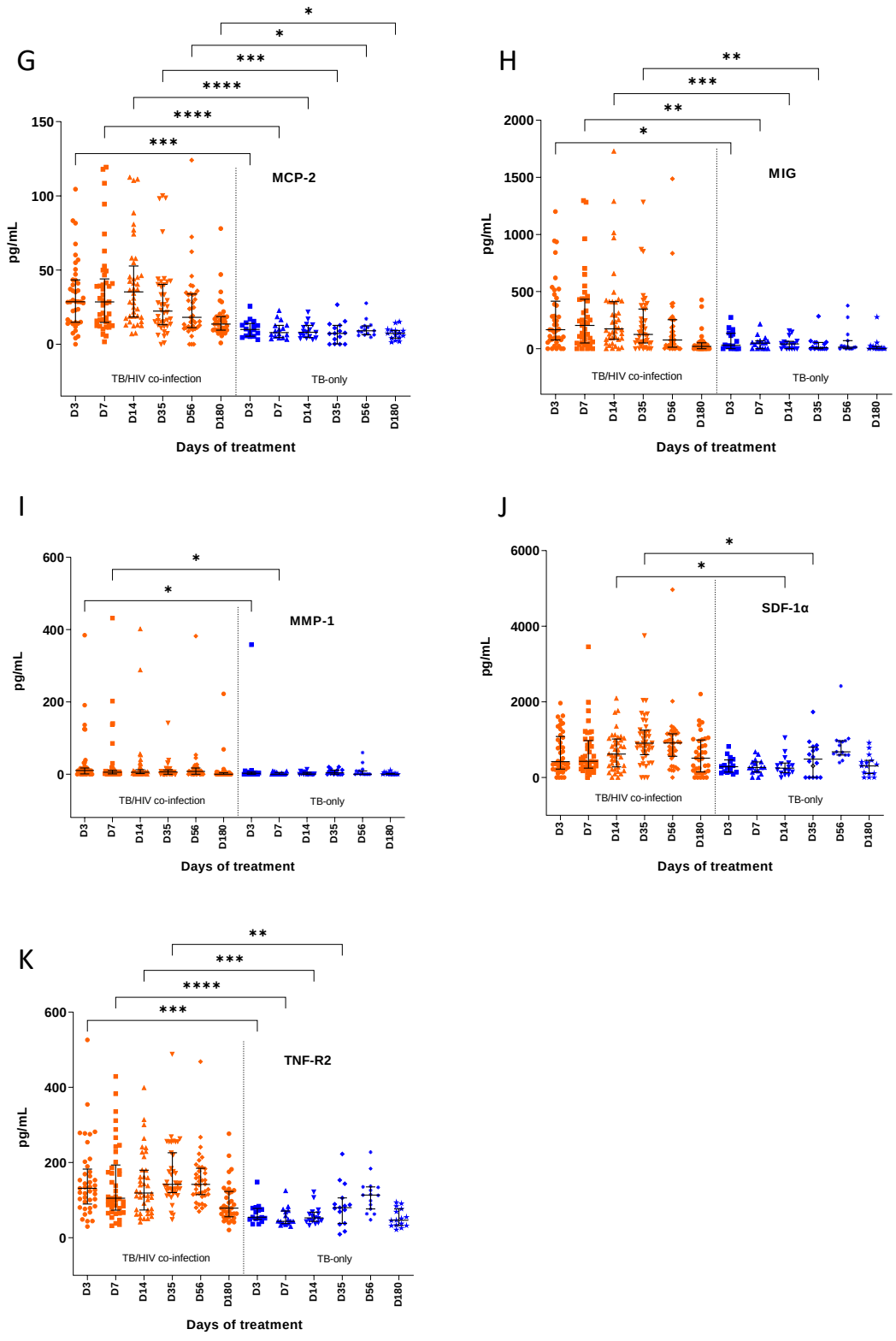

Figure 3.12. Comparison of cytokine profiles between HIV/TB co-infected and TB infected during treatment. Orange and blue dots represents HIV/TB co-infected and TB-only infected patients, respectively. The results are expressed in pg/mL and were analysed by the non-parametric Kruskal-wallis test, with significance *P <0.01; **P < 0.001; ***P < 0.001; ***P < 0.0001 (post hoc corrected by Dunn's multiple comparisons).

Next, we attempted to correlate changes in cytokine profiles with CD4 T cell counts and viral loads in HIV/TB co-infected patients.

3.17. Correlation of plasma cytokine/chemokine levels with viral load and CD4 count in HIV/TB co-infected individuals.

We analysed the correlation between concentrations of cytokines on day 3, which was our baseline sample, with viral load, as well CD4 T cell count, in the HIV/TB co-infected group. There was a significant negative correlation between the levels of IL-2 and viral load, **Figure 3.13A**. We also observed a significant negative correlation between CD4+ T cells and the concentration levels of IL-1α, IP-10, I-TAC, VEGF-A, MIF, MIG, TNF-R2 and MIP-1β, and as shown in **Figure 3.13B, C, D, F, G, H, I** and **J**, respectively.

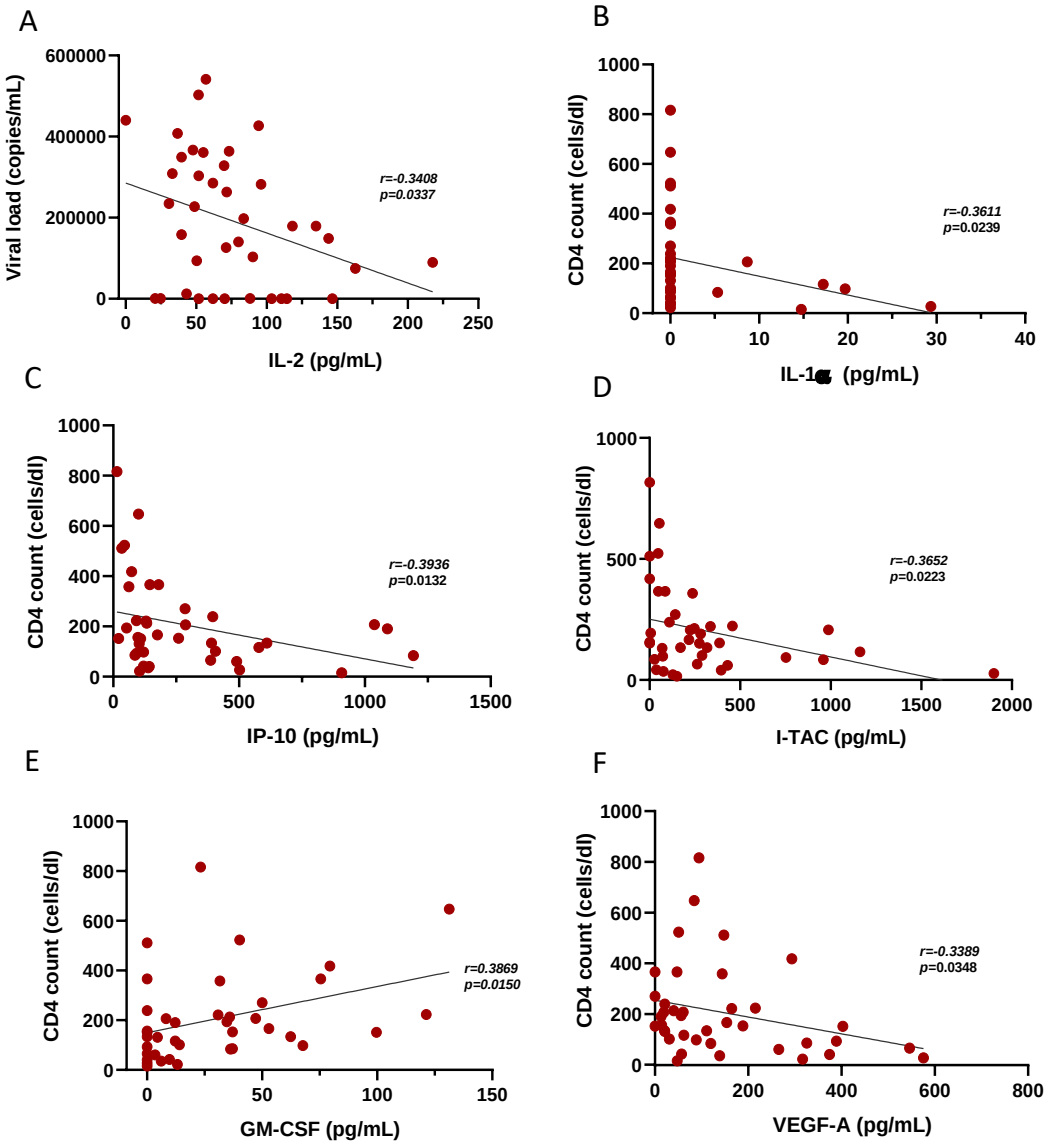

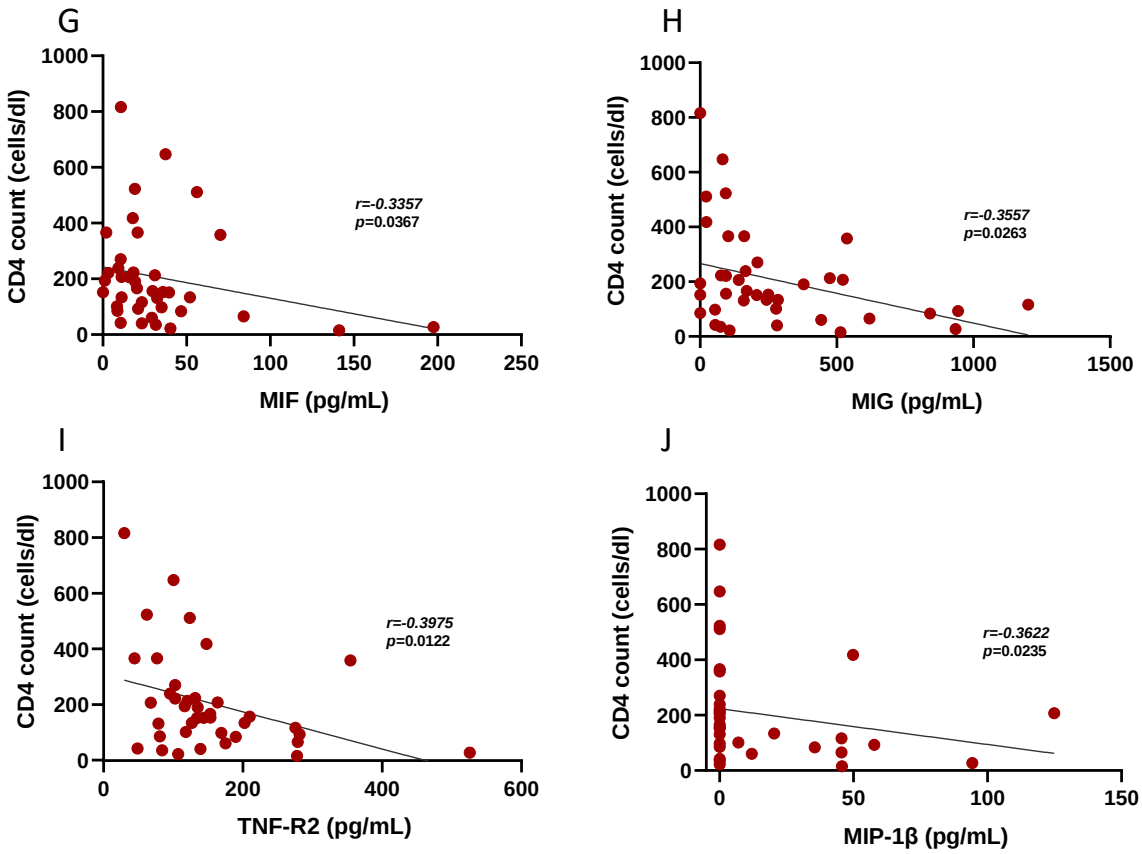

Figure 3.13. Correlations between viral load and CD4 T cell count with levels of plasma cytokines. In the illustration, only cytokines that were significantly correlated in the analysis are depicted. The results of the Spearman correlation analysis are shown as rho and p values in the graphs.

Moreover, a significant positive correlation was found between the number of CD4+ T cells and the levels of GM-CSF, **Figure13E**.

Up to this point, the differences in cytokine profiles described are based on time post treatment and were analysed relative to their control groups. This enabled us to get a sense of cytokine expression in the cohort, together with the relative contribution of HIV. Next, we incorporated the DCTB response patterns into our analytical approach.

3.18. Heat map analysis of cytokine/chemokine associated DCTB treatment response.

Heat map analysis was done for the 65 cytokines, chemokines and growth factors to differentiate the DCTB treatment response groups, which were stratified by their HIV status. An overview of the profile between the treatment-responsive, delayed-responsive and non-responsive can be seen in **Figure 3.14**, where the concentrations of the 65 immune mediators

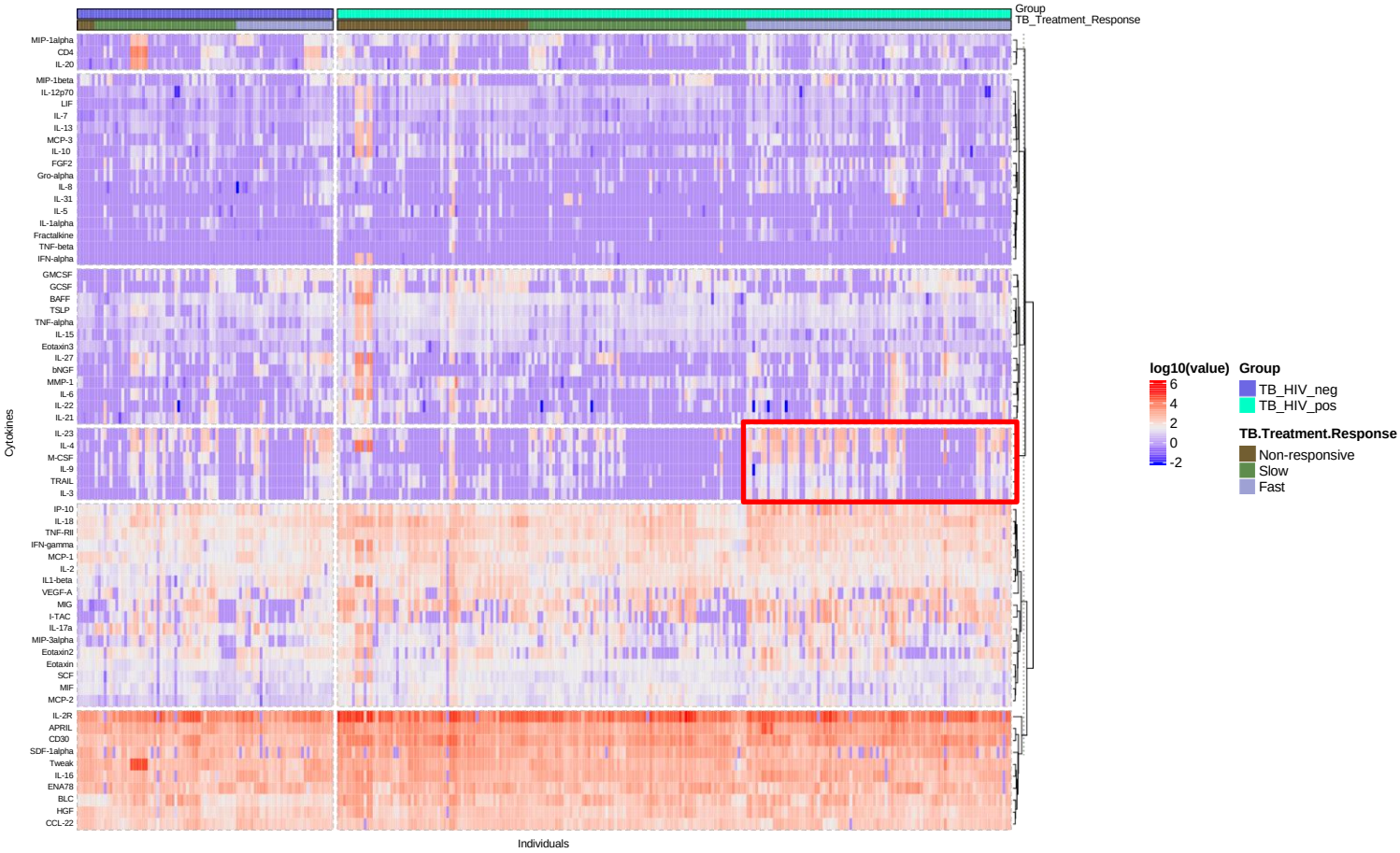

Figure 3:14. Heat map of cytokine and chemokine concentrations among the DCTB treatment groups stratified by HIV status in the TB patients. The heat map represents an unsupervised clustering of cytokine and chemokine concentrations in the inflammatory immune response of 57 individuals (every column indicates one patient) and cytokines/chemokines abundance (rows). Heat map colour corresponds to the Log-transformed concentrations of cytokines at day 3. The spectrum of red to blue corresponds to decreasing gradient of chemokine/cytokine concentrations. The red block represents cytokines that were modulated in the fast-responding TB/HIV group.

are presented as a colour-coded heat map created using unsupervised hierarchical clustering. We did not observe any distinct pattern between the groups however, certain trends emerged. For example, IL-23 IL-4, M-CSF, IL-9, TRAIL, and IL-3 emerged as cluster of cytokines that appeared to be differentially modulated in the treatment responsive, TB/HIV group, **Figure 3.14**.

3.19. Analysis of host markers in plasma between healthy controls, Treatment responsive, Delayed-responsive and Non-responsive groups, using PCA analysis.

Given that immediately trends did not emerge from the clustering analysis, we next used PCA to investigate the distribution of cytokine profiles among the DCTB treatment response groups. A clear distinction appeared between fast (TR-treatment responsive), slow (DR-treatment responsive) and non-responsive at day 3, 7, 14, 35, 56 and 180 of TB treatment as seen from the PCA analysis (**Figure. 3.15A**). This analysis revealed that IL-4, IL-23, M-CSF, IL-20, CD40L, IL-2R, and G-CSF were the most important factors determining the discrimination power of the PCA model between the groups in PC1 and PC2. This analysis included the cytokine profiles from healthy controls (HCs). When only including TB infected participants, the cytokines IL-4, M-CSF, IL-9, I-TAC, IL-2R, G-CSF, SDF-1α, and VEGF-A captured in PC1 and PC2 showed a discriminatory power in the three DCTB treatment response groups as shown in **Figure 3.15B**.

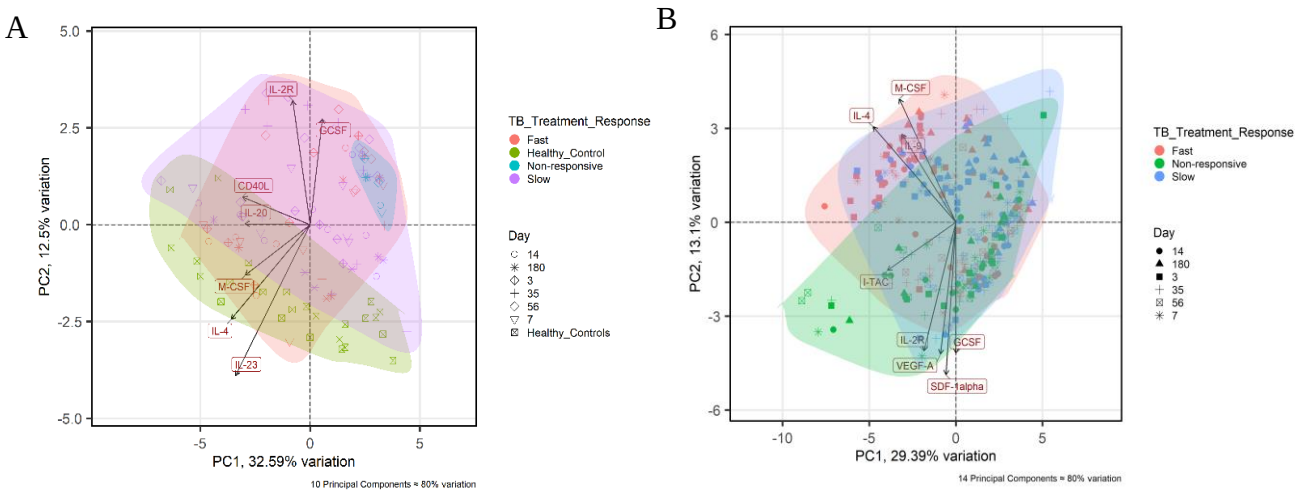

Figure 3.15. Principal Component Analysis (PCA) of cytokines and chemokines from plasma stratified by DCTB responses. (A) PCA plot highlighting the variations between healthy controls, fast (TR-treatment responsive), slow (DR-treatment responsive) and non-responders at day 3, 7, 14, 35, 56 and 180 of TB treatment, based on variability captured in PC1 and PC2. (B) PCA plot highlighting the variations between fast (TR-treatment responsive), slow (DR-delayed responsive) and non-responsive at day 3, 7, 14, 35, 56 and 180 of TB treatment, based on variability captured in PC1 and PC2.

To further unpack the data emerging from the PCA analysis, we next plotted individual cytokines from the different DCTB response groups and compared them with controls.

3.20. Analysis of host markers in plasma between healthy controls, Treatment responsive, Delayed-responsive and Non-responsive groups.

When the plasma levels obtained in both the TB only and TB/HIV co-infected DCTB treatment responsive groups were compared to the levels observed in the HCs significant differences were observed in forty-two cytokine markers as shown in **Figure 3.16**. The levels of CD30, ENA-78, G-CSF, IL-2R, IL-3, IL-4, IL-7, IL-15, IL-17A, IL-23, IP-10, MCP-1, M-CSF, MIF, MIG, MMP-1, TNF-R2, SDF-1α and VEGF-A, as shown in **Figure 3.16A, E, I, K, M, O, P, W, X, Z, CC, EE, GG, II, JJ, KK, MM, NN** and **OO,** respectively, were significantly different between HCsand all the DCTB treatment response groups.

In all the DCTB response groups compared to HCs, the levels of CD30, ENA-78, IL-2R, IL-3, IL-4, IL-23, MIF, MIG, MMP-1, TNF-R2, SDF-1α, and VEGF-A were all significantly different at more than two time periods. Due to the size of these graphs, most significant statistical relationships between groups are indicated (maximum of 6) per graph as shown in **Figure 3.16**. The graphs displaying all the significance are shown in **Figure A3** in appendix A. The levels of IL-6, IL-8, IL-13, IL-12p70, I-TAC and TNF-α (**Figure 3.16N, Q, R, V, BB** and **HH**, respectively) were only significantly different between HC and treatment-responsive group. There were significant differences in the levels of TRAIL and TSLP between the HCs and the delayed-responsive group as shown in **Figure 3.16 LL** and **PP**, respectively. Increased concentrations of APRIL, BAFF and Eotaxin-3 (**Figure 3.16B, C** and **H**) were observed in the non-responsive group as compared to HCs at different days of TB treatment. The concentrations of BLC, Eotaxin, Eotaxin-2, IFN-γ, IL-10, IL-1β, IL-18, IL-22, LIF, and MCP-2, were also not specific in distinguishing controls from treatment-responsive, delayed-responsive or non-responsive as they were significantly different in HCs vs any two groups (**Figure 3.16D, F, G, J, L, U, Y, AA, DD, and FF** respectively). In this case, all individuals were compared to HCs as stratifying the DCTB treatment responsive patterns by HIV status yields small numbers of individuals in each group. This was not conducive for robust statistical analysis.

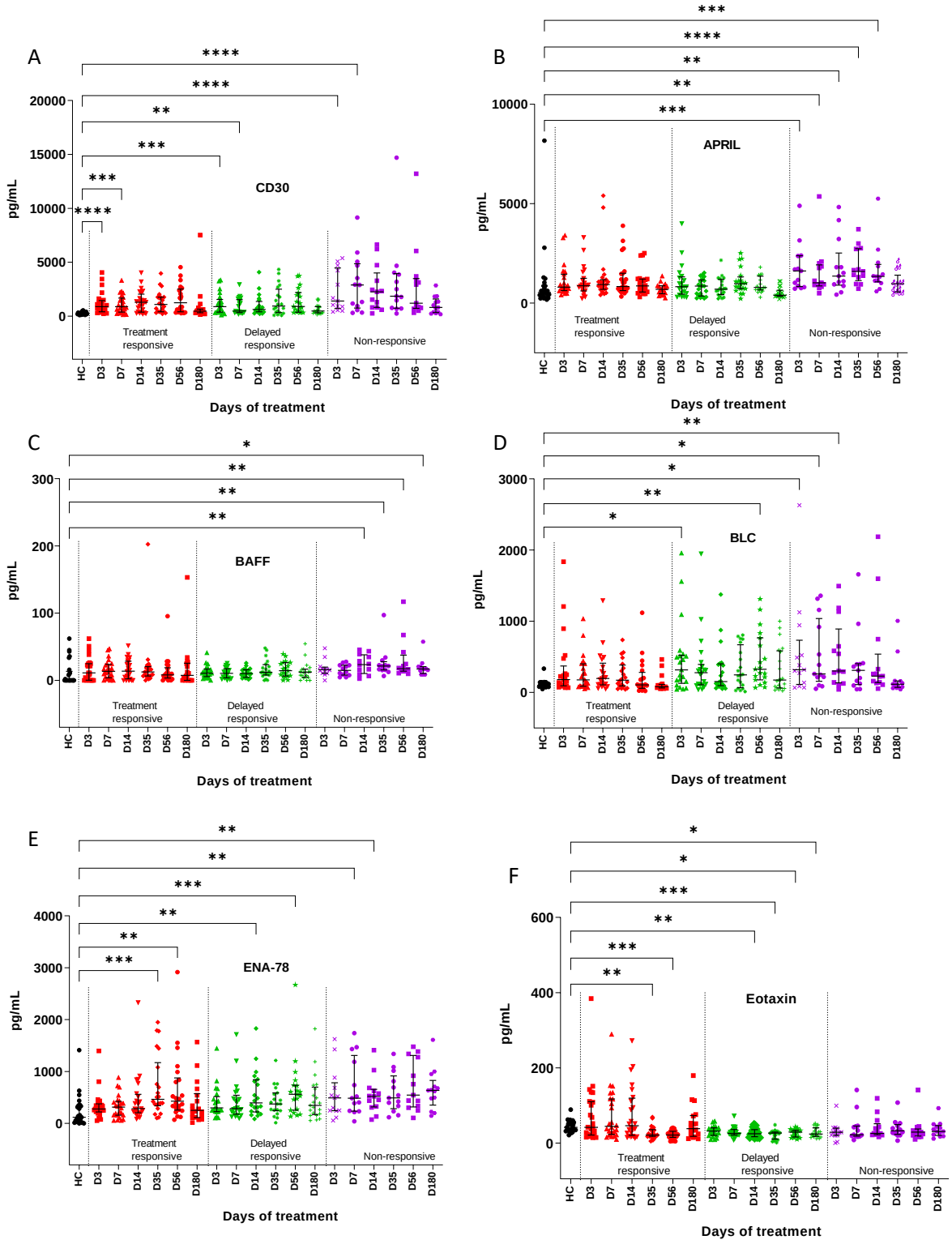
A
CD30
pg/mL
Treatment responsive
Delayed responsive
Non-responsive
B
APRIL
C
BAFF
D
BLC
E
ENA-78
F
Eotaxin
HC
D3
D7
D14
D35
D56
D180
Days of treatment

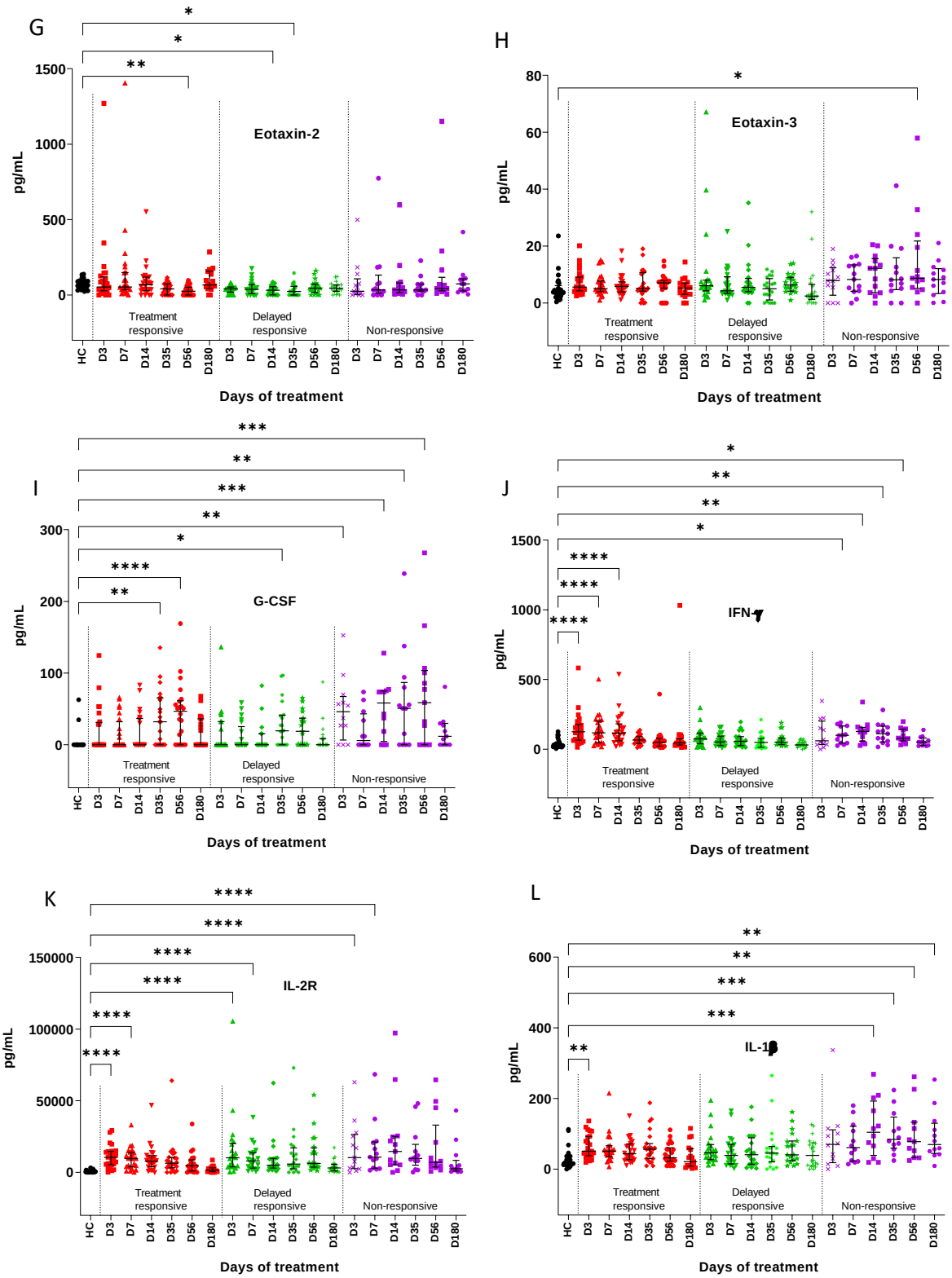
G
Eotaxin-2
pg/mL
Treatment responsive
Delayed responsive
Non-responsive
Days of treatment
H
Eotaxin-3
pg/mL
Treatment responsive
Delayed responsive
Non-responsive
Days of treatment
I
G-CSF
pg/mL
Treatment responsive
Delayed responsive
Non-responsive
Days of treatment
J
IFN-γ
pg/mL
Treatment responsive
Delayed responsive
Non-responsive
Days of treatment
K
IL-2R
pg/mL
Treatment responsive
Delayed responsive
Non-responsive
Days of treatment
L
IL-1β
pg/mL
Treatment responsive
Delayed responsive
Non-responsive
Days of treatment

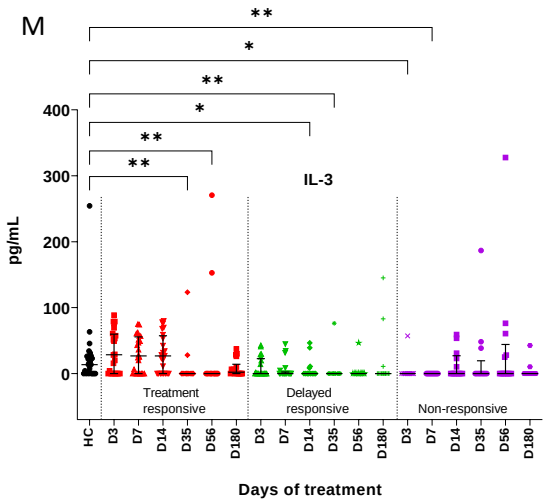
M
IL-3
pg/mL
Treatment responsive
Delayed responsive
Non-responsive
Days of treatment

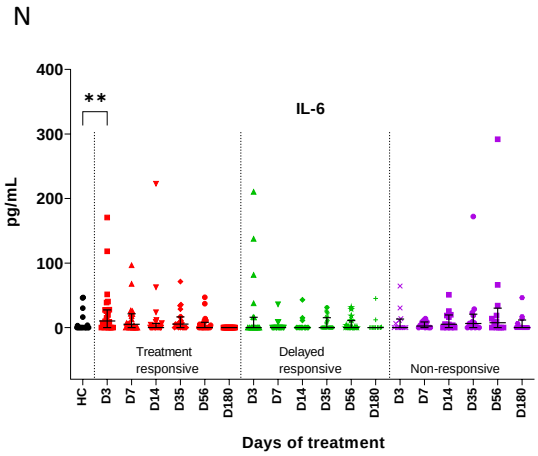
N
IL-6
pg/mL
Treatment responsive
Delayed responsive
Non-responsive
Days of treatment

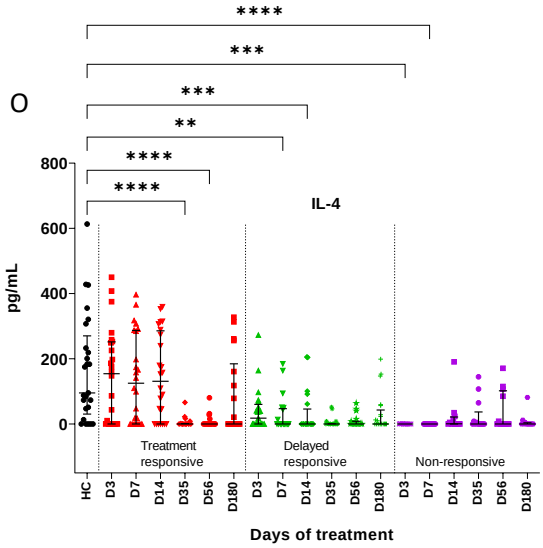
O
IL-4
pg/mL
Treatment responsive
Delayed responsive
Non-responsive
Days of treatment

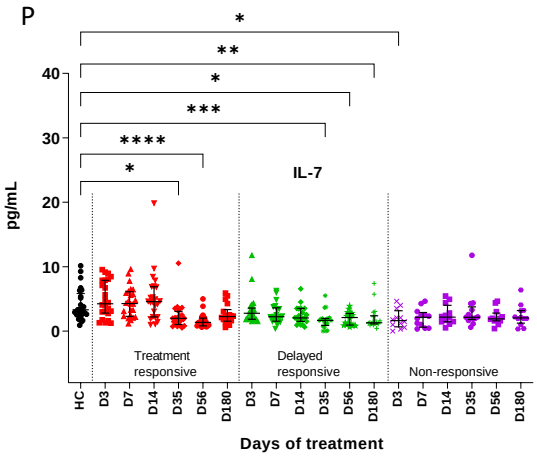
P
IL-7
pg/mL
Treatment responsive
Delayed responsive
Non-responsive
Days of treatment

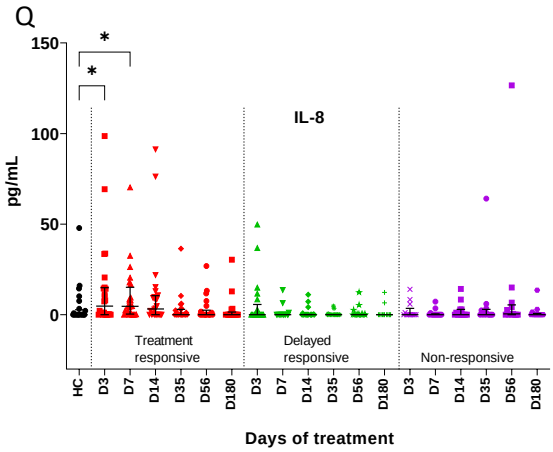
Q
IL-8
pg/mL
Treatment responsive
Delayed responsive
Non-responsive
Days of treatment

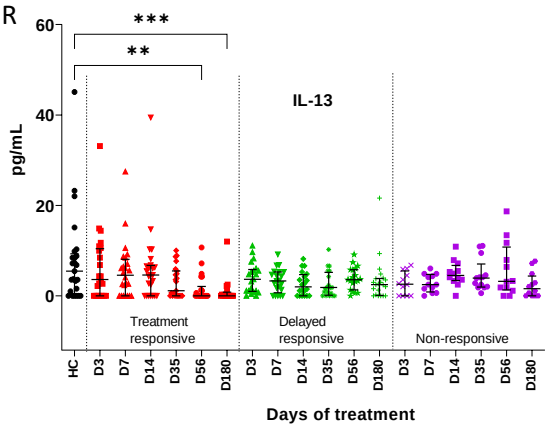
R
IL-13
pg/mL
Treatment responsive
Delayed responsive
Non-responsive
Days of treatment

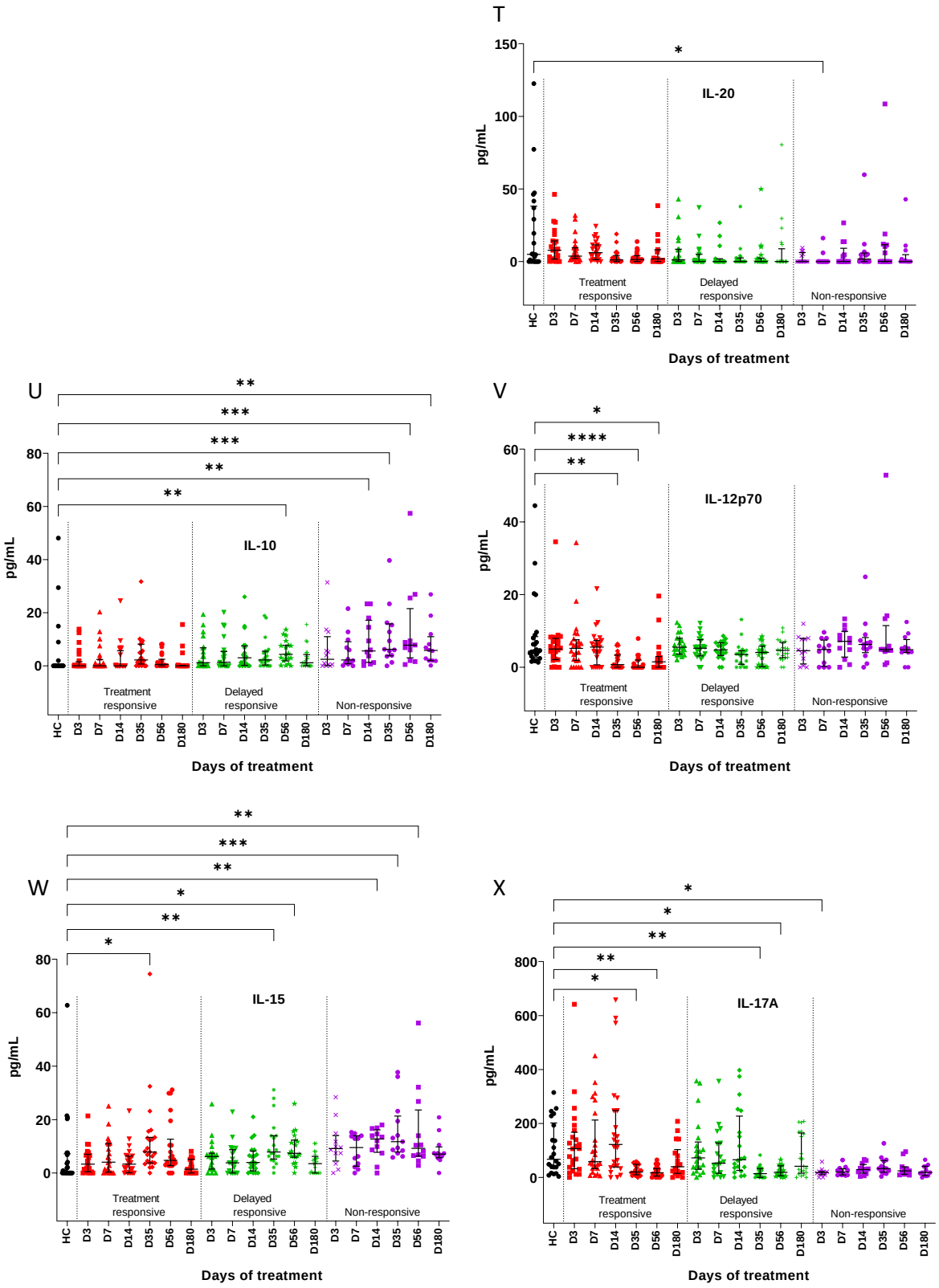
T
IL-20
pg/mL
Treatment responsive
Delayed responsive
Non-responsive
Days of treatment
U
IL-10
pg/mL
Treatment responsive
Delayed responsive
Non-responsive
Days of treatment
V
IL-12p70
pg/mL
Treatment responsive
Delayed responsive
Non-responsive
Days of treatment
W
IL-15
pg/mL
Treatment responsive
Delayed responsive
Non-responsive
Days of treatment
X
IL-17A
pg/mL
Treatment responsive
Delayed responsive
Non-responsive
Days of treatment

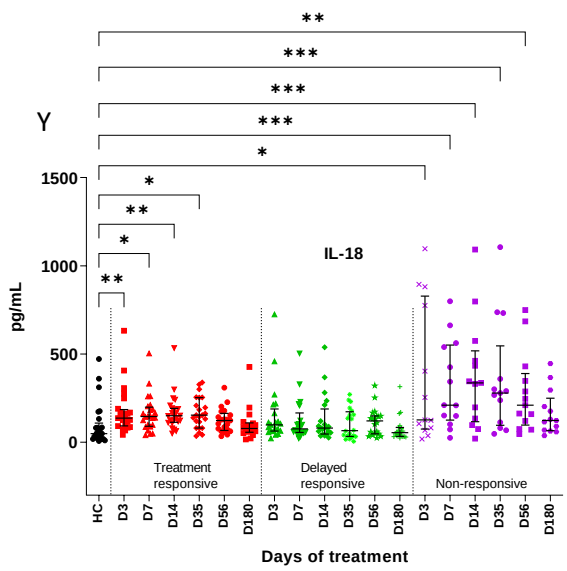
Y
IL-18
pg/mL
Treatment responsive
Delayed responsive
Non-responsive
Days of treatment

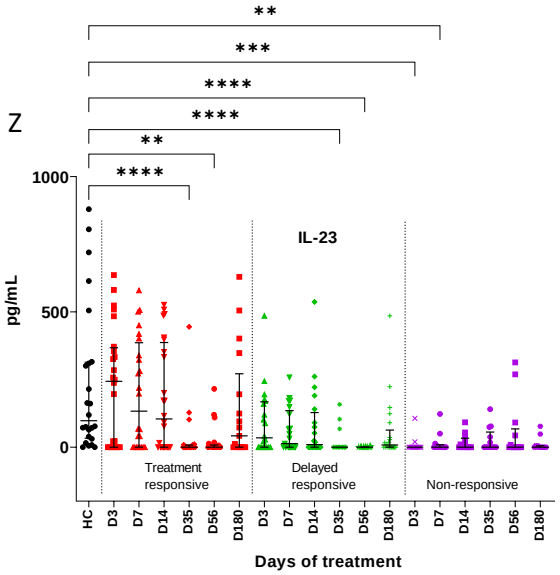
Z
IL-23
pg/mL
Treatment responsive
Delayed responsive
Non-responsive
Days of treatment

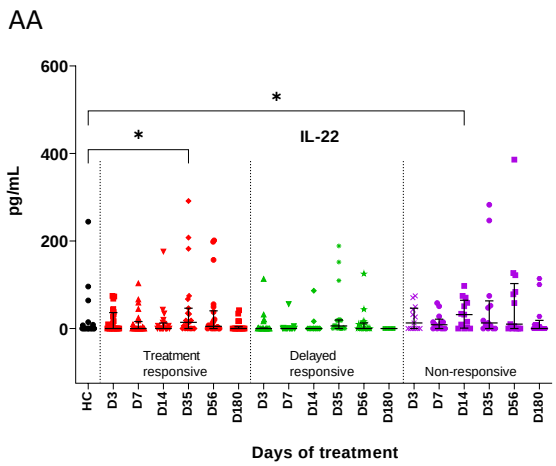
AA
IL-22
pg/mL
Treatment responsive
Delayed responsive
Non-responsive
Days of treatment

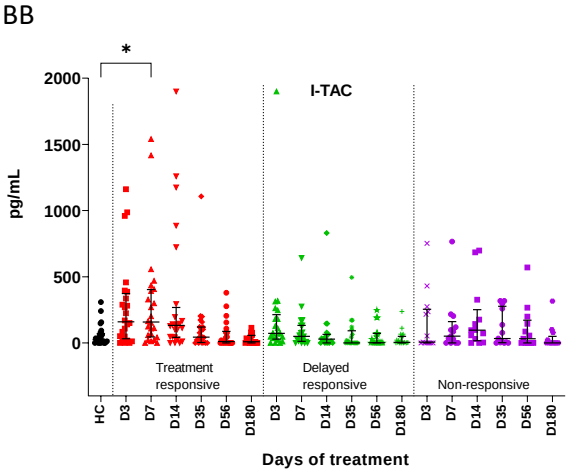
BB
I-TAC
pg/mL
Treatment responsive
Delayed responsive
Non-responsive
Days of treatment

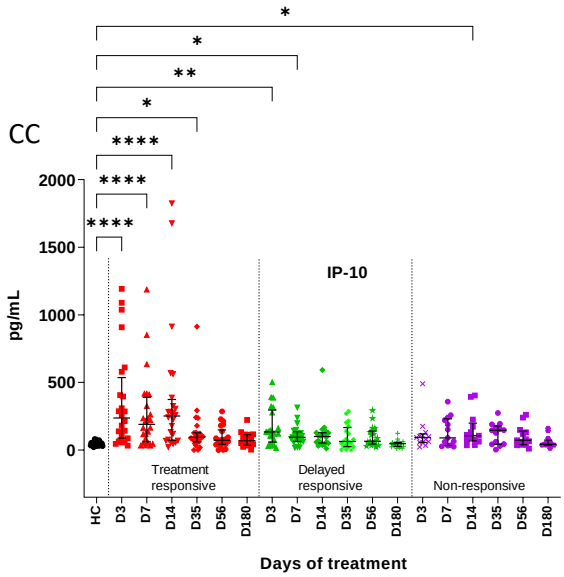
CC
IP-10
pg/mL
Treatment responsive
Delayed responsive
Non-responsive
Days of treatment

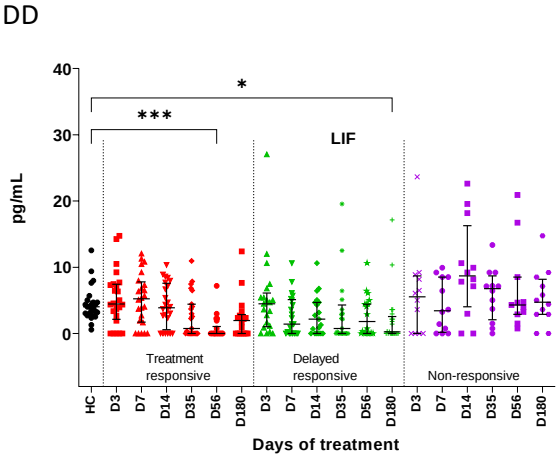
DD
LIF
pg/mL
Treatment responsive
Delayed responsive
Non-responsive
Days of treatment

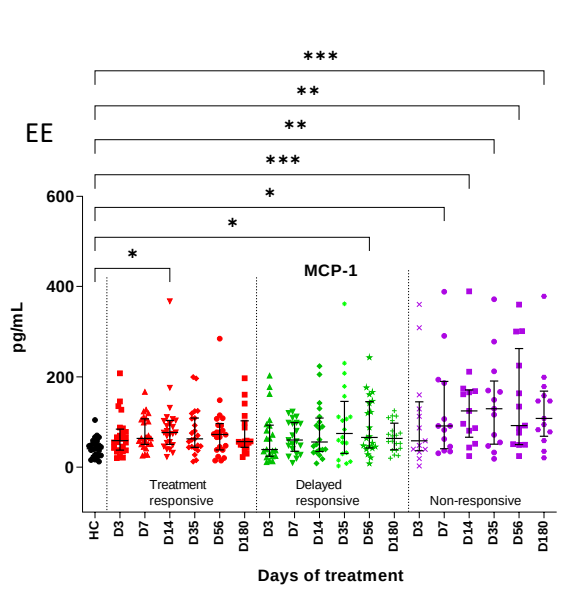
EE
MCP-1
pg/mL
Treatment responsive
Delayed responsive
Non-responsive
Days of treatment

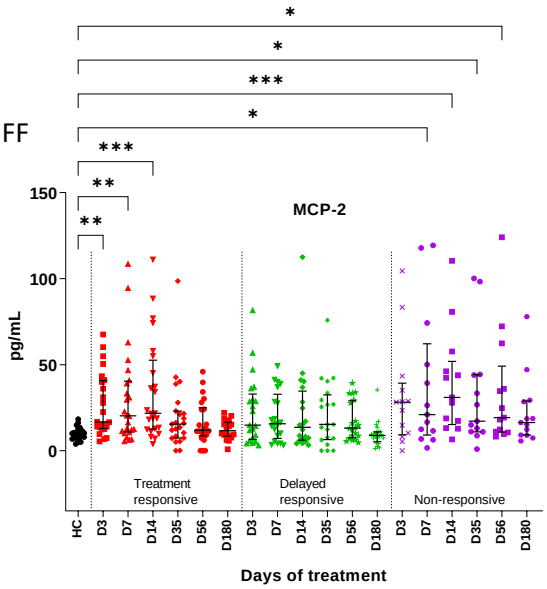
FF
MCP-2
pg/mL
Treatment responsive
Delayed responsive
Non-responsive
Days of treatment

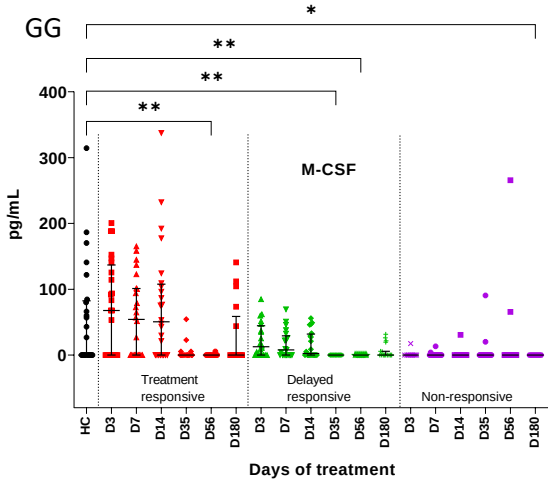
GG
M-CSF
pg/mL
Treatment responsive
Delayed responsive
Non-responsive
Days of treatment

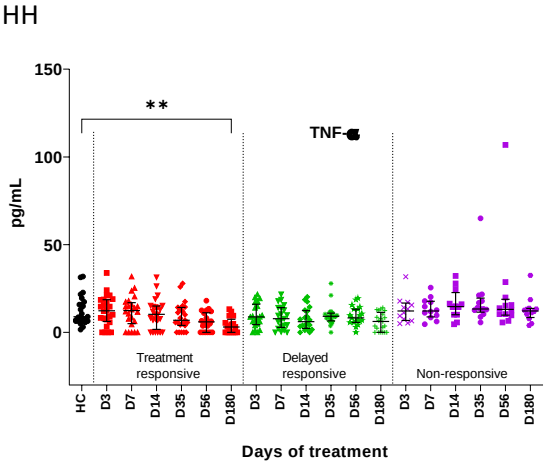
HH
TNF
pg/mL
Treatment responsive
Delayed responsive
Non-responsive
Days of treatment

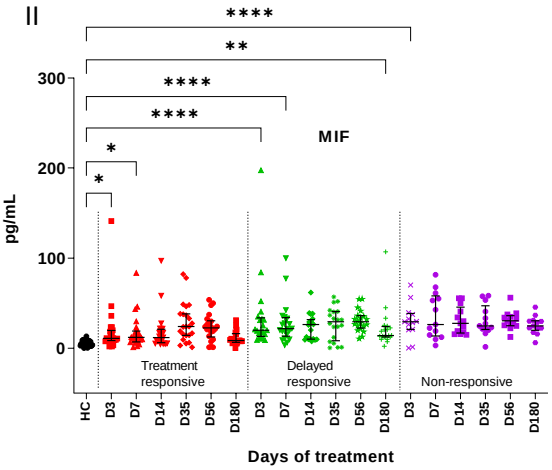
II
MIF
pg/mL
Treatment responsive
Delayed responsive
Non-responsive
Days of treatment

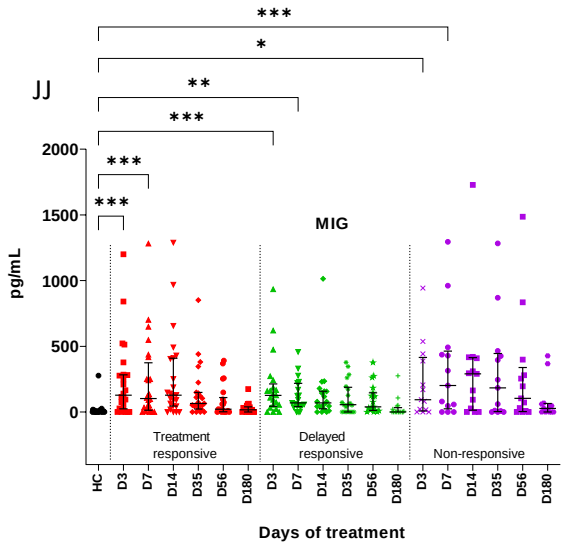
JJ
MIG
pg/mL
Treatment responsive
Delayed responsive
Non-responsive
Days of treatment

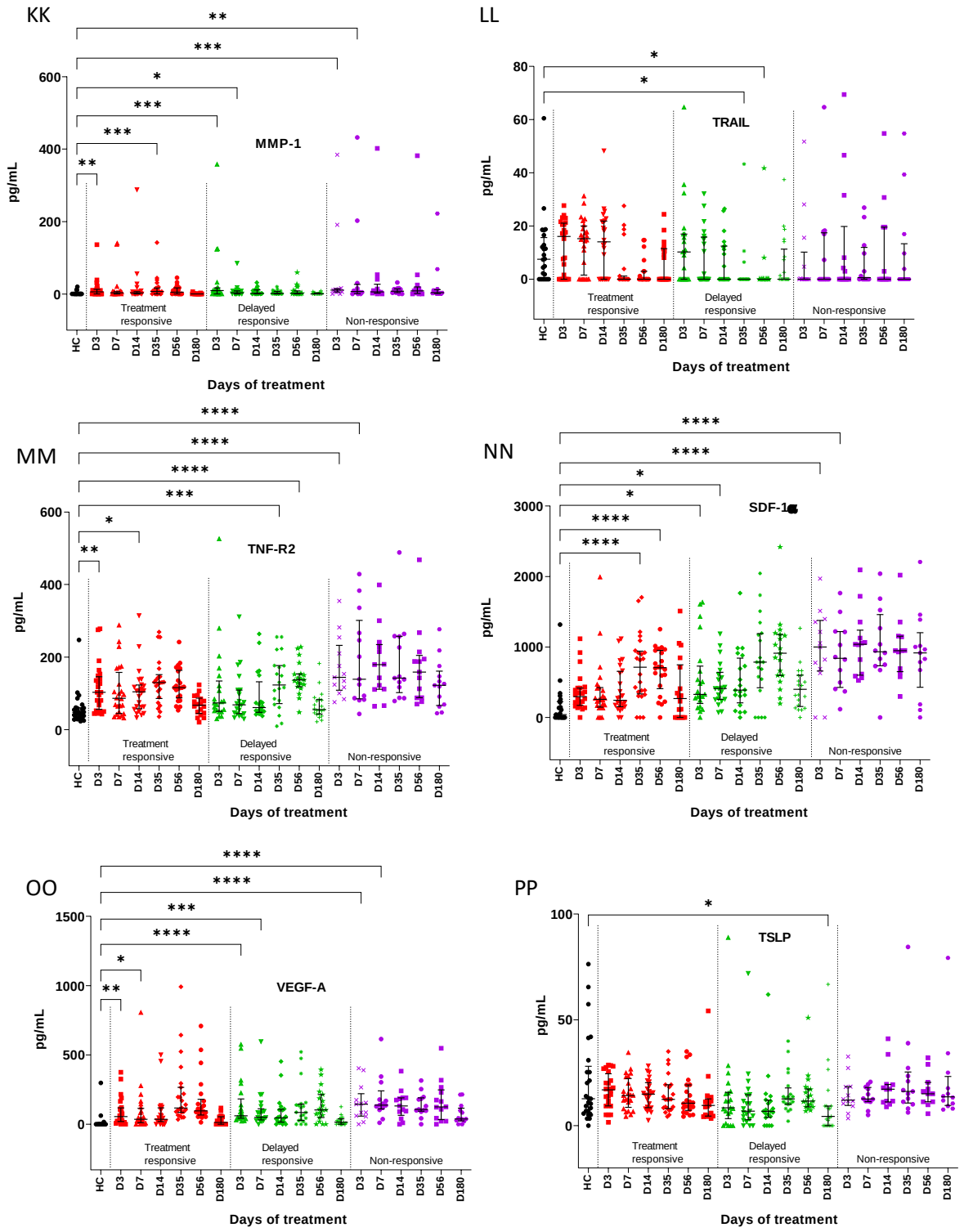

Figure 3.16. Changes in biomarkers between healthy controls, DCTB Treatment responsive, Delayed-responsive and Non-responsive groups. Black dots represent healthy controls; red: treatment-responsive; green: delayed-responsive and purple: non-responsive DCTB groups. The results are expressed in pg/mL and were analysed by the non-parametric Kruskal-wallis test, with significance significance *P <0.01; **P < 0.001; ***P < 0.001; ****P < 0.0001 (post hoc corrected by multiple comparisons).

Our analysis thus far allowed for the identification of cytokine signatures that change specifically with respect to DCTB response patterns. We next wanted to determine if these would enable the development of a predictive signature that could potentially be used to classify individuals into treatment responsive, delayed responsive or non-responsive DCTB groups. For this ROC analysis was carried out.

3.21. Plasma cytokines that can robustly distinguish treatment-responsive, delayed responsive and non-responsive DCTB response patterns.

We performed ROC analysis to estimate the discriminatory power of cytokines that showed greatest variations in the PCA model between healthy vs TB/HIV+ and TB patient treatment groups at different time points (**Figure 3.15**). The area under the curve (AUC) score of cytokines showing strongest discriminatory capacity between the different groups are highlighted in yellow in **Table 3.5**. As the DCTB treatment response groups were not based on the HIV status of individuals, HCs were employed for comparison in this analysis for both TB only and TB/HIV co-infected patients. ROC curves for cytokines highlighted in yellow in **Table 3.5** that show significant discriminatory power are given in **Figure 3.17**. I-TAC was the only cytokine that showed any discriminatory power with high AUC values (0.91, 0.94, 0.89, 0.72) in HCs vs treatment-responders with TB/HIV coinfection at day 3, 7, 14 and 35 (**Figure 3.17 A-B**), respectively. GCSF (AUC 0.92, 0.82, 0.89, 0.82) and VEGF-A (AUC 0.92 and 0.85) [**Figure 3.17C-E**)], demonstrated discriminatory power with high AUC values in HCs vs non-responders with TB only and TB/HIV coinfection at day 3, 14 and 180. No cytokines/cytokine signatures that were specific for the delayed responsive group were identified.

Table 3.5: Receiver operating characteristic (ROC) analysis of healthy controls vs TB/HIV+ and TB patient treatment groups at different time points

Cytokines	Days of TB treatment																	
	3			7			14			35			56			180		
	TR	DR	NR	TR	DR	NR	TR	DR	NR	TR	DR	NR	TR	DR	NR	TR	DR	NR
GCSF	0.63	0.52	0.92	0.62	0.52	0.46	0.63	0.52	0.46	0.87	0.78	0.46	0.78	0.71	0.46	0.65	0.52	0.46
	0.59	0.69	0.82	0.62	0.68	0.73	0.59	0.66	0.89	0.71	0.78	0.83	0.83	0.76	0.84	0.64	0.68	0.82
IL-2R	0.97	0.9	0.96	0.91	0.95	0.88	0.94	0.94	0.8	0.76	0.62	0.92	0.9	0.97	0.92	0.75	0.74	0.88
	1	0.96	0.87	1	0.96	0.99	1	0.98	0.91	0.94	0.98	0.92	0.86	1	0.96	0.77	0.85	0.87
SDF-1alpha	0.77	0.8	0.96	0.6	0.82	0.92	0.72	0.74	0.96	0.66	0.68	0.96	0.95	0.96	0.96	0.62	0.7	0.96
	0.81	0.85	0.82	0.79	0.9	0.93	0.76	0.89	0.97	0.9	0.91	0.91	0.86	0.92	0.96	0.61	0.89	0.85
VEGF-A	0.85	0.93	0.92	0.76	0.88	0.88	0.77	0.86	0.88	0.95	0.9	0.92	0.94	0.96	0.92	0.73	0.73	0.92
	0.88	0.95	0.9	0.84	0.94	0.97	0.85	0.86	0.91	0.96	0.87	0.92	0.96	0.82	0.91	0.62	0.77	0.85
I-TAC	0.55	0.63	0.16	0.55	0.6	0.16	0.55	0.53	0.16	0.34	0.41	0.16	0.34	0.38	0.16	0.42	0.5	0.16
	0.91	0.71	0.62	0.94	0.59	0.67	0.89	0.47	0.78	0.72	0.38	0.63	0.56	0.43	0.58	0.46	0.32	0.38
IL-23	0.44	0.38	0.04	0.41	0.27	0.04	0.45	0.3	0.04	0.16	0.13	0.04	0.09	0.03	0.04	0.34	0.26	0.04
	0.51	0.32	0.1	0.48	0.24	0.12	0.45	0.23	0.15	0.1	0.08	0.15	0.16	0.04	0.19	0.47	0.18	0.11
IL-27	0.69	0.55	0.34	0.56	0.58	0.34	0.69	0.58	0.34	0.54	0.52	0.34	0.56	0.51	0.64	0.62	0.51	0.64
	0.53	0.46	0.44	0.54	0.43	0.43	0.52	0.41	0.6	0.61	0.47	0.49	0.57	0.57	0.59	0.43	0.44	0.43
IL-4	0.41	0.36	0.1	0.39	0.28	0.1	0.45	0.3	0.1	0.12	0.16	0.2	0.13	0.13	0.1	0.26	0.26	0.2
	0.52	0.17	0.2	0.52	0.14	0.18	0.51	0.15	0.27	0.14	0.12	0.17	0.14	0.15	0.31	0.39	0.18	0.22
MCSF	0.56	0.57	0.26	0.53	0.51	0.26	0.61	0.5	0.26	0.31	0.26	0.26	0.26	0.26	0.26	0.37	0.43	0.26
	0.64	0.45	0.29	0.59	0.38	0.31	0.63	0.35	0.29	0.31	0.26	0.33	0.28	0.26	0.36	0.5	0.36	0.26

Patient analysis: Healthy Controls versus TB/HIV-, Healthy Controls versus TB/HIV+
Optimal discrimination calculations between the different subgroups are indicated by a yellow box fill.
Abbreviations: TR-treatment responsive, DR-delayed responsive, NR- non responsive.
ROC AUC (area under the curve) score

A

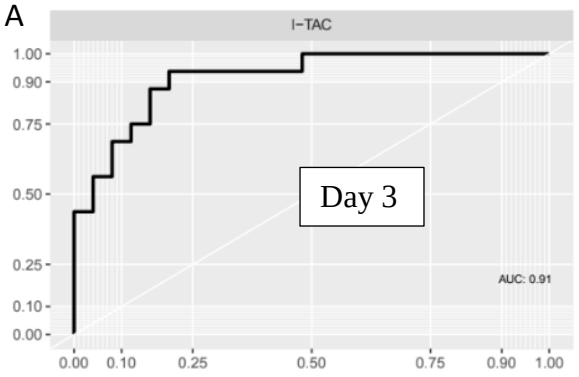
I-TAC
1.00
0.90
0.75
0.50
0.25
0.10
0.00
Day 3
AUC: 0.91
0.00 0.10 0.25 0.50 0.75 0.90 1.00

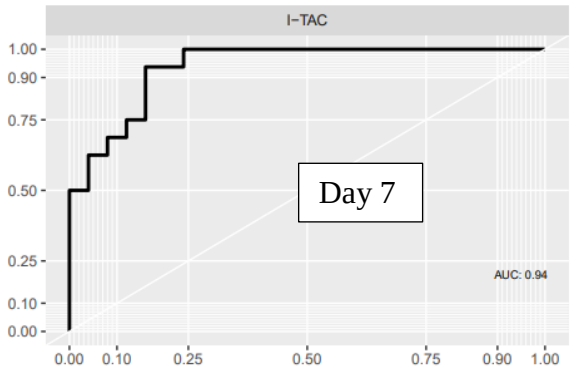
I-TAC
1.00
0.90
0.75
0.50
0.25
0.10
0.00
Day 7
AUC: 0.94
0.00 0.10 0.25 0.50 0.75 0.90 1.00

B

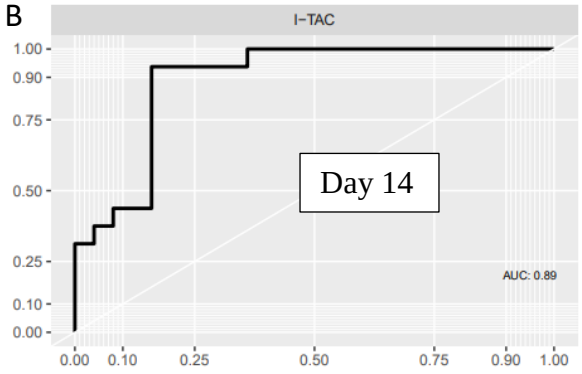
I-TAC
1.00
0.90
0.75
0.50
0.25
0.10
0.00
Day 14
AUC: 0.89
0.00 0.10 0.25 0.50 0.75 0.90 1.00

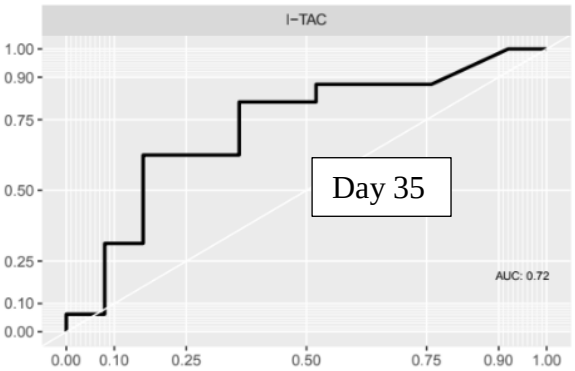
I-TAC
1.00
0.90
0.75
0.50
0.25
0.10
0.00
Day 35
AUC: 0.72
0.00 0.10 0.25 0.50 0.75 0.90 1.00

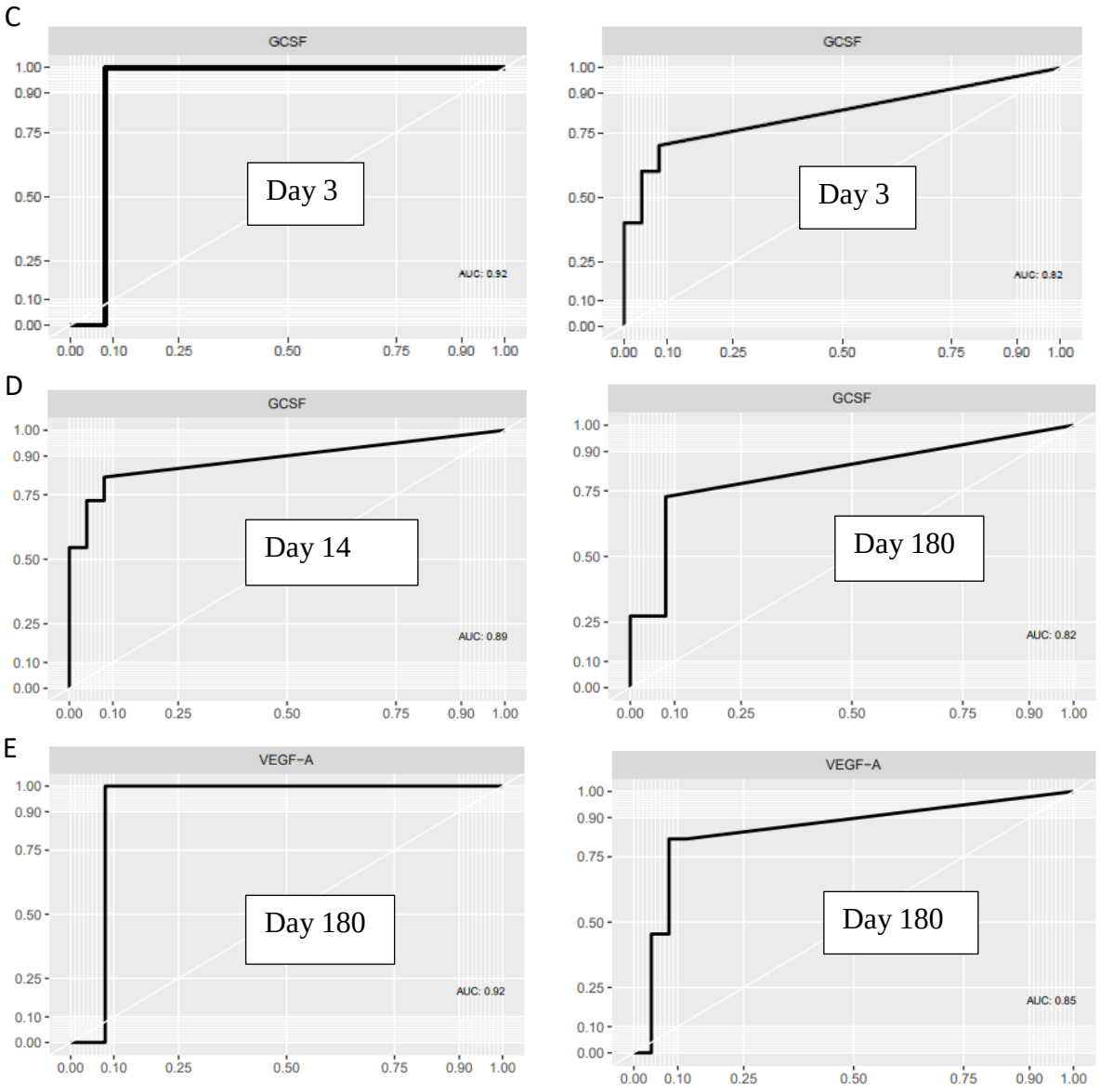

Figure 3:17. ROC analysis to estimate the discriminatory power of plasma cytokines in DCTB treatment responsive, slow delayed responsive and non-responders with and without HIV infection. ROC analysis to estimate the sensitivity, specificity and AUC was performed using cytokines that showed greatest variations in the PCA model. These data are derived from AUC values given in **Table 3.5**. The ROC of I-TAC for its ability to distinguish the treatment responsive group from the others, for TB/HIV co-infected individuals, at days 3 and 7 is given in (A) and for days 14 and 35 is given in (B). The ROC for G-CSF to distinguish the non-responsive group from others, for both TB only and TB-HIV infected groups, for day 3 is given in (C), left and right panels, respectively. The ROC for G-CSF to distinguish the non-responsive group from others, for TB-HIV infected individuals at days 14 and 180, is given in (D). The ROC for VEGF-A to distinguish the non-responsive group from others, for TB only and TB-HIV infected individuals at 180, is given in (E), left and right panels, respectively.

Summary of cytokine responses: Our analysis revealed I-TAC as a cytokine that is specific for the DCTB treatment responsive pattern for individuals with TB-HIV co-infection for days 3, 7, 14 and 35, suggesting that this cytokine can report on DCTB early treatment response. For the DCTB non-responsive group, G-CSF in individuals with TB/HIV co-infection, had discriminatory power at days

3, 14 and 180. Also in this group, VEGF-A, had discriminatory power at day 180 for TB only and TB-HIV infected individuals.

Finally, we conducted some secondary analysis to determine (I) if there were any cytokines that appeared to be different within groups during treatment response, (II) if Mtb strain type had an effect, and (III) if the presence of residual DCTB upon treatment completion affected cytokine profiles. A brief summary of these data is given next.

3.22. Changes in the concentrations of host biomarkers during the course of TB treatment within the Treatment-responsive, Delayed-responsive and Non-responsive groups.

We analysed whether there were differences in cytokine profiles within in each treatment group and noted some significant differences. **Figure A3** (in Appendix A) illustrates all the significant differences seen in each treatment responsive group. There were a few host biomarkers (BLC, Eotaxin, Eotaxin-2, Fractalkine, HGF, IL-2, IL-3, IL-4, IL-7, IL-10, IL-6, IL-12p70, IL-18, IL-20, IL-21, I-TAC, LIF, MCP-2, MCP-3, MIF, MIP-3α, SCF, and TNF-α) that could possibly be used to monitor treatment response specifically within the treatment-responsive group. These are shown in **Figure A3** panels B, C, D, E, F, H, K, L, M, N, O, P, S, T, U, Y, Z, AA, BB, CC, DD, GG, II, KK, LL, MM, and OO, respectively. In the delayed responsive group, three markers (APRIL, MIP-1β and TSLP in **Figure A3A, FF** and **NN**) that showed significant differences during treatment duration. IL-1α was the only marker that showed a significant change during treatment response in the non-responsive group of patients as shown in **Figure A3PP**.

3.23. The effect of strain type on cytokine profiles during TB treatment.

Next, we assessed whether the genotype of the infecting Mtb strain affect cytokine responses during TB treatment. We selected three of the most prevalent genotypes in our cohort including, LAM, Beijing and T-strains. The former two were also investigated in chapter 2 for their propensity to simulate the immune response when in the DCTB state. We found no significant differences in cytokine profiles when stratified by strain type, **Figure A4** in Appendix A.

3.24. The effect of residual DCTB at the end of treatment.

In prior work from our lab using this cohort, it was demonstrated that ca. two-thirds of individuals in the cohort had residual, viable DCTB at treatment completion (Peters et al., 2023). We stratified the 57 individuals selected for this study by the presence of DCTB upon treatment completion and compared whether there were differences in cytokine responses. We found no significant differences in cytokine abundance between individuals with and without DCTB at the end of treatment. The data are given in **Figure A5** in Appendix A.

3.25. A summary of the analysis plan and key observations of the differences of cytokines, chemokines and growth factors observed in each group of patients.

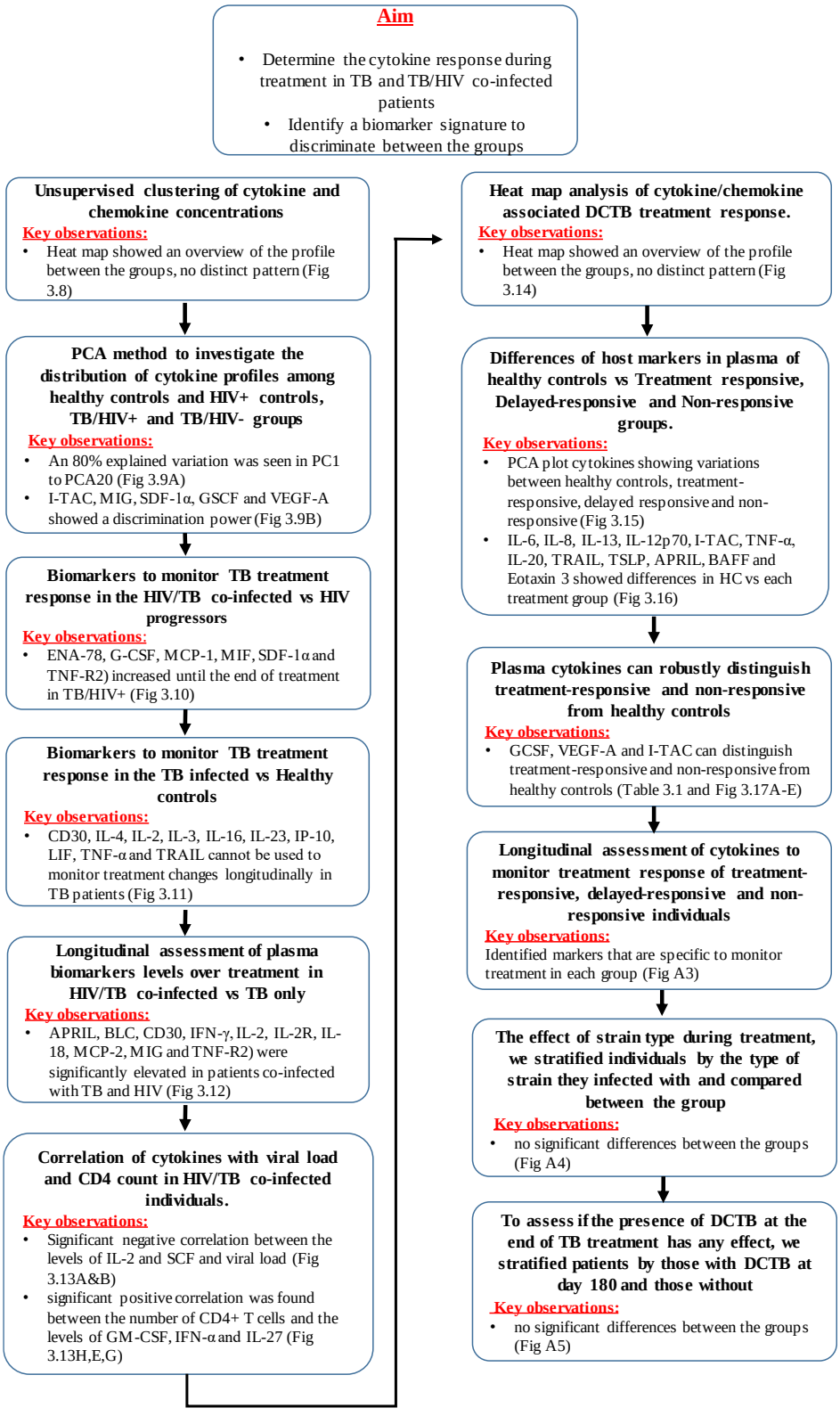

Figure 3.18. A Flow diagram summarising the changes in cytokines between the different groups of patients.

DISCUSSION

There is an urgent need for prognostic biomarkers of TB treatment efficacy, preferably those that allow identification of individuals at high risk of treatment failure, even before treatment begins, in order to provide tailored management (Walzl et al., 2018). There is also broad scientific agreement that such predictive tools must be based on bio-signatures rather than single biomarkers. Multiplex assays based on transcriptional or soluble protein biomarkers in peripheral blood are thus appropriate analysis platforms for discovery of these signatures (Maertzdorf et al., 2015). Previous studies have reported changes in bio-signatures during treatment, together with evaluating their predictive capacity for specific treatment outcomes. Studies using RNA profiling in peripheral whole blood evaluated the potential use of transcriptional signatures in improving TB diagnosis and treatment monitoring (Bloom et al., 2012, Cliff et al., 2013, Sweeney et al., 2016, Zak et al., 2016). Another study obtained a novel PREDICT 29 TB signature that consisted of 29 genes which were mostly associated with innate immune response. The authors demonstrated that the signature was able significantly discriminate progressors from non-progressors in a Brazil cohort with an (AUC) value of 0.911. In addition, the performance of PREDICT29 signature to previously published ACS-COR and RISK4 signatures for TB progression risk was superior in their cohort. It was concluded that PREDICT29 can predict likelihood of progression/reactivation to TB in individuals who have been recently exposed, at least five years before disease development (Leong et al., 2020). Our study compared the cytokine expression profiles of HCs, individuals with active TB, TB/HIV co-infected individuals and HIV progressors. Unlike other published work, we stratified our cohort into groups based on DCTB response patterns including treatment-responsive, delayed-responsive, and non-responsive patients. Our hypothesis was that as DCTB represent drug tolerant organisms, their differential rates of clearance would impact on immune responses.

Cytokines have a big impact on how susceptible the host is to TB and how quickly disease spreads (Hassuna et al., 2021). Infection with Mtb is regulated by mRNA expression, which leads to the generation of cytokines and other proteins that activate many different cell types (Wawrocki et al., 2020). Inflammatory cytokines and chemokines are produced by alveolar macrophages during Mtb infection. To confine infection and stop the spread of bacteria, monocytes, neutrophils, and lymphocytes move to the site of the infection. This group of inflammatory cells creates an immunological and physical barrier in the form of a granuloma (Lin and Flynn, 2010). The interaction of pro-inflammatory and anti-inflammatory signals, following infection is crucial for forming the granuloma and determining its ultimate course

(Kumar et al., 2019). Despite the fact that a Th1 profile is required for a protective response, it can also result in immunopathologic damage. As a result, either regulatory T cells or a Th2 response play crucial regulatory roles in protecting the patient from unintended host tissue damage (Geffner et al., 2009). Chemokines are crucial components in the inflammatory response of Mtb infection as they aid in cell migration, which leads to the formation of granulomas (Sasindran and Torrelles, 2011).

Upon conducting cytokine profiling, we first set out to conduct an analysis comparing controls with TB infected groups. Assuming that there wouldn't have been any changes in the immune response as early as day 3 of treatment, we used day 3 of treatment as our baseline for the patients on treatment. Whilst large patterns did not emerge between groups, we did note some distinct differences in select cytokines and investigated this further using pairwise comparisons of all 65 cytokines in HIV+ progressors vs TB/HIV co-infected individuals and HCs versus the TB infected group. Additionally, to monitor treatment effectiveness, we longitudinally analysed the changes in concentrations in each patient group.

We employed PCA to investigate cytokine profiles among the HCs, HIV progressors and patient groups at day 3 of treatment. A clear distinction appeared between HCs, HIV+ controls, TB/HIV+ and TB/HIV- from the PCA analysis (**Figure 3.9B**). This analysis revealed that I-TAC, MIG, SDF-1α, GSCF and VEGF-A were the most important biomarkers determining the discrimination power of the PCA model between HCs and HIV+ controls, TB/HIV+ and TB/HIV- groups. These data strongly implied that it was possible to search for potential biomarkers to distinguish HIV+ controls from TB/HIV+ individuals and TB/HIV- infected individuals from HCs. Plasma concentrations of six host markers (ENA-78, G-CSF, MCP-1, MIF, SDF-1α and TNF-R2) were significantly higher in TB/HIV+ individuals until the end of treatment when compared to the HIV progressors. The concentrations of I-TAC, BLC, IL-6, IL-8, IFN-γ, IL-15, IL-22, MCP-2, and MIP-3α were not significantly different between HIV controls and HIV/TB co-infected patients at any of the treatment days. Changes in the concentrations of all the 65 markers over the treatment period in the TB/HIV+ patients demonstrated that the cytokines ENA-78, Eotaxin-3, MCP-1, LIF, IL-9, G-CSF and IL-4 cannot be used to monitor treatment changes longitudinally in this group of patients as they yielded no material differences over time.

HIV infection affects both innate and adaptive immune responses. Through the release of cytokines that control the immunological response, CD4+ T helper cells are essential for the

immune system (Osuji et al., 2018). HIV and TB have synergistic negative effects on the immune system, which can activate viral replication and impair T cell activation (Nosik et al., 2021). It is yet unclear how Mtb co-infection affects immunological activation when HIV is present. Pro-inflammatory pathways and type I interferon gene signalling are particularly upregulated in *in vitro* models of macrophage co-infection, suggesting that Mtb-derived gene expression predominates over that of HIV infection (Tsang et al., 2009). The impact of TB treatment on plasma cytokine response and viral load in HIV-infected people with TB is poorly understood, with some research demonstrating an increase in pro-inflammatory immune response and a decrease in HIV viral load in response to TB therapy (Dean et al., 2002), while other studies do not show a similar effect (Kalou et al., 2005). At six months of anti-TB treatment without antiretroviral therapy, there was no significant differences in the restoration of IFN-γ, IL-2, IL-17, and IP-10 cytokines in the HIV/TB co-infected patients (Kassa et al., 2016). To some extent, our data reproduced these findings. A recent review article also showed that the concentrations of IFN-γ, IL-2, IL-6, and IL-10 were higher in HIV-positive patients receiving anti-TB therapy (Bhopale, 2021).

The immunological response during TB treatment in patients who are HIV positive is expected to be different from that in patients who are HIV negative. Longitudinal assessment of plasma cytokines in this group, showed that the levels of pro-inflammatory host cytokines (APRIL, BLC, CD30, IFN-γ, IL-18, TNF-R2) and chemokines (MIG, MCP-2) are significantly higher in HIV/TB co-infected patients compared to those who were infected with TB only during anti-TB treatment. In contrast to TB patients, who had a reduction in bacterial load following TB therapy, the majority of non-responders in our cohort were TB/HIV patients (as reported in (Peters et al., 2023), who experienced no significant change in DCTB levels during treatment. In people with HIV, anti-TB treatment considerably raises the level of chemokines and Th1 cytokines without restoring the immunological response (Mihret et al., 2014). Our results suggest that the increased level of select cytokines and chemokines in HIV/TB patients could be due to the ongoing inflammatory immune response as compared to TB only patients due to the TB treatment not clearing the bacterial burden in the former group.

Characterizing early cytokine responses is important to find biomarkers that could be targeted to reduce HIV-induced immune damage (Leeansyah et al., 2013). The frequency of exhausted CD4 T cells and CD8 T cells was shown to be significantly correlated with TNFR2 and sCD27 levels when assessing the relationship between early HIV infection T-cell phenotypes and plasma biomarker levels (Pastor et al., 2018). Bivariate analysis revealed a relationship

between elevated peak viral load and IL-16, SCGF, MCP-3, IL-12p40, and SCF concentrations (Ngcobo et al., 2022). The levels of IL-2 had a strong negative relationship with viral load (**Figure 3.13A**). We found a negative correlation between CD4+ T cells and the concentration levels of IL-1α, IP-10, I-TAC, MIF, MIG, MIP-1β, TNF-R2, and VEGF-A. Moreover, a strong positive association between the quantity of CD4+ T cells and the concentrations of GM-CSF was noted. Given the differences in cytokine profiles observed, our longitudinal study offers new insight into potential associations between innate and cellular responses as well as viral load in TB/HIV co-infected individuals. It should be noted however, that our study does have limitations in this regard. We did not have complete information on how long our participants had been infected with HIV on average, which could have an impact on the inflammatory profile. Secondly, the participants with HIV infection who were on ART at enrolment had possibly varying ART initiation times/adherence.

Biomarkers required for monitoring treatment response are necessary for clinical decision making. We showed that the concentration of 26 cytokines were significantly different at the different time points of treatment between HCs and TB patients, with Eotaxin concentrations that were high till the end of treatment. We also note that the concentrations of CD30, IL-4, IL-2, IL-3, IL-16, IL-23, IP-10, LIF, TNF-α and TRAIL cannot be used to monitor treatment changes longitudinally in this group of patients. When compared to those with TB/HIV co-infection, participants with Mtb only infection had more cytokines that could be utilized to monitor TB treatment response. The concentration of these cytokines was either significantly lower or at similar levels as the HCs at treatment completion. This suggests that HIV infection has a significant impact on the immune system during TB treatment, reducing the number of potential biomarkers that can be used to monitor TB treatment response. This should be carefully considered in future biomarker studies.

The TNF-α family of ligands, includes B cell activating factor/a proliferation-inducing ligand (BAFF/APRIL), which are essential for B cell survival, development, and immune system modulation (Kathamuthu et al., 2018). Cynomolgus macaques with peripheral B-cell depletion showed decreased levels of inflammation, altered T-cell and cytokine responses, and higher bacterial load upon examination of individual granulomas (Phuah et al., 2016). Additionally, studies have demonstrated the function of B cells in inflammatory responses in granulomas by regulating neutrophil influx and Th17 responses (Kozakiewicz et al., 2013). The CD30 ligand (Tnfsf8) and CD30 (Tnfrsf8) receptor pair has attracted interest as a potential IFN-independent signalling mechanism during Mtb infection. Tnfsf8-/- mice die more quickly than wild-type

mice after infection (Sallin et al., 2018), and higher frequencies of Mtb specific Tnfsf8+ CD4 T cells in humans are associated with a reduced bacterial load in the lungs (Du Bruyn et al., 2021). TNF is a pleotropic cytokine that functions through the tumour necrosis factor receptor 1 (TNFR1) and TNFR2 receptors (Ward-Kavanagh et al., 2016). TNFR1 is expressed by all cells, but TNFR2 expression is induced and commonly thought to be limited to lymphoid lineage cells (Faustman and Davis, 2013). T cell growth and effector differentiation depend on the co-stimulatory signal produced by TNFR2 in activated T cells. To express TNFR2, naive T cells need activation signals (Ward-Kavanagh et al., 2016). Despite its importance, it appears that TNF-α levels were not sufficiently discriminatory to report on changes in DCTB levels in our cohort.

The family of type I cytokine receptors includes cell surface-expressed transmembrane receptors that can detect four-helix bundle cytokines including IL-2, IL-4, IL-6, IL-12, and IL-23, as well as granulocyte colony-stimulating factor (G-CSF) and granulocyte-macrophage colony-stimulating factor (GM-CSF) (Druszczyńska et al., 2022). T helper 17 (Th17)-related cytokines include IL-17A (IL-17A), IL-21, IL-22, and IL-23, which are either produced by Th17/Th22 cells or involved in their development (Shen and Chen, 2018). Antigen-presenting cells are the primary producers of a heterodimeric cytokine IL-23 (Khader et al., 2007). By focusing on cells that express IL-23R, IL-23 can affect both innate and acquired immunity (Che Mat et al., 2011). Shen et al. (2015) discovered that IL-23's capacity to promote the proliferation of activated Vγ2Vδ2 T cells and the production of cytokines including IL-17, IL-22, IL-2, and IFN-γ was elevated in macaques with Mtb infection. With the exception of IL-17, these cytokines appear to be differentially regulated in our cohort however, they did not reach the discriminatory power for predicting treatment response.

IL-2, also referred to as a significant T-lymphocyte growth factor, regulates the proliferation of B cells and the activity of natural killer (NK) cells in addition to promoting the maturation and expansion of activated T cells (Malek and Castro, 2010). The functioning IL-2 receptor (IL-2R) is the first short-chain type I cytokine whose receptor structure has been determined (Damoiseaux, 2020). Regardless of HIV status, a study found greater IL-2Ra levels in TB patients compared to LTBI (Chendi et al., 2021). Whilst IL-2 was detected in our cohort, this cytokine was not useful to monitor treatment response.

Members of the IL-1 family include the pro-inflammatory cytokines IL-1α, IL-1β and IL-18 (Dinarello, 1991). A significant mediator of inflammation and a factor in the host's ability to

withstand Mtb is the pro-inflammatory cytokine IL-1β (Krishnan et al., 2013). The antimicrobial activity of IL-1β serves as a barrier against the development of TB illness, but persistent expression may result in increasing tissue damage (Zhang et al., 2014). In another study, the pro-inflammatory cytokines levels of IL-1β and IL-18, were considerably lower in TB compared to LTBI. However, after receiving anti-TB therapy, there was a considerable rise in IL-1β and IL-18 levels (Kathamuthu et al., 2017). IL-18, is a cytokine that promotes inflammation and is essential to the inflammatory cascade (Chang et al., 2000). IFN-γ production and mycobacterial defense immunity are strongly correlated with IL-18 production in response to mycobacterial antigens (Lee et al., 2011). The expression of adhesion molecules, the generation of the enzyme nitric oxide synthase, and the creation of chemokines are all increased by IL-18 (Wawrocki et al., 2020). Animals unable to generate IL-18 in a mouse model showed greater sensitivity to Mtb infection (Schneider et al., 2010). A meta-analysis of IL-18 levels in the TB and HC groups demonstrated that patients with TB had higher levels of IL-18 than those in the HC group, proving that TB patients also had high levels of IL-18 (Zhang et al., 2021a). Similarly, we found that IL-18 levels were higher in TB infected patients, but levels were not significantly different between the different DCTB response groups.

The pro-inflammatory chemokine MCP-2/CCL8 is produced in inflamed tissues by resident and infiltrated cells, primarily monocytes and macrophages, following paracrine stimulation of T-cells by pro-inflammatory cytokines like interferons (IFNs) and other cytokines, or by innate mechanisms in response to contact with bacterial, viral, and fungal agents (Ragno et al., 2001, Van Damme et al., 1994). When (Goletti et al., 2006) compared MCP-2 responses to specific ESAT-6/CFP-10 peptides in TB cases and controls, they discovered that active TB patients had noticeably higher responses. Furthermore, (Wei et al., 2015) also showed that after stimulation with TB-specific antigen, the expression levels of MCP-2, IL-1β, and CCL3 (MIP-1α) were considerably increased in both active and latent TB infections compared to those in the HC group. We found that the changes in the concentration levels of MCP-2, could possibly be used to monitor treatment response specifically within the treatment-responsive group.

Monocytes and macrophages are the main cell types that express MIG (CXCL9). IFN-γ, but not IFN-α/β or other T-cell cytokines implicated in the production of IP-10, substantially induce MIG. Although TNF-α cannot induce MIG on its own, it can do so when combined with IFN-γ (Groom and Luster, 2011b, Ohmori et al., 1993). When MIG binds to the CXCR3 receptor, IP-10 and I-TAC-like immune effector activities are also induced. As a result, it takes part in a sophisticated cooperative network in which MIG is the one of a few agonists

responsible for providing the signal of adaptive immune response (Groom and Luster, 2011a, Groom and Luster, 2011b). Consistent with this, MIG emerged as a cytokine that has strong discriminatory power between TB infected groups and controls. MIG also appeared to have some discriminatory power between TB and TB/HIV infected individuals however, it was not able to discriminate effectively between treatment response groups.

IP-10 (CXCL10), is a chemokine that is known to trigger apoptosis, and chemotaxis of lymphocytes particularly in activated T cells (Liu et al., 2011, Sauty et al., 1999). The involvement of IP-10 in the development of TB and the potential for utilising IP-10 as a biomarker of TB response to treatment have both been noted in a number of studies. This cytokine is also known to be high in people living with HIV not on antiretroviral therapy (Lei et al., 2019). During pleural and meningeal TB, MIG and IP-10 traffic to the site of the disease and their levels decline after anti-TB therapy (Yang et al., 2014). IP-10 levels in the plasma of TB patients was high compared to controls (Blauenfeldt et al., 2018). Another study by Petrone et al. (2019) demonstrated that patients with active TB exhibited considerably greater baseline levels of total and agonist IP-10 in comparison with HCs. Additionally, near the end of treatment, a decrease in total urine IP-10 was seen in patients with active TB. In our hands, this cytokine did not emerge as a useful marker to monitor TB treatment response.

It has been established that migration inhibitory factor (MIF), a cytokine with pro-inflammatory chemokine-like properties, is crucial in initiating a range of immune responses to invading pathogens and may be linked to the beginning and/or progression of TB (Rossato Silva et al., 2019). MIF is likely the first cytokine to emerge during the TB inflammatory response; it limits macrophage movement, enhances macrophage accumulation, and activates T cells in inflamed TB lesions (Gómez et al., 2007). Patients with advanced TB disease and drug-resistant TB had median MIF values that were significantly higher than those with mild to moderate, non-disseminated TB, and drug-sensitive TB. The increase in serum levels of MIF was associated with higher mortality in pulmonary TB patients and could therefore be used as a biomarker for predicting death (Wang et al., 2019). Serum levels of MIF have been shown to be a helpful measure for evaluating the effectiveness of treatment. Prior to treatment, MIF serum levels were substantially higher in patients with active TB than in control participants, but after 2, 4, and 6 months of treatment, the levels were significantly lower (Shang et al., 2018). Similarly, in our cohort there were changes in MIF levels that could be used to report on treatment response but not on patterns of DCTB clearance.

Stromal cell-derived factor-1alpha (SDF-1α) also called CXCL12 is a chemokine, which has numerous activities, one of which is controlling circulation of lymphocytes (Janssens et al., 2018). SDF-1α is one of the most effective T lymphocyte chemoattractants and activators, it was discovered to be related to the development of pulmonary granulomas, organized lymphoid structure, the presence of T cells, and neutrophils in guinea pigs. A successful response to anti-TB therapy is linked to CXCL12 expression in guinea pigs which modulated at 10 weeks post infection. (Rawat et al., 2018). The rate of increased CXCL12 was noticeably higher in active TB patients than HCs. It was discovered that elevated CXCL12 levels were independently influenced by bacterial load, radiological severity, and the degree of chest x-ray involvement (Kalkan et al., 2021). In our work, this cytokine was able to distinguish TB infection from controls, with levels of this cytokine remaining somewhat high at the end of treatment.

Vascular endothelial growth factor (VEGF), which is produced by macrophages and released into the extracellular spaces, is also induced by Mtb. VEGF induces angiogenesis, a physiological process that results in the formation of blood vessels and increases vascular permeability. It is unclear why angiogenesis occurs in TB granulomas, possibly the emerging blood vessels provide a quick route for immune cells to travel to the granuloma and try to combat the infection (Batista et al., 2020). In nearly every granulomatous disease in humans where it has been studied, including pulmonary TB, high levels of VEGF-A have been discovered (Alatas et al., 2004). There have been several findings pointing to the impact of VEGF-A-mediated angiogenesis during mycobacterial infections. These studies found that VEGF-A suppression reduced mycobacterial survival and proliferation in low-vascularized regions (Oehlers et al., 2015). Serum levels of VEGF are higher in patients with active TB compared to HCs without other respiratory diseases, including those with latent TB infection or uninfected individuals, according to the first meta-analysis comparing VEGF levels between patients with TB and various control conditions (Saghazadeh and Rezaei, 2022). This cytokine was able to distinguish TB infected groups from controls and appeared to have an effect at distinguishing DCTB treatment response patterns.

A clear distinction with select cytokines appeared between treatment responsive, delayed responsive and non-responsive groups at day 3, 7, 14, 35, 56 and 180 of TB treatment as seen from the PCA analysis. This analysis revealed that IL-4, IL-23, M-CSF, IL-20, CD40L, IL-2R and G-CSF were the biomarkers determining the discrimination power of the PCA model between the groups in PC1 and PC2. The three DCTB treatment response groups could be distinguished by the cytokines IL-4, M-CSF, IL-9, I-TAC, G-CSF, SDF-1, and VEGF-A

captured in PC1 and PC2. The only group with statistically different levels of IL-6, IL-8, IL-13, IL-12p70, I-TAC, and TNF-α was the treatment-responsive group when compared with HCs. There were significant variations in the levels of IL-20, TRAIL, and TSLP between the HCs and the delayed-responsive group. Increased concentrations of APRIL, BAFF and Eotaxin-3 were observed in the non-responsive group as compared to healthy controls at different days of TB treatment. The levels of Eotaxin, Eotaxin-2, IFN-, IL-1, IL-18, IL-22, MCP, BLC, IL-10, and LIF were insufficient to distinguish HCs from treatment-responsive, delayed-responsive, or non-responsive patients since they were significantly higher in the controls compared to the other groups. Several host biomarkers (BLC, Eotaxin, Eotaxin-2, Fractalkine, HGF, IL-2, IL-3, IL-4, IL-7, IL-10, IL-6, IL-12p70, IL-18, IL-20, IL-21, I-TAC, LIF, M-CSF, MCP-2, MCP-3, MIF, MIP-3α, SCF, TNF-α, TNF-R2, TRAIL and VEGF-A) showed significant changes over treatment and these can possibly be used to monitor treatment response specifically in the treatment-responsive group but are not sufficient to discriminate between DCTB response groups. APRIL, MIP-1beta, and TSLP in the delayed responding group showed significant change during treatment. The only marker in the non-responsive group of patients that significantly changed throughout treatment response was IL-1α.

Macrophages and mesenchymal cells both release the pleiotropic cytokine hepatocyte growth factor (HGF). The development of many organs, including the lung, as well as normal embryogenesis depend on it (Sonnenberg et al., 1993, Yamamoto et al., 2007). HGF might be crucial for controlling inflammation. Activated T cells and a range of pro-inflammatory cytokines, including IFN-γ, IL-1α/β, and TNF-α both induce the expression of HGF (Matsumoto et al., 1992, Skibinski et al., 2001). To date only one recent study has shown a relationship between HGF and TB. They found significant increase of HGF in healthy donors compared to LTBI and active TB patients (He et al., 2020). A crucial hematopoietic cytokine called stem cell factor (SCF) collaborates with other cytokines to maintain the viability of hematopoietic stem and progenitor cells, to control how they enter the cell cycle, and to promote their proliferation and differentiation (Hassan and Zander, 1996). Thymic stromal lymphopoietin (TSLP) has been identified as a crucial inflammatory cytokine in immune homeostasis (Yu et al., 2019). There hasn't been any research demonstrating a link between SCF, TSLP and TB. In our cohort, we observed significant changes in the concentrations of SCF and TSLP that could possibly be used to monitor treatment response specifically within the treatment-responsive and delayed responsive group, respectively. Their relationship to the effectiveness of TB treatment needs to be confirmed in a larger study.

IL-17A is one of the six cytokines that make up the IL-17 family (Tateosian et al., 2017). Early during Mtb infection, IL-17A is induced and helps to attract neutrophils (Lombard et al., 2016). Anti-TB treatment can enhance CD4+ T cell production of IL-17A and decrease PD-1 expression (Bandaru et al., 2014). Lower IL-17A levels were seen in active TB patients with a 2-month sputum smear non-conversion and in those with a 2-month sputum culture non-conversion (Feng et al., 2021). In contrast to the incredibly low levels in the non-responsive group, we have seen an increase in the concentration levels of IL-17A in treatment responsive and delayed responsive patients as early as 7 days into therapy, pointing to the movement of neutrophils to the infection site.

Using ROCs, we evaluated which cytokines yielded AUC values that were significantly different between the three DCTB response groups. I-TAC was the only cytokine that showed a discriminatory power with high AUC values (0.91, 0.94, 0.89, 0.72) in HCs vs treatment-responders with TB/HIV coinfection at day 3, 7, 14 and 35. At days 3, 14, and 180, GCSF (AUC 0.92, 0.82, 0.89, 0.82) and VEGF-A (AUC 0.92 and 0.85) [**Figure 3:17 C-E**] showed strong discriminating power between HCs and non-responders with TB alone and TB/HIV co-infection.

These three cytokines represent novel immune biomarkers that can be evaluated in larger cohorts or clinical trials aimed at treatment shortening. Given that DCTB assays are complex and difficult to execute *en masse* in clinical trials, these cytokines provide the opportunity to correlate changes in immune profiles with clearance of drug tolerant bacteria.

CHAPTER 4: SUMMARY

4.1 Conclusion

Reversing the negative trajectory of TB disease in human society will require the discovery and deployment of novel tools that enable rapid diagnosis of disease. Linking these individuals to appropriate care will effectively eliminate TB transmission. Furthermore, the ability to identify those individuals with subclinical/incipient/latent TB infection who will ultimately progress to full blown disease will enable more strategic deployment of health resources. Finally, identifying those individuals who will benefit from shorter durations of therapy will reduce the prevalence of antibiotic related side-effects and increase treatment adherence. Biomarkers are critical for achieving success with all these aspects. Whilst there has been significant effort in the last decade to identify immune biomarkers that predict risk of disease progression, treatment response and risk of recurrence, there has been very little work looking at biomarkers based on the pathogen. Herein, we set out to evaluate whether DCTB, which appear to comprise a novel biomarker for response to TB treatment, could be correlated with immune responses. Our outlook was to provide a novel biomarker signature that would integrate both host and pathogen-specific responses.

In the first component of our work, we explored whether bacilli that exist in the DCTB state induce differential immune responses when compared to their conventionally culturable counterparts. Our demonstration that Beijing and LAM isolates in a DCTB state produce significantly less IFN-γ, when compared to conventionally culturable preparations of the same strains provides preliminary evidence that drug tolerant bacteria may affect immunity in a manner that is distinct from the larger bacterial population. The data also suggest that the immune response measured in TB infected individuals comprises the sum of both culturable and DCTB populations, both of which may be unique effects on the immune system.

Following this, we explored whether patterns of DCTB clearance were associated with distinct immune signatures. Treatment success in patients with active TB is determined by chemotherapy in partnership with the production of pro-inflammatory, chemokines, and growth factors that cause the formation of granulomas and the stimulation of macrophages and T cells. Hence, cytokine signatures play an important role in reporting on clearance of infection. We found that the levels of I-TAC, G-CSF and VEGF-A could potentially be used to differentiate between TB patients with different amounts of DCTB in their sputum.

4.2. Limitations of the study

Our research has several limitations. We only tested the ability of a select set of clinical isolates to establish the DCTB state. Using a broader set of geographically diverse strains may yield more clinical isolates with strong inherent propensities to adopt the DCTB state. In this component of our work, we also only evaluated 6 cytokines. Using a broader set may yield interesting findings.

With regards to the cohort study, we did not have sufficient information on how long our participants had been infected with HIV, which could have an impact on the inflammatory profile. Also, participants with HIV infection who were on ART at enrolment had possibly varying ART initiation times. Considering this, we have been careful to draw conclusions with the TB/HIV infected group. Finally, the lack of a baseline specimen likely affected our comparisons at baseline (where we used a day 3 sample) with controls.

4.3. Future studies

Future work will entail exploring establishment of DCTB populations using different laboratory models, with possible sorting of DCTB from conventionally culturable cells for macrophage infections. Using specific knockout macrophages to study molecular mechanisms will also be a priority. Further successful validation of these immunological biomarkers in other cohorts and geographical areas may contribute to the development of potential diagnostic tests that are important for monitoring the efficacy of TB treatment as well as how DCTB contribute to treatment response. Further investigation on determining the best cut-off for cytokine abundance, and testing these in larger cohorts, may enable the development of a robust point-of-care test.

5. REFERENCES

ABRAHAMS, K. A. & BESRA, G. S. 2018. Mycobacterial cell wall biosynthesis: a multifaceted antibiotic target. *Parasitology,* 145**,** 116-133.

ABRAHEM, R., CHIANG, E., HAQUANG, J., NHAM, A., TING, Y. S. & VENKETARAMAN, V. 2020. The Role of Dendritic Cells in TB and HIV Infection. *J Clin Med,* 9.

ABU-RADDAD, L. J., SABATELLI, L., ACHTERBERG, J. T., SUGIMOTO, J. D., LONGINI JR, I. M., DYE, C. & HALLORAN, M. E. 2009. Epidemiological benefits of more-effective tuberculosis vaccines, drugs, and diagnostics. *Proceedings of the National Academy of Sciences,* 106**,** 13980-13985.

ACHARYA, B., ACHARYA, A., GAUTAM, S., GHIMIRE, S. P., MISHRA, G., PARAJULI, N. & SAPKOTA, B. 2020. Advances in diagnosis of Tuberculosis: an update into molecular diagnosis of *Mycobacterium tuberculosis*. *Molecular Biology Reports,* 47**,** 4065-4075.

ACHKAR, J. M. & JENNY-AVITAL, E. R. 2011. Incipient and subclinical tuberculosis: defining early disease states in the context of host immune response. *Journal of Infectious Diseases,* 204**,** S1179-S1186.

ADAMS, L., DINAUER, M., MORGENSTERN, D. & KRAHENBUHL, J. 1997. Comparison of the roles of reactive oxygen and nitrogen intermediates in the host response to *Mycobacterium tuberculosis* using transgenic mice. *Tubercle and Lung Disease,* 78**,** 237-246.

AGRANOFF, D., FERNANDEZ-REYES, D., PAPADOPOULOS, M. C., ROJAS, S. A., HERBSTER, M., LOOSEMORE, A., TARELLI, E., SHELDON, J., SCHWENK, A. & POLLOK, R. 2006. Identification of diagnostic markers for tuberculosis by proteomic fingerprinting of serum. *The Lancet,* 368**,** 1012-1021.

AGUILAR, C., MANO, M. & EULALIO, A. 2019. MicroRNAs at the host–bacteria interface: host defense or bacterial offense. *Trends in microbiology,* 27**,** 206-218.

AHMED, A., RAKSHIT, S. & VYAKARNAM, A. 2016. HIV–TB co-infection: mechanisms that drive reactivation of *Mycobacterium tuberculosis* in HIV infection. *Oral diseases,* 22**,** 53-60.

AL-KASSIMI, F. A., AL-HAJJAJ, M. S., AL-ORAINEY, I. O. & BAMGBOYE, E. A. 1995. Does the protective effect of neonatal BCG correlate with vaccine-induced tuberculin reaction? *American journal of respiratory and critical care medicine,* 152**,** 1575-1578.

ALAHARI, A., TRIVELLI, X., GUÉRARDEL, Y., DOVER, L. G., BESRA, G. S., SACCHETTINI, J. C., REYNOLDS, R. C., COXON, G. D. & KREMER, L. 2007. Thiacetazone, an antitubercular drug that inhibits cyclopropanation of cell wall mycolic acids in mycobacteria. *PloS one,* 2**,** e1343.

ALATAS, F., METINTAS, M., ERGINEL, S. & YILDIRIM, H. 2004. Vascular endothelial growth factor levels in active pulmonary tuberculosis. *Chest,* 125**,** 2156-2159.

ALDERWICK, L. J., HARRISON, J., LLOYD, G. S. & BIRCH, H. L. 2015. The mycobacterial cell wall—peptidoglycan and arabinogalactan. *Cold Spring Harbor perspectives in medicine,* 5**,** a021113.

AMARAL, J. J., ANTUNES, L. C. M., DE MACEDO, C. S., MATTOS, K. A., HAN, J., PAN, J., CANDÉA, A. L., HENRIQUES, M. D. G. M., RIBEIRO-ALVES, M. & BORCHERS, C. H. 2013. Metabonomics reveals drastic changes in anti-

inflammatory/pro-resolving polyunsaturated fatty acids-derived lipid mediators in leprosy disease. *Plos Neglected Tropical Diseases,* 7**,** e2381.
ANTONELLI, L. R., MAHNKE, Y., HODGE, J. N., PORTER, B. O., BARBER, D. L., DERSIMONIAN, R., GREENWALD, J. H., ROBY, G., MICAN, J. & SHER, A. 2010. Elevated frequencies of highly activated CD4+ T cells in HIV+ patients developing immune reconstitution inflammatory syndrome. *Blood, The Journal of the American Society of Hematology,* 116**,** 3818-3827.
ARBUÉS, A., SCHMIDIGER, S., KAMMÜLLER, M. & PORTEVIN, D. 2021. Extracellular matrix-induced GM-CSF and hypoxia promote immune control of *Mycobacterium tuberculosis* in human in vitro granulomas. *Frontiers in Immunology,* 12**,** 727508.
ARMITIGE, L. Y., JAGANNATH, C., WANGER, A. R. & NORRIS, S. J. 2000. Disruption of the genes encoding antigen 85A and antigen 85B of *Mycobacterium tuberculosis* H37Rv: effect on growth in culture and in macrophages. *Infection and immunity,* 68**,** 767-778.
ASTON, C., ROM, W. N., TALBOT, A. T. & REIBMAN, J. 1998. Early inhibition of mycobacterial growth by human alveolar macrophages is not due to nitric oxide. *American journal of respiratory and critical care medicine,* 157**,** 1943-1950.
BABAKI, M. K. Z., SOLEIMANPOUR, S. & REZAEE, S. A. 2017. Antigen 85 complex as a powerful *Mycobacterium tuberculosis* immunogene: Biology, immune-pathogenicity, applications in diagnosis, and vaccine design. *Microbial pathogenesis,* 112**,** 20-29.
BAFFONE, W., CASAROLI, A., CITTERIO, B., PIERFELICI, L., CAMPANA, R., VITTORIA, E., GUAGLIANONE, E. & DONELLI, G. 2006. Campylobacter jejuni loss of culturability in aqueous microcosms and ability to resuscitate in a mouse model. *International journal of food microbiology,* 107**,** 83-91.
BANDARU, A., DEVALRAJU, K. P., PAIDIPALLY, P., DHIMAN, R., VENKATASUBRAMANIAN, S., BARNES, P. F., VANKAYALAPATI, R. & VALLURI, V. 2014. Phosphorylated STAT3 and PD-1 regulate IL-17 production and IL-23 receptor expression in *Mycobacterium tuberculosis* infection. *European journal of immunology,* 44**,** 2013-2024.
BANDARU, R., SAHOO, D., NAIK, R., KESHARWANI, P. & DANDELA, R. 2020. Pathogenesis, biology, and immunology of tuberculosis. 1-25.
BARBER, D. L., ANDRADE, B. B., MCBERRY, C., SERETI, I. & SHER, A. 2014. Role of IL-6 in Mycobacterium avium–associated immune reconstitution inflammatory syndrome. *The Journal of Immunology,* 192**,** 676-682.
BARKA, E. A., VATSA, P., SANCHEZ, L., GAVEAU-VAILLANT, N., JACQUARD, C., KLENK, H.-P., CLÉMENT, C., OUHDOUCH, Y. & VAN WEZEL, G. P. 2016. Taxonomy, physiology, and natural products of Actinobacteria. *Microbiology and Molecular Biology Reviews,* 80**,** 1-43.
BARKAN, D., HEDHLI, D., YAN, H.-G., HUYGEN, K. & GLICKMAN, M. S. 2012. *Mycobacterium tuberculosis* lacking all mycolic acid cyclopropanation is viable but highly attenuated and hyperinflammatory in mice. *Infection and immunity,* 80**,** 1958-1968.
BARRIOS-PAYÁN, J., AGUILAR-LEÓN, D., LASCURAIN-LEDEZMA, R. & HERNÁNDEZ-PANDO, R. 2006. [Neutrophil participation in early control and immune activation during experimental pulmonary tuberculosis]. *Gac Med Mex,* 142**,** 273-81.
BARRY, C. E., BOSHOFF, H. I., DARTOIS, V., DICK, T., EHRT, S., FLYNN, J., SCHNAPPINGER, D., WILKINSON, R. J. & YOUNG, D. 2009. The spectrum of

latent tuberculosis: rethinking the biology and intervention strategies. *Nature Reviews Microbiology,* 7**,** 845-855.
BARRY, C. E., CRICK, D. C. & MCNEIL, M. R. 2007. Targeting the formation of the cell wall core of M. tuberculosis. *Infectious Disorders-Drug Targets (Formerly Current Drug Targets-Infectious Disorders),* 7**,** 182-202.
BARTEK, I., RUTHERFORD, R., GRUPPO, V., MORTON, R., MORRIS, R., KLEIN, M., VISCONTI, K., RYAN, G., SCHOOLNIK, G. & LENAERTS, A. 2009. The DosR regulon of M. tuberculosis and antibacterial tolerance. *Tuberculosis,* 89**,** 310-316.
BASARABA, R. J. 2008. Experimental tuberculosis: the role of comparative pathology in the discovery of improved tuberculosis treatment strategies. *Tuberculosis,* 88**,** S35-S47.
BATISTA, L. A. F., SILVA, K. J. S., E SILVA, L. M. D. C., DE MOURA, Y. F. & ZUCCHI, F. C. R. 2020. Tuberculosis: A granulomatous disease mediated by epigenetic factors. *Tuberculosis,* 123**,** 101943.
BATYRSHINA, Y. & SCHWARTZ, Y. 2020. New in vitro model of *Mycobacterium tuberculosis* dormancy. Eur Respiratory Soc.
BATYRSHINA, Y. R. & SCHWARTZ, Y. S. 2019. Modeling of *Mycobacterium tuberculosis* dormancy in bacterial cultures. *Tuberculosis,* 117**,** 7-17.
BEHR, M. A., EDELSTEIN, P. H. & RAMAKRISHNAN, L. 2018. Revisiting the timetable of tuberculosis. *Bmj,* 362.
BEHR, M. A., KAUFMANN, E., DUFFIN, J., EDELSTEIN, P. H. & RAMAKRISHNAN, L. 2021. Latent tuberculosis: two centuries of confusion. *American Journal of Respiratory and Critical Care Medicine,* 204**,** 142-148.
BEKMURZAYEVA, A., SYPABEKOVA, M. & KANAYEVA, D. 2013. Tuberculosis diagnosis using immunodominant, secreted antigens of *Mycobacterium tuberculosis*. *Tuberculosis,* 93**,** 381-388.
BELL, L. C. K. & NOURSADEGHI, M. 2017. Pathogenesis of HIV-1 and *Mycobacterium tuberculosis* co-infection. *Nature Reviews Microbiology,* 16**,** 80-90.
BELTON, M., BRILHA, S., MANAVAKI, R., MAURI, F., NIJRAN, K., HONG, Y. T., PATEL, N. H., DEMBEK, M., TEZERA, L. & GREEN, J. 2016. Hypoxia and tissue destruction in pulmonary TB. *Thorax,* 71**,** 1145-1153.
BELTRAN, C. G., HEUNIS, T., GALLANT, J., VENTER, R., DU PLESSIS, N., LOXTON, A. G., TROST, M., WINTER, J., MALHERBE, S. T. & KANA, B. D. 2020. Investigating non-sterilizing cure in TB patients at the end of successful anti-TB therapy. *Frontiers in Cellular and Infection Microbiology,* 10**,** 443.
BERRY, M. P., GRAHAM, C. M., MCNAB, F. W., XU, Z., BLOCH, S. A., ONI, T., WILKINSON, K. A., BANCHEREAU, R., SKINNER, J., WILKINSON, R. J., QUINN, C., BLANKENSHIP, D., DHAWAN, R., CUSH, J. J., MEJIAS, A., RAMILO, O., KON, O. M., PASCUAL, V., BANCHEREAU, J., CHAUSSABEL, D. & O'GARRA, A. 2010. An interferon-inducible neutrophil-driven blood transcriptional signature in human tuberculosis. *Nature,* 466**,** 973-7.
BETTS, J. C., LUKEY, P. T., ROBB, L. C., MCADAM, R. A. & DUNCAN, K. 2002. Evaluation of a nutrient starvation model of *Mycobacterium tuberculosis* persistence by gene and protein expression profiling. *Molecular microbiology,* 43**,** 717-731.
BHOPALE, M. K. 2021. Aspects of Cytokine Response to HIV-1 and Tuberculosis Co-Infection. *International J. of Biomed Research,* 1(9).
BISHT, D., SHARMA, D., SHARMA, D., SINGH, R. & GUPTA, V. K. 2019. Recent insights into *Mycobacterium tuberculosis* through proteomics and implications for the clinic. *Expert Review of Proteomics,* 16**,** 443-456.
BISHWAL, S. C., DAS, M. K., BADIREDDY, V. K., DABRAL, D., DAS, A., MAHAPATRA, A. R., SAHU, S., MALAKAR, D., SINGH, I. I. & MAZUMDAR,

H. 2019. Sputum proteomics reveals a shift in vitamin D-binding protein and antimicrobial protein axis in tuberculosis patients. *Scientific reports,* 9**,** 1-9.
BLAUENFELDT, T., PETRONE, L., DEL NONNO, F., BAIOCCHINI, A., FALASCA, L., CHIACCHIO, T., BONDET, V., VANINI, V., PALMIERI, F. & GALLUCCIO, G. 2018. Interplay of DDP4 and IP-10 as a potential mechanism for cell recruitment to tuberculosis lesions. *Frontiers in immunology,* 9**,** 1456.
BLIGHE, K., LEWIS, M., LUN, A. & BLIGHE, M. K. 2019. Package 'PCAtools.'. PCAtools.
BLOOM, C. I., GRAHAM, C. M., BERRY, M. P., WILKINSON, K. A., ONI, T., ROZAKEAS, F., XU, Z., ROSSELLO-URGELL, J., CHAUSSABEL, D. & BANCHEREAU, J. 2012. Detectable changes in the blood transcriptome are present after two weeks of antituberculosis therapy.
BONI, F. G., HAMDI, I., KOUNDI, L. M., SHRESTHA, K. & XIE, J. 2022. Cytokine storm in tuberculosis and IL-6 involvement. *Infection, Genetics and Evolution,* 97**,** 105166.
BOROWSKA-STRUGIŃSKA, B., DRUSZCZYŃSKA, M., LORKIEWICZ, W., SZEWCZYK, R. & ŻĄDZIŃSKA, E. 2014. Mycolic acids as markers of osseous tuberculosis in the Neolithic skeleton from Kujawy region (central Poland). *AnthropologicAl review,* 77**,** 137-149.
BRENNAN, P. J. & NIKAIDO, H. 1995. The envelope of mycobacteria. *Annual review of biochemistry,* 64**,** 29-63.
BREWER, T. F. 2000. Preventing tuberculosis with bacillus Calmette-Guerin vaccine: a meta-analysis of the literature. *Clinical Infectious Diseases,* 31**,** S64-S67.
BRITES, D. & GAGNEUX, S. 2015. Co-evolution of M ycobacterium tuberculosis and H omo sapiens. *Immunological reviews,* 264**,** 6-24.
BROOKS-POLLOCK, E., BECERRA, M. C., GOLDSTEIN, E., COHEN, T. & MURRAY, M. B. 2011. Epidemiologic inference from the distribution of tuberculosis cases in households in Lima, Peru. *Journal of Infectious Diseases,* 203**,** 1582-1589.
BROWN, G. C. 2001. Regulation of mitochondrial respiration by nitric oxide inhibition of cytochrome c oxidase. *Biochimica et Biophysica Acta (BBA)-Bioenergetics,* 1504**,** 46-57.
BUCK, J. 1979. The plate count in aquatic microbiology. *Native aquatic bacteria: enumeration, activity and ecology,* 1**,** 19-28.
BULTERYS, M. A., WAGNER, B., REDARD-JACOT, M., SURESH, A., POLLOCK, N. R., MOREAU, E., DENKINGER, C. M., DRAIN, P. K. & BROGER, T. 2019. Point-of-care urine LAM tests for tuberculosis diagnosis: a status update. *Journal of clinical medicine,* 9**,** 111.
CAMPANIÇO, A., HARJIVAN, S. G., WARNER, D. F., MOREIRA, R. & LOPES, F. 2020. Addressing latent tuberculosis: new advances in mimicking the disease, discovering key targets, and designing hit compounds. *International Journal of Molecular Sciences,* 21**,** 8854.
CAÑO-MUÑIZ, S., ANTHONY, R., NIEMANN, S. & ALFFENAAR, J.-W. C. 2018. New approaches and therapeutic options for *Mycobacterium tuberculosis* in a dormant state. *Clinical microbiology reviews,* 31**,** e00060-17.
CARPENTER, G. H. 2013. The secretion, components, and properties of saliva. *Annual review of food science and technology,* 4**,** 267-276.
CARRANZA, C., PEDRAZA-SANCHEZ, S., DE OYARZABAL-MENDEZ, E. & TORRES, M. 2020. Diagnosis for latent tuberculosis infection: New alternatives. *Frontiers in immunology***,** 2006.
CHANG, J. T., SEGAL, B. M., NAKANISHI, K., OKAMURA, H. & SHEVACH, E. M. 2000. The costimulatory effect of IL-18 on the induction of antigen-specific IFN-γ

production by resting T cells is IL-12 dependent and is mediated by up-regulation of the IL-12 receptor β2 subunit. *European journal of immunology,* 30**,** 1113-1119.
CHAO, M. C. & RUBIN, E. J. 2010. Letting sleeping dos lie: does dormancy play a role in tuberculosis? *Annual review of microbiology,* 64**,** 293-311.
CHE MAT, N. F., ZHANG, X., GUZZO, C. & GEE, K. 2011. Interleukin-23-induced interleukin-23 receptor subunit expression is mediated by the Janus kinase/signal transducer and activation of transcription pathway in human CD4 T cells. *Journal of Interferon & Cytokine Research,* 31**,** 363-371.
CHEGOU, N. N., BLACK, G. F., KIDD, M., VAN HELDEN, P. D. & WALZL, G. 2009. Host markers in QuantiFERON supernatants differentiate active TB from latent TB infection: preliminary report. *BMC pulmonary medicine,* 9**,** 1-12.
CHENDI, B. H., JOOSTE, T., SCRIBA, T. J., KIDD, M., MENDELSOHN, S., TONBY, K., WALZL, G., DYRHOL-RIISE, A. M. & CHEGOU, N. N. 2023. Utility of a three-gene transcriptomic signature in the diagnosis of tuberculosis in a low-endemic hospital setting. *Infectious Diseases,* 55**,** 44-54.
CHENDI, B. H., TVEITEN, H., SNYDERS, C. I., TONBY, K., JENUM, S., NIELSEN, S. D., HOVE-SKOVSGAARD, M., WALZL, G., CHEGOU, N. N. & DYRHOL-RIISE, A. M. 2021. CCL1 and IL-2Ra differentiate Tuberculosis disease from latent infection Irrespective of HIV infection in low TB burden countries. *Journal of Infection,* 83**,** 433-443.
CHENGALROYEN, M. D., BEUKES, G. M., GORDHAN, B. G., STREICHER, E. M., CHURCHYARD, G., HAFNER, R., WARREN, R., OTWOMBE, K., MARTINSON, N. & KANA, B. D. 2016. Detection and quantification of differentially culturable tubercle bacteria in sputum from patients with tuberculosis. *American journal of respiratory and critical care medicine,* 194**,** 1532-1540.
CHO, S. H., WARIT, S., WAN, B., HWANG, C. H., PAULI, G. F. & FRANZBLAU, S. G. 2007. Low-oxygen-recovery assay for high-throughput screening of compounds against nonreplicating *Mycobacterium tuberculosis*. *Antimicrobial agents and chemotherapy,* 51**,** 1380-1385.
CHOUDHARY, E., SHARMA, R., PAL, P. & AGARWAL, N. 2022. Deciphering the Proteomic Landscape of *Mycobacterium tuberculosis* in Response to Acid and Oxidative Stresses. *ACS omega,* 7**,** 26749-26766.
CHURCHYARD, G., KIM, P., SHAH, N. S., RUSTOMJEE, R., GANDHI, N., MATHEMA, B., DOWDY, D., KASMAR, A. & CARDENAS, V. 2017. What We Know About Tuberculosis Transmission: An Overview. *The Journal of Infectious Diseases,* 216**,** S629-S635.
CLIFF, J. M., CHO, J.-E., LEE, J.-S., RONACHER, K., KING, E. C., VAN HELDEN, P., WALZL, G. & DOCKRELL, H. M. 2016. Excessive cytolytic responses predict tuberculosis relapse after apparently successful treatment. *The Journal of infectious diseases,* 213**,** 485-495.
CLIFF, J. M., LEE, J.-S., CONSTANTINOU, N., CHO, J.-E., CLARK, T. G., RONACHER, K., KING, E. C., LUKEY, P. T., DUNCAN, K. & VAN HELDEN, P. D. 2013. Distinct phases of blood gene expression pattern through tuberculosis treatment reflect modulation of the humoral immune response. *The Journal of infectious diseases,* 207**,** 18-29.
COLLINS, J. M., KEMPKER, R. R., ZIEGLER, T. R., BLUMBERG, H. M. & JONES, D. P. 2016. Metabolomics and mycobacterial disease: don't forget the bioinformatics. *Annals of the American Thoracic Society,* 13**,** 141-142.
COMBRINK, M., DU PREEZ, I., RONACHER, K., WALZL, G. & LOOTS, D. T. 2019. Time-dependent changes in urinary metabolome before and after intensive phase

tuberculosis therapy: a pharmacometabolomics study. *OMICS: A Journal of Integrative Biology,* 23**,** 560-572.
CONDE, R., LAIRES, R., GONÇALVES, L., RIZVI, A., BARROSO, C., VILLAR, M., MACEDO, R., SIMÕES, M., GADDAM, S. & LAMOSA, P. 2021. Discovery of serum biomarkers for diagnosis of tuberculosis by NMR metabolomics including cross-validation with a second cohort. *Biomedical Journal*.
COOPER, A. M. & KHADER, S. A. 2008. The role of cytokines in the initiation, expansion, and control of cellular immunity to tuberculosis. *Immunological reviews,* 226**,** 191-204.
CORREIA-NEVES, M., FRÖBERG, G., KORSHUN, L., VIEGAS, S., VAZ, P., RAMANLAL, N., BRUCHFELD, J., HAMASUR, B., BRENNAN, P. & KÄLLENIUS, G. 2019. Biomarkers for tuberculosis: the case for lipoarabinomannan. *ERJ open research,* 5.
CORTES, T., SCHUBERT, O. T., BANAEI-ESFAHANI, A., COLLINS, B. C., AEBERSOLD, R. & YOUNG, D. B. 2017. Delayed effects of transcriptional responses in *Mycobacterium tuberculosis* exposed to nitric oxide suggest other mechanisms involved in survival. *Scientific reports,* 7**,** 1-9.
CUDAHY, P. & SHENOI, S. V. 2016. Diagnostics for pulmonary tuberculosis. *Postgraduate medical journal,* 92**,** 187-193.
DA COSTA, L. L., DELCROIX, M., DALLA COSTA, E. R., PRESTES, I. V., MILANO, M., FRANCIS, S. S., UNIS, G., SILVA, D. R., RILEY, L. W. & ROSSETTI, M. L. 2015. A real-time PCR signature to discriminate between tuberculosis and other pulmonary diseases. *Tuberculosis,* 95**,** 421-425.
DAFFE, M. & REYRAT, J.-M. 2008. *The mycobacterial cell envelope,* ASM Press.
DAMOISEAUX, J. 2020. The IL-2–IL-2 receptor pathway in health and disease: The role of the soluble IL-2 receptor. *Clinical Immunology,* 218**,** 108515.
DARBOE, F., MBANDI, S. K., NAIDOO, K., YENDE-ZUMA, N., LEWIS, L., THOMPSON, E. G., DUFFY, F. J., FISHER, M., FILANDER, E. & VAN ROOYEN, M. 2019. Detection of tuberculosis recurrence, diagnosis and treatment response by a blood transcriptomic risk signature in HIV-infected persons on antiretroviral therapy. *Frontiers in microbiology,* 10**,** 1441.
DARTOIS, V., SAITO, K., WARRIER, T. & NATHAN, C. 2016. New evidence for the complexity of the population structure of *Mycobacterium tuberculosis* increases the diagnostic and biologic challenges. American Thoracic Society.
DE ARAUJO, L. S., RIBEIRO-ALVES, M., LEAL-CALVO, T., LEUNG, J., DURÁN, V., SAMIR, M., TALBOT, S., TALLAM, A., MELLO, F. C. D. Q. & GEFFERS, R. 2019. Reprogramming of small noncoding RNA populations in peripheral blood reveals host biomarkers for latent and active *Mycobacterium tuberculosis* infection. *MBio,* 10**,** e01037-19.
DE ARAUJO, L. S., RIBEIRO-ALVES, M., WIPPERMAN, M. F., VORKAS, C. K., PESSLER, F. & SAAD, M. H. F. 2021. Transcriptomic Biomarkers for Tuberculosis: Validation of NPC2 as a Single mRNA Biomarker to Diagnose TB, Predict Disease Progression, and Monitor Treatment Response. *Cells,* 10**,** 2704.
DE ARAUJO, L. S., VAAS, L. A., RIBEIRO-ALVES, M., GEFFERS, R., MELLO, F. C., DE ALMEIDA, A. S., MOREIRA, A. D. S., KRITSKI, A. L., LAPA E SILVA, J. R. & MORAES, M. O. 2016. Transcriptomic biomarkers for tuberculosis: evaluation of DOCK9. EPHA4, and NPC2 mRNA expression in peripheral blood. *Frontiers in microbiology,* 7**,** 1586.
DE GROOTE, M. A., STERLING, D. G., HRAHA, T., RUSSELL, T. M., GREEN, L. S., WALL, K., KRAEMER, S., OSTROFF, R., JANJIC, N. & OCHSNER, U. A. 2017.

Discovery and validation of a six-marker serum protein signature for the diagnosis of active pulmonary tuberculosis. *Journal of clinical microbiology,* 55**,** 3057-3071.
DE MARTINO, M., LODI, L., GALLI, L. & CHIAPPINI, E. 2019. Immune Response to *Mycobacterium tuberculosis*: A Narrative Review. *Frontiers in Pediatrics,* 7.
DEAN, G. L., EDWARDS, S. G., IVES, N. J., MATTHEWS, G., FOX, E. F., NAVARATNE, L., FISHER, M., TAYLOR, G. P., MILLER, R. & TAYLOR, C. B. 2002. Treatment of tuberculosis in HIV-infected persons in the era of highly active antiretroviral therapy. *Aids,* 16**,** 75-83.
DEB, C., LEE, C.-M., DUBEY, V. S., DANIEL, J., ABOMOELAK, B., SIRAKOVA, T. D., PAWAR, S., ROGERS, L. & KOLATTUKUDY, P. E. 2009. A novel in vitro multiple-stress dormancy model for *Mycobacterium tuberculosis* generates a lipid-loaded, drug-tolerant, dormant pathogen. *PloS one,* 4**,** e6077.
DENHOLM, J., BAKER, A.-M. & TIMLIN, M. 2020. Latent tuberculosis in the general practice context. *Australian journal of general practice,* 49**,** 107-110.
DEVALRAJU, K. P., NEELA, V. S. K., CHINTALA, S., KROVVIDI, S. S. & VALLURI, V. L. 2019. Transforming Growth Factor-β Suppresses Interleukin (IL)-2 and IL-1β Production in HIV-Tuberculosis Co-Infection. *Journal of Interferon & Cytokine Research,* 39**,** 355-363.
DEY, B. & BISHAI, W. R. Crosstalk between *Mycobacterium tuberculosis* and the host cell. Seminars in immunology, 2014. Elsevier, 486-496.
DHAR, N. & MCKINNEY, J. D. 2007. Microbial phenotypic heterogeneity and antibiotic tolerance. *Current opinion in microbiology,* 10**,** 30-38.
DI PIETRANTONIO, T., HERNANDEZ, C., GIRARD, M., VERVILLE, A., ORLOVA, M., BELLEY, A., BEHR, M. A., LOREDO-OSTI, J. C. & SCHURR, E. 2010. Strain-specific differences in the genetic control of two closely related mycobacteria. *PLoS pathogens,* 6**,** e1001169.
DINARELLO, C. A. 1991. Interleukin-1 and interleukin-1 antagonism.
DINKELE, R., GESSNER, S., MCKERRY, A., LEONARD, B., LEUKES, J., SELDON, R., WARNER, D. F. & WOOD, R. 2022. Aerosolization of *Mycobacterium tuberculosis* by tidal breathing. *American Journal of Respiratory and Critical Care Medicine,* 206**,** 206-216.
DOMENECH, P., ZOU, J., AVERBACK, A., SYED, N., CURTIS, D., DONATO, S. & REED, M. B. 2017. Unique regulation of the DosR regulon in the Beijing lineage of *Mycobacterium tuberculosis*. *Journal of bacteriology,* 199**,** e00696-16.
DOMINGO-GONZALEZ, R., PRINCE, O., COOPER, A. & KHADER, S. A. 2016. Cytokines and chemokines in *Mycobacterium tuberculosis* infection. *Microbiology spectrum,* 4**,** 4.5. 23.
DOWNING, K. J., BETTS, J., YOUNG, D., MCADAM, R., KELLY, F., YOUNG, M. & MIZRAHI, V. 2004. Global expression profiling of strains harbouring null mutations reveals that the five rpf-like genes of *Mycobacterium tuberculosis* show functional redundancy. *Tuberculosis,* 84**,** 167-179.
DOWNING, K. J., MISCHENKO, V. V., SHLEEVA, M. O., YOUNG, D. I., YOUNG, M., KAPRELYANTS, A. S., APT, A. S. & MIZRAHI, V. 2005. Mutants of *Mycobacterium tuberculosis* lacking three of the five rpf-like genes are defective for growth in vivo and for resuscitation in vitro. *Infection and immunity,* 73**,** 3038-3043.
DRAIN, P. K., BAJEMA, K. L., DOWDY, D., DHEDA, K., NAIDOO, K., SCHUMACHER, S. G., MA, S., MEERMEIER, E., LEWINSOHN, D. M. & SHERMAN, D. R. 2018. Incipient and subclinical tuberculosis: a clinical review of early stages and progression of infection. *Clinical microbiology reviews,* 31**,** e00021-18.

DRUSZCZYŃSKA, M., GODKOWICZ, M., KULESZA, J., WAWROCKI, S. & FOL, M. 2022. Cytokine Receptors—Regulators of Antimycobacterial Immune Response. *International Journal of Molecular Sciences,* 23**,** 1112.

DU BRUYN, E., RUZIVE, S., LINDESTAM ARLEHAMN, C. S., SETTE, A., SHER, A., BARBER, D. L., WILKINSON, R. J. & RIOU, C. 2021. *Mycobacterium tuberculosis*-specific CD4 T cells expressing CD153 inversely associate with bacterial load and disease severity in human tuberculosis. *Mucosal immunology,* 14**,** 491-499.

DUSTHACKEER, A., BALASUBRAMANIAN, M., SHANMUGAM, G., PRIYA, S., NIRMAL, C. R., SAM EBENEZER, R., BALASUBRAMANIAN, A., MONDAL, R. K., THIRUVENKADAM, K. & HEMANTH KUMAR, A. 2019. Differential culturability of *Mycobacterium tuberculosis* in culture-negative sputum of patients with pulmonary tuberculosis and in a simulated model of dormancy. *Frontiers in Microbiology,* 10**,** 2381.

DUTTA, N. K., TORNHEIM, J. A., FUKUTANI, K. F., PARADKAR, M., TIBURCIO, R. T., KINIKAR, A., VALVI, C., KULKARNI, V., PRADHAN, N. & SHIVAKUMAR, S. V. B. Y. 2020. Integration of metabolomics and transcriptomics reveals novel biomarkers in the blood for tuberculosis diagnosis in children. *Scientific reports,* 10**,** 1-11.

EHLERS, S. & SCHAIBLE, U. E. 2013. The granuloma in tuberculosis: dynamics of a host–pathogen collusion. *Frontiers in immunology,* 3**,** 411.

ESMAIL, H., BARRY 3RD, C., YOUNG, D. & WILKINSON, R. 2014. The ongoing challenge of latent tuberculosis. *Philosophical Transactions of the Royal Society B: Biological Sciences,* 369**,** 20130437.

ESTELLER, M. 2011. Non-coding RNAs in human disease. *Nature reviews genetics,* 12**,** 861-874.

ETNA, M. P., GIACOMINI, E., SEVERA, M. & COCCIA, E. M. 2014. Pro- and anti-inflammatory cytokines in tuberculosis: a two-edged sword in TB pathogenesis. *Semin Immunol,* 26**,** 543-51.

EUM, S.-Y., KONG, J.-H., HONG, M.-S., LEE, Y.-J., KIM, J.-H., HWANG, S.-H., CHO, S.-N., VIA, L. E. & BARRY III, C. E. 2010. Neutrophils are the predominant infected phagocytic cells in the airways of patients with active pulmonary TB. *Chest,* 137**,** 122-128.

FAKRUDDIN, M., MANNAN, K. S. B. & ANDREWS, S. 2013. Viable but nonculturable bacteria: food safety and public health perspective. *International Scholarly Research Notices,* 2013.

FALKINHAM, I., JO 2009. Surrounded by mycobacteria: nontuberculous mycobacteria in the human environment. *Journal of applied microbiology,* 107**,** 356-367.

FAUSTMAN, D. L. & DAVIS, M. 2013. TNF receptor 2 and disease: autoimmunity and regenerative medicine. *Frontiers in immunology,* 4**,** 478.

FENG, C. G., KAVIRATNE, M., ROTHFUCHS, A. G., CHEEVER, A., HIENY, S., YOUNG, H. A., WYNN, T. A. & SHER, A. 2006. NK cell-derived IFN-γ differentially regulates innate resistance and neutrophil response in T cell-deficient hosts infected with *Mycobacterium tuberculosis*. *The Journal of Immunology,* 177**,** 7086-7093.

FENG, J.-Y., HO, L.-I., CHUANG, F.-Y., PAN, S.-W., CHEN, Y.-Y., TUNG, C.-L., LI, C.-P. & SU, W.-J. 2021. Depression and recovery of IL-17A secretion in mitogen responses in patients with active tuberculosis-a prospective observational study. *Journal of the Formosan Medical Association,* 120**,** 1080-1089.

FENG, S., DU, Y.-Q., ZHANG, L., ZHANG, L., FENG, R.-R. & LIU, S.-Y. 2015. Analysis of serum metabolic profile by ultra-performance liquid chromatography-mass

spectrometry for biomarkers discovery: application in a pilot study to discriminate patients with tuberculosis. *Chinese medical journal,* 128**,** 159-168.
FLANAGAN, J. M., STEWARD, S., HANKINS, J. S., HOWARD, T. M., NEALE, G. & WARE, R. E. 2009. Microarray analysis of liver gene expression in iron overloaded patients with sickle cell anemia and beta-thalassemia. *American journal of hematology,* 84**,** 328-334.
FLEPISI, B. T., BOUIC, P., SISSOLAK, G. & ROSENKRANZ, B. 2014. Biomarkers of HIV-associated Cancer. *Biomarkers in cancer,* 6**,** BIC. S15056.
FLYNN, J. & KLEIN, E. 2011. Pulmonary tuberculosis in monkeys In: Leong J, Dick T, eds. A Color Atlas of Comparative Pulmonary Tuberculosis Histopathology. Boca Raton, FL: CRC Press, Taylor & Francis.
FLYNN, J. L. & CHAN, J. 2001. Immunology of tuberculosis. *Annual review of immunology,* 19**,** 93-129.
FLYNN, J. L., CHAN, J. & LIN, P. 2011. Macrophages and control of granulomatous inflammation in tuberculosis. *Mucosal immunology,* 4**,** 271-278.
FOREMAN, T. W., MEHRA, S., LOBATO, D. N., MALEK, A., ALVAREZ, X., GOLDEN, N. A., BUCŞAN, A. N., DIDIER, P. J., DOYLE-MEYERS, L. A. & RUSSELL-LODRIGUE, K. E. 2016. CD4+ T-cell–independent mechanisms suppress reactivation of latent tuberculosis in a macaque model of HIV coinfection. *Proceedings of the National Academy of Sciences,* 113**,** E5636-E5644.
FORRELLAD, M. A., KLEPP, L. I., GIOFFRÉ, A., SABIO Y GARCIA, J., MORBIDONI, H. R., SANTANGELO, M. D. L. P., CATALDI, A. A. & BIGI, F. 2013. Virulence factors of the *Mycobacterium tuberculosis* complex. *Virulence,* 4**,** 3-66.
FRANCISCO, N. M., FANG, Y.-M., DING, L., FENG, S., YANG, Y., WU, M., JACOBS, M., RYFFEL, B. & HUANG, X. 2017. Diagnostic accuracy of a selected signature gene set that discriminates active pulmonary tuberculosis and other pulmonary diseases. *Journal of Infection,* 75**,** 499-510.
FREDIANI, J. K., JONES, D. P., TUKVADZE, N., UPPAL, K., SANIKIDZE, E., KIPIANI, M., TRAN, V. T., HEBBAR, G., WALKER, D. I. & KEMPKER, R. R. 2014. Plasma metabolomics in human pulmonary tuberculosis disease: a pilot study. *PloS one,* 9**,** e108854.
FRYER, R. M., RANDALL, J., YOSHIDA, T., HSIAO, L.-L., BLUMENSTOCK, J., JENSEN, K. E., DIMOFTE, T., JENSEN, R. V. & GULLANS, S. R. 2002. Global analysis of gene expression: methods, interpretation, and pitfalls. *Nephron Experimental Nephrology,* 10**,** 64-74.
GALAGAN, J. E., MINCH, K., PETERSON, M., LYUBETSKAYA, A., AZIZI, E., SWEET, L., GOMES, A., RUSTAD, T., DOLGANOV, G. & GLOTOVA, I. 2013. The *Mycobacterium tuberculosis* regulatory network and hypoxia. *Nature,* 499**,** 178-183.
GAO, B. & GUPTA, R. S. 2012. Phylogenetic framework and molecular signatures for the main clades of the phylum Actinobacteria. *Microbiology and molecular biology reviews,* 76**,** 66-112.
GEFFNER, L., YOKOBORI, N., BASILE, J., SCHIERLOH, P., BALBOA, L., ROMERO, M. M., RITACCO, V., VESCOVO, M., GONZALEZ MONTANER, P. & LOPEZ, B. 2009. Patients with multidrug-resistant tuberculosis display impaired Th1 responses and enhanced regulatory T-cell levels in response to an outbreak of multidrug-resistant *Mycobacterium tuberculosis* M and Ra strains. *Infection and immunity,* 77**,** 5025-5034.
GENGENBACHER, M. & KAUFMANN, S. H. 2012. *Mycobacterium tuberculosis*: success through dormancy. *FEMS microbiology reviews,* 36**,** 514-532.

GERNAEY, A. M., MINNIKIN, D. E., COPLEY, M., DIXON, R. A., MIDDLETON, J. & ROBERTS, C. 2001. Mycolic acids and ancient DNA confirm an osteological diagnosis of tuberculosis. *Tuberculosis,* 81**,** 259-265.

GIBSON, S. E., HARRISON, J. & COX, J. A. 2018. Modelling a silent epidemic: a review of the in vitro models of latent tuberculosis. *Pathogens,* 7**,** 88.

GIDEON, H. P., PHUAH, J., JUNECKO, B. A. & MATTILA, J. T. 2019. Neutrophils express pro- and anti-inflammatory cytokines in granulomas from *Mycobacterium tuberculosis*-infected cynomolgus macaques. *Mucosal Immunol,* 12**,** 1370-1381.

GILL, C. M., DOLAN, L., PIGGOTT, L. M. & MCLAUGHLIN, A. M. 2022. New developments in tuberculosis diagnosis and treatment. *Breathe,* 18.

GLICKMAN, M. S., COX, J. S. & JACOBS JR, W. R. 2000. A novel mycolic acid cyclopropane synthetase is required for cording, persistence, and virulence of *Mycobacterium tuberculosis*. *Molecular cell,* 5**,** 717-727.

GOLETTI, D., CARRARA, S., VINCENTI, D., SALTINI, C., RIZZI, E. B., SCHININA, V., IPPOLITO, G., AMICOSANTE, M. & GIRARDI, E. 2006. Accuracy of an immune diagnostic assay based on RD1 selected epitopes for active tuberculosis in a clinical setting: a pilot study. *Clinical microbiology and infection,* 12**,** 544-550.

GOLETTI, D., LEE, M. R., WANG, J. Y., WALTER, N. & OTTENHOFF, T. H. 2018. Update on tuberculosis biomarkers: from correlates of risk, to correlates of active disease and of cure from disease. *Respirology,* 23**,** 455-466.

GOLETTI, D., PETRUCCIOLI, E., JOOSTEN, S. A. & OTTENHOFF, T. H. 2016. Tuberculosis biomarkers: from diagnosis to protection. *Infectious disease reports,* 8**,** 24-32.

GÓMEZ, L., SANCHEZ, E., RUIZ-NARVAEZ, E., LÓPEZ-NEVOT, M., ANAYA, J. M. & MARTIN, J. 2007. Macrophage migration inhibitory factor gene influences the risk of developing tuberculosis in northwestern Colombian population. *Tissue antigens,* 70**,** 28-33.

GOODING, S., CHOWDHURY, O., HINKS, T., RICHELDI, L., LOSI, M., EWER, K., MILLINGTON, K., GUNATHEESAN, R., CERRI, S. & MCNALLY, J. 2007. Impact of a T cell-based blood test for tuberculosis infection on clinical decision-making in routine practice. *Journal of Infection,* 54**,** e169-e174.

GORDHAN, B. G., PETERS, J. S., MCIVOR, A., MACHOWSKI, E. E., EALAND, C., WAJA, Z., MARTINSON, N. & KANA, B. D. 2021. Detection of differentially culturable tubercle bacteria in sputum using mycobacterial culture filtrates. *Scientific Reports,* 11**,** 1-11.

GORDHAN, B. G., SEWCHARRAN, A., LETSOALO, M., CHINAPPA, T., YENDE-ZUMA, N., PADAYATCHI, N., NAIDOO, K. & KANA, B. D. 2022. Detection of differentially culturable tubercle bacteria in sputum from drug-resistant tuberculosis patients. *Frontiers in Cellular and Infection Microbiology***,** 1305.

GREENLEE-WACKER, M. C. 2016. Clearance of apoptotic neutrophils and resolution of inflammation. *Immunol Rev,* 273**,** 357-70.

GRIFFIN, J. E., PANDEY, A. K., GILMORE, S. A., MIZRAHI, V., MCKINNEY, J. D., BERTOZZI, C. R. & SASSETTI, C. M. 2012. Cholesterol catabolism by *Mycobacterium tuberculosis* requires transcriptional and metabolic adaptations. *Chemistry & biology,* 19**,** 218-227.

GROOM, J. R. & LUSTER, A. D. 2011a. CXCR3 in T cell function. *Experimental cell research,* 317**,** 620-631.

GROOM, J. R. & LUSTER, A. D. 2011b. CXCR3 ligands: redundant, collaborative and antagonistic functions. *Immunology and cell biology,* 89**,** 207-215.

GROSSET, J. 2003. *Mycobacterium tuberculosis* in the extracellular compartment: an underestimated adversary. *Antimicrobial agents and chemotherapy,* 47**,** 833-836.
GU, Z., EILS, R. & SCHLESNER, M. 2016. Complex heatmaps reveal patterns and correlations in multidimensional genomic data. *Bioinformatics,* 32**,** 2847-2849.
GUIRADO, E. & SCHLESINGER, L. S. 2013. Modeling the *Mycobacterium tuberculosis* granuloma–the critical battlefield in host immunity and disease. *Frontiers in immunology,* 4**,** 98.
GUO, J., ZHANG, X., CHEN, X. & CAI, Y. 2022. Proteomics in Biomarker Discovery for Tuberculosis: Current Status and Future Perspectives. *Frontiers in Microbiology,* 13.
GUPTA, R. K., TURNER, C. T., VENTURINI, C., ESMAIL, H., RANGAKA, M. X., COPAS, A., LIPMAN, M., ABUBAKAR, I. & NOURSADEGHI, M. 2020. Concise whole blood transcriptional signatures for incipient tuberculosis: a systematic review and patient-level pooled meta-analysis. *The Lancet Respiratory Medicine,* 8**,** 395-406.
HAILEMARIAM, M., EGUEZ, R. V., SINGH, H., BEKELE, S., AMENI, G., PIEPER, R. & YU, Y. 2018. S-Trap, an ultrafast sample-preparation approach for shotgun proteomics. *Journal of proteome research,* 17**,** 2917-2924.
HALLIDAY, A., MASONOU, T., TOLOSA-WRIGHT, M., MANDAGERE, V. & LALVANI, A. 2019. Immunodiagnosis of active tuberculosis. *Expert Review of Respiratory Medicine,* 13**,** 521-532.
HAMASUR, B., BRUCHFELD, J., HAILE, M., PAWLOWSKI, A., BJORVATN, B., KÄLLENIUS, G. & SVENSON, S. B. 2001. Rapid diagnosis of tuberculosis by detection of mycobacterial lipoarabinomannan in urine. *Journal of microbiological methods,* 45**,** 41-52.
HAMASUR, B., BRUCHFELD, J., VAN HELDEN, P., KÄLLENIUS, G. & SVENSON, S. 2015. A sensitive urinary lipoarabinomannan test for tuberculosis. *PLoS One,* 10**,** e0123457.
HAN, X., M. HOLTZMAN, D., W. MCKEEL JR, D., KELLEY, J. & MORRIS, J. C. 2002. Substantial sulfatide deficiency and ceramide elevation in very early Alzheimer's disease: potential role in disease pathogenesis. *Journal of neurochemistry,* 82**,** 809-818.
HASSAN, H. & ZANDER, A. 1996. Stem cell factor as a survival and growth factor in human normal and malignant hematopoiesis. *Molecular Biology of Hematopoiesis 5***,** 549-558.
HASSUNA, N. A., EL FEKY, M., HUSSEIN, A. A. M., MAHMOUD, M. A., IDRISS, N. K., ABDELWAHAB, S. F. & IBRAHIM, M. A. 2021. Interleukin-18 and interferon-γ single nucleotide polymorphisms in Egyptian patients with tuberculosis. *Plos one,* 16**,** e0244949.
HE, J., FAN, Y., SHEN, D., YU, M., SHI, L., DING, S. & LI, L. 2020. Characterization of cytokine profile to distinguish latent tuberculosis from active tuberculosis and healthy controls. *Cytokine,* 135**,** 155218.
HETT, E. C., CHAO, M. C., DENG, L. L. & RUBIN, E. J. 2008. A mycobacterial enzyme essential for cell division synergizes with resuscitation-promoting factor. *PLoS pathogens,* 4**,** e1000001.
HORNE, D. J., ROYCE, S. E., GOOZE, L., NARITA, M., HOPEWELL, P. C., NAHID, P. & STEINGART, K. R. 2010. Sputum monitoring during tuberculosis treatment for predicting outcome: systematic review and meta-analysis. *The Lancet infectious diseases,* 10**,** 387-394.
HORSBURGH JR, C. R. & RUBIN, E. J. 2011. Latent tuberculosis infection in the United States. *New England Journal of Medicine,* 364**,** 1441-1448.

HU, Y., COATES, A. & MITCHISON, D. 2006. Sterilising action of pyrazinamide in models of dormant and rifampicin-tolerant *Mycobacterium tuberculosis*. *The International Journal of Tuberculosis and Lung Disease,* 10**,** 317-322.

IDH, J., WESTMAN, A., ELIAS, D., MOGES, F., GETACHEW, A., GELAW, A., SUNDQVIST, T., FORSLUND, T., ALEMU, A. & AYELE, B. 2008. Nitric oxide production in the exhaled air of patients with pulmonary tuberculosis in relation to HIV co-infection. *BMC Infectious Diseases,* 8**,** 1-8.

ILLIG, T., GIEGER, C., ZHAI, G., RÖMISCH-MARGL, W., WANG-SATTLER, R., PREHN, C., ALTMAIER, E., KASTENMÜLLER, G., KATO, B. S. & MEWES, H.-W. 2010. A genome-wide perspective of genetic variation in human metabolism. *Nature genetics,* 42**,** 137-141.

ISKANDAR, A., NURSILONINGRUM, E., ARTHAMIN, M. Z., OLIVIANTO, E. & CHANDRAKUSUMA, M. S. 2017. The diagnostic value of urine lipoarabinomannan (LAM) antigen in childhood tuberculosis. *Journal of clinical and diagnostic research: JCDR,* 11**,** EC32.

JACQUIER, N., FRANDI, A., PILLONEL, T., VIOLLIER, P. H. & GREUB, G. 2014. Cell wall precursors are required to organize the chlamydial division septum. *Nature communications,* 5**,** 3578.

JAMES, B. W., BACON, J., HAMPSHIRE, T., MORLEY, K. & MARSH, P. D. 2002. In vitro gene expression dissected: chemostat surgery for *Mycobacterium tuberculosis*. Wiley Online Library.

JANSSENS, R., STRUYF, S. & PROOST, P. 2018. The unique structural and functional features of CXCL12. *Cellular & molecular immunology,* 15**,** 299-311.

JEFFREY NORTH, E., JACKSON, M. & E LEE, R. 2014. New approaches to target the mycolic acid biosynthesis pathway for the development of tuberculosis therapeutics. *Current pharmaceutical design,* 20**,** 4357-4378.

JENNE, C. N., WONG, C. H., ZEMP, F. J., MCDONALD, B., RAHMAN, M. M., FORSYTH, P. A., MCFADDEN, G. & KUBES, P. 2013. Neutrophils recruited to sites of infection protect from virus challenge by releasing neutrophil extracellular traps. *Cell Host Microbe,* 13**,** 169-80.

JÚNIOR, P. S. A., CASTELLANI, L. G. S., PERES, R. L., COMBADAO, J., TRISTÃO, T. C., DIETZE, R., HADAD, D. J. & PALACI, M. 2020. Differentially culturable tubercle bacteria dynamics during standard anti-tuberculosis treatment: a prospective cohort study. *Tuberculosis,* 124**,** 101945.

JUSTICE, A. C., ERLANDSON, K. M., HUNT, P. W., LANDAY, A., MIOTTI, P. & TRACY, R. P. 2018. Can biomarkers advance HIV research and care in the antiretroviral therapy era? *The Journal of infectious diseases,* 217**,** 521-528.

KACZOR-URBANOWICZ, K. E., MARTIN CARRERAS-PRESAS, C., ARO, K., TU, M., GARCIA-GODOY, F. & WONG, D. T. 2017. Saliva diagnostics–Current views and directions. *Experimental Biology and Medicine,* 242**,** 459-472.

KAEWSEEKHAO, B., ROYTRAKUL, S., YINGCHUTRAKUL, Y., SALAO, K., REECHAIPICHITKUL, W. & FAKSRI, K. 2020. Proteomic analysis of infected primary human leucocytes revealed PSTK as potential treatment-monitoring marker for active and latent tuberculosis. *Plos one,* 15**,** e0231834.

KAFOROU, M., WRIGHT, V. J., ONI, T., FRENCH, N., ANDERSON, S. T., BANGANI, N., BANWELL, C. M., BRENT, A. J., CRAMPIN, A. C. & DOCKRELL, H. M. 2013. Detection of tuberculosis in HIV-infected and-uninfected African adults using whole blood RNA expression signatures: a case-control study. *PLoS medicine,* 10**,** e1001538.

KALKAN, I. K., GOZU, A., TANSEL, E., KALAC, S. N., SAMURKASOGLU, B. & SIMSEK, H. 2021. The Diagnostic and prognostic value of CXCL12 (SDF-1α) level in *Mycobacterium tuberculosis* infection and disease. *The Journal of Infection in Developing Countries,* 15**,** 81-88.

KALOU, M., SASSAN-MOROKRO, M., ABOUYA, L., BILE, C., MAURICE, C., MARAN, M., TOSSOU, O., ROELS, T., GREENBERG, A. E. & WIKTOR, S. Z. 2005. Changes in HIV RNA viral load, CD4+ T-cell counts, and levels of immune activation markers associated with anti-tuberculosis therapy and cotrimoxazole prophylaxis among HIV-infected tuberculosis patients in Abidjan, Cote d'Ivoire. *Journal of medical virology,* 75**,** 202-208.

KANA, B. D., GORDHAN, B. G., DOWNING, K. J., SUNG, N., VOSTROKTUNOVA, G., MACHOWSKI, E. E., TSENOVA, L., YOUNG, M., KAPRELYANTS, A. & KAPLAN, G. 2008. The resuscitation-promoting factors of *Mycobacterium tuberculosis* are required for virulence and resuscitation from dormancy but are collectively dispensable for growth in vitro. *Molecular microbiology,* 67**,** 672-684.

KANA, B. D. & MIZRAHI, V. 2010. Resuscitation-promoting factors as lytic enzymes for bacterial growth and signaling. *FEMS Immunology & Medical Microbiology,* 58**,** 39-50.

KARAKOUSIS, P. C., YOSHIMATSU, T., LAMICHHANE, G., WOOLWINE, S. C., NUERMBERGER, E. L., GROSSET, J. & BISHAI, W. R. 2004. Dormancy phenotype displayed by extracellular *Mycobacterium tuberculosis* within artificial granulomas in mice. *The Journal of experimental medicine,* 200**,** 647-657.

KASHYAP, R. S., DOBOS, K. M., BELISLE, J. T., PUROHIT, H. J., CHANDAK, N. H., TAORI, G. M. & DAGINAWALA, H. F. 2005. Demonstration of components of antigen 85 complex in cerebrospinal fluid of tuberculous meningitis patients. *Clinical and Vaccine Immunology,* 12**,** 752-758.

KASSA, D., DE JAGER, W., GEBREMICHAEL, G., ALEMAYEHU, Y., RAN, L., FRANSEN, J., WOLDAY, D., MESSELE, T., TEGBARU, B. & OTTENHOFF, T. H. 2016. The effect of HIV coinfection, HAART and TB treatment on cytokine/chemokine responses to *Mycobacterium tuberculosis* (Mtb) antigens in active TB patients and latently Mtb infected individuals. *Tuberculosis,* 96**,** 131-140.

KATHAMUTHU, G. R., MOIDEEN, K., BANUREKHA, V. V., NAIR, D., SRIDHAR, R., BASKARAN, D. & BABU, S. 2018. Altered circulating levels of B cell growth factors and their modulation upon anti-tuberculosis treatment in pulmonary tuberculosis and tuberculous lymphadenitis. *Plos one,* 13**,** e0207404.

KATHAMUTHU, G. R., MOIDEEN, K., BHASKARAN, D., SEKAR, G., SRIDHAR, R., VIDYAJAYANTHI, B., GAJENDRARAJ, G. & BABU, S. 2017. Reduced systemic and mycobacterial antigen-stimulated concentrations of IL-1β and IL-18 in tuberculous lymphadenitis. *Cytokine,* 90**,** 66-72.

KAUFMANN, S. H. 2002. Protection against tuberculosis: cytokines, T cells, and macrophages. *Annals of the rheumatic diseases,* 61**,** ii54-ii58.

KAUR, P., DATTA, S., SHANDIL, R. K., KUMAR, N., ROBERT, N., SOKHI, U. K., GUPTHA, S., NARAYANAN, S., ANBARASU, A. & RAMAIAH, S. 2016. Unravelling the secrets of mycobacterial cidality through the lens of antisense. *Plos one,* 11**,** e0154513.

KAVALLARIS, M. & MARSHALL, G. M. 2005. Proteomics and disease: opportunities and challenges. *Medical journal of Australia,* 182**,** 575-579.

KEIKHA, M. & MAJIDZADEH, M. 2021. Beijing genotype of *Mycobacterium tuberculosis* is associated with extensively drug-resistant tuberculosis: A global analysis. *New Microbes and New Infections,* 43**,** 100921.

KERKHOFF, A. D., SOSSEN, B., SCHUTZ, C., REIPOLD, E. I., TROLLIP, A., MOREAU, E., SCHUMACHER, S. G., BURTON, R., WARD, A. & NICOL, M. P. 2020. Diagnostic sensitivity of SILVAMP TB-LAM (FujiLAM) point-of-care urine assay for extra-pulmonary tuberculosis in people living with HIV. *European Respiratory Journal,* 55.

KERKHOFF, A. D., WOOD, R., VOGT, M. & LAWN, S. D. 2014. Prognostic value of a quantitative analysis of lipoarabinomannan in urine from patients with HIV-associated tuberculosis. *PLoS One,* 9**,** e103285.

KFUTWAH, A., LEMÉE, V., NGONO, H. V., DE OLIVEIRA, F., NJOUOM, R. & PLANTIER, J.-C. 2013. Field evaluation of the Abbott Architect HIV Ag/Ab combo immunoassay. *Journal of Clinical Virology,* 58**,** e70-e75.

KHADER, S. A., BELL, G. K., PEARL, J. E., FOUNTAIN, J. J., RANGEL-MORENO, J., CILLEY, G. E., SHEN, F., EATON, S. M., GAFFEN, S. L. & SWAIN, S. L. 2007. IL-23 and IL-17 in the establishment of protective pulmonary CD4+ T cell responses after vaccination and during *Mycobacterium tuberculosis* challenge. *Nature immunology,* 8**,** 369-377.

KHAN, N., VIDYARTHI, A., PAHARI, S. & AGREWALA, J. N. 2016. Distinct Strategies Employed by Dendritic Cells and Macrophages in Restricting *Mycobacterium tuberculosis* Infection: Different Philosophies but Same Desire. *Int Rev Immunol,* 35**,** 386-398.

KIM, B. & KIM, T. H. 2018. Fundamental role of dendritic cells in inducing Th2 responses. *Korean J Intern Med,* 33**,** 483-489.

KIM, J.-S., RYU, M.-J., BYUN, E.-H., KIM, W. S., WHANG, J., MIN, K.-N., SHONG, M., KIM, H.-J. & SHIN, S. J. 2011. Differential immune response of adipocytes to virulent and attenuated *Mycobacterium tuberculosis*. *Microbes and infection,* 13**,** 1242-1251.

KOHONEN, P., PARKKINEN, J. A., WILLIGHAGEN, E. L., CEDER, R., WENNERBERG, K., KASKI, S. & GRAFSTRÖM, R. C. 2017. A transcriptomics data-driven gene space accurately predicts liver cytopathology and drug-induced liver injury. *Nature communications,* 8**,** 1-15.

KOLIBAB, K., YANG, A., PARRA, M., DERRICK, S. & MORRIS, S. 2014. Time to detection of *Mycobacterium tuberculosis* using the MGIT 320 system correlates with colony counting in preclinical testing of new vaccines. *Clinical and Vaccine Immunology,* 21**,** 453-455.

KOLLOLI, A., SINGH, P. & SUBBIAN, S. 2018. Granulomatous response to *Mycobacterium tuberculosis* infection. *Understanding the Host Immune Response Against Mycobacterium tuberculosis Infection.* Springer.

KORB, V. C., CHUTURGOON, A. A. & MOODLEY, D. 2016. *Mycobacterium tuberculosis*: manipulator of protective immunity. *International journal of molecular sciences,* 17**,** 131.

KOZAKIEWICZ, L., CHEN, Y., XU, J., WANG, Y., DUNUSSI-JOANNOPOULOS, K., OU, Q., FLYNN, J. L., PORCELLI, S. A., JACOBS JR, W. R. & CHAN, J. 2013. B cells regulate neutrophilia during *Mycobacterium tuberculosis* infection and BCG vaccination by modulating the interleukin-17 response. *PLoS pathogens,* 9**,** e1003472.

KRISHNAN, N., ROBERTSON, B. D. & THWAITES, G. 2013. Pathways of IL-1β secretion by macrophages infected with clinical *Mycobacterium tuberculosis* strains. *Tuberculosis,* 93**,** 538-547.

KROON, E. E., COUSSENS, A. K., KINNEAR, C., ORLOVA, M., MOLLER, M., SEEGER, A., WILKINSON, R. J., HOAL, E. G. & SCHURR, E. 2018. Neutrophils: Innate Effectors of TB Resistance? *Front Immunol,* 9**,** 2637.

KRUGER, P., SAFFARZADEH, M., WEBER, A. N., RIEBER, N., RADSAK, M., VON BERNUTH, H., BENARAFA, C., ROOS, D., SKOKOWA, J. & HARTL, D. 2015. *Neutrophils: between host defence, immune modulation, and tissue injury.* 11.

KUMAR, A., TOLEDO, J. C., PATEL, R. P., LANCASTER JR, J. R. & STEYN, A. J. 2007. *Mycobacterium tuberculosis* DosS is a redox sensor and DosT is a hypoxia sensor. *Proceedings of the National Academy of Sciences,* 104**,** 11568-11573.

KUMAR, G., DAGUR, P. K., SINGH, P. K., SHANKAR, H., YADAV, V. S., KATOCH, V. M., BAJAJ, B., GUPTA, R., SENGUPTA, U. & JOSHI, B. 2010. Serodiagnostic efficacy of *Mycobacterium tuberculosis* 30/32-kDa mycolyl transferase complex, ESAT-6, and CFP-10 in patients with active tuberculosis. *Archivum immunologiae et therapiae experimentalis,* 58**,** 57-65.

KUMAR, N. P., MOIDEEN, K., BANUREKHA, V. V., NAIR, D. & BABU, S. Plasma proinflammatory cytokines are markers of disease severity and bacterial burden in pulmonary tuberculosis. Open forum infectious diseases, 2019. Oxford University Press US, ofz257.

KWAN, C. K. & ERNST, J. D. 2011. HIV and tuberculosis: a deadly human syndemic. *Clinical microbiology reviews,* 24**,** 351-376.

LA MANNA, M. P., ORLANDO, V., LI DONNI, P., SIRECI, G., DI CARLO, P., CASCIO, A., DIELI, F. & CACCAMO, N. 2018. Identification of plasma biomarkers for discrimination between tuberculosis infection/disease and pulmonary non tuberculosis disease. *PLoS One,* 13**,** e0192664.

LANGLEY, R. J., TSALIK, E. L., VELKINBURGH, J. C. V., GLICKMAN, S. W., RICE, B. J., WANG, C., CHEN, B., CARIN, L., SUAREZ, A. & MOHNEY, R. P. 2013. An integrated clinico-metabolomic model improves prediction of death in sepsis. *Science translational medicine,* 5**,** 195ra95-195ra95.

LATORRE, I., LEIDINGER, P., BACKES, C., DOMÍNGUEZ, J., DE SOUZA-GALVÃO, M. L., MALDONADO, J., PRAT, C., RUIZ-MANZANO, J., SÁNCHEZ, F. & CASAS, I. 2015. A novel whole-blood miRNA signature for a rapid diagnosis of pulmonary tuberculosis. *European Respiratory Journal,* 45**,** 1173-1176.

LAUB, M. T., MCADAMS, H. H., FELDBLYUM, T., FRASER, C. M. & SHAPIRO, L. 2000. Global analysis of the genetic network controlling a bacterial cell cycle. *Science,* 290**,** 2144-2148.

LAWN, S. D. 2012. Point-of-care detection of lipoarabinomannan (LAM) in urine for diagnosis of HIV-associated tuberculosis: a state of the art review. *BMC infectious diseases,* 12**,** 1-12.

LAWN, S. D., WOOD, R. & WILKINSON, R. J. 2011. Changing concepts of "latent tuberculosis infection" in patients living with HIV infection. *Clinical and Developmental Immunology,* 2011.

LEE, S., CHOI, I., JEON, Y., PARK, S., LEE, H., LEE, Y., CHANG, C., KIM, Y., LEE, M. & PARK, S. K. 2011. Association between the interleukin-18 promoter polymorphism and pulmonary tuberculosis in a Korean population. *The International journal of tuberculosis and lung disease,* 15**,** 1246-1251.

LEEANSYAH, E., MALONE, D. F., ANTHONY, D. D. & SANDBERG, J. K. 2013. Soluble biomarkers of HIV transmission, disease progression and comorbidities. *Current opinion in HIV and AIDS,* 8**,** 117-124.

LEEM, A. Y., SONG, J. H., LEE, E. H., LEE, H., SIM, B., KIM, S. Y., CHUNG, K. S., KIM, E. Y., JUNG, J. Y. & PARK, M. S. 2018. Changes in cytokine responses to TB antigens ESAT-6, CFP-10 and TB 7.7 and inflammatory markers in peripheral blood during therapy. *Scientific reports,* 8**,** 1-8.

LEI, J., YIN, X., SHANG, H. & JIANG, Y. 2019. IP-10 is highly involved in HIV infection. *Cytokine,* 115**,** 97-103.
LEISTIKOW, R. L., MORTON, R. A., BARTEK, I. L., FRIMPONG, I., WAGNER, K. & VOSKUIL, M. I. 2010. The *Mycobacterium tuberculosis* DosR regulon assists in metabolic homeostasis and enables rapid recovery from nonrespiring dormancy. *Journal of bacteriology,* 192**,** 1662-1670.
LEONG, S., ZHAO, Y., RIBEIRO-RODRIGUES, R., JONES-LÓPEZ, E. C., ACUÑA-VILLAORDUÑA, C., RODRIGUES, P. M., PALACI, M., ALLAND, D., DIETZE, R. & ELLNER, J. J. 2020. Cross-validation of existing signatures and derivation of a novel 29-gene transcriptomic signature predictive of progression to TB in a Brazilian cohort of household contacts of pulmonary TB. *Tuberculosis,* 120**,** 101898.
LERNER, T. R., BOREL, S. & GUTIERREZ, M. G. 2015. The innate immune response in human tuberculosis. *Cell Microbiol,* 17**,** 1277-85.
LI, L., MENDIS, N., TRIGUI, H., OLIVER, J. D. & FAUCHER, S. P. 2014. The importance of the viable but non-culturable state in human bacterial pathogens. *Frontiers in microbiology,* 5**,** 258.
LI, Y.-J., PETROFSKY, M. & BERMUDEZ, L. E. 2002. *Mycobacterium tuberculosis* uptake by recipient host macrophages is influenced by environmental conditions in the granuloma of the infectious individual and is associated with impaired production of interleukin-12 and tumor necrosis factor alpha. *Infection and immunity,* 70**,** 6223-6230.
LIN, P. L. & FLYNN, J. L. 2010. Understanding latent tuberculosis: a moving target. *The Journal of Immunology,* 185**,** 15-22.
LIN, P. L. & FLYNN, J. L. 2018. The End of the Binary Era: Revisiting the Spectrum of Tuberculosis. *J Immunol,* 201**,** 2541-2548.
LINH, N. N., VINEY, K., GEGIA, M., FALZON, D., GLAZIOU, P., FLOYD, K., TIMIMI, H., ISMAIL, N., ZIGNOL, M. & KASAEVA, T. 2021. World Health Organization treatment outcome definitions for tuberculosis: 2021 update. Eur Respiratory Soc.
LIPWORTH, S., HAMMOND, R., BARON, V., HU, Y., COATES, A. & GILLESPIE, S. 2016. Defining dormancy in mycobacterial disease. *Tuberculosis,* 99**,** 131-142.
LIU, A., TETZLAFF, M. T., VANBELLE, P., ELDER, D., FELDMAN, M., TOBIAS, J. W., SEPULVEDA, A. R. & XU, X. 2009. MicroRNA expression profiling outperforms mRNA expression profiling in formalin-fixed paraffin-embedded tissues. *International journal of clinical and experimental pathology,* 2**,** 519.
LIU, C. H., LIU, H. & GE, B. 2017. Innate immunity in tuberculosis: host defense vs pathogen evasion. *Cellular & molecular immunology,* 14**,** 963-975.
LIU, L., DENG, J., YANG, Q., WEI, C., LIU, B., ZHANG, H., XIN, H., PAN, S., LIU, Z. & WANG, D. 2021. Urinary proteomic analysis to identify a potential protein biomarker panel for the diagnosis of tuberculosis. *IUBMB life,* 73**,** 1073-1083.
LIU, M., GUO, S., HIBBERT, J. M., JAIN, V., SINGH, N., WILSON, N. O. & STILES, J. K. 2011. CXCL10/IP-10 in infectious diseases pathogenesis and potential therapeutic implications. *Cytokine & growth factor reviews,* 22**,** 121-130.
LODDENKEMPER, R., LIPMAN, M. & ZUMLA, A. 2016. Clinical aspects of adult tuberculosis. *Cold Spring Harbor perspectives in medicine,* 6**,** a017848.
LOEBEL, R., SHORR, E. & RICHARDSON, H. 1933a. The influence of adverse conditions upon the respiratory metabolism and growth of human tubercle bacilli. *Journal of bacteriology,* 26**,** 167-200.
LOEBEL, R., SHORR, E. & RICHARDSON, H. 1933b. The influence of foodstuffs upon the respiratory metabolism and growth of human tubercle bacilli. *Journal of bacteriology,* 26**,** 139-166.

LOMBARD, R., DOZ, E., CARRERAS, F., EPARDAUD, M., LE VERN, Y., BUZONI-GATEL, D. & WINTER, N. 2016. IL-17RA in non-hematopoietic cells controls CXCL-1 and 5 critical to recruit neutrophils to the lung of mycobacteria-infected mice during the adaptive immune response. *PloS one,* 11**,** e0149455.

LOOTS, D. T. 2014. An altered *Mycobacterium tuberculosis* metabolome induced by katG mutations resulting in isoniazid resistance. *Antimicrobial Agents and Chemotherapy,* 58**,** 2144-2149.

LORAINE, J., PU, F., TURAPOV, O. & MUKAMOLOVA, G. V. 2016. Development of an in vitro assay for detection of drug-induced resuscitation-promoting-factor-dependent mycobacteria. *Antimicrobial Agents and Chemotherapy,* 60**,** 6227-6233.

LOURENS, M., PHILIPS, L., KLEINHANS, C. C., FRIEDRICH, S. O., MARTINSON, N., VENTER, A., VAN DER MERWE, L. & DIACON, A. H. 2019. Liquid mycobacterial culture outcomes after different sputum collection techniques before and during treatment. *Tuberculosis,* 116**,** 17-21.

LYADOVA, I. V. 2017. Neutrophils in Tuberculosis: Heterogeneity Shapes the Way? *Mediators Inflamm,* 2017**,** 8619307.

MACK, U., MIGLIORI, G. B., SESTER, M., RIEDER, H. L., EHLERS, S., GOLETTI, D., BOSSINK, A., MAGDORF, K., HOLSCHER, C., KAMPMANN, B., AREND, S. M., DETJEN, A., BOTHAMLEY, G., ZELLWEGER, J. P., MILBURN, H., DIEL, R., RAVN, P., COBELENS, F., CARDONA, P. J., KAN, B., SOLOVIC, I., DUARTE, R. & CIRILLO, D. M. 2009. LTBI: latent tuberculosis infection or lasting immune responses to M. tuberculosis? A TBNET consensus statement. *European Respiratory Journal,* 33**,** 956-973.

MACLEAN, E., BROGER, T., YERLIKAYA, S., FERNANDEZ-CARBALLO, B. L., PAI, M. & DENKINGER, C. M. 2019. A systematic review of biomarkers to detect active tuberculosis. *Nature microbiology,* 4**,** 748-758.

MACLEAN, E., KOHLI, M., WEBER, S. F., SURESH, A., SCHUMACHER, S. G., DENKINGER, C. M. & PAI, M. 2020. Advances in molecular diagnosis of tuberculosis. *Journal of Clinical Microbiology,* 58**,** e01582-19.

MACMICKING, J. D., NORTH, R. J., LACOURSE, R., MUDGETT, J. S., SHAH, S. K. & NATHAN, C. F. 1997. Identification of nitric oxide synthase as a protective locus against tuberculosis. *Proceedings of the National Academy of Sciences,* 94**,** 5243-5248.

MAERTZDORF, J., KAUFMANN, S. H. & WEINER, J. 2015. Toward a unified biosignature for tuberculosis. *Cold Spring Harbor perspectives in medicine,* 5**,** a018531.

MAERTZDORF, J., REPSILBER, D., PARIDA, S. K., STANLEY, K., ROBERTS, T., BLACK, G., WALZL, G. & KAUFMANN, S. H. 2011. Human gene expression profiles of susceptibility and resistance in tuberculosis. *Genes & Immunity,* 12**,** 15-22.

MAGDALENA, D., MICHAL, S., MARTA, S., MAGDALENA, K.-P., ANNA, P., MAGDALENA, G. & RAFAŁ, S. 2022. Targeted metabolomics analysis of serum and *Mycobacterium tuberculosis* antigen-stimulated blood cultures of pediatric patients with active and latent tuberculosis. *Scientific reports,* 12**,** 1-13.

MAGOMBEDZE, G., PASIPANODYA, J. G. & GUMBO, T. 2021. Bacterial load slopes represent biomarkers of tuberculosis therapy success, failure, and relapse. *Communications biology,* 4**,** 1-13.

MALEK, T. R. & CASTRO, I. 2010. Interleukin-2 receptor signaling: at the interface between tolerance and immunity. *Immunity,* 33**,** 153-165.

MANTOVANI, A., CASSATELLA, M. A., COSTANTINI, C. & JAILLON, S. 2011. Neutrophils in the activation and regulation of innate and adaptive immunity. *Nat Rev Immunol,* 11**,** 519-31.

MARAKALALA, M. J., MARTINEZ, F. O., PLÜDDEMANN, A. & GORDON, S. 2018. Macrophage heterogeneity in the immunopathogenesis of tuberculosis. *Frontiers in microbiology,* 9**,** 1028.

MARAKALALA, M. J., RAJU, R. M., SHARMA, K., ZHANG, Y. J., EUGENIN, E. A., PRIDEAUX, B., DAUDELIN, I. B., CHEN, P.-Y., BOOTY, M. G. & KIM, J. H. 2016. Inflammatory signaling in human tuberculosis granulomas is spatially organized. *Nature medicine,* 22**,** 531.

MARRERO, J., RHEE, K. Y., SCHNAPPINGER, D., PETHE, K. & EHRT, S. 2010. Gluconeogenic carbon flow of tricarboxylic acid cycle intermediates is critical for *Mycobacterium tuberculosis* to establish and maintain infection. *Proceedings of the National Academy of Sciences,* 107**,** 9819-9824.

MATEOS, J., ESTÉVEZ, O., GONZÁLEZ-FERNÁNDEZ, Á., ANIBARRO, L., PALLARÉS, Á., RELJIC, R., GALLARDO, J. M., MEDINA, I. & CARRERA, M. 2019. High-resolution quantitative proteomics applied to the study of the specific protein signature in the sputum and saliva of active tuberculosis patients and their infected and uninfected contacts. *Journal of proteomics,* 195**,** 41-52.

MATHEMA, B., KUREPINA, N., FALLOWS, D. & KREISWIRTH, B. N. Lessons from molecular epidemiology and comparative genomics. Seminars in respiratory and critical care medicine, 2008. © Thieme Medical Publishers, 467-480.

MATSUMOTO, K., OKAZAKI, H. & NAKAMURA, T. 1992. Up-regulation of hepatocyte growth factor gene expression by interleukin-1 in human skin fibroblasts. *Biochemical and biophysical research communications,* 188**,** 235-243.

MATTILA, J. T., OJO, O. O., KEPKA-LENHART, D., MARINO, S., KIM, J. H., EUM, S. Y., VIA, L. E., BARRY, C. E., KLEIN, E. & KIRSCHNER, D. E. 2013. Microenvironments in tuberculous granulomas are delineated by distinct populations of macrophage subsets and expression of nitric oxide synthase and arginase isoforms. *The Journal of Immunology,* 191**,** 773-784.

MBONGUE, J., NICHOLAS, D., FIREK, A. & LANGRIDGE, W. 2014. The role of dendritic cells in tissue-specific autoimmunity. *Journal of immunology research,* 2014.

MCAULAY, K., SAITO, K., WARRIER, T., WALSH, K. F., MATHURIN, L. D., ROYAL-MARDI, G., LEE, M. H., OCHERETINA, O., PAPE, J. W. & FITZGERALD, D. W. 2018. Differentially detectable *Mycobacterium tuberculosis* cells in sputum from treatment-naive subjects in Haiti and their proportionate increase after initiation of treatment. *MBio,* 9**,** e02192-18.

MCIVOR, A., GORDHAN, B. G., WAJA, Z., OTWOMBE, K., MARTINSON, N. A. & KANA, B. D. 2021. Supplementation of sputum cultures with culture filtrate to detect tuberculosis in a cross-sectional study of HIV-infected individuals. *Tuberculosis,* 129**,** 102103.

MCNERNEY, R. & DALEY, P. 2011. Towards a point-of-care test for active tuberculosis: obstacles and opportunities. *Nature Reviews Microbiology,* 9**,** 204-213.

MCNERNEY, R., MAEURER, M., ABUBAKAR, I., MARAIS, B., MCHUGH, T. D., FORD, N., WEYER, K., LAWN, S., GROBUSCH, M. P. & MEMISH, Z. 2012. Tuberculosis diagnostics and biomarkers: needs, challenges, recent advances, and opportunities. *Journal of Infectious Diseases,* 205**,** S147-S158.

MCSHANE, H., PATHAN, A. A., SANDER, C. R., KEATING, S. M., GILBERT, S. C., HUYGEN, K., FLETCHER, H. A. & HILL, A. V. 2004. Recombinant modified

vaccinia virus Ankara expressing antigen 85A boosts BCG-primed and naturally acquired antimycobacterial immunity in humans. *Nature medicine,* 10**,** 1240-1244.
MEDJAHED, H., GAILLARD, J.-L. & REYRAT, J.-M. 2010. Mycobacterium abscessus: a new player in the mycobacterial field. *Trends in microbiology,* 18**,** 117-123.
MEHTA, A. & BALTIMORE, D. 2016. MicroRNAs as regulatory elements in immune system logic. *Nature Reviews Immunology,* 16**,** 279-294.
MELLMAN, I. & STEINMAN, R. M. 2001. Dendritic cells: specialized and regulated antigen processing machines. *Cell,* 106**,** 255-258.
MENSAH, G. I., BOAKYE, A. N., BASINGNAA, A., OWUSU, E., ANTWI-BAFFOUR, S., OFORI, M. F., ADDO, K. K., JACKSON-SILLAH, D. & ADEKAMBI, T. 2021. Identification of Serum Cytokine Biomarkers Associated with Multidrug Resistant Tuberculosis (MDR-TB). *Immuno,* 1**,** 400-409.
MIHRET, A. 2012. The role of dendritic cells in *Mycobacterium tuberculosis* infection. *Virulence,* 3**,** 654-9.
MIHRET, A. & ABEBE, M. 2013. Mycobacterial Diseases.
MIHRET, A., ABEBE, M., BEKELE, Y., ASEFFA, A., WALZL, G. & HOWE, R. 2014. Impact of HIV co-infection on plasma level of cytokines and chemokines of pulmonary tuberculosis patients. *BMC infectious diseases,* 14**,** 1-7.
MIOTTO, P., MWANGOKA, G., VALENTE, I. C., NORBIS, L., SOTGIU, G., BOSU, R., AMBROSI, A., CODECASA, L. R., GOLETTI, D. & MATTEELLI, A. 2013. miRNA signatures in sera of patients with active pulmonary tuberculosis. *PloS one,* 8**,** e80149.
MISHRA, B. B., RATHINAM, V. A., MARTENS, G. W., MARTINOT, A. J., KORNFELD, H., FITZGERALD, K. A. & SASSETTI, C. M. 2013. Nitric oxide controls the immunopathology of tuberculosis by inhibiting NLRP3 inflammasome–dependent processing of IL-1β. *Nature immunology,* 14**,** 52-60.
MONTORO, E., LEMUS, D., ECHEMENDIA, M., MARTIN, A., PORTAELS, F. & PALOMINO, J. C. 2005. Comparative evaluation of the nitrate reduction assay, the MTT test, and the resazurin microtitre assay for drug susceptibility testing of clinical isolates of *Mycobacterium tuberculosis*. *Journal of Antimicrobial Chemotherapy,* 55**,** 500-505.
MORTAZ, E., ADCOCK, I. M., TABARSI, P., MASJEDI, M. R., MANSOURI, D., VELAYATI, A. A., CASANOVA, J.-L. & BARNES, P. J. 2014. Interaction of Pattern Recognition Receptors with *Mycobacterium tuberculosis*. *Journal of Clinical Immunology,* 35**,** 1-10.
MOURIK, B. C., DE STEENWINKEL, J. E., DE KNEGT, G. J., HUIZINGA, R., VERBON, A., OTTENHOFF, T. H., VAN SOOLINGEN, D. & LEENEN, P. J. 2019. *Mycobacterium tuberculosis* clinical isolates of the Beijing and East-African Indian lineage induce fundamentally different host responses in mice compared to H37Rv. *Scientific reports,* 9**,** 19922.
MUEFONG, C. N. & SUTHERLAND, J. S. 2020. Neutrophils in Tuberculosis-Associated Inflammation and Lung Pathology. *Front Immunol,* 11**,** 962.
MUKAMOLOVA, G. V., KAPRELYANTS, A. S., YOUNG, D. I., YOUNG, M. & KELL, D. B. 1998. A bacterial cytokine. *Proceedings of the National Academy of Sciences,* 95**,** 8916-8921.
MUKAMOLOVA, G. V., TURAPOV, O., MALKIN, J., WOLTMANN, G. & BARER, M. R. 2010. Resuscitation-promoting factors reveal an occult population of tubercle bacilli in sputum. *American journal of respiratory and critical care medicine,* 181**,** 174-180.

MUKAMOLOVA, G. V., TURAPOV, O. A., YOUNG, D. I., KAPRELYANTS, A. S., KELL, D. B. & YOUNG, M. 2002. A family of autocrine growth factors in *Mycobacterium tuberculosis*. *Molecular microbiology,* 46**,** 623-635.

MUNIR, M. K., REHMAN, S., AASIM, M., IQBAL, R. & SAEED, S. 2015. Comparison of Ziehl Neelsen microscopy with GeneXpert for detection of *Mycobacterium tuberculosis*. *IOSR J Dent Med Sci,* 14**,** 56-60.

MUTAVHATSINDI, H., CALDER, B., MCANDA, S., MALHERBE, S. T., STANLEY, K., KIDD, M., WALZL, G. & CHEGOU, N. N. 2021. Identification of novel salivary candidate protein biomarkers for tuberculosis diagnosis: a preliminary biomarker discovery study. *Tuberculosis,* 130**,** 102118.

NAEEM, A., RAI, S. N. & PIERRE, L. 2018. Histology, alveolar macrophages.

NAKIYINGI, L., SSENGOOBA, W., NAKANJAKO, D., ARMSTRONG, D., HOLSHOUSER, M., KIRENGA, B. J., SHAH, M., MAYANJA-KIZZA, H., JOLOBA, M. L. & ELLNER, J. J. 2015. Predictors and outcomes of mycobacteremia among HIV-infected smear-negative presumptive tuberculosis patients in Uganda. *BMC infectious Diseases,* 15**,** 1-8.

NARASIMHAN, P., WOOD, J., MACINTYRE, C. R. & MATHAI, D. 2013. Risk factors for tuberculosis. *Pulmonary medicine,* 2013.

NARENDRAN, G., ANDRADE, B. B., PORTER, B. O., CHANDRASEKHAR, C., VENKATESAN, P., MENON, P. A., SUBRAMANIAN, S., ANBALAGAN, S., BHAVANI, K. P. & SEKAR, S. 2013. Paradoxical tuberculosis immune reconstitution inflammatory syndrome (TB-IRIS) in HIV patients with culture confirmed pulmonary tuberculosis in India and the potential role of IL-6 in prediction. *PloS one,* 8**,** e63541.

NATHAN, C. & EHRT, S. 2004. Nitric oxide in tuberculosis. *Tuberculosis,* 84**,** 215-235.

NATHAN, C. & SHILOH, M. U. 2000. Reactive oxygen and nitrogen intermediates in the relationship between mammalian hosts and microbial pathogens. *Proceedings of the National Academy of Sciences,* 97**,** 8841-8848.

NDLANDLA, F., EJOH, V., STOLTZ, A., NAICKER, B., CROMARTY, A., VAN WYNGAARDT, S., KHATI, M., ROTHERHAM, L., LEMMER, Y. & NIEBUHR, J. 2016. Standardization of natural mycolic acid antigen composition and production for use in biomarker antibody detection to diagnose active tuberculosis. *Journal of Immunological Methods,* 435**,** 50-59.

NEWSON, J., STABLES, M., KARRA, E., ARCE-VARGAS, F., QUEZADA, S., MOTWANI, M., MACK, M., YONA, S., AUDZEVICH, T. & GILROY, D. W. 2014. Resolution of acute inflammation bridges the gap between innate and adaptive immunity. *Blood,* 124**,** 1748-1764.

NGCOBO, S., MOLATLHEGI, R. P., OSMAN, F., NGCAPU, S., SAMSUNDER, N., GARRETT, N. J., ABDOOL KARIM, S. S., ABDOOL KARIM, Q., MCKINNON, L. R. & SIVRO, A. 2022. Pre-infection plasma cytokines and chemokines as predictors of HIV disease progression. *Scientific Reports,* 12**,** 1-8.

NGUYEN, T. N. A., BERRE, A.-L., BAÑULS, A.-L. & NGUYEN, T. V. A. 2019. Molecular diagnosis of drug-resistant tuberculosis; a literature review. *Frontiers in microbiology,* 10**,** 794.

NICHOLSON, S., BONECINI-ALMEIDA, M. D. G., LAPA E SILVA, J., NATHAN, C., XIE, Q., MUMFORD, R., WEIDNER, J. R., CALAYCAY, J., GENG, J. & BOECHAT, N. 1996. Inducible nitric oxide synthase in pulmonary alveolar macrophages from patients with tuberculosis. *The Journal of experimental medicine,* 183**,** 2293-2302.

NICOLÁS-ÁVILA, J. Á., ADROVER, J. M. & HIDALGO, A. 2017. Neutrophils in Homeostasis, Immunity, and Cancer. *Immunity,* 46**,** 15-28.
NIKITUSHKIN, V. D., DEMINA, G. R., SHLEEVA, M. O., GURYANOVA, S. V., RUGGIERO, A., BERISIO, R. & KAPRELYANTS, A. S. 2015. A product of RpfB and RipA joint enzymatic action promotes the resuscitation of dormant mycobacteria. *The FEBS journal,* 282**,** 2500-2511.
NONKULA, B. 2022. *Assessing the propensity of drug resistant tuberculosis to enter and exit the differentially culturable state.* Master of Science, University of the Witwatersrand.
NORDENFELT, P. & TAPPER, H. 2011. Phagosome dynamics during phagocytosis by neutrophils. *J Leukoc Biol,* 90**,** 271-84.
NOSIK, M., RYZHOV, K., RYMANOVA, I., SOBKIN, A., KRAVTCHENKO, A., KUIMOVA, U., POKROVSKY, V., ZVEREV, V. & SVITICH, O. 2021. Dynamics of plasmatic levels of pro-and anti-inflammatory cytokines in HIV-infected individuals with M. tuberculosis co-infection. *Microorganisms,* 9**,** 2291.
NYKA, W. 1974. Studies on the effect of starvation on mycobacteria. *Infection and immunity,* 9**,** 843-850.
O'CALLAGHAN, A. & VAN SINDEREN, D. 2016. Bifidobacteria and their role as members of the human gut microbiota. *Frontiers in microbiology,* 7**,** 925.
OEHLERS, S. H., CRONAN, M. R., SCOTT, N. R., THOMAS, M. I., OKUDA, K. S., WALTON, E. M., BEERMAN, R. W., CROSIER, P. S. & TOBIN, D. M. 2015. Interception of host angiogenic signalling limits mycobacterial growth. *Nature,* 517**,** 612-615.
OHMORI, Y., WYNER, L., NARUMI, S., ARMSTRONG, D., STOLER, M. & HAMILTON, T. A. 1993. Tumor necrosis factor-alpha induces cell type and tissue-specific expression of chemoattractant cytokines in vivo. *The American journal of pathology,* 142**,** 861.
OJHA, A. K., BAUGHN, A. D., SAMBANDAN, D., HSU, T., TRIVELLI, X., GUERARDEL, Y., ALAHARI, A., KREMER, L., JACOBS JR, W. R. & HATFULL, G. F. 2008. Growth of *Mycobacterium tuberculosis* biofilms containing free mycolic acids and harbouring drug-tolerant bacteria. *Molecular microbiology,* 69**,** 164-174.
OLIVER, J. D. 2000. The public health significance of viable but nonculturable bacteria. *Nonculturable microorganisms in the environment***,** 277-300.
OLIVER, J. D. 2016. The viable but nonculturable state for bacteria: status update. *Microbe,* 11**,** 159-164.
OPIE, E. L. 1927. Tubercle bacilli in latent tuberculous lesions and in the lung tissue without tuberculous lesions. *Arch. Pathol. Lab. Med.,* 4**,** 1-21.
ORME, I. M. & BASARABA, R. J. The formation of the granuloma in tuberculosis infection. Seminars in immunology, 2014. Elsevier, 601-609.
OSUJI, F. N., ONYENEKWE, C. C., AHANEKU, J. E. & UKIBE, N. R. 2018. The effects of highly active antiretroviral therapy on the serum levels of pro-inflammatory and anti-inflammatory cytokines in HIV infected subjects. *Journal of biomedical science,* 25**,** 1-8.
PADARATH, K. 2020. *The emergence of differentially culturable tubercle bacteria in clinical drug sensitive Mycobacterium tuberculosis strains.* Master of Science (MSc), University of the Witwatersrand.
PAI, M., BEHR, M. A., DOWDY, D., DHEDA, K., DIVANGAHI, M., BOEHME, C. C., GINSBERG, A., SWAMINATHAN, S., SPIGELMAN, M., GETAHUN, H., MENZIES, D. & RAVIGLIONE, M. 2016. Tuberculosis. *Nature Reviews Disease Primers,* 2.

PAI, M., RAMSAY, A. & O'BRIEN, R. 2008. Evidence-based tuberculosis diagnosis. *PLoS Medicine,* 5**,** e156.
PANKLA, R., BUDDHISA, S., BERRY, M., BLANKENSHIP, D. M., BANCROFT, G. J., BANCHEREAU, J., LERTMEMONGKOLCHAI, G. & CHAUSSABEL, D. 2009. Genomic transcriptional profiling identifies a candidate blood biomarker signature for the diagnosis of septicemic melioidosis. *Genome biology,* 10**,** 1-22.
PARIDA, S. K. & KAUFMANN, S. H. 2010. The quest for biomarkers in tuberculosis. *Drug discovery today,* 15**,** 148-157.
PARK, H. D., GUINN, K. M., HARRELL, M. I., LIAO, R., VOSKUIL, M. I., TOMPA, M., SCHOOLNIK, G. K. & SHERMAN, D. R. 2003. Rv3133c/dosR is a transcription factor that mediates the hypoxic response of *Mycobacterium tuberculosis*. *Molecular microbiology,* 48**,** 833-843.
PASTOR, L., URREA, V., CARRILLO, J., PARKER, E., FUENTE-SORO, L., JAIROCE, C., MANDOMANDO, I., NANICHE, D. & BLANCO, J. 2018. Dynamics of CD4 and CD8 T-cell subsets and inflammatory biomarkers during early and chronic HIV infection in Mozambican adults. *Frontiers in Immunology,* 8**,** 1925.
PEDDIREDDY, V., DODDAM, S. N. & AHMED, N. 2017. Mycobacterial dormancy systems and host responses in tuberculosis. *Frontiers in immunology,* 8**,** 84.
PENN-NICHOLSON, A., MBANDI, S. K., THOMPSON, E., MENDELSOHN, S. C., SULIMAN, S., CHEGOU, N. N., MALHERBE, S. T., DARBOE, F., ERASMUS, M. & HANEKOM, W. A. 2020. RISK6, a 6-gene transcriptomic signature of TB disease risk, diagnosis and treatment response. *Scientific reports,* 10**,** 1-21.
PETERS, J. S., ISMAIL, N., DIPPENAAR, A., MA, S., SHERMAN, D. R., WARREN, R. M. & KANA, B. D. 2020. Genetic diversity in *Mycobacterium tuberculosis* clinical isolates and resulting outcomes of tuberculosis infection and disease. *Annual Review of Genetics,* 54**,** 511-537.
PETERS, J. S., MCIVOR, A., PAPADOPOULOS, A. O., MASANGANA, T., GORDHAN, B. G., WAJA, Z., OTWOMBE, K., LETUTU, M., KAMARIZA, M. & STERLING, T. R. 2023. Differentially culturable tubercle bacteria as a measure of tuberculosis treatment response. *Frontiers in Cellular and Infection Microbiology,* 12**,** 1976.
PETRONE, L., BONDET, V., VANINI, V., CUZZI, G., PALMIERI, F., PALUCCI, I., DELOGU, G., CICCOSANTI, F., FIMIA, G. M. & BLAUENFELDT, T. 2019. First description of agonist and antagonist IP-10 in urine of patients with active TB. *International Journal of Infectious Diseases,* 78**,** 15-21.
PHUAH, J., WONG, E. A., GIDEON, H. P., MAIELLO, P., COLEMAN, M. T., HENDRICKS, M. R., RUDEN, R., CIRRINCIONE, L. R., CHAN, J. & LIN, P. L. 2016. Effects of B cell depletion on early *Mycobacterium tuberculosis* infection in cynomolgus macaques. *Infection and immunity,* 84**,** 1301-1311.
PILCHER, C. D., FISCUS, S. A., NGUYEN, T. Q., FOUST, E., WOLF, L., WILLIAMS, D., ASHBY, R., O'DOWD, J. O., MCPHERSON, J. T. & STALZER, B. 2005. Detection of acute infections during HIV testing in North Carolina. *New England Journal of Medicine,* 352**,** 1873-1883.
PINTO, D., SANTOS, M. A. & CHAMBEL, L. 2015. Thirty years of viable but nonculturable state research: unsolved molecular mechanisms. *Critical reviews in microbiology,* 41**,** 61-76.
PITALOKA, D. A. E., SYAMSUNARNO, M. R. A. A., ABDULAH, R. & CHAIDIR, L. 2022. Omics Biomarkers for Monitoring Tuberculosis Treatment: A Mini-Review of Recent Insights and Future Approaches. *Infection and Drug Resistance,* 15**,** 2703.
PONNUSAMY, N. & ARUMUGAM, M. 2022. Interaction of Host Pattern Recognition Receptors (PRRs) with *Mycobacterium tuberculosis* and Ayurvedic Management of

Tuberculosis: A Systemic Approach. *Infectious Disorders-Drug Targets (Formerly Current Drug Targets-Infectious Disorders),* 22**,** 28-40.
PREEZ, I. D., LUIES, L. & LOOTS, D. T. 2017. Metabolomics biomarkers for tuberculosis diagnostics: current status and future objectives. *Biomarkers in medicine,* 11**,** 179-194.
PUISSEGUR, M. P., BOTANCH, C., DUTEYRAT, J. L., DELSOL, G., CARATERO, C. & ALTARE, F. 2004. An in vitro dual model of mycobacterial granulomas to investigate the molecular interactions between mycobacteria and human host cells. *Cellular microbiology,* 6**,** 423-433.
QIAN, X., NGUYEN, D. T., LI, Y., LYU, J., GRAVISS, E. A. & HU, T. Y. 2016. Predictive value of serum bradykinin and desArg9-bradykinin levels for chemotherapeutic responses in active tuberculosis patients: A retrospective case series. *Tuberculosis,* 101**,** S109-S118.
QUEVAL, C. J., BROSCH, R. & SIMEONE, R. 2017. The Macrophage: A Disputed Fortress in the Battle against *Mycobacterium tuberculosis*. *Front Microbiol,* 8**,** 2284.
RAGNO, S., ROMANO, M., HOWELL, S., PAPPIN, D. J., JENNER, P. J. & COLSTON, M. J. 2001. Changes in gene expression in macrophages infected with *Mycobacterium tuberculosis*: a combined transcriptomic and proteomic approach. *Immunology,* 104**,** 99-108.
RATLEDGE, C. & STANFORD, J. 1982. *The biology of the mycobacteria*.
RAWAT, K. D., CHAHAR, M., SRIVASTAVA, N., GUPTA, U., NATRAJAN, M., KATOCH, V., KATOCH, K. & CHAUHAN, D. 2018. Expression profile of CXCL12 chemokine during M. tuberculosis infection with different therapeutic interventions in guinea pig. *Indian Journal of Tuberculosis,* 65**,** 152-158.
REDFORD, P. S., BOONSTRA, A., READ, S., PITT, J., GRAHAM, C., STAVROPOULOS, E., BANCROFT, G. J. & O'GARRA, A. 2010. Enhanced protection to *Mycobacterium tuberculosis* infection in IL-10-deficient mice is accompanied by early and enhanced Th1 responses in the lung. *European journal of immunology,* 40**,** 2200-2210.
RIAZ, M., MAHMOOD, Z., JAVED, M. T., JAVED, I., SHAHID, M., ABBAS, M. & EHTISHAM-UL-HAQUE, S. 2016. Drug resistant strains of *Mycobacterium tuberculosis* identified through PCR-RFLP from patients of Central Punjab, Pakistan. *International journal of immunopathology and pharmacology,* 29**,** 443-449.
ROBERTS, D. M., LIAO, R. P., WISEDCHAISRI, G., HOL, W. G. & SHERMAN, D. R. 2004. Two sensor kinases contribute to the hypoxic response of *Mycobacterium tuberculosis*. *Journal of Biological Chemistry,* 279**,** 23082-23087.
ROCHA, D. M., VIVEIROS, M., SARAIVA, M. & OSÓRIO, N. S. 2021. The neglected contribution of streptomycin to the tuberculosis drug resistance problem. *Genes,* 12**,** 2003.
ROCKWOOD, N., DU BRUYN, E., MORRIS, T. & WILKINSON, R. J. 2016. Assessment of treatment response in tuberculosis. *Expert review of respiratory medicine,* 10**,** 643-654.
RONNING, D. R., KLABUNDE, T., BESRA, G. S., VISSA, V. D., BELISLE, J. T. & SACCHETTINI, J. C. 2000. Crystal structure of the secreted form of antigen 85C reveals potential targets for mycobacterial drugs and vaccines. *Nature structural biology,* 7**,** 141-146.
ROSSATO SILVA, D., GEHLEN, M., BERNARDI, R., ANTON, C., MACHADO, F., COSTA, E. & ROSSETTI, M. 2019. Single Nucleotide Polymorphism in the Gene Encoding Macrophage Migration Inhibitory Factor (MIF) and Its Association with

Active Pulmonary Tuberculosis. *B110. MYCOBACTERIAL HOST DEFENSE AND PATHOGENESIS.* American Thoracic Society.
ROSSER, A., PAREEK, M., TURAPOV, O., WISELKA, M. J. & MUKAMOLOVA, G. V. 2018. Differentially culturable tubercule bacilli are generated during nonpulmonary tuberculosis infection. *American Journal of Respiratory and Critical Care Medicine,* 197**,** 818-821.
ROSZAK, D., GRIMES, D. & COLWELL, R. 1984. Viable but nonrecoverable stage of Salmonella enteritidis in aquatic systems. *Canadian journal of microbiology,* 30**,** 334-338.
RUHL, S. 2012. The scientific exploration of saliva in the post-proteomic era: from database back to basic function. *Expert review of proteomics,* 9**,** 85-96.
RUSSELL-GOLDMAN, E., XU, J., WANG, X., CHAN, J. & TUFARIELLO, J. M. 2008. A *Mycobacterium tuberculosis* Rpf double-knockout strain exhibits profound defects in reactivation from chronic tuberculosis and innate immunity phenotypes. *Infection and immunity,* 76**,** 4269-4281.
RUSSELL, D. G. 2011. *Mycobacterium tuberculosis* and the intimate discourse of a chronic infection. *Immunological reviews,* 240**,** 252-268.
RUSTAD, T. R., HARRELL, M. I., LIAO, R. & SHERMAN, D. R. 2008. The enduring hypoxic response of *Mycobacterium tuberculosis*. *PloS one,* 3**,** e1502.
RYNDAK, M. B., SINGH, K. K., PENG, Z. & LAAL, S. 2015. Transcriptional profile of *Mycobacterium tuberculosis* replicating in type II alveolar epithelial cells. *PloS one,* 10**,** e0123745.
SABIR, N., HUSSAIN, T., SHAH, S. Z. A., PERAMO, A., ZHAO, D. & ZHOU, X. 2018. miRNAs in tuberculosis: new avenues for diagnosis and host-directed therapy. *Frontiers in microbiology,* 9**,** 602.
SAGHAZADEH, A. & REZAEI, N. 2022. Vascular endothelial growth factor levels in tuberculosis: A systematic review and meta-analysis. *PloS one,* 17**,** e0268543.
SAITO, K., WARRIER, T., SOMERSAN-KARAKAYA, S., KAMINSKI, L., MI, J., JIANG, X., PARK, S., SHIGYO, K., GOLD, B. & ROBERTS, J. 2017. Rifamycin action on RNA polymerase in antibiotic-tolerant *Mycobacterium tuberculosis* results in differentially detectable populations. *Proceedings of the National Academy of Sciences,* 114**,** E4832-E4840.
SALAM, N., GUPTA, S., SHARMA, S., PAHUJANI, S., SINHA, A., SAXENA, R. K. & NATARAJAN, K. 2008. Protective immunity to *Mycobacterium tuberculosis* infection by chemokine and cytokine conditioned CFP-10 differentiated dendritic cells. *PLoS One,* 3**,** e2869.
SALEK, R. M., MAGUIRE, M. L., BENTLEY, E., RUBTSOV, D. V., HOUGH, T., CHEESEMAN, M., NUNEZ, D., SWEATMAN, B. C., HASELDEN, J. N. & COX, R. 2007. A metabolomic comparison of urinary changes in type 2 diabetes in mouse, rat, and human. *Physiological genomics,* 29**,** 99-108.
SALINA, E. G., WADDELL, S. J., HOFFMANN, N., ROSENKRANDS, I., BUTCHER, P. D. & KAPRELYANTS, A. S. 2014. Potassium availability triggers *Mycobacterium tuberculosis* transition to, and resuscitation from, non-culturable (dormant) states. *Open biology,* 4**,** 140106.
SALLIN, M. A., KAUFFMAN, K. D., RIOU, C., DU BRUYN, E., FOREMAN, T. W., SAKAI, S., HOFT, S. G., MYERS, T. G., GARDINA, P. J. & SHER, A. 2018. Host resistance to pulmonary *Mycobacterium tuberculosis* infection requires CD153 expression. *Nature microbiology,* 3**,** 1198-1205.

SAMIR, M. & PESSLER, F. 2016. Small non-coding RNAs associated with viral infectious diseases of veterinary importance: potential clinical applications. *Frontiers in Veterinary Science,* 3**,** 22.
SARDIWAL, S., KENDALL, S. L., MOVAHEDZADEH, F., RISON, S. C., STOKER, N. G. & DJORDJEVIC, S. 2005. A GAF domain in the hypoxia/NO-inducible *Mycobacterium tuberculosis* DosS protein binds haem. *Journal of molecular biology,* 353**,** 929-936.
SASINDRAN, S. J. & TORRELLES, J. B. 2011. *Mycobacterium tuberculosis* Infection and Inflammation: what is Beneficial for the Host and for the Bacterium? *Frontiers in microbiology,* 2**,** 2.
SAUTY, A., DZIEJMAN, M., TAHA, R. A., IAROSSI, A. S., NEOTE, K., GARCIA-ZEPEDA, E. A., HAMID, Q. & LUSTER, A. D. 1999. The T cell-specific CXC chemokines IP-10, Mig, and I-TAC are expressed by activated human bronchial epithelial cells. *The Journal of Immunology,* 162**,** 3549-3558.
SCHNAPPINGER, D., EHRT, S., VOSKUIL, M. I., LIU, Y., MANGAN, J. A., MONAHAN, I. M., DOLGANOV, G., EFRON, B., BUTCHER, P. D. & NATHAN, C. 2003. Transcriptional adaptation of *Mycobacterium tuberculosis* within macrophages: insights into the phagosomal environment. *The Journal of experimental medicine,* 198**,** 693-704.
SCHNEIDER, B. E., KORBEL, D., HAGENS, K., KOCH, M., RAUPACH, B., ENDERS, J., KAUFMANN, S. H., MITTRÜCKER, H. W. & SCHAIBLE, U. E. 2010. A role for IL-18 in protective immunity against *Mycobacterium tuberculosis*. *European journal of immunology,* 40**,** 396-405.
SCHROEDER, E., DE SOUZA, O. N., SANTOS, D., BLANCHARD, J. & BASSO, L. 2002. Drugs that inhibit mycolic acid biosynthesis in *Mycobacterium tuberculosis*. *Current pharmaceutical biotechnology,* 3**,** 197-225.
SCHUTZ, C., MEINTJES, G., ALMAJID, F., WILKINSON, R. J. & POZNIAK, A. 2010. Clinical management of tuberculosis and HIV-1 co-infection. Eur Respiratory Soc.
SCORDO, J. M., KNOELL, D. L. & TORRELLES, J. B. 2016. Alveolar Epithelial Cells in *Mycobacterium tuberculosis* Infection: Active Players or Innocent Bystanders? *J Innate Immun,* 8**,** 3-14.
SEILER, P., AICHELE, P., RAUPACH, B., ODERMATT, B., STEINHOFF, U. & KAUFMANN, S. H. 2000. Rapid neutrophil response controls fast-replicating intracellular bacteria but not slow-replicating *Mycobacterium tuberculosis*. *The Journal of infectious diseases,* 181**,** 671-680.
SHANG, Z.-B., WANG, J., KUAI, S.-G., ZHANG, Y.-Y., OU, Q.-F., PEI, H. & HUANG, L.-H. 2018. Serum macrophage migration inhibitory factor as a biomarker of active pulmonary tuberculosis. *Annals of laboratory medicine,* 38**,** 9.
SHARAN, R., BUCŞAN, A. N., GANATRA, S., PAIARDINI, M., MOHAN, M., MEHRA, S., KHADER, S. A. & KAUSHAL, D. 2020. Chronic immune activation in TB/HIV co-infection. *Trends in microbiology,* 28**,** 619-632.
SHARMA, D., BOSE, A., SHAKILA, H., DAS, T. K., TYAGI, J. S. & RAMANATHAN, V. 2006. Expression of mycobacterial cell division protein, FtsZ, and dormancy proteins, DevR and Acr, within lung granulomas throughout guinea pig infection. *FEMS Immunology & Medical Microbiology,* 48**,** 329-336.
SHEN, H. & CHEN, Z. W. 2018. The crucial roles of Th17-related cytokines/signal pathways in M. tuberculosis infection. *Cellular & molecular immunology,* 15**,** 216-225.
SHEN, H., WANG, Y., CHEN, C. Y., FRENCHER, J., HUANG, D., YANG, E., RYAN-PAYSEUR, B. & CHEN, Z. W. 2015. Th17-related cytokines contribute to recall-like

expansion/effector function of HMBPP-specific Vγ2Vδ2 T cells after *Mycobacterium tuberculosis* infection or vaccination. *European journal of immunology,* 45**,** 442-451.
SHEN, Y., XUN, J., SONG, W., WANG, Z., WANG, J., LIU, L., ZHANG, R., QI, T., TANG, Y. & CHEN, J. 2020. Discovery of potential plasma biomarkers for tuberculosis in HIV-infected patients by data-independent acquisition-based quantitative proteomics. *Infection and Drug Resistance,* 13**,** 1185.
SHILOH, M. U., MANZANILLO, P. & COX, J. S. 2008. *Mycobacterium tuberculosis* senses host-derived carbon monoxide during macrophage infection. *Cell host & microbe,* 3**,** 323-330.
SHLEEVA, M., BAGRAMYAN, K., TELKOV, M., MUKAMOLOVA, G., YOUNG, M., KELL, D. & KAPRELYANTS, A. 2002. Formation and resuscitation of 'non-culturable'cells of Rhodococcus rhodochrous and *Mycobacterium tuberculosis* in prolonged stationary phase. *Microbiology,* 148**,** 1581-1591.
SHLEEVA, M., SALINA, E. & KAPRELYANTS, A. 2010. Dormant forms of mycobacteria. *Microbiology,* 79**,** 1-12.
SHUI, G., BENDT, A. K., JAPPAR, I. A., LIM, H. M., LANEELLE, M., HERVÉ, M., VIA, L. E., CHUA, G. H., BRATSCHI, M. W. & ZAINUL RAHIM, S. Z. 2012. Mycolic acids as diagnostic markers for tuberculosis case detection in humans and drug efficacy in mice. *EMBO molecular medicine,* 4**,** 27-37.
SIGAL, G., SEGAL, M., MATHEW, A., JARLSBERG, L., WANG, M., BARBERO, S., SMALL, N., HAYNESWORTH, K., DAVIS, J. & WEINER, M. 2017. Biomarkers of tuberculosis severity and treatment effect: a directed screen of 70 host markers in a randomized clinical trial. *EBioMedicine,* 25**,** 112-121.
SILVA, D., PONTE, C. G., HACKER, M. A. & ANTAS, P. R. 2013. A whole blood assay as a simple, broad assessment of cytokines and chemokines to evaluate human immune responses to *Mycobacterium tuberculosis* antigens. *Acta tropica,* 127**,** 75-81.
SILVEIRA-MATTOS, P. S., NARENDRAN, G., AKRAMI, K., FUKUTANI, K. F., ANBALAGAN, S., NAYAK, K., SUBRAMANYAM, S., SUBRAMANI, R., VINHAES, C. L. & SOUZA, D. O.-D. 2019. Differential expression of CXCR3 and CCR6 on CD4+ T-lymphocytes with distinct memory phenotypes characterizes tuberculosis-associated immune reconstitution inflammatory syndrome. *Scientific reports,* 9**,** 1-9.
SINGER, S. N., NDUMNEGO, O. C., KIM, R. S., NDUNG'U, T., ANASTOS, K., FRENCH, A., CHURCHYARD, G., PARAMITHIOTHIS, E., KASPROWICZ, V. O. & ACHKAR, J. M. 2022. Plasma host protein biomarkers correlating with increasing *Mycobacterium tuberculosis* infection activity prior to tuberculosis diagnosis in people living with HIV. *EBioMedicine,* 75**,** 103787.
SINGH, P. R., VIJJAMARRI, A. K. & SARKAR, D. 2020. Metabolic switching of *Mycobacterium tuberculosis* during hypoxia is controlled by the virulence regulator PhoP. *Journal of bacteriology,* 202**,** e00705-19.
SKIBINSKI, G., SKIBINSKA, A. & JAMES, K. 2001. The role of hepatocyte growth factor and its receptor c-met in interactions between lymphocytes and stromal cells in secondary human lymphoid organs. *Immunology,* 102**,** 506-514.
SOHN, H., LEE, K. S., KIM, S. Y., SHIN, D. M., SHIN, S. J., JO, E. K., PARK, J. K. & KIM, H. J. 2009. Induction of cell death in human macrophages by a highly virulent Korean Isolate of *Mycobacterium tuberculosis* and the virulent strain H37Rv. *Scandinavian journal of immunology,* 69**,** 43-50.
SOMASUNDARAM, S., RAM, A. & SANKARANARAYANAN, L. 2014. Isoniazid and rifampicin as therapeutic regimen in the current era: a review. *Journal of Tuberculosis Research,* 2014.

SONNENBERG, E., WEIDNER, K. & BIRCHMEIER, C. 1993. Expression of the met-receptor and its ligand, HGF-SF during mouse embryogenesis. *Exs,* 65**,** 381-394.
SOVERSHAEVA, E., KRANZER, K., MCHUGH, G., BANDASON, T., MAJONGA, E. D., USMANI, O. S., ROWLAND-JONES, S., GUTTEBERG, T., FLÆGSTAD, T. & FERRAND, R. A. 2019. History of tuberculosis is associated with lower exhaled nitric oxide levels in HIV-infected children. *AIDS (London, England),* 33**,** 1711.
STALEY, J. T. & KONOPKA, A. 1985. Measurement of in situ activities of nonphotosynthetic microorganisms in aquatic and terrestrial habitats. *Annual review of microbiology,* 39**,** 321-346.
STINEAR, T. P., SEEMANN, T., PIDOT, S., FRIGUI, W., REYSSET, G., GARNIER, T., MEURICE, G., SIMON, D., BOUCHIER, C. & MA, L. 2007. Reductive evolution and niche adaptation inferred from the genome of Mycobacterium ulcerans, the causative agent of Buruli ulcer. *Genome research,* 17**,** 192-200.
STOLPOVSKY, K., MARTINEZ-LAVANCHY, P., HEIPIEPER, H. J., VAN CAPPELLEN, P. & THULLNER, M. 2011. Incorporating dormancy in dynamic microbial community models. *Ecological Modelling,* 222**,** 3092-3102.
SUBRAMANIAN, I., VERMA, S., KUMAR, S., JERE, A. & ANAMIKA, K. 2020. Multi-omics data integration, interpretation, and its application. *Bioinformatics and biology insights,* 14**,** 1177932219899051.
SUGAWARA, I., UDAGAWA, T. & YAMADA, H. 2004. Rat neutrophils prevent the development of tuberculosis. *Infect Immun,* 72**,** 1804-6.
SUN, Y., LIU, S., QIAO, Z., SHANG, Z., XIA, Z., NIU, X., QIAN, L., ZHANG, Y., FAN, L. & CAO, C.-X. 2017. Systematic comparison of exosomal proteomes from human saliva and serum for the detection of lung cancer. *Analytica chimica acta,* 982**,** 84-95.
SWAMINATHAN, S. & NARENDRAN, G. 2008. HIV and tuberculosis in India. *Journal of biosciences,* 33**,** 527-537.
SWEENEY, T. E., BRAVIAK, L., TATO, C. M. & KHATRI, P. 2016. Genome-wide expression for diagnosis of pulmonary tuberculosis: a multicohort analysis. *The Lancet Respiratory Medicine,* 4**,** 213-224.
ŚWIERZKO, A. S., BARTŁOMIEJCZYK, M. A., BRZOSTEK, A., ŁUKASIEWICZ, J., MICHALSKI, M., DZIADEK, J. & CEDZYŃSKI, M. 2016. Mycobacterial antigen 85 complex (Ag85) as a target for ficolins and mannose-binding lectin. *International Journal of Medical Microbiology,* 306**,** 212-221.
TANEJA, N. K. & TYAGI, J. S. 2007. Resazurin reduction assays for screening of anti-tubercular compounds against dormant and actively growing *Mycobacterium tuberculosis*, Mycobacterium bovis BCG and Mycobacterium smegmatis. *Journal of antimicrobial chemotherapy,* 60**,** 288-293.
TANG, X., DENG, W. & XIE, J. 2012. Novel insights into Mycobacterium antigen Ag85 biology and implications in countermeasures for M. tuberculosis. *Critical Reviews™ in Eukaryotic Gene Expression,* 22.
TATEOSIAN, N. L., PELLEGRINI, J. M., AMIANO, N. O., ROLANDELLI, A., CASCO, N., PALMERO, D. J., COLOMBO, M. I. & GARCÍA, V. E. 2017. IL17A augments autophagy in *Mycobacterium tuberculosis*-infected monocytes from patients with active tuberculosis in association with the severity of the disease. *Autophagy,* 13**,** 1191-1204.
TECCHIO, C. & CASSATELLA, M. A. 2016. Neutrophil-derived chemokines on the road to immunity. *Semin Immunol,* 28**,** 119-28.
TEITELBAUM, R., SCHUBERT, W., GUNTHER, L., KRESS, Y., MACALUSO, F., POLLARD, J. W., MCMURRAY, D. N. & BLOOM, B. R. 1999. The M cell as a

portal of entry to the lung for the bacterial pathogen *Mycobacterium tuberculosis*. *Immunity,* 10**,** 641-650.
THOMPSON, E. G., DU, Y., MALHERBE, S. T., SHANKAR, S., BRAUN, J., VALVO, J., RONACHER, K., TROMP, G., TABB, D. L. & ALLAND, D. 2017. Host blood RNA signatures predict the outcome of tuberculosis treatment. *Tuberculosis,* 107**,** 48-58.
TONG, J., LIU, Q., WU, J., JIANG, Y., TAKIFF, H. E. & GAO, Q. 2020. *Mycobacterium tuberculosis* strains of the modern Beijing sublineage excessively accumulate triacylglycerols in vitro. *Tuberculosis,* 120**,** 101892.
TRAUNER, A., LOUGHEED, K. E., BENNETT, M. H., HINGLEY-WILSON, S. M. & WILLIAMS, H. D. 2012. The dormancy regulator DosR controls ribosome stability in hypoxic mycobacteria. *Journal of Biological Chemistry,* 287**,** 24053-24063.
TSANG, J., CHAIN, B. M., MILLER, R. F., WEBB, B. L., BARCLAY, W., TOWERS, G. J., KATZ, D. R. & NOURSADEGHI, M. 2009. HIV-1 infection of macrophages is dependent on evasion of innate immune cellular activation. *AIDS (London, England),* 23**,** 2255.
TUCCI, P., GONZÁLEZ-SAPIENZA, G. & MARIN, M. 2014. Pathogen-derived biomarkers for active tuberculosis diagnosis. *Frontiers in microbiology,* 5**,** 549.
TUFARIELLO, J. M., JACOBS JR, W. R. & CHAN, J. 2004. Individual *Mycobacterium tuberculosis* resuscitation-promoting factor homologues are dispensable for growth in vitro and in vivo. *Infection and immunity,* 72**,** 515-526.
VAEZIPOUR, N., FRITSCHI, N., BRASIER, N., BÉLARD, S., DOMÍNGUEZ, J., TEBRUEGGE, M., PORTEVIN, D. & RITZ, N. 2022. Towards accurate point-of-care tests for tuberculosis in children. *Pathogens,* 11**,** 327.
VAN DAMME, J., PROOST, P., PUT, W., ARENS, S., LENAERTS, J., CONINGS, R., OPDENAKKER, G., HEREMANS, H. & BILLIAU, A. 1994. Induction of monocyte chemotactic proteins MCP-1 and MCP-2 in human fibroblasts and leukocytes by cytokines and cytokine inducers. Chemical synthesis of MCP-2 and development of a specific RIA. *The Journal of Immunology,* 152**,** 5495-5502.
VAN RENSBURG, I. C. & LOXTON, A. G. 2015. Transcriptomics: the key to biomarker discovery during tuberculosis? *Biomarkers in medicine,* 9**,** 483-495.
VIA, L. E., LIN, P. L., RAY, S. M., CARRILLO, J., ALLEN, S. S., EUM, S. Y., TAYLOR, K., KLEIN, E., MANJUNATHA, U. & GONZALES, J. 2008. Tuberculous granulomas are hypoxic in guinea pigs, rabbits, and nonhuman primates. *Infection and immunity,* 76**,** 2333-2340.
VIGNESH, R., SWATHIRAJAN, C. R., SOLOMON, S. S., SHANKAR, E. M. & MURUGAVEL, K. G. 2017. Risk factors and frequency of tuberculosis-associated immune reconstitution inflammatory syndrome among HIV/Tuberculosis co-infected patients in Southern India. *Indian Journal of Medical Microbiology,* 35**,** 279-281.
VILCHÈZE, C. 2020. Mycobacterial cell wall: a source of successful targets for old and new drugs. *Applied Sciences,* 10**,** 2278.
VOSKUIL, M. I., SCHNAPPINGER, D., VISCONTI, K. C., HARRELL, M. I., DOLGANOV, G. M., SHERMAN, D. R. & SCHOOLNIK, G. K. 2003. Inhibition of respiration by nitric oxide induces a *Mycobacterium tuberculosis* dormancy program. *The Journal of experimental medicine,* 198**,** 705-713.
WALLIS, R. S., KIM, P., COLE, S., HANNA, D., ANDRADE, B. B., MAEURER, M., SCHITO, M. & ZUMLA, A. 2013. Tuberculosis biomarkers discovery: developments, needs, and challenges. *The Lancet infectious diseases,* 13**,** 362-372.
WALLIS, R. S., PAI, M., MENZIES, D., DOHERTY, T. M., WALZL, G., PERKINS, M. D. & ZUMLA, A. 2010. Biomarkers and diagnostics for tuberculosis: progress, needs, and translation into practice. *The lancet,* 375**,** 1920-1937.

WALLIS, R. S., PATIL, S., CHEON, S.-H., EDMONDS, K., PHILLIPS, M., PERKINS, M. D., JOLOBA, M., NAMALE, A., JOHNSON, J. L. & TEIXEIRA, L. 1999. Drug tolerance in *Mycobacterium tuberculosis*. *Antimicrobial agents and chemotherapy,* 43**,** 2600-2606.

WALLIS, R. S. & PEPPARD, T. 2015. Early biomarkers and regulatory innovation in multidrug-resistant tuberculosis. *Clinical Infectious Diseases,* 61**,** S160-S163.

WALZL, G., MCNERNEY, R., DU PLESSIS, N., BATES, M., MCHUGH, T. D., CHEGOU, N. N. & ZUMLA, A. 2018. Tuberculosis: advances and challenges in development of new diagnostics and biomarkers. *The Lancet Infectious Diseases,* 18**,** e199-e210.

WALZL, G., RONACHER, K., HANEKOM, W., SCRIBA, T. J. & ZUMLA, A. 2011. Immunological biomarkers of tuberculosis. *Nature Reviews Immunology,* 11**,** 343-354.

WANCHU, A., BHATNAGAR, A., TALREJA, J., SAPRA, S., SURYANARAYANA, B. & SURESH, P. 2009. Immunophenotypic and intracellular cytokine profile of Indian patients with tuberculosis with and without human immunodeficiency virus co-infection. *The Indian journal of chest diseases & allied sciences,* 51**,** 207-211.

WANG, C., LIU, C., LIN, H., YU, C., CHUNG, K. & KUO, H. 1998. Increased exhaled nitric oxide in active pulmonary tuberculosis due to inducible NO synthase upregulation in alveolar macrophages. *European Respiratory Journal,* 11**,** 809-815.

WANG, C., YANG, S., LIU, C.-M., JIANG, T.-T., CHEN, Z.-L., TU, H.-H., MAO, L.-G., LI, Z.-J. & LI, J.-C. 2018. Screening and identification of four serum miRNAs as novel potential biomarkers for cured pulmonary tuberculosis. *Tuberculosis,* 108**,** 26-34.

WANG, Q., HAN, W., NIU, J., SUN, B., DONG, W. & LI, G. 2019. Prognostic value of serum macrophage migration inhibitory factor levels in pulmonary tuberculosis. *Respiratory research,* 20**,** 1-10.

WARD-KAVANAGH, L. K., LIN, W. W., ŠEDÝ, J. R. & WARE, C. F. 2016. The TNF receptor superfamily in co-stimulating and co-inhibitory responses. *Immunity,* 44**,** 1005-1019.

WARSINSKE, H. C., RAO, A. M., MOREIRA, F. M., SANTOS, P. C. P., LIU, A. B., SCOTT, M., MALHERBE, S. T., RONACHER, K., WALZL, G. & WINTER, J. 2018. Assessment of validity of a blood-based 3-gene signature score for progression and diagnosis of tuberculosis, disease severity, and treatment response. *JAMA network open,* 1**,** e183779-e183779.

WAWROCKI, S., KIELNIEROWSKI, G., RUDNICKA, W., SEWERYN, M. & DRUSZCZYNSKA, M. 2020. Interleukin-18, functional IL-18 receptor and IL-18 binding protein expression in active and latent tuberculosis. *Pathogens,* 9**,** 451.

WAYNE, L. & HAYES, L. 1998. Nitrate reduction as a marker for hypoxic shiftdown of *Mycobacterium tuberculosis*. *Tubercle and Lung Disease,* 79**,** 127-132.

WAYNE, L. G. 1976. Dynamics of submerged growth of *Mycobacterium tuberculosis* under aerobic and microaerophilic conditions. *American Review of Respiratory Disease,* 114**,** 807-811.

WAYNE, L. G. & HAYES, L. G. 1996. An in vitro model for sequential study of shiftdown of *Mycobacterium tuberculosis* through two stages of nonreplicating persistence. *Infection and immunity,* 64**,** 2062-2069.

WEI, M., WU, Z., LIN, J., LI, Y., QIAN, Z., XIE, Y., SU, H. & ZHOU, W. 2015. Regulation network of serum cytokines induced by tuberculosis-specific antigens reveals biomarkers for tuberculosis diagnosis. *Genet Mol Res,* 14**,** 17182-92.

WEI, Z., LI, Y., WEI, C., LI, Y., XU, H., WU, Y., JIA, Y., GUO, R., JIA, J. & QI, X. 2020. The meta-analysis for ideal cytokines to distinguish the latent and active TB infection. *BMC Pulmonary Medicine,* 20**,** 1-12.

WEINER 3RD, J., PARIDA, S. K., MAERTZDORF, J., BLACK, G. F., REPSILBER, D., TELAAR, A., MOHNEY, R. P., ARNDT-SULLIVAN, C., GANOZA, C. A. & FAE, K. C. 2012. Biomarkers of inflammation, immunosuppression and stress are revealed by metabolomic profiling of tuberculosis patients. *PloS one,* 7**,** e40221.

WEINER, J., MAERTZDORF, J., SUTHERLAND, J. S., DUFFY, F. J., THOMPSON, E., SULIMAN, S., MCEWEN, G., THIEL, B., PARIDA, S. K. & ZYLA, J. 2018. Metabolite changes in blood predict the onset of tuberculosis. *Nature communications,* 9**,** 1-12.

WHO 2019. Lateral flow urine lipoarabinomannan assay (LF-LAM) for the diagnosis of active tuberculosis in people living with HIV: policy update (2019): evidence to decision tables https://www.who.int/publications/i/item/9789241565714 accessed 15/06/2023. World Health Organization.

WHO, G. 2020. Global tuberculosis report 2020 https://www.who.int/publications/i/item/9789240013131 Accessed 15/06/2023. *Glob. Tuberc. Rep*.

WHO, G. 2022. Global tuberculosis report 2022. <https://www.who.int/teams/global-tuberculosis-programme/tb-reports/global-tuberculosis-report-2022 Accessed 15/06/2023>. *Glob Tuberc. Rep*.

WON, E.-J., CHOI, J.-H., CHO, Y.-N., JIN, H.-M., KEE, H. J., PARK, Y.-W., KWON, Y.-S. & KEE, S.-J. 2017. Biomarkers for discrimination between latent tuberculosis infection and active tuberculosis disease. *Journal of Infection,* 74**,** 281-293.

WYKOWSKI, J. H., PHILLIPS, C., NGO, T. & DRAIN, P. K. 2021. A systematic review of potential screening biomarkers for active TB disease. *Journal of Clinical Tuberculosis and Other Mycobacterial Diseases,* 25**,** 100284.

XU, H.-S., ROBERTS, N., SINGLETON, F., ATTWELL, R., GRIMES, D. J. & COLWELL, R. 1982. Survival and viability of nonculturableEscherichia coli andVibrio cholerae in the estuarine and marine environment. *Microbial ecology,* 8**,** 313-323.

YAMAMOTO, H., YUN, E. J., GERBER, H.-P., FERRARA, N., WHITSETT, J. A. & VU, T. H. 2007. Epithelial–vascular cross talk mediated by VEGF-A and HGF signaling directs primary septae formation during distal lung morphogenesis. *Developmental biology,* 308**,** 44-53.

YANG, C.-T., CAMBIER, C. J., DAVIS, J. M., HALL, CHRISTOPHER J., CROSIER, PHILIP S. & RAMAKRISHNAN, L. 2012. Neutrophils Exert Protection in the Early Tuberculous Granuloma by Oxidative Killing of Mycobacteria Phagocytosed from Infected Macrophages. *Cell Host & Microbe,* 12**,** 301-312.

YANG, E., YANG, R., GUO, M., HUANG, D., WANG, W., ZHANG, Z., CHEN, C., WANG, F., HO, W. & SHEN, L. 2018. Multidrug-resistant tuberculosis (MDR-TB) strain infection in macaques results in high bacilli burdens in airways, driving broad innate/adaptive immune responses. *Emerging Microbes & Infections,* 7**,** 1-12.

YANG, Q., CAI, Y., ZHAO, W., WU, F., ZHANG, M., LUO, K., ZHANG, Y., LIU, H., ZHOU, B. & KORNFELD, H. 2014. IP-10 and MIG are compartmentalized at the site of disease during pleural and meningeal tuberculosis and are decreased after antituberculosis treatment. *Clinical and vaccine immunology,* 21**,** 1635-1644.

YI, W.-J., HAN, Y.-S., WEI, L.-L., SHI, L.-Y., HUANG, H., JIANG, T.-T., LI, Z.-B., CHEN, J., HU, Y.-T. & TU, H.-H. 2019. l-Histidine, arachidonic acid, biliverdin, and l-cysteine-glutathione disulfide as potential biomarkers for cured pulmonary tuberculosis. *Biomedicine & Pharmacotherapy,* 116**,** 108980.

YONG, Y. K., TAN, H. Y., SAEIDI, A., WONG, W. F., VIGNESH, R., VELU, V., ERI, R., LARSSON, M. & SHANKAR, E. M. 2019. Immune biomarkers for diagnosis and treatment monitoring of tuberculosis: current developments and future prospects. *Frontiers in microbiology,* 10**,** 2789.

YOTSU, R. R., SUZUKI, K., SIMMONDS, R. E., BEDIMO, R., ABLORDEY, A., YEBOAH-MANU, D., PHILLIPS, R. & ASIEDU, K. 2018. Buruli ulcer: a review of the current knowledge. *Current tropical medicine reports,* 5**,** 247-256.

YOUNG, B. L., MLAMLA, Z., GQAMANA, P. P., SMIT, S., ROBERTS, T., PETER, J., THERON, G., GOVENDER, U., DHEDA, K. & BLACKBURN, J. 2014. The identification of tuberculosis biomarkers in human urine samples. *European Respiratory Journal,* 43**,** 1719-1729.

YU, Q., LI, Y., WANG, H. & XIONG, H. 2019. TSLP induces a proinflammatory phenotype in circulating innate cells and predicts prognosis in sepsis patients. *FEBS Open bio,* 9**,** 2137-2148.

YU, T., PARK, Y., LI, S. & JONES, D. P. 2013. Hybrid feature detection and information accumulation using high-resolution LC–MS metabolomics data. *Journal of proteome research,* 12**,** 1419-1427.

ZAINABADI, K., WALSH, K. F., VILBRUN, S. C., MATHURIN, L. D., LEE, M. H., SAITO, K., MISHRA, S., OCHERETINA, O., PAPE, J. W. & NATHAN, C. 2021. Characterization of differentially detectable *Mycobacterium tuberculosis* in the sputum of subjects with drug-sensitive or drug-resistant tuberculosis before and after two months of therapy. *Antimicrobial Agents and Chemotherapy,* 65**,** e00608-21.

ZAK, D. E., PENN-NICHOLSON, A., SCRIBA, T. J., THOMPSON, E., SULIMAN, S., AMON, L. M., MAHOMED, H., ERASMUS, M., WHATNEY, W. & HUSSEY, G. D. 2016. A blood RNA signature for tuberculosis disease risk: a prospective cohort study. *The Lancet,* 387**,** 2312-2322.

ZELLWEGER, J.-P., SOTGIU, G., CORRADI, M. & DURANDO, P. 2020. The diagnosis of latent tuberculosis infection (LTBI): currently available tests, future developments, and perspectives to eliminate tuberculosis (TB). *La Medicina del lavoro,* 111**,** 170.

ZHANG, B., XIAO, L., QIU, Q., MIAO, L., YAN, S. & ZHOU, S. 2021a. Association between IL-18, IFN-γ and TB susceptibility: a systematic review and meta-analysis. *Annals of Palliative Medicine,* 10**,** 10878-10886.

ZHANG, G., ZHOU, B., LI, S., YUE, J., YANG, H., WEN, Y., ZHAN, S., WANG, W., LIAO, M. & ZHANG, M. 2014. Allele-specific induction of IL-1β expression by C/EBPβ and PU. 1 contributes to increased tuberculosis susceptibility. *PLoS pathogens,* 10**,** e1004426.

ZHANG, X.-H., AHMAD, W., ZHU, X.-Y., CHEN, J. & AUSTIN, B. 2021b. Viable but nonculturable bacteria and their resuscitation: implications for cultivating uncultured marine microorganisms. *Marine Life Science & Technology,* 3**,** 189-203.

ZHAO, S., FUNG-LEUNG, W.-P., BITTNER, A., NGO, K. & LIU, X. 2014. Comparison of RNA-Seq and microarray in transcriptome profiling of activated T cells. *PloS one,* 9**,** e78644.

ZIJENAH, L. S., KADZIRANGE, G., BANDASON, T., CHIPITI, M. M., GWAMBIWA, B., MAKOGA, F., CHUNGU, P., KAGURU, P. & DHEDA, K. 2015. Comparative performance characteristics of the urine lipoarabinomannan strip test and sputum smear microscopy in hospitalized HIV-infected patients with suspected tuberculosis in Harare, Zimbabwe. *BMC infectious diseases,* 16**,** 1-9.

ZIMMER, A. J., LAINATI, F., AGUILERA VASQUEZ, N., CHEDID, C., MCGRATH, S., BENEDETTI, A., MACLEAN, E., RUHWALD, M., DENKINGER, C. M. & KOHLI, M. 2022. Biomarkers that correlate with active pulmonary tuberculosis

treatment response: a systematic review and meta-analysis. *Journal of clinical microbiology*, 60**,** e01859-21.

APPENDICES

APPENDIX A

Supplementary figures

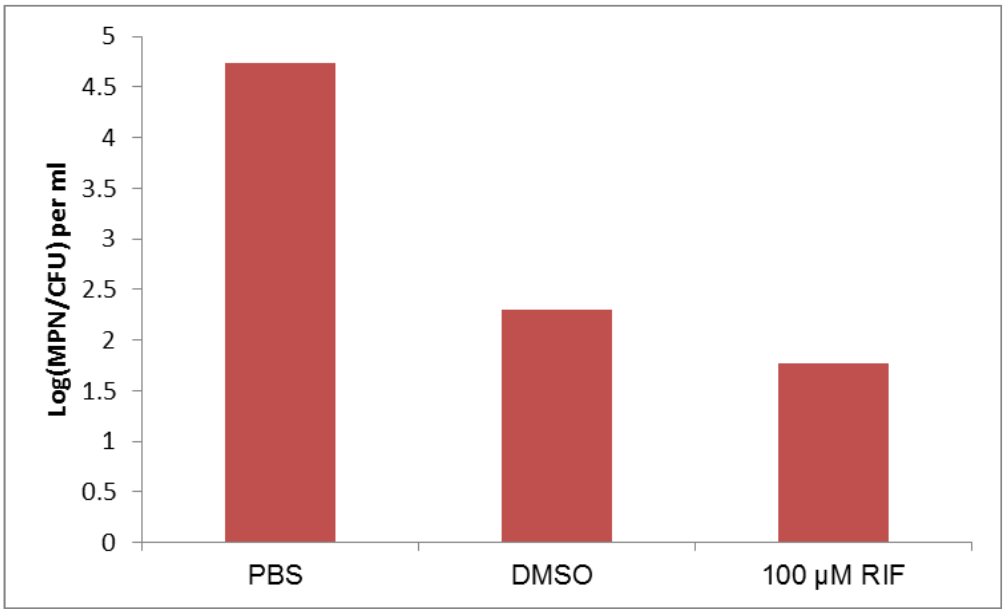

Figure A1. The log difference of cells in the MPN wells as compared to CFU in the PBS-starvation, 1% DMSO and 100 µM Rifampicin (RIF)-treated cultures. Resuscitation of DCTB, measured as the MPN (most probably number) normalized by CFU of starved bacteria during treatment with RIF.

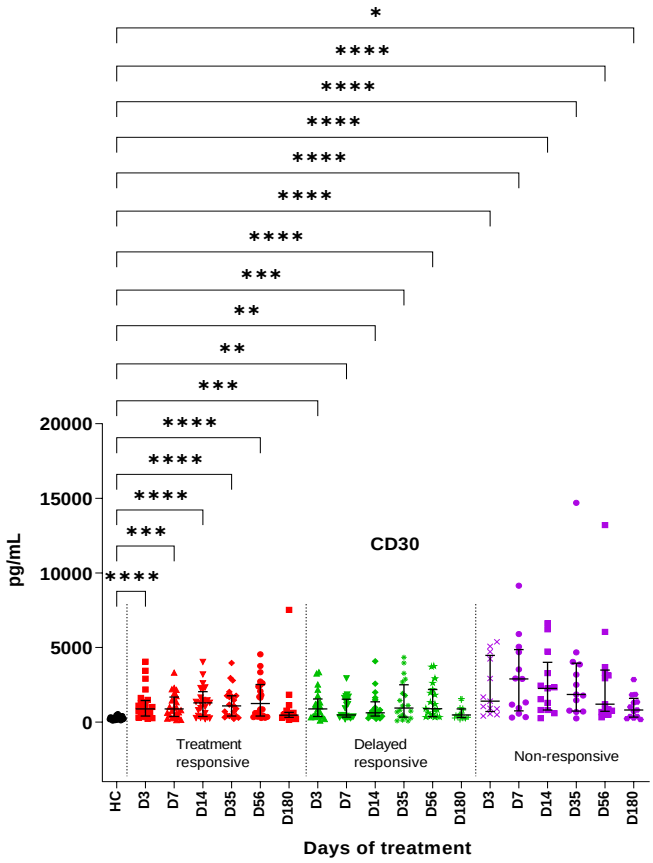
CD30
pg/mL
20000
15000
10000
5000
0
Treatment responsive
Delayed responsive
Non-responsive
HC D3 D7 D14 D35 D56 D180 D3 D7 D14 D35 D56 D180 D3 D7 D14 D35 D56 D180
Days of treatment

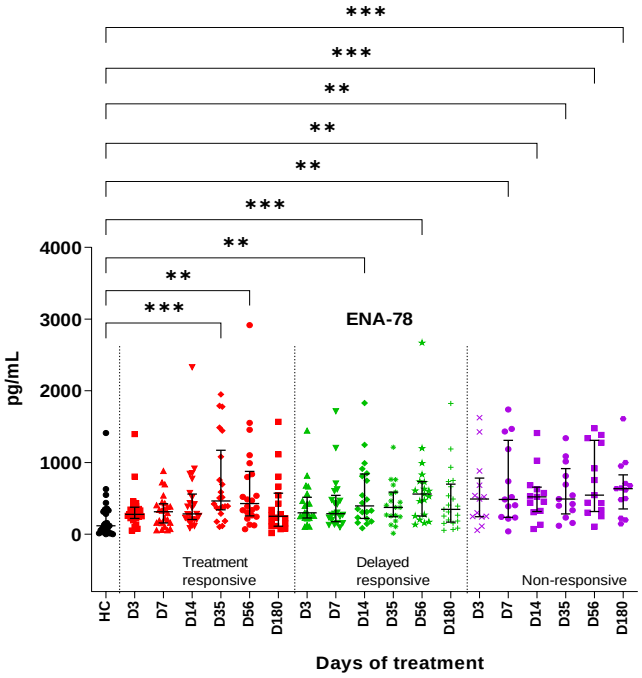
ENA-78
pg/mL
4000
3000
2000
1000
0
Treatment responsive
Delayed responsive
Non-responsive
HC D3 D7 D14 D35 D56 D180 D3 D7 D14 D35 D56 D180 D3 D7 D14 D35 D56 D180
Days of treatment

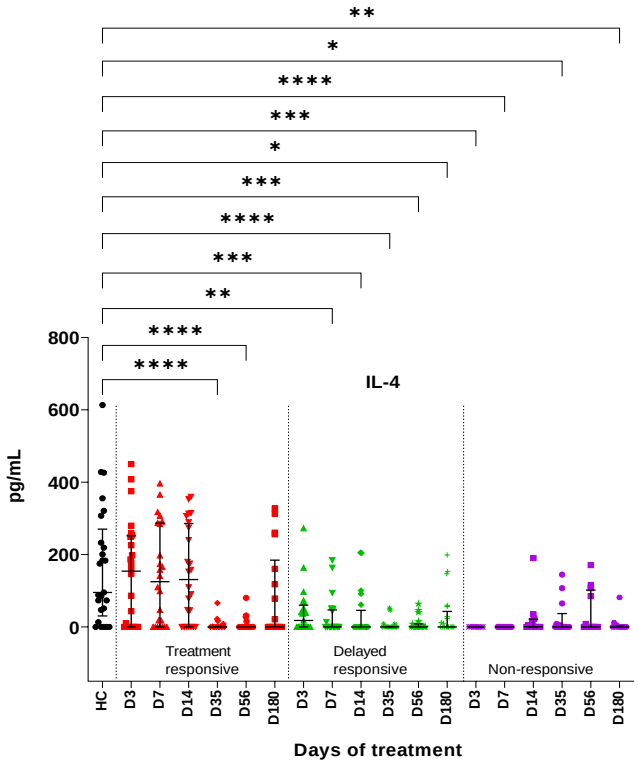
IL-4
pg/mL
800
600
400
200
0
Treatment responsive
Delayed responsive
Non-responsive
HC D3 D7 D14 D35 D56 D180 D3 D7 D14 D35 D56 D180 D3 D7 D14 D35 D56 D180
Days of treatment

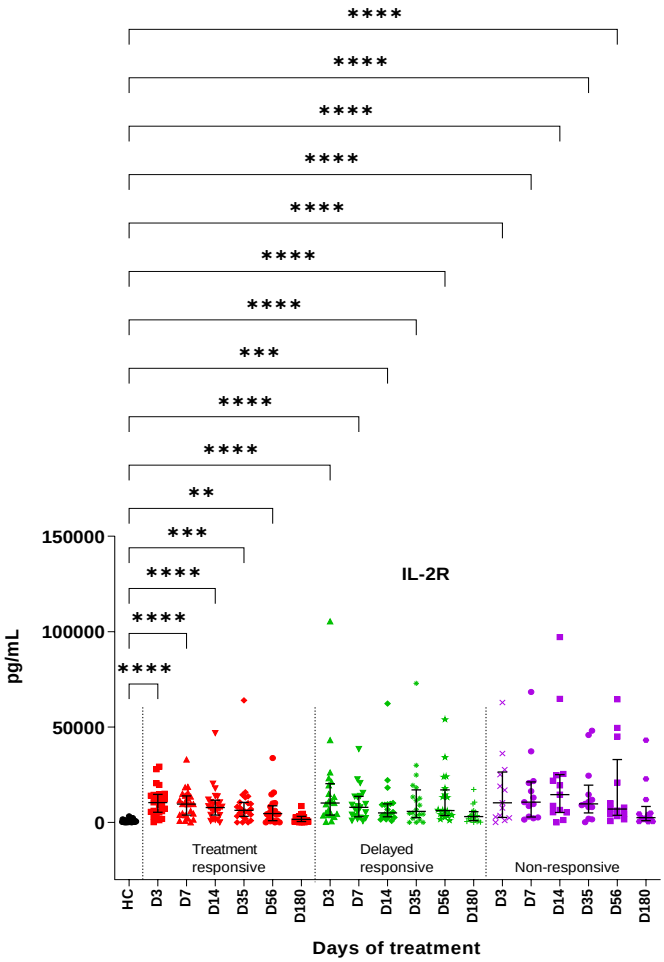
IL-2R
pg/mL
150000
100000
50000
0
Treatment responsive
Delayed responsive
Non-responsive
HC D3 D7 D14 D35 D56 D180 D3 D7 D14 D35 D56 D180 D3 D7 D14 D35 D56 D180
Days of treatment

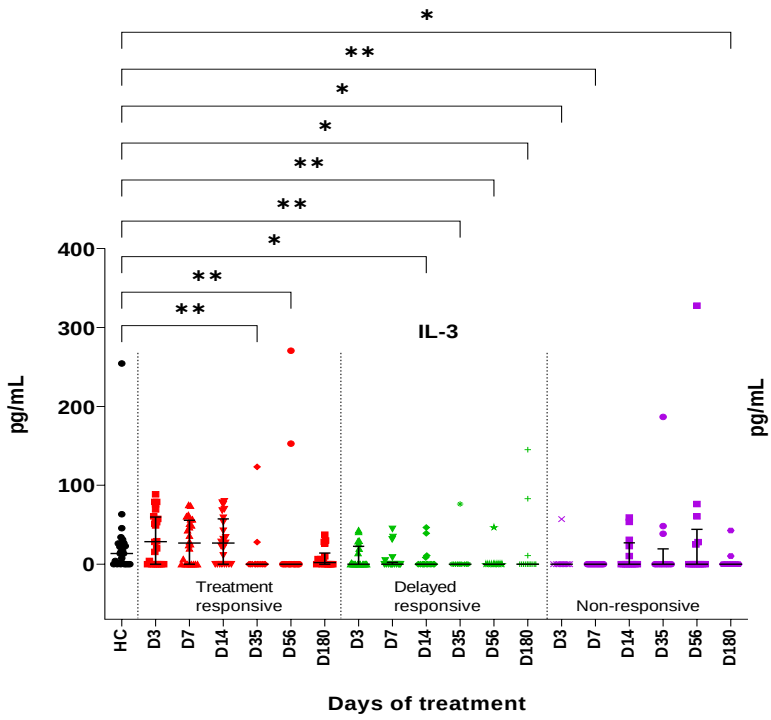
IL-3
pg/mL
400
300
200
100
0
Treatment responsive
Delayed responsive
Non-responsive
HC
D3
D7
D14
D35
D56
D180
Days of treatment

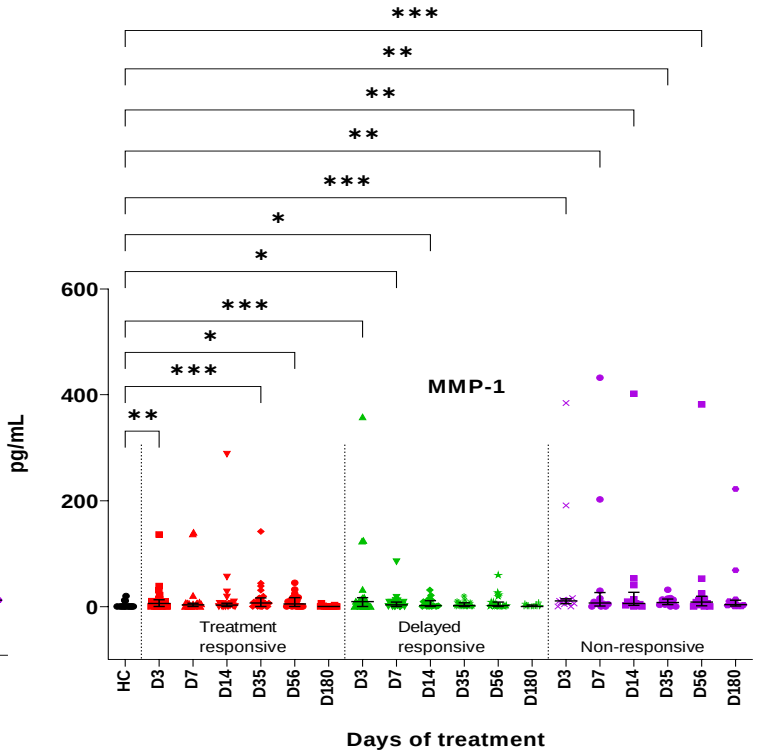
MMP-1
pg/mL
600
400
200
0
Treatment responsive
Delayed responsive
Non-responsive
HC
D3
D7
D14
D35
D56
D180
Days of treatment

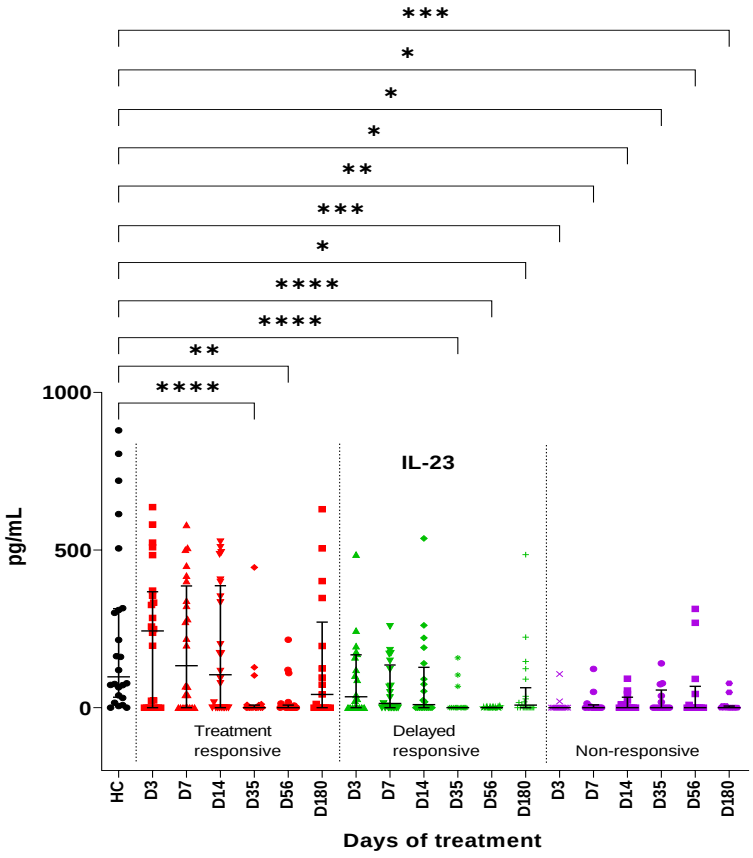
IL-23
pg/mL
1000
500
0
Treatment responsive
Delayed responsive
Non-responsive
HC
D3
D7
D14
D35
D56
D180
Days of treatment

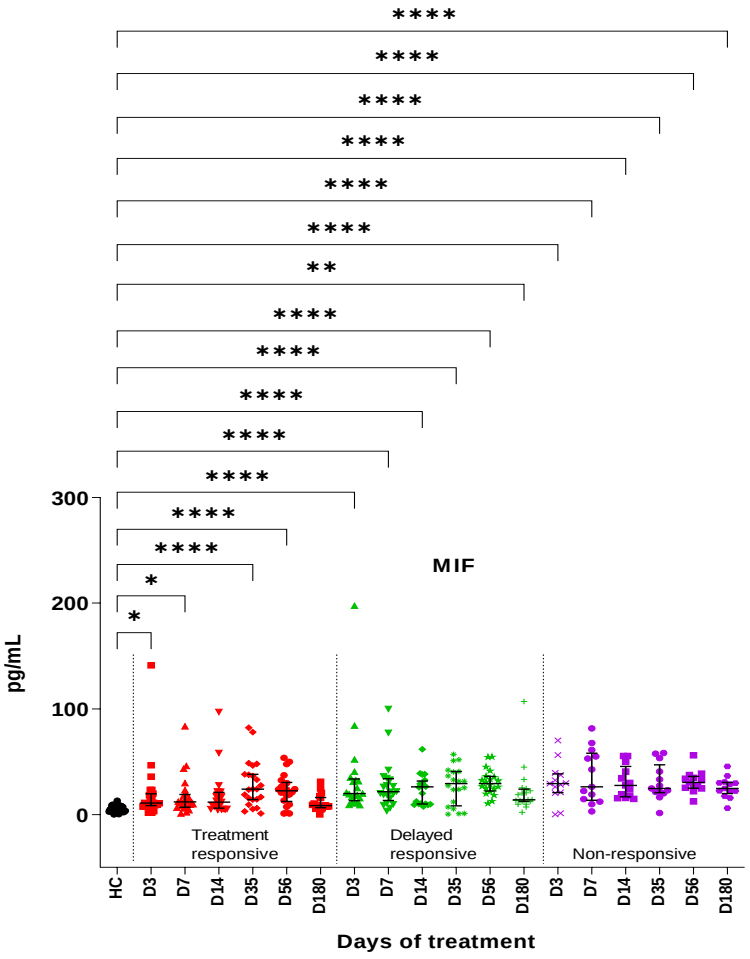
MIF
pg/mL
300
200
100
0
Treatment responsive
Delayed responsive
Non-responsive
HC
D3
D7
D14
D35
D56
D180
Days of treatment

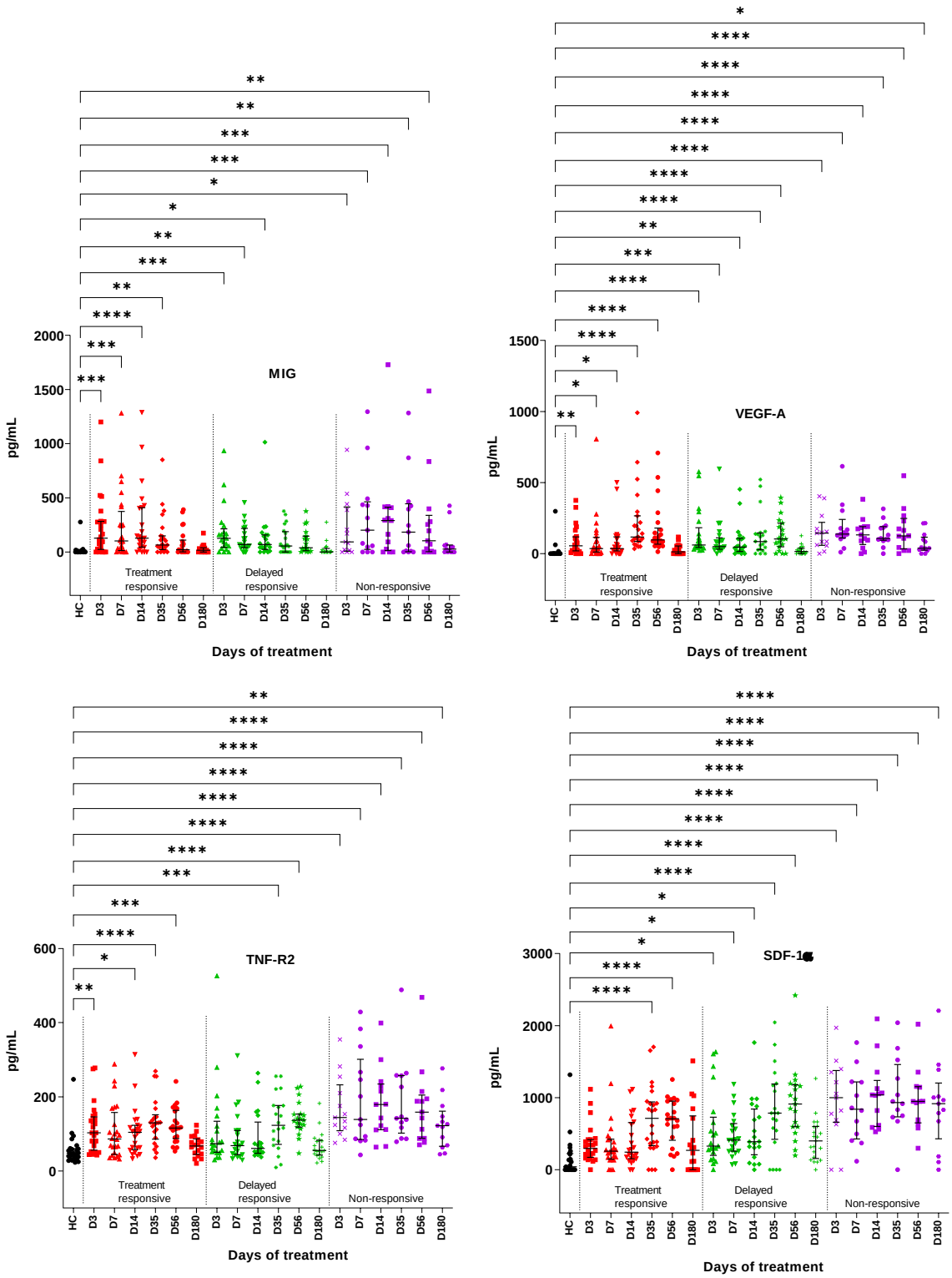

Figure A2. Changes in biomarkers between healthy controls, DCTB Treatment responsive, Delayed-responsive and Non-responsive groups. Black dots represent healthy controls; red: treatment-responsive; green: delayed-responsive and purple: non-responsive DCTB groups. The results are expressed in pg/mL and were analysed by the non-parametric Kruskal-wallis test, with significance *P <0.01; **P < 0.001; ***P < 0.001; ****P < 0.001 (post hoc corrected by multiple comparisons).

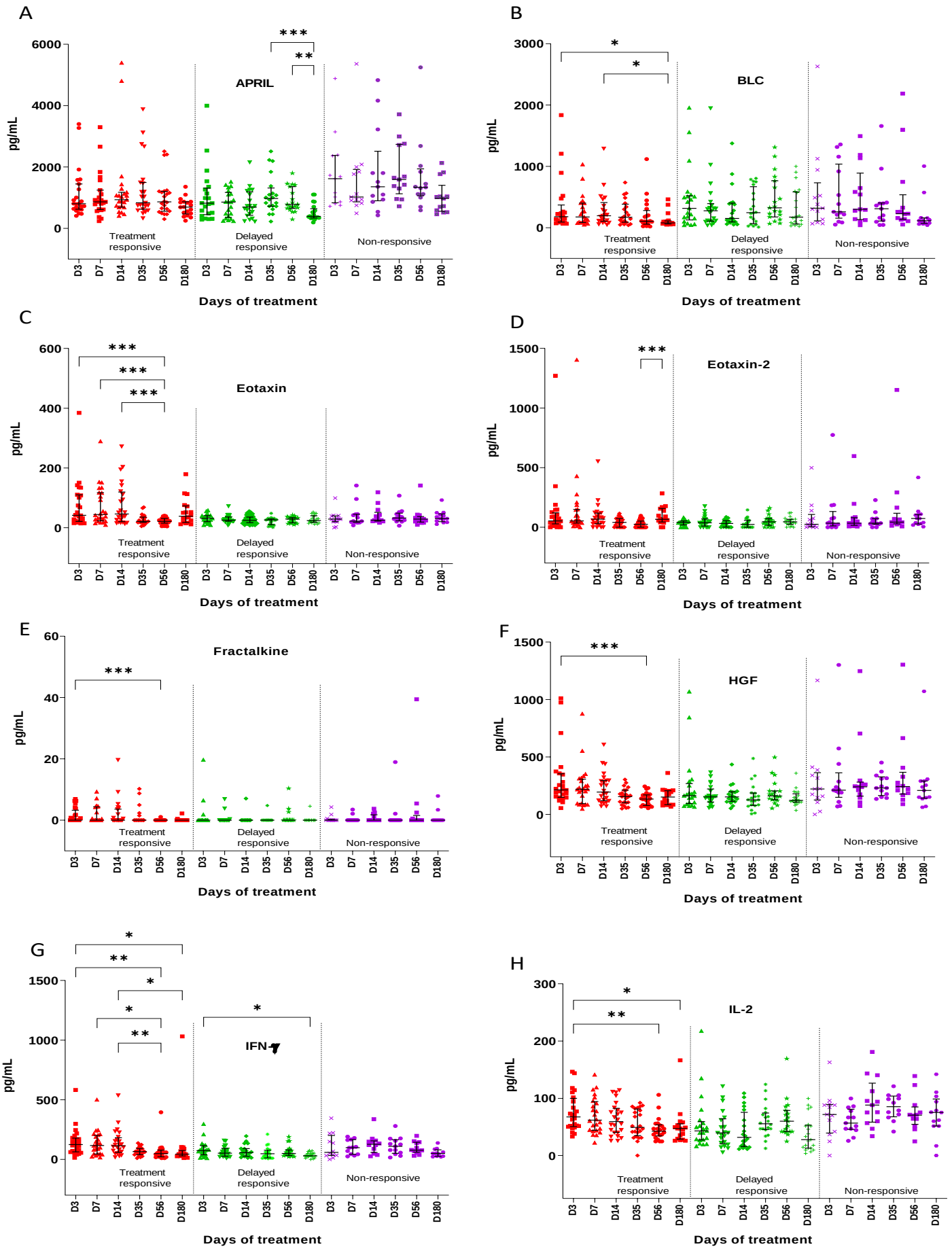
A
APRIL
pg/mL
6000
4000
2000
0
***
**
Treatment responsive
Delayed responsive
Non-responsive
D3 D7 D14 D35 D56 D180
Days of treatment
B
BLC
3000
2000
1000
0
*
*
C
Eotaxin
600
400
200
0
***
***
***
D
Eotaxin-2
1500
1000
500
0
***
E
Fractalkine
60
40
20
0
***
F
HGF
1500
1000
500
0
***
G
IFN-γ
1500
1000
500
0
*
**
*
*
**
*
H
IL-2
300
200
100
0
*
**

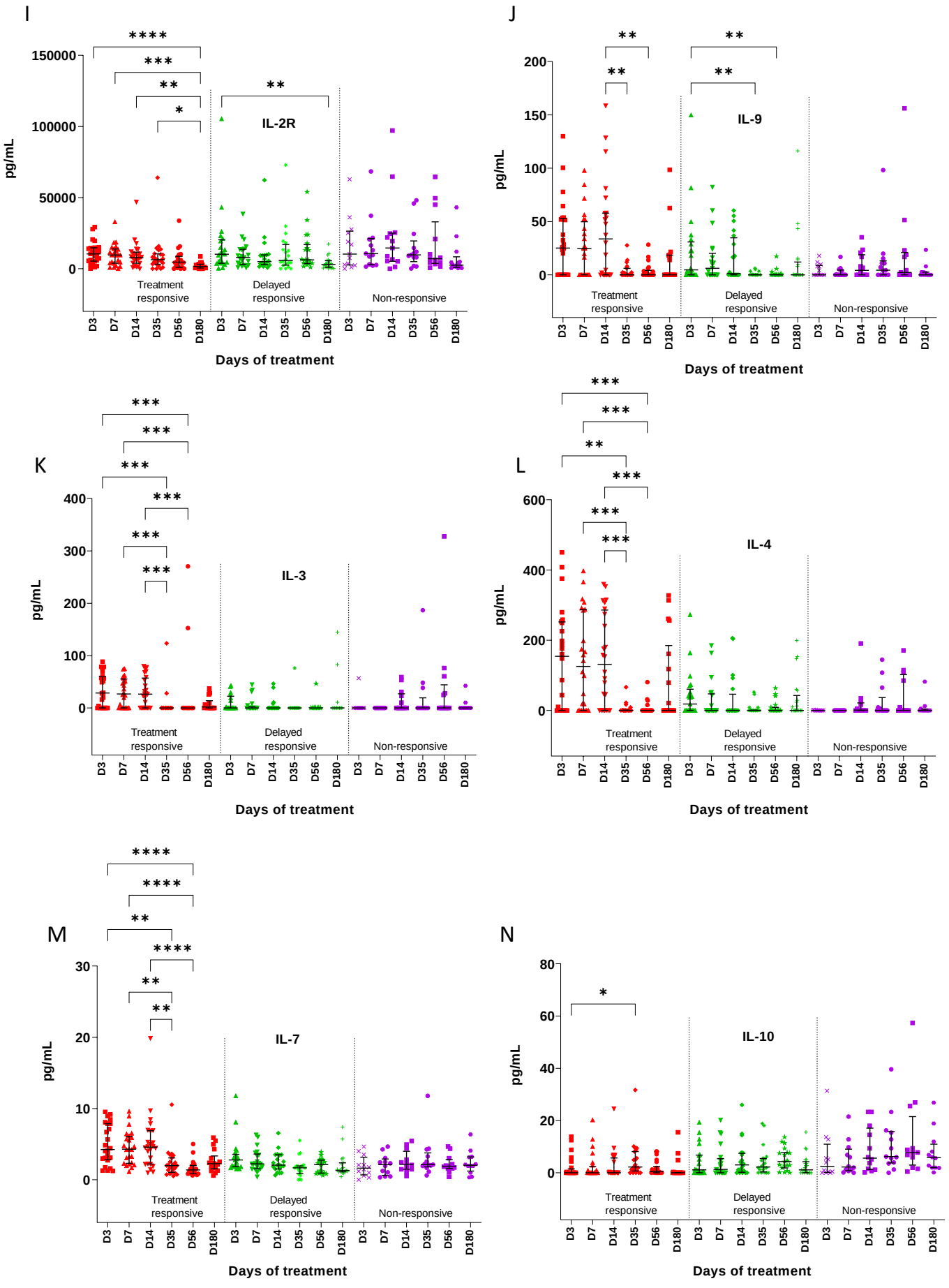
I
IL-2R
pg/mL
Treatment responsive
Delayed responsive
Non-responsive
Days of treatment
J
IL-9
K
IL-3
L
IL-4
M
IL-7
N
IL-10

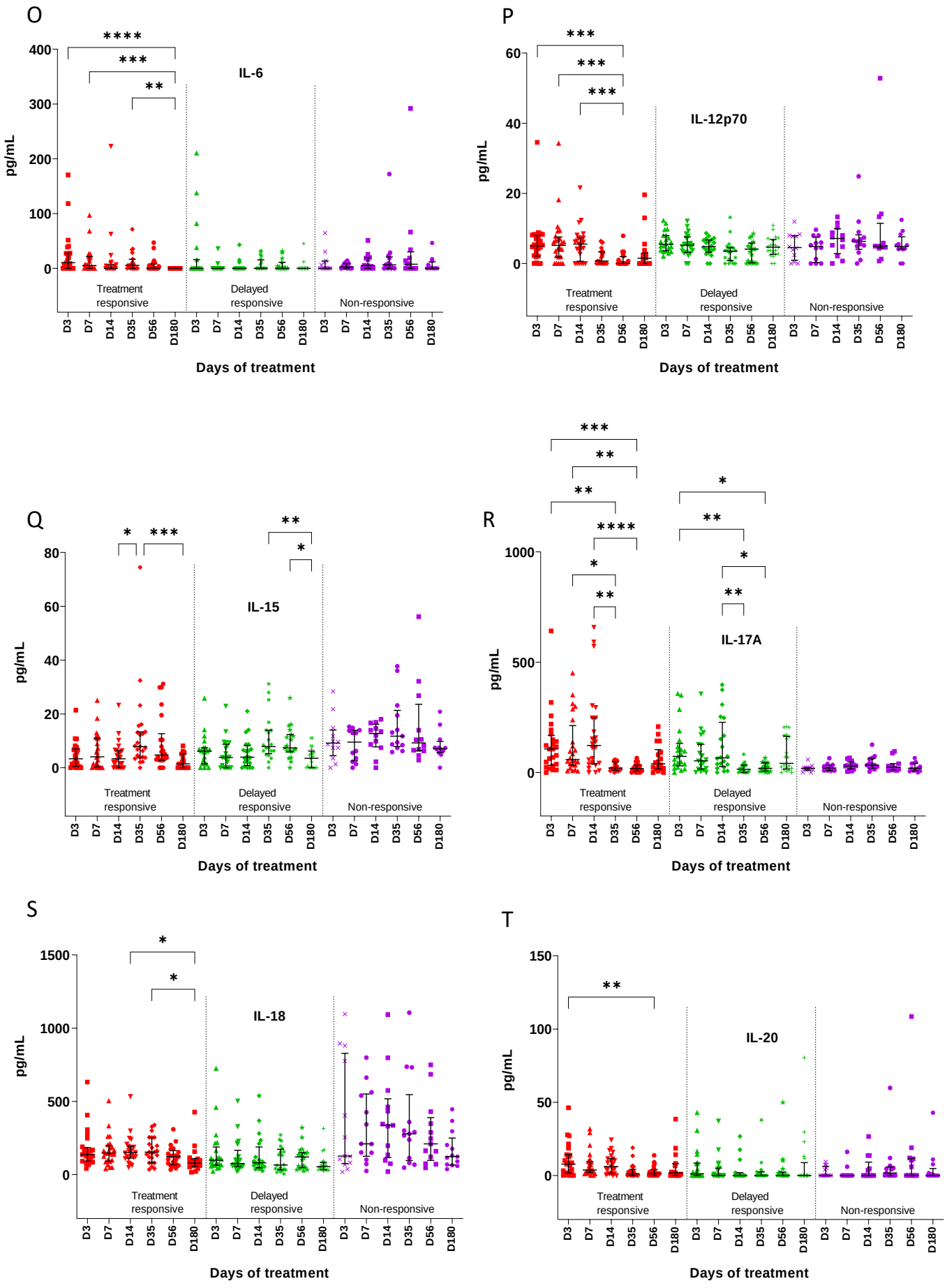
O
IL-6
pg/mL
Treatment responsive
Delayed responsive
Non-responsive
Days of treatment
P
IL-12p70
pg/mL
Treatment responsive
Delayed responsive
Non-responsive
Days of treatment
Q
IL-15
pg/mL
Treatment responsive
Delayed responsive
Non-responsive
Days of treatment
R
IL-17A
pg/mL
Treatment responsive
Delayed responsive
Non-responsive
Days of treatment
S
IL-18
pg/mL
Treatment responsive
Delayed responsive
Non-responsive
Days of treatment
T
IL-20
pg/mL
Treatment responsive
Delayed responsive
Non-responsive
Days of treatment

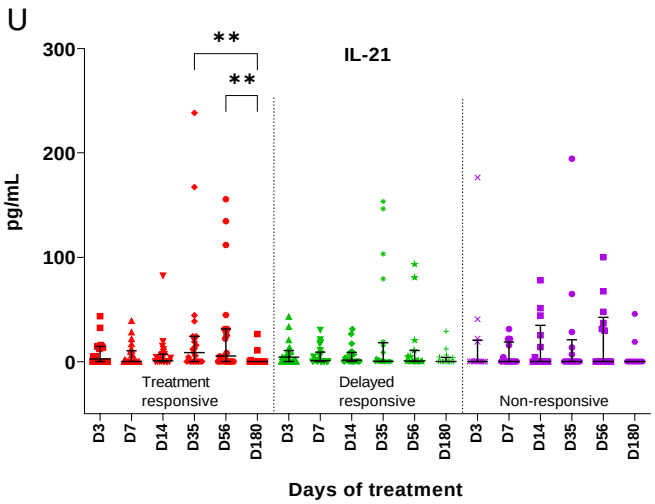
U
IL-21
pg/mL
300
200
100
0
**
**
Treatment responsive
Delayed responsive
Non-responsive
D3 D7 D14 D35 D56 D180
Days of treatment

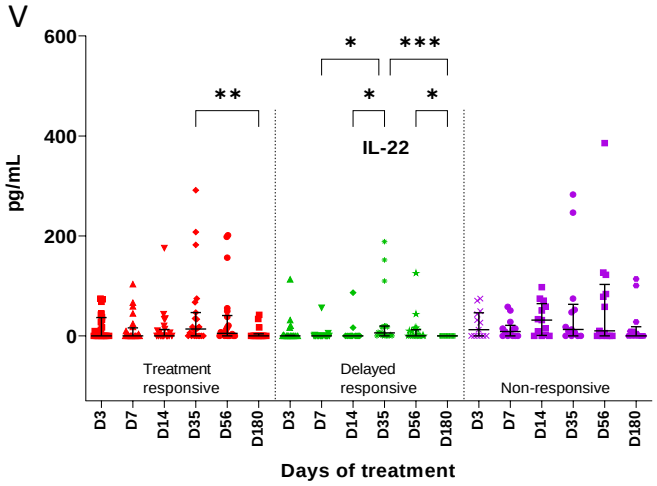
V
IL-22
pg/mL
600
400
200
0
**
*
***
*
*
Treatment responsive
Delayed responsive
Non-responsive
D3 D7 D14 D35 D56 D180
Days of treatment

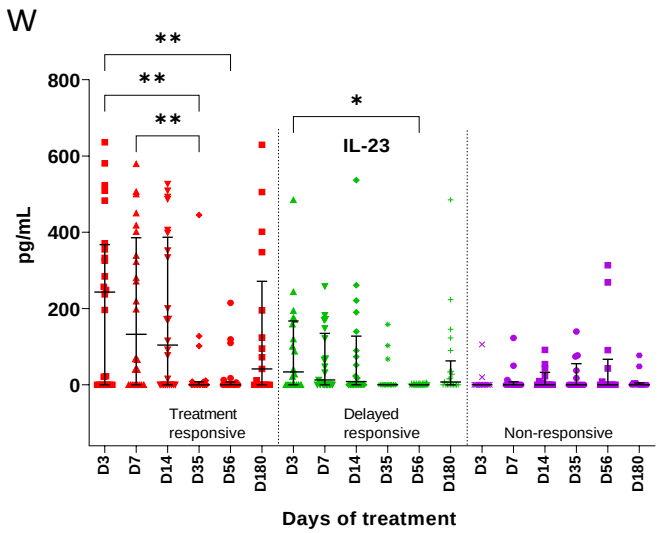
W
IL-23
pg/mL
800
600
400
200
0
**
**
**
*
Treatment responsive
Delayed responsive
Non-responsive
D3 D7 D14 D35 D56 D180
Days of treatment

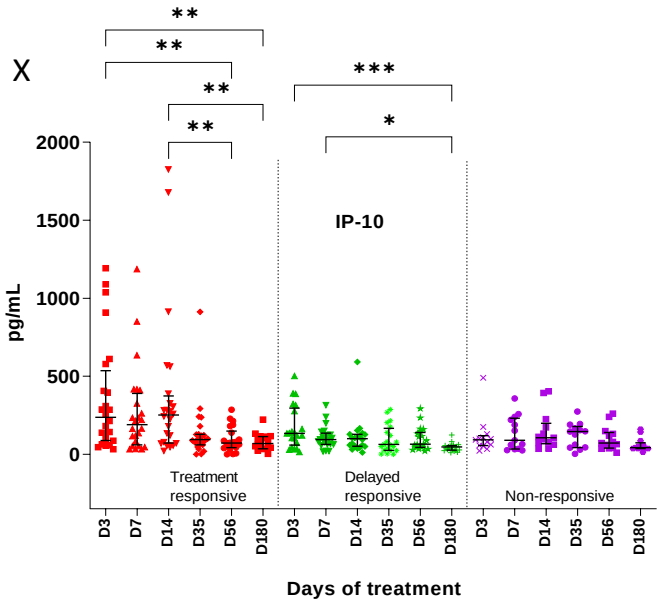
X
IP-10
pg/mL
2000
1500
1000
500
0
**
**
**
**
***
*
Treatment responsive
Delayed responsive
Non-responsive
D3 D7 D14 D35 D56 D180
Days of treatment

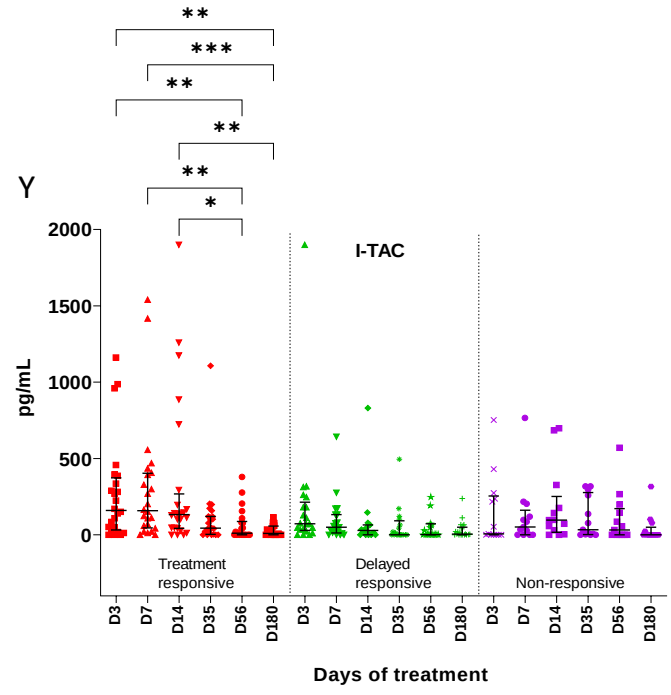
Y
I-TAC
pg/mL
2000
1500
1000
500
0
**
***
**
**
**
*
Treatment responsive
Delayed responsive
Non-responsive
D3 D7 D14 D35 D56 D180
Days of treatment

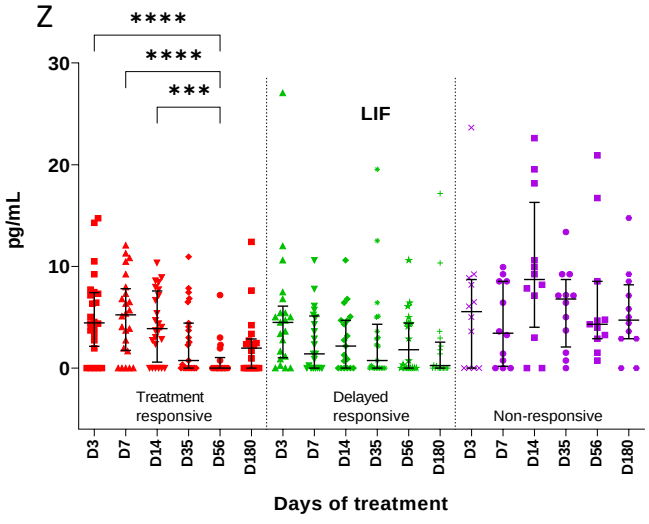
Z
LIF
pg/mL
30
20
10
0
****
****
***
Treatment responsive
Delayed responsive
Non-responsive
D3 D7 D14 D35 D56 D180
Days of treatment

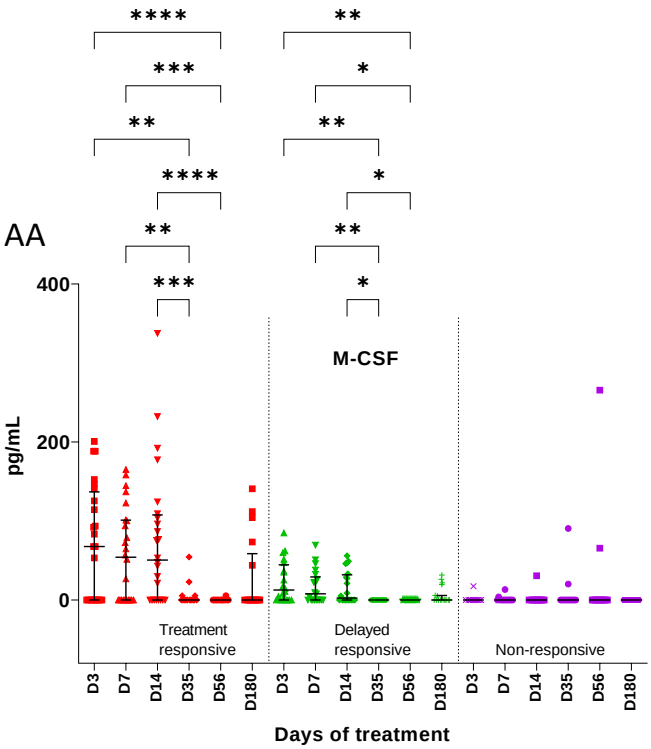
AA
M-CSF
pg/mL
400
200
0
Treatment responsive
Delayed responsive
Non-responsive
D3 D7 D14 D35 D56 D180
Days of treatment

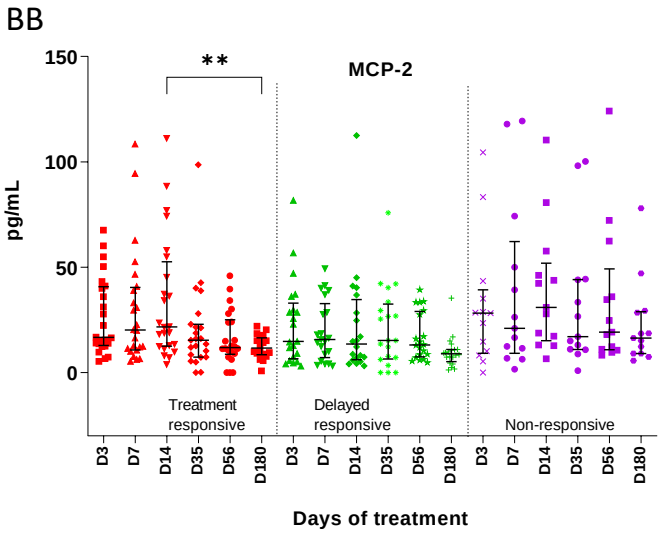
BB
MCP-2
pg/mL
150
100
50
0
Treatment responsive
Delayed responsive
Non-responsive
D3 D7 D14 D35 D56 D180
Days of treatment

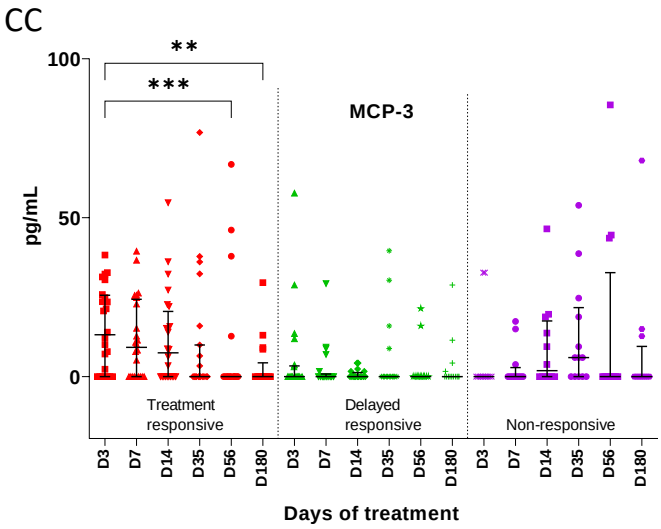
CC
MCP-3
pg/mL
100
50
0
Treatment responsive
Delayed responsive
Non-responsive
D3 D7 D14 D35 D56 D180
Days of treatment

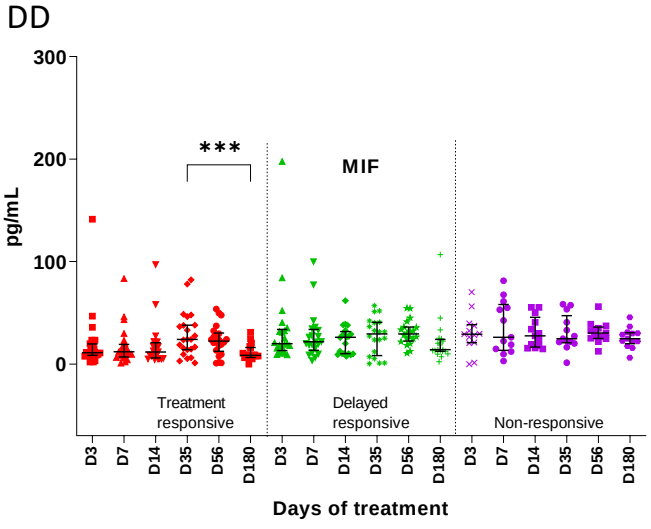
DD
MIF
pg/mL
300
200
100
0
Treatment responsive
Delayed responsive
Non-responsive
D3 D7 D14 D35 D56 D180
Days of treatment

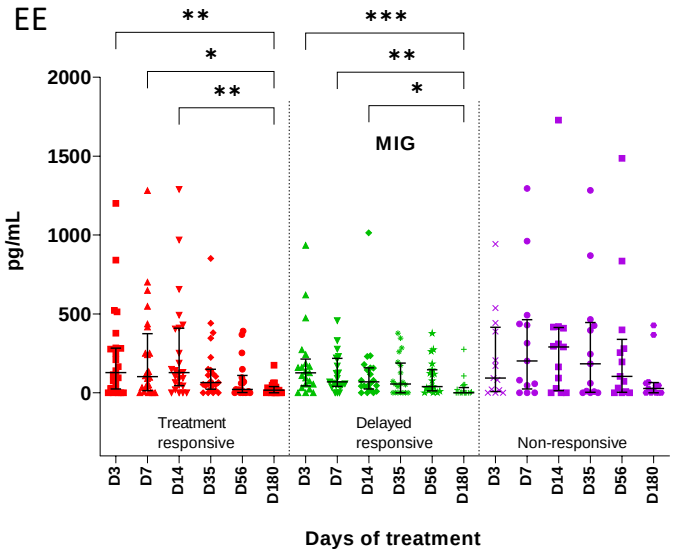
EE
MIG
pg/mL
2000
1500
1000
500
0
Treatment responsive
Delayed responsive
Non-responsive
D3 D7 D14 D35 D56 D180
Days of treatment

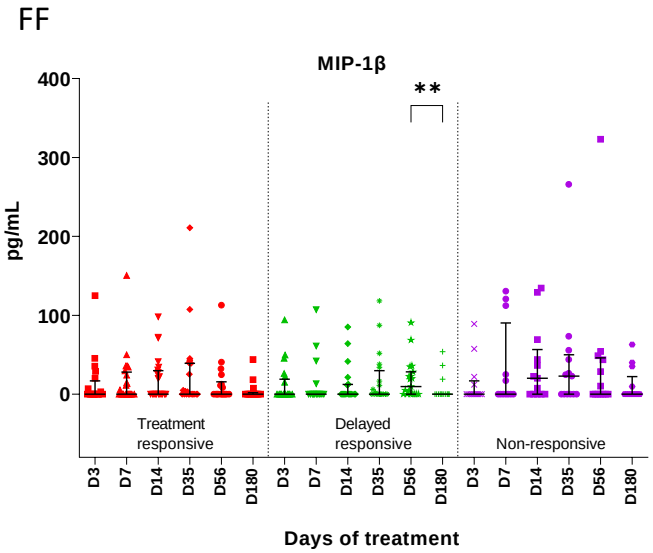
FF
MIP-1β
pg/mL
400
300
200
100
0
Treatment responsive
Delayed responsive
Non-responsive
D3 D7 D14 D35 D56 D180
Days of treatment

GG

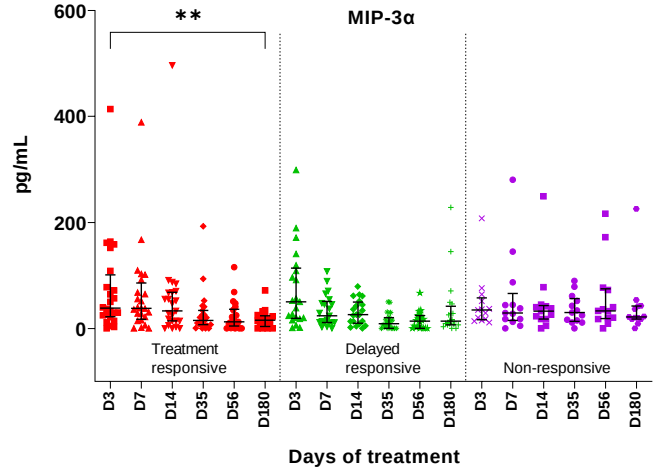

HH

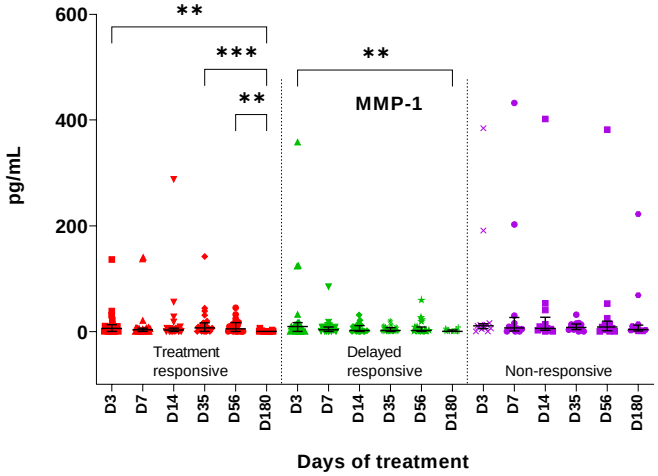

II

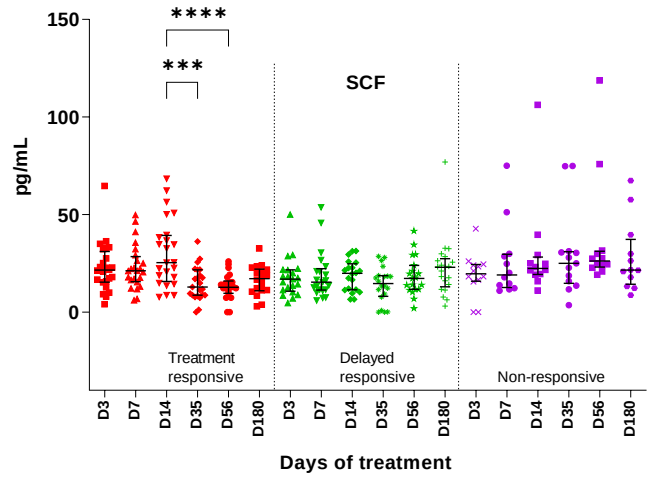

JJ

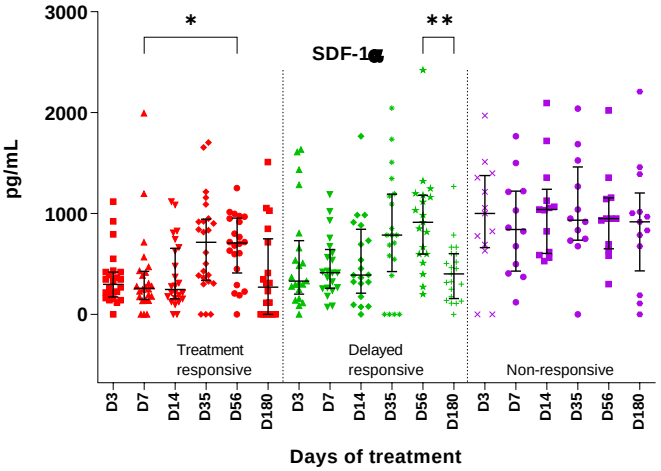

KK

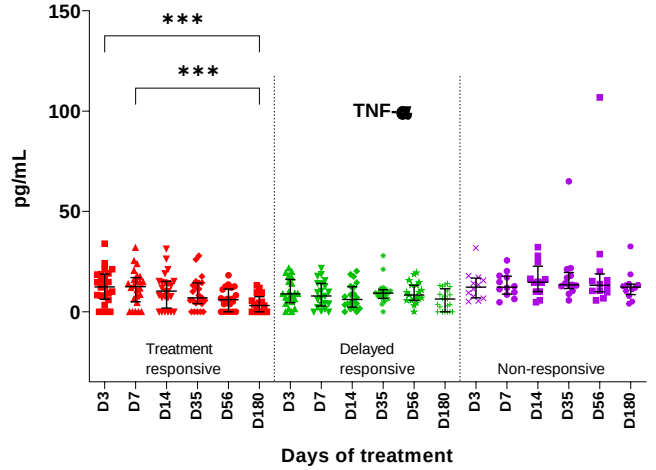

LL

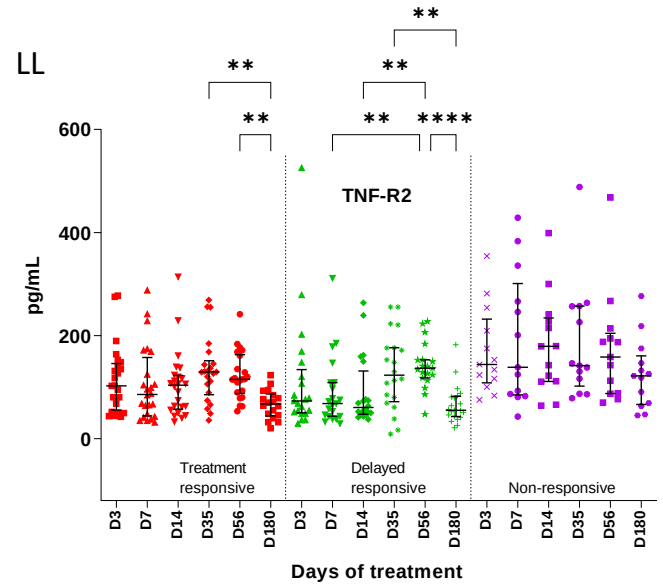

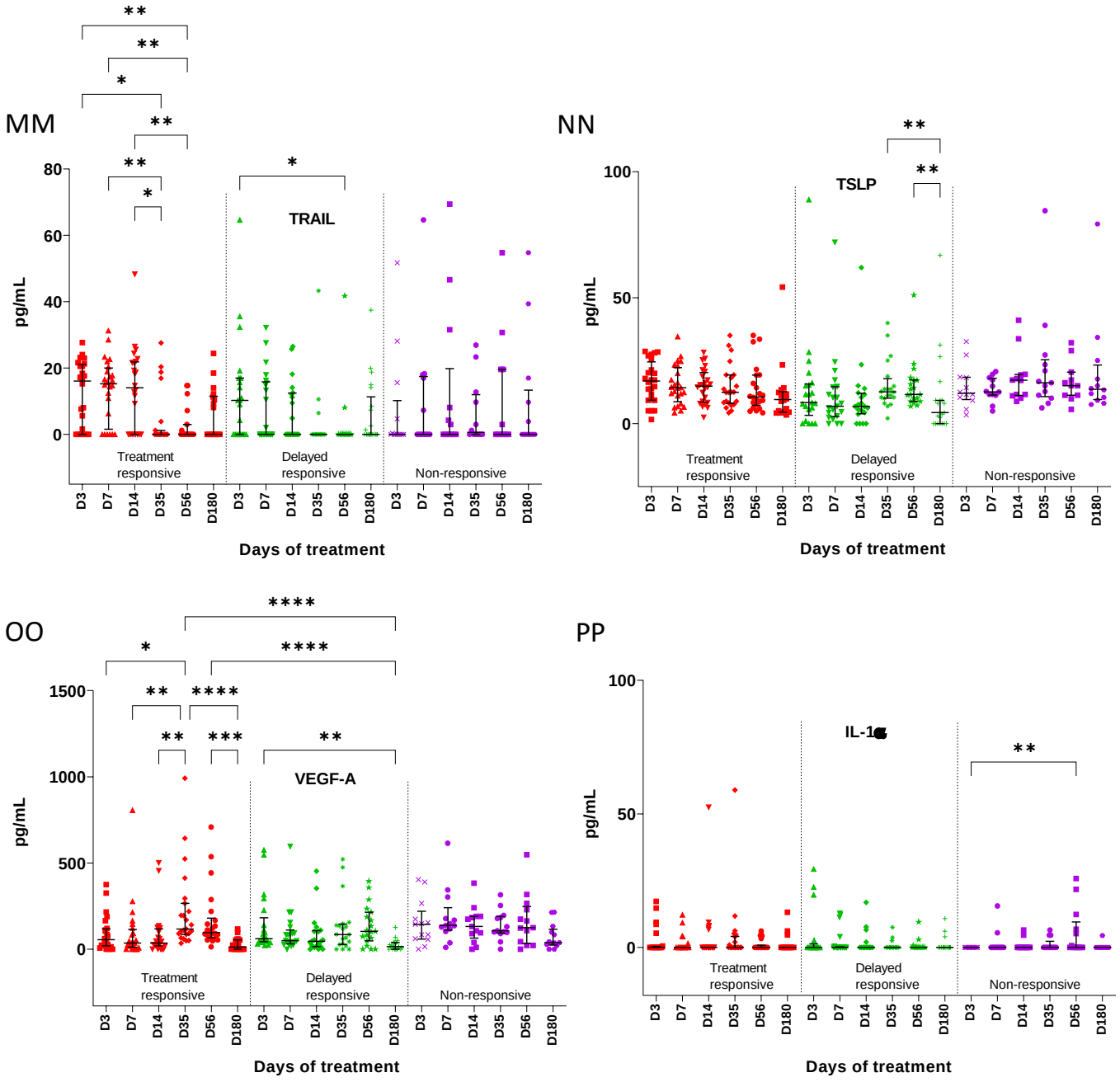

Figure A3. Longitudinal assessment of cytokines to monitor treatment response of treatment-responsive, delayed-responsive and non-responsive individuals. Red, green and purple dots represents samples in the treatment-responsive, delayed-responsive and non-responsive group respectively. The concentrations are expressed in pg/mL and were analysed by the non-parametric Kruskal-wallis test, with significance *P <0.01; **P < 0.001; ***P < 0.001; ****P < 0.001 (Post hoc corrected by Dunn's multiple comparisons).

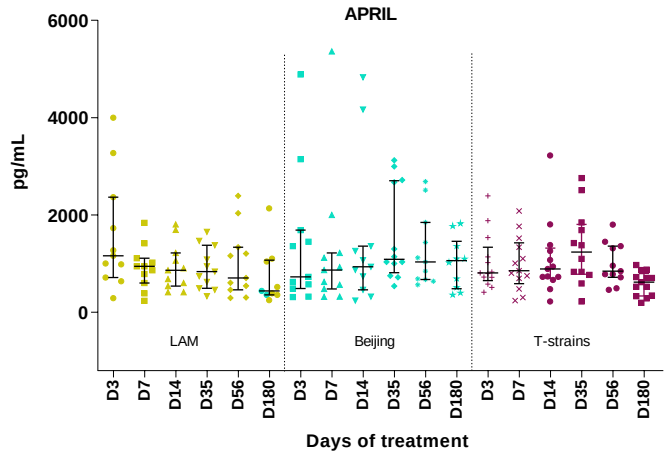
APRIL
pg/mL
6000
4000
2000
0
LAM
Beijing
T-strains
D3 D7 D14 D35 D56 D180 D3 D7 D14 D35 D56 D180 D3 D7 D14 D35 D56 D180
Days of treatment

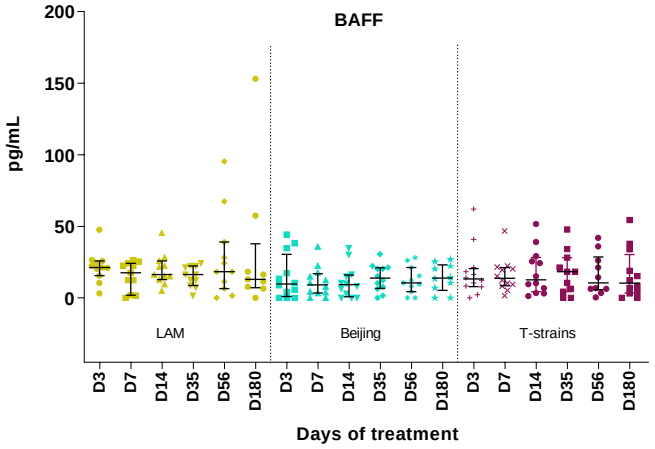
BAFF
pg/mL
200
150
100
50
0
LAM
Beijing
T-strains
D3 D7 D14 D35 D56 D180 D3 D7 D14 D35 D56 D180 D3 D7 D14 D35 D56 D180
Days of treatment

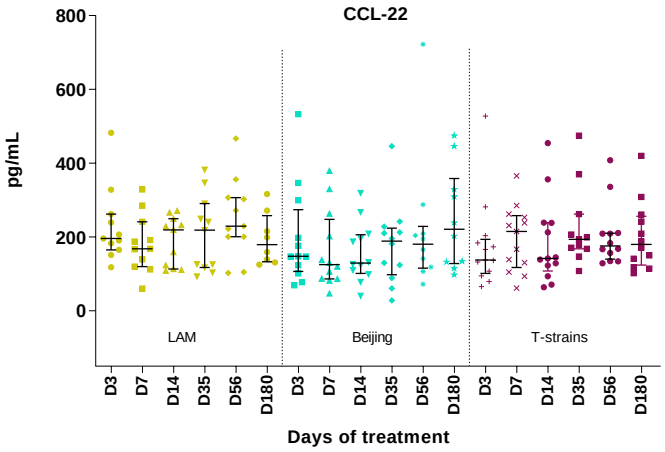
CCL-22
pg/mL
800
600
400
200
0
LAM
Beijing
T-strains
D3 D7 D14 D35 D56 D180 D3 D7 D14 D35 D56 D180 D3 D7 D14 D35 D56 D180
Days of treatment

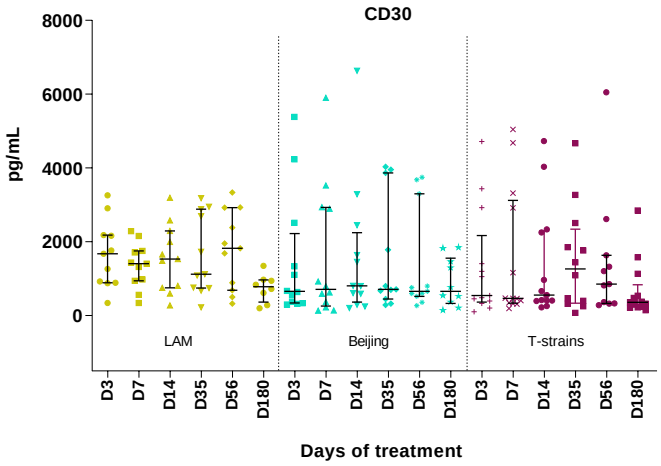
CD30
pg/mL
8000
6000
4000
2000
0
LAM
Beijing
T-strains
D3 D7 D14 D35 D56 D180 D3 D7 D14 D35 D56 D180 D3 D7 D14 D35 D56 D180
Days of treatment

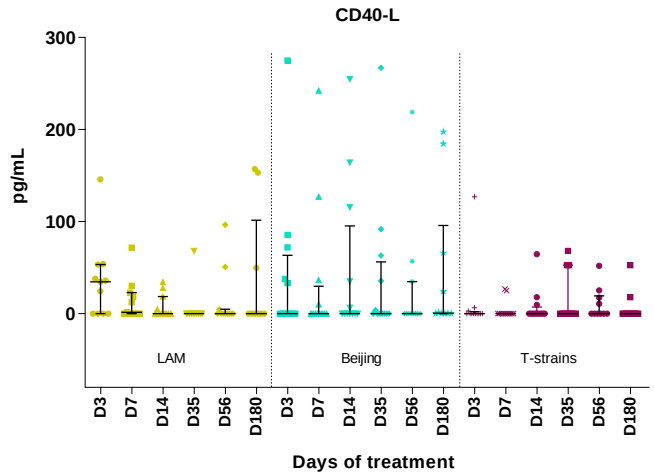
CD40-L
pg/mL
300
200
100
0
LAM
Beijing
T-strains
D3 D7 D14 D35 D56 D180 D3 D7 D14 D35 D56 D180 D3 D7 D14 D35 D56 D180
Days of treatment

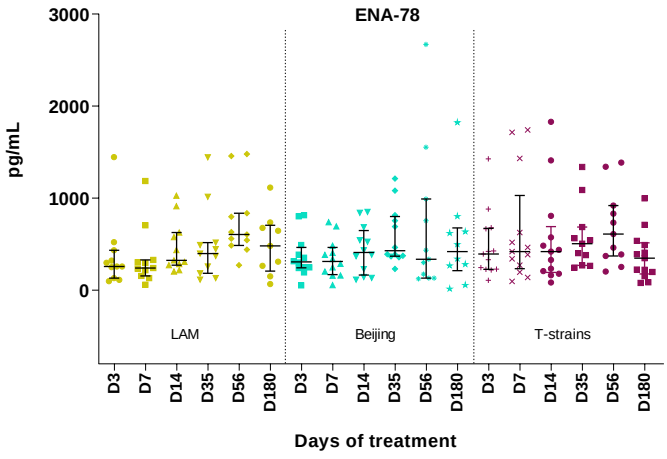
ENA-78
pg/mL
3000
2000
1000
0
LAM
Beijing
T-strains
D3 D7 D14 D35 D56 D180 D3 D7 D14 D35 D56 D180 D3 D7 D14 D35 D56 D180
Days of treatment

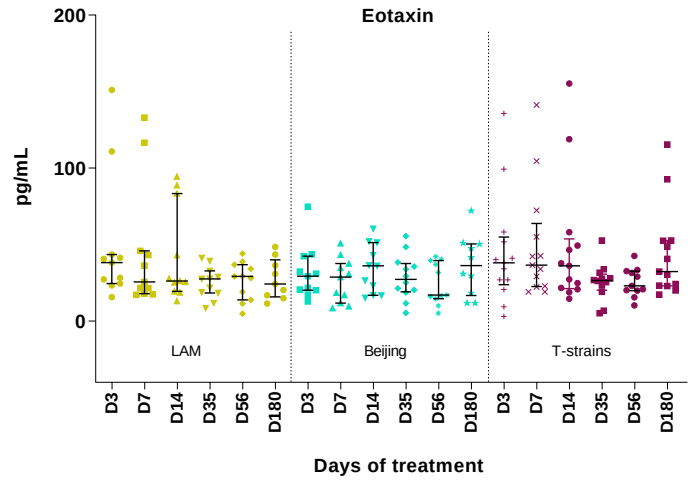
Eotaxin
pg/mL
200
100
0
LAM
Beijing
T-strains
D3 D7 D14 D35 D56 D180
Days of treatment

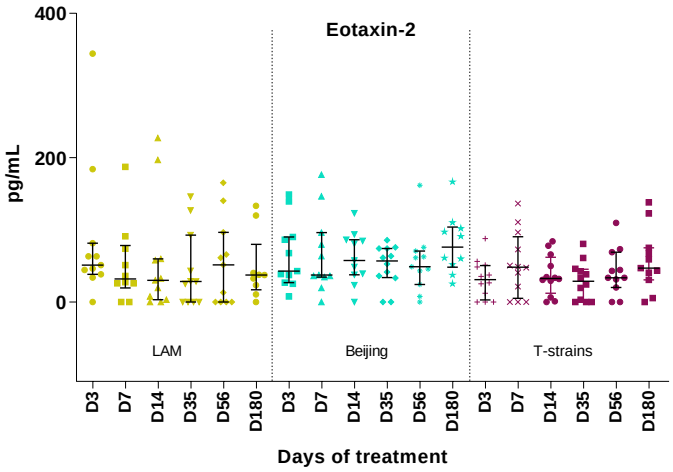
Eotaxin-2
pg/mL
400
200
0
LAM
Beijing
T-strains
D3 D7 D14 D35 D56 D180
Days of treatment

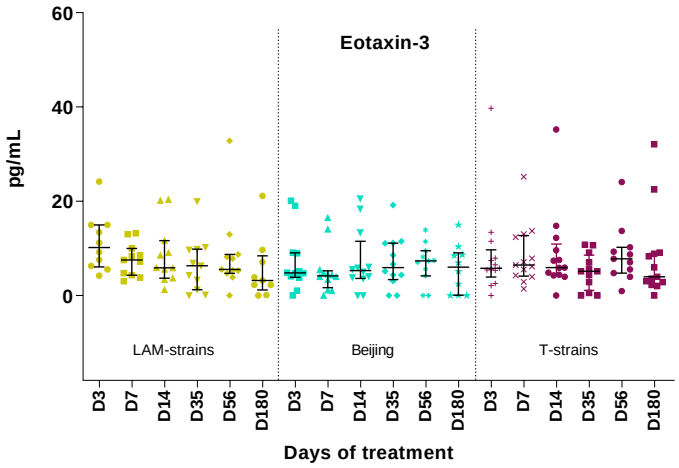
Eotaxin-3
pg/mL
60
40
20
0
LAM-strains
Beijing
T-strains
D3 D7 D14 D35 D56 D180
Days of treatment

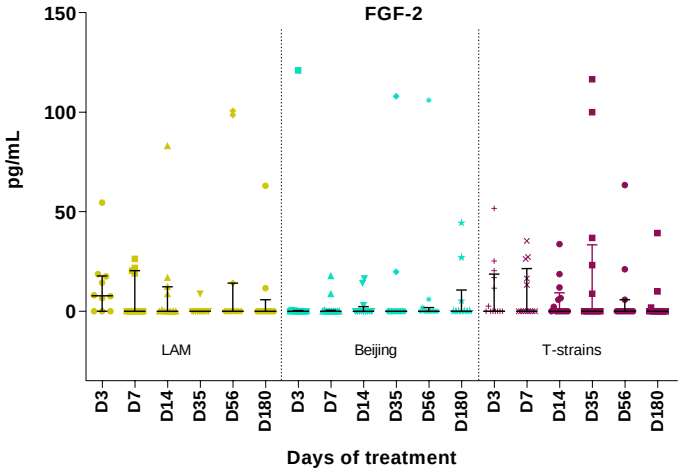
FGF-2
pg/mL
150
100
50
0
LAM
Beijing
T-strains
D3 D7 D14 D35 D56 D180
Days of treatment

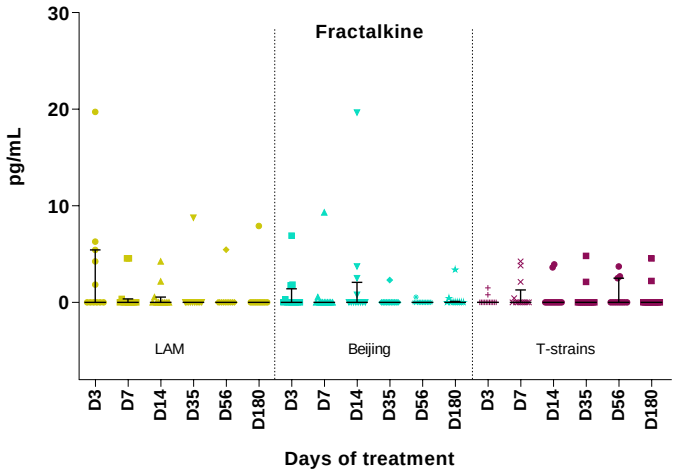
Fractalkine
pg/mL
30
20
10
0
LAM
Beijing
T-strains
D3 D7 D14 D35 D56 D180
Days of treatment

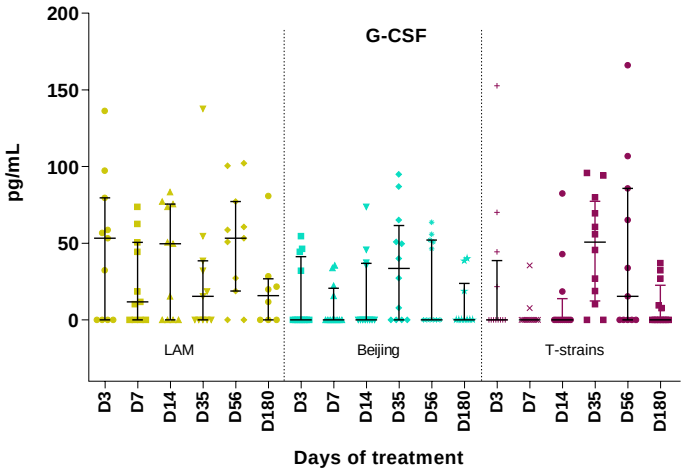
G-CSF
pg/mL
200
150
100
50
0
LAM
Beijing
T-strains
D3 D7 D14 D35 D56 D180
Days of treatment

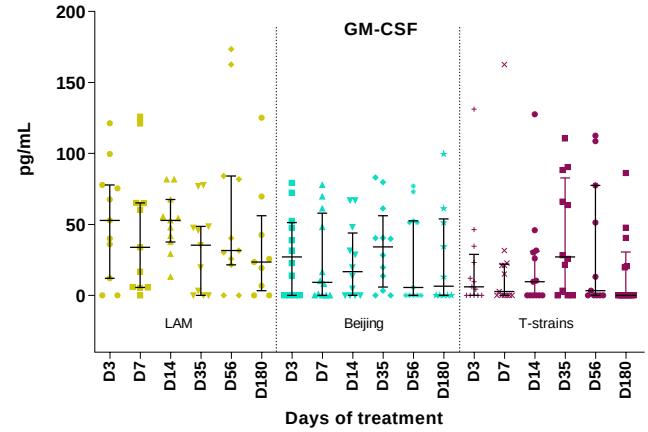
GM-CSF
pg/mL
200
150
100
50
0
LAM
Beijing
T-strains
D3 D7 D14 D35 D56 D180 D3 D7 D14 D35 D56 D180 D3 D7 D14 D35 D56 D180
Days of treatment

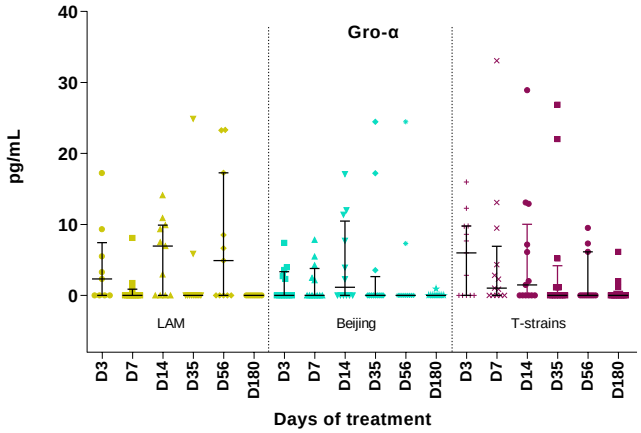
Gro-α
pg/mL
40
30
20
10
0
LAM
Beijing
T-strains
D3 D7 D14 D35 D56 D180 D3 D7 D14 D35 D56 D180 D3 D7 D14 D35 D56 D180
Days of treatment

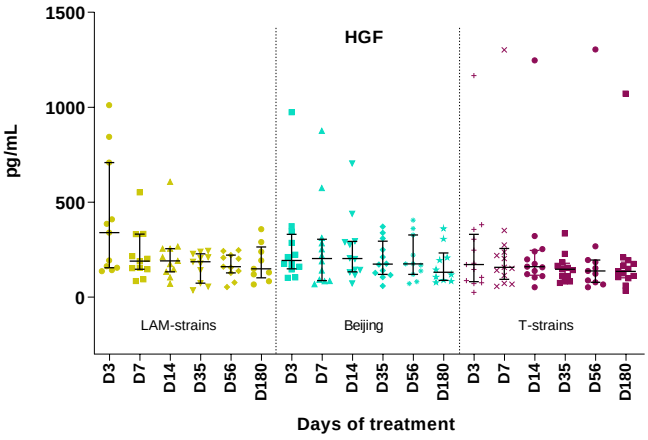
HGF
pg/mL
1500
1000
500
0
LAM-strains
Beijing
T-strains
D3 D7 D14 D35 D56 D180 D3 D7 D14 D35 D56 D180 D3 D7 D14 D35 D56 D180
Days of treatment

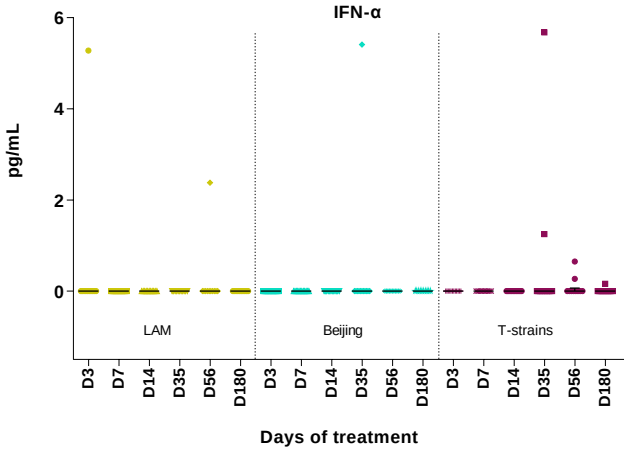
IFN-α
pg/mL
6
4
2
0
LAM
Beijing
T-strains
D3 D7 D14 D35 D56 D180 D3 D7 D14 D35 D56 D180 D3 D7 D14 D35 D56 D180
Days of treatment

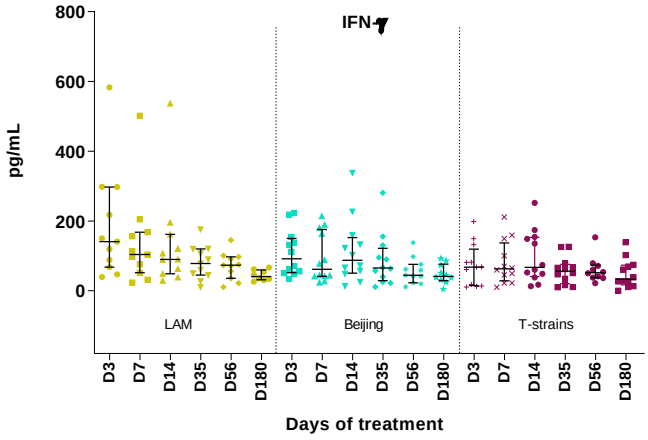
IFN-γ
pg/mL
800
600
400
200
0
LAM
Beijing
T-strains
D3 D7 D14 D35 D56 D180 D3 D7 D14 D35 D56 D180 D3 D7 D14 D35 D56 D180
Days of treatment

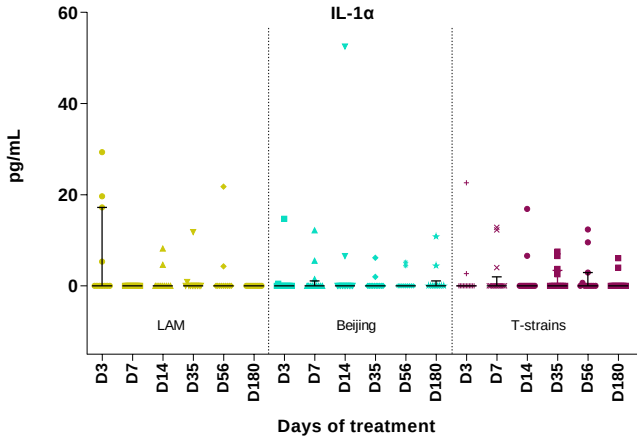
IL-1α
pg/mL
60
40
20
0
LAM
Beijing
T-strains
D3 D7 D14 D35 D56 D180 D3 D7 D14 D35 D56 D180 D3 D7 D14 D35 D56 D180
Days of treatment

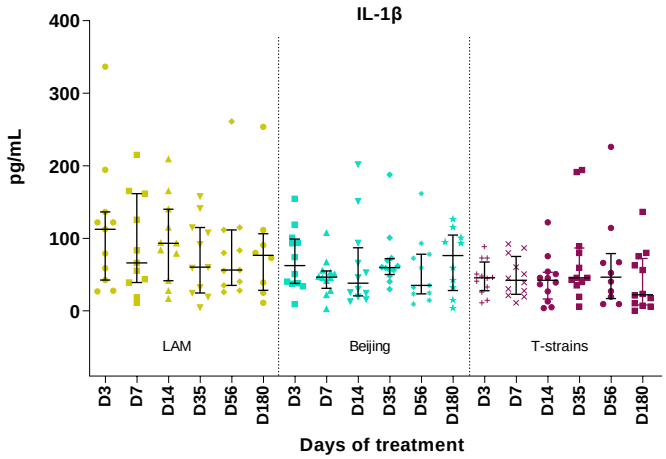
IL-1β
pg/mL
400
300
200
100
0
LAM
Beijing
T-strains
D3 D7 D14 D35 D56 D180 D3 D7 D14 D35 D56 D180 D3 D7 D14 D35 D56 D180
Days of treatment

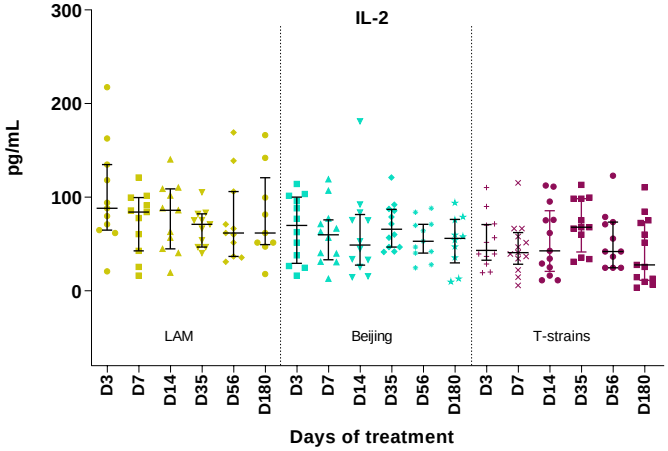
IL-2
pg/mL
300
200
100
0
LAM
Beijing
T-strains
D3 D7 D14 D35 D56 D180 D3 D7 D14 D35 D56 D180 D3 D7 D14 D35 D56 D180
Days of treatment

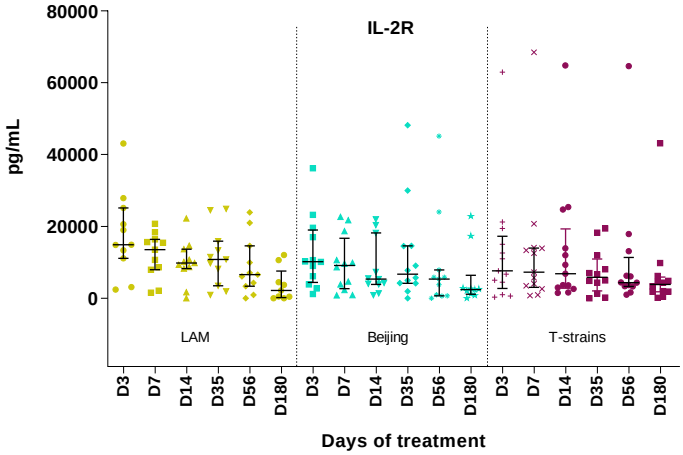
IL-2R
pg/mL
80000
60000
40000
20000
0
LAM
Beijing
T-strains
D3 D7 D14 D35 D56 D180 D3 D7 D14 D35 D56 D180 D3 D7 D14 D35 D56 D180
Days of treatment

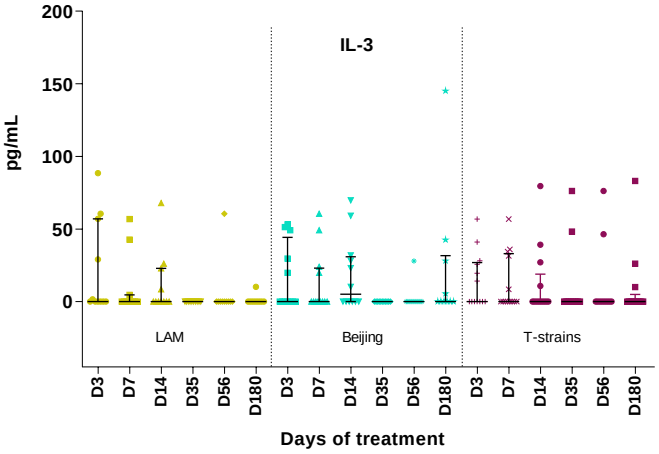
IL-3
pg/mL
200
150
100
50
0
LAM
Beijing
T-strains
D3 D7 D14 D35 D56 D180 D3 D7 D14 D35 D56 D180 D3 D7 D14 D35 D56 D180
Days of treatment

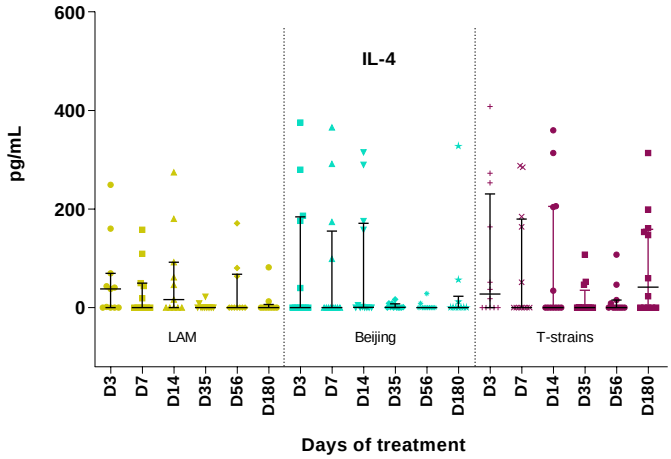
IL-4
pg/mL
600
400
200
0
LAM
Beijing
T-strains
D3 D7 D14 D35 D56 D180 D3 D7 D14 D35 D56 D180 D3 D7 D14 D35 D56 D180
Days of treatment

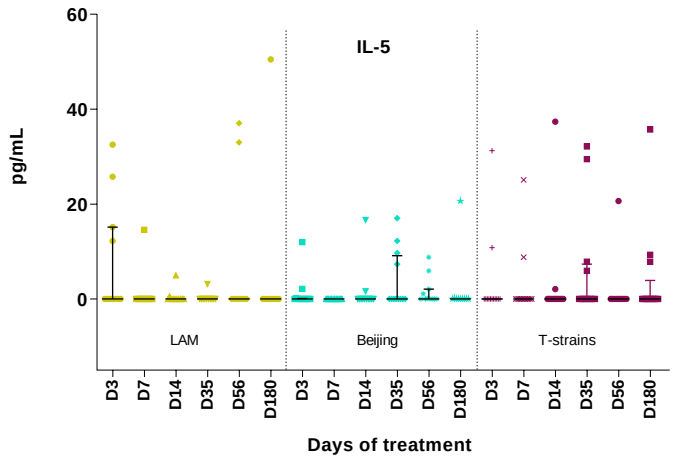
IL-5
pg/mL
60
40
20
0
LAM
Beijing
T-strains
D3 D7 D14 D35 D56 D180 D3 D7 D14 D35 D56 D180 D3 D7 D14 D35 D56 D180
Days of treatment

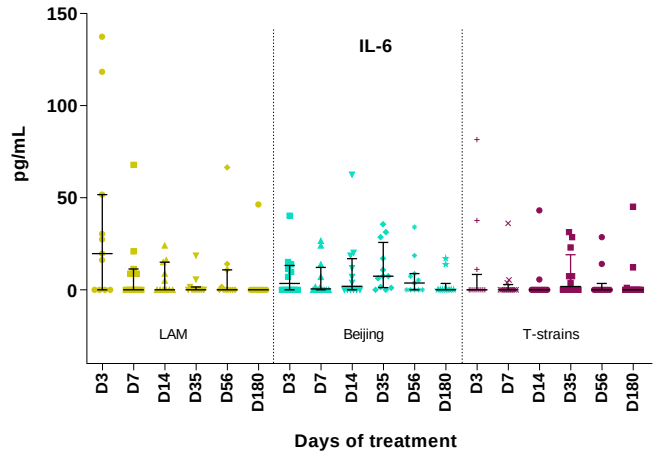
IL-6
pg/mL
150
100
50
0
LAM
Beijing
T-strains
D3
D7
D14
D35
D56
D180
Days of treatment

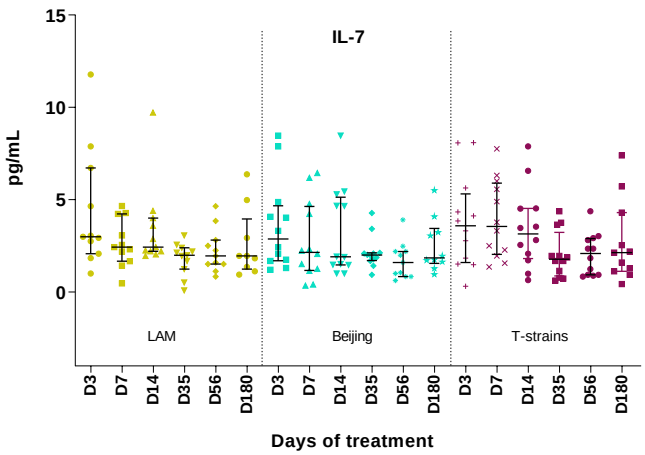
IL-7
pg/mL
15
10
5
0
LAM
Beijing
T-strains
D3
D7
D14
D35
D56
D180
Days of treatment

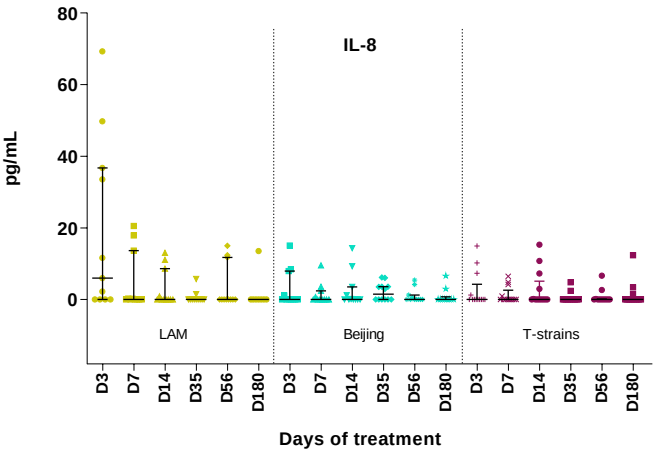
IL-8
pg/mL
80
60
40
20
0
LAM
Beijing
T-strains
D3
D7
D14
D35
D56
D180
Days of treatment

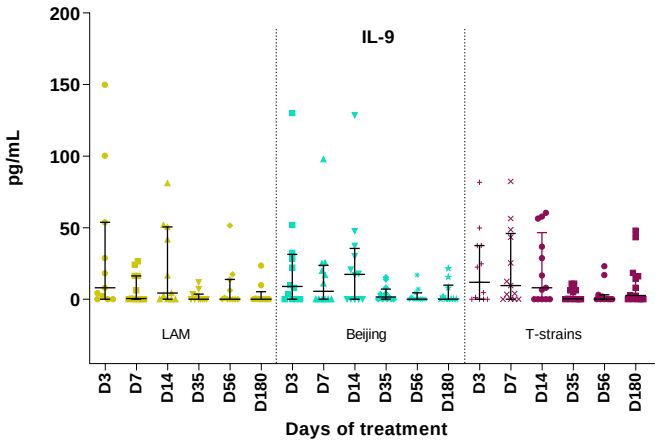
IL-9
pg/mL
200
150
100
50
0
LAM
Beijing
T-strains
D3
D7
D14
D35
D56
D180
Days of treatment

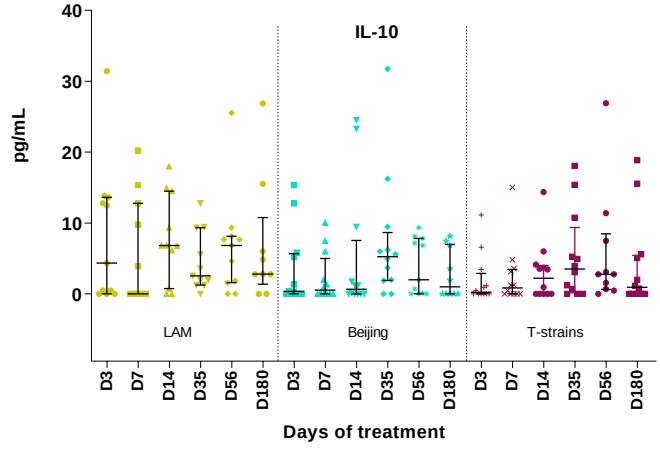
IL-10
pg/mL
40
30
20
10
0
LAM
Beijing
T-strains
D3
D7
D14
D35
D56
D180
Days of treatment

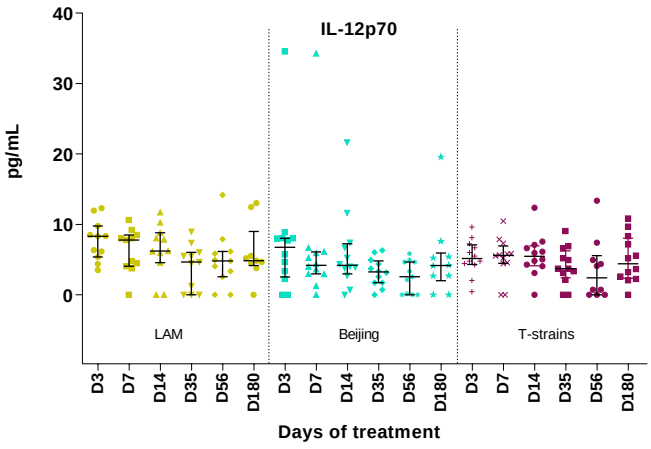
IL-12p70
pg/mL
40
30
20
10
0
LAM
Beijing
T-strains
D3
D7
D14
D35
D56
D180
Days of treatment

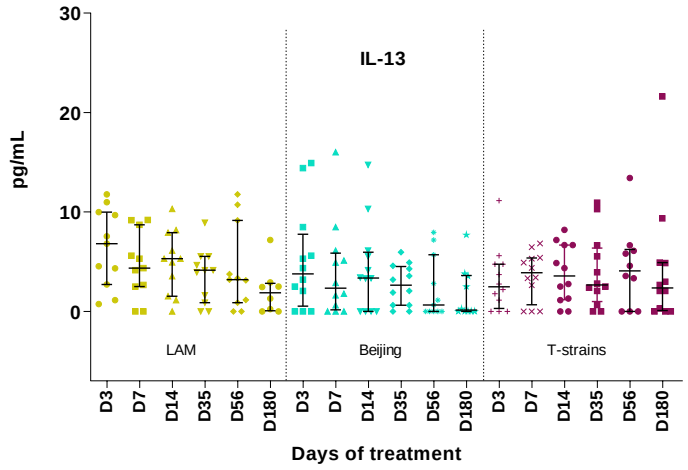
IL-13
pg/mL
30
20
10
0
LAM
Beijing
T-strains
D3 D7 D14 D35 D56 D180 D3 D7 D14 D35 D56 D180 D3 D7 D14 D35 D56 D180
Days of treatment

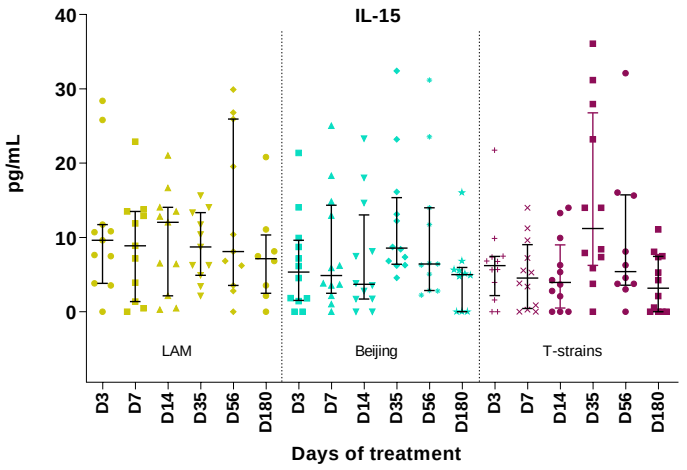
IL-15
pg/mL
40
30
20
10
0
LAM
Beijing
T-strains
D3 D7 D14 D35 D56 D180 D3 D7 D14 D35 D56 D180 D3 D7 D14 D35 D56 D180
Days of treatment

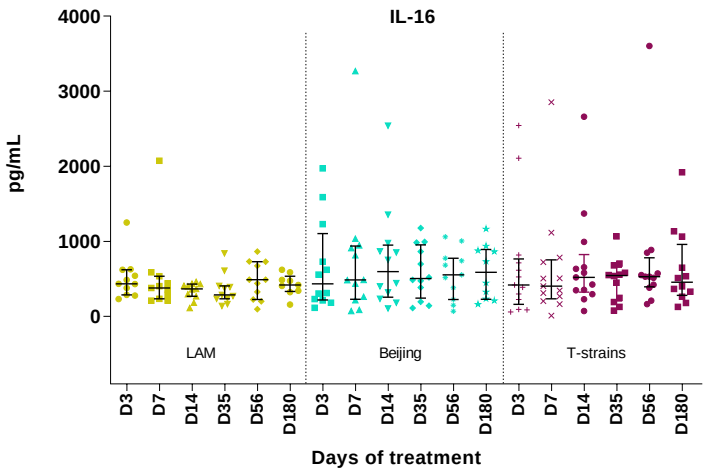
IL-16
pg/mL
4000
3000
2000
1000
0
LAM
Beijing
T-strains
D3 D7 D14 D35 D56 D180 D3 D7 D14 D35 D56 D180 D3 D7 D14 D35 D56 D180
Days of treatment

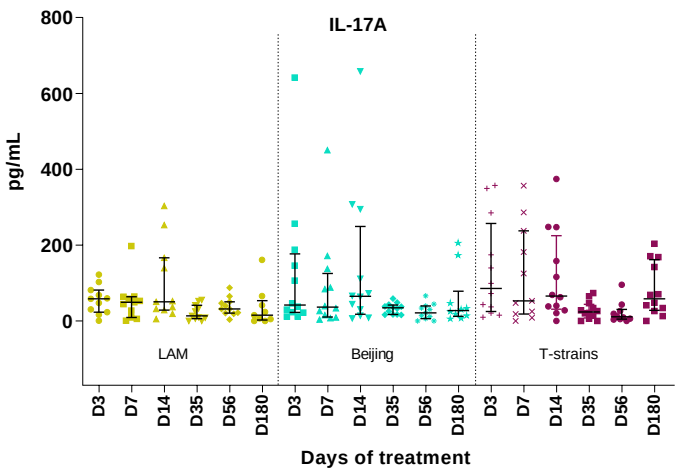
IL-17A
pg/mL
800
600
400
200
0
LAM
Beijing
T-strains
D3 D7 D14 D35 D56 D180 D3 D7 D14 D35 D56 D180 D3 D7 D14 D35 D56 D180
Days of treatment

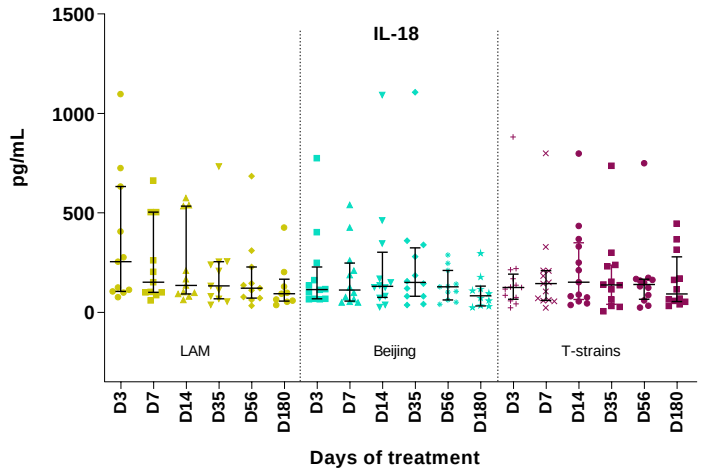
IL-18
pg/mL
1500
1000
500
0
LAM
Beijing
T-strains
D3 D7 D14 D35 D56 D180 D3 D7 D14 D35 D56 D180 D3 D7 D14 D35 D56 D180
Days of treatment

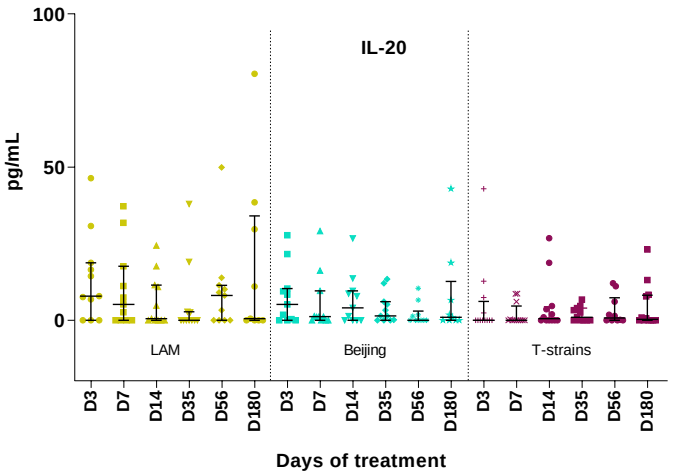
IL-20
pg/mL
100
50
0
LAM
Beijing
T-strains
D3 D7 D14 D35 D56 D180 D3 D7 D14 D35 D56 D180 D3 D7 D14 D35 D56 D180
Days of treatment

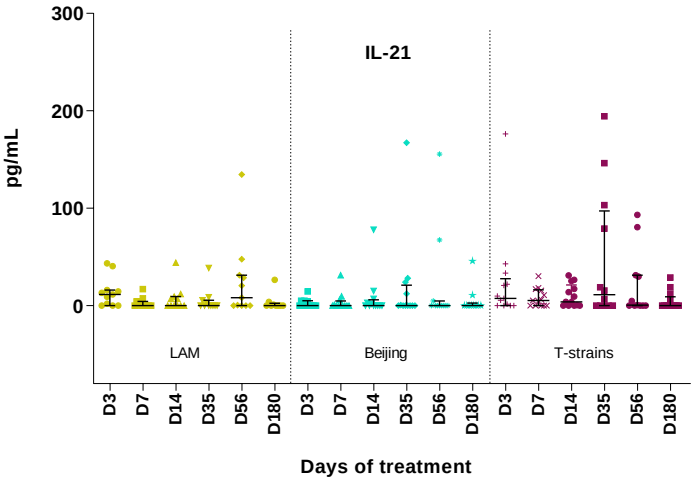
IL-21
pg/mL
300
200
100
0
LAM
Beijing
T-strains
D3 D7 D14 D35 D56 D180 D3 D7 D14 D35 D56 D180 D3 D7 D14 D35 D56 D180
Days of treatment

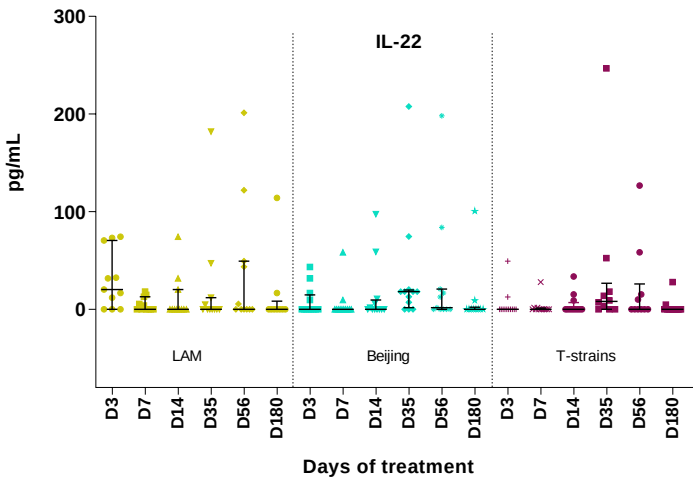
IL-22
pg/mL
300
200
100
0
LAM
Beijing
T-strains
D3 D7 D14 D35 D56 D180 D3 D7 D14 D35 D56 D180 D3 D7 D14 D35 D56 D180
Days of treatment

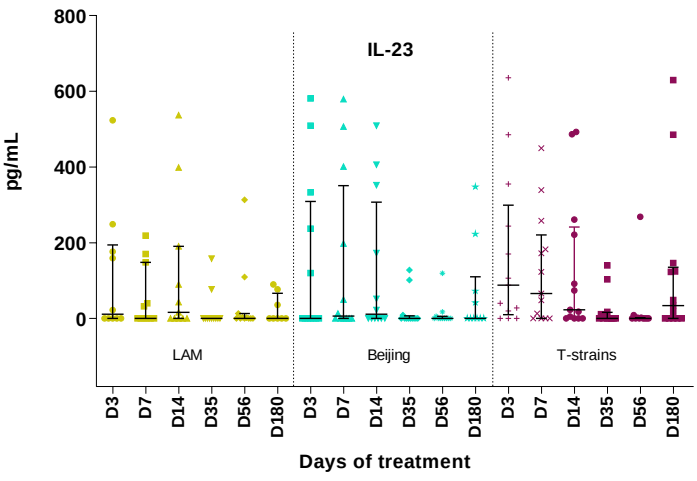
IL-23
pg/mL
800
600
400
200
0
LAM
Beijing
T-strains
D3 D7 D14 D35 D56 D180 D3 D7 D14 D35 D56 D180 D3 D7 D14 D35 D56 D180
Days of treatment

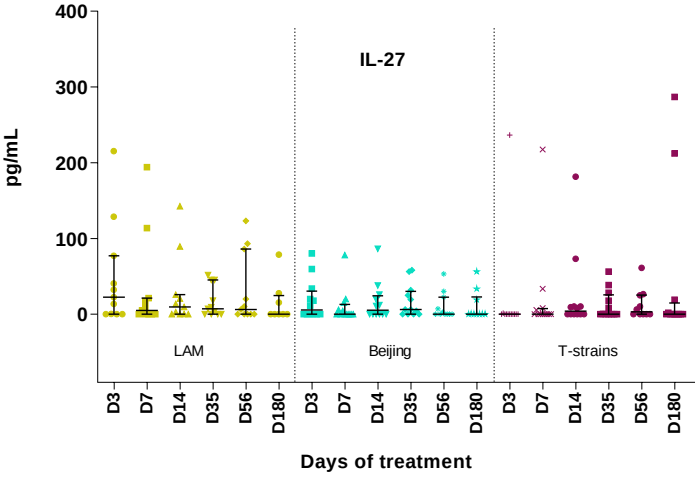
IL-27
pg/mL
400
300
200
100
0
LAM
Beijing
T-strains
D3 D7 D14 D35 D56 D180 D3 D7 D14 D35 D56 D180 D3 D7 D14 D35 D56 D180
Days of treatment

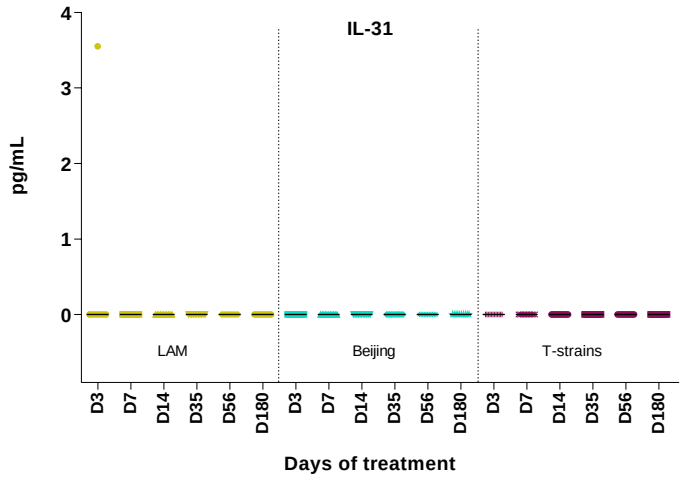
IL-31
pg/mL
4
3
2
1
0
LAM
Beijing
T-strains
D3 D7 D14 D35 D56 D180 D3 D7 D14 D35 D56 D180 D3 D7 D14 D35 D56 D180
Days of treatment

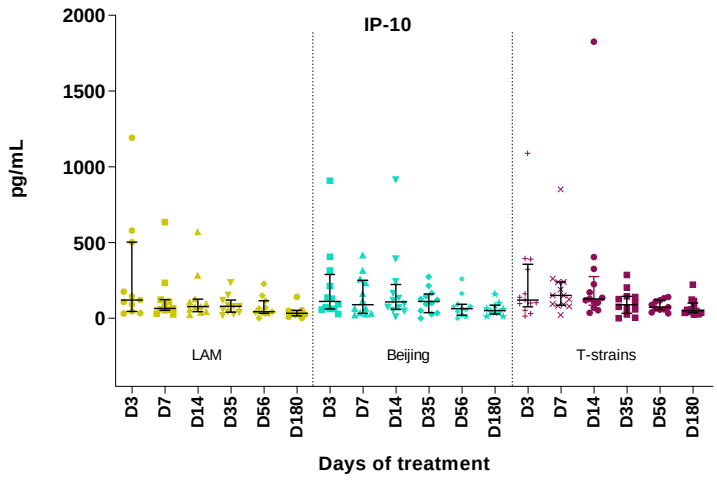
IP-10
pg/mL
2000
1500
1000
500
0
LAM
Beijing
T-strains
D3 D7 D14 D35 D56 D180 D3 D7 D14 D35 D56 D180 D3 D7 D14 D35 D56 D180
Days of treatment

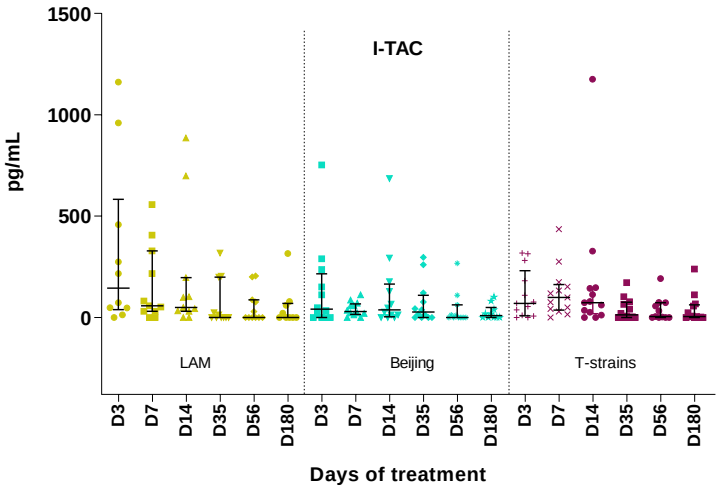
I-TAC
pg/mL
1500
1000
500
0
LAM
Beijing
T-strains
D3 D7 D14 D35 D56 D180
Days of treatment

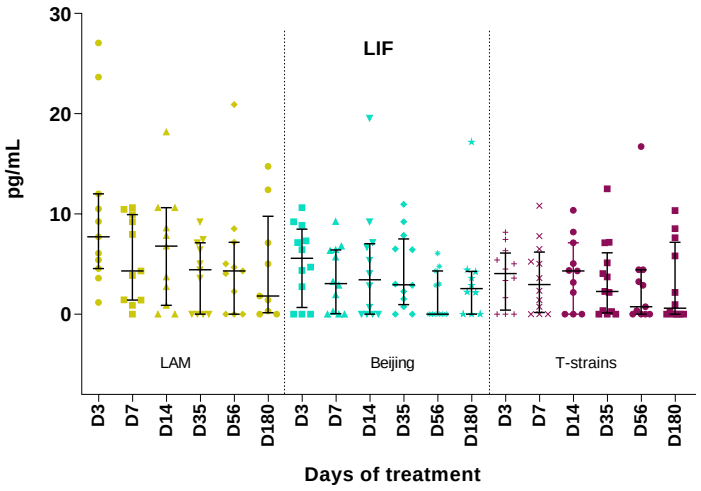
LIF
pg/mL
30
20
10
0
LAM
Beijing
T-strains
D3 D7 D14 D35 D56 D180
Days of treatment

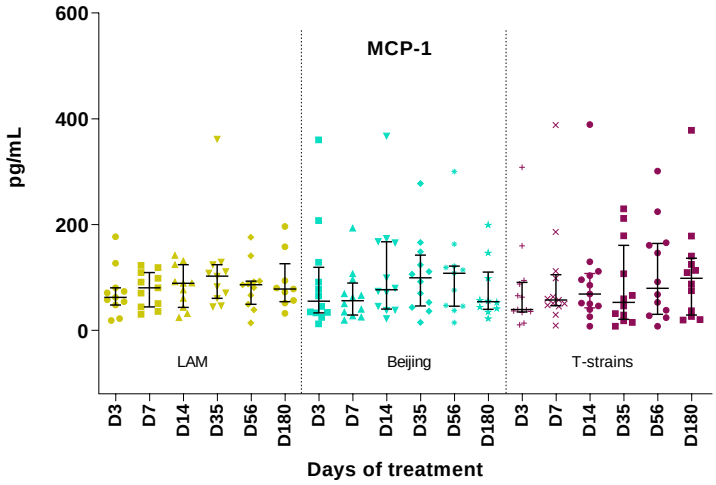
MCP-1
pg/mL
600
400
200
0
LAM
Beijing
T-strains
D3 D7 D14 D35 D56 D180
Days of treatment

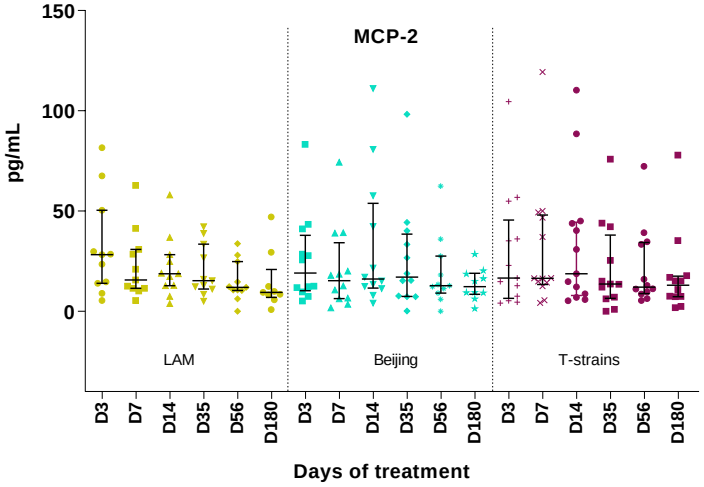
MCP-2
pg/mL
150
100
50
0
LAM
Beijing
T-strains
D3 D7 D14 D35 D56 D180
Days of treatment

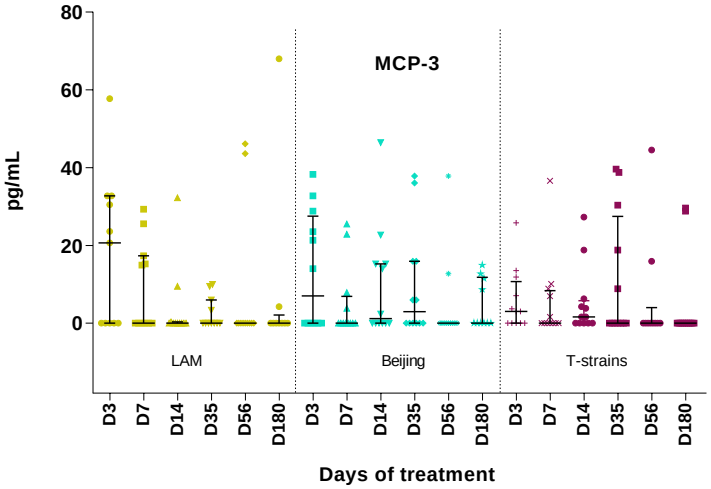
MCP-3
pg/mL
80
60
40
20
0
LAM
Beijing
T-strains
D3 D7 D14 D35 D56 D180
Days of treatment

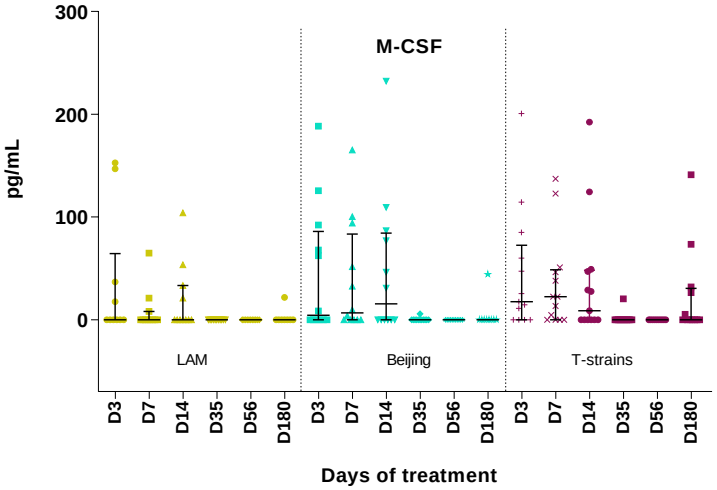
M-CSF
pg/mL
300
200
100
0
LAM
Beijing
T-strains
D3 D7 D14 D35 D56 D180
Days of treatment

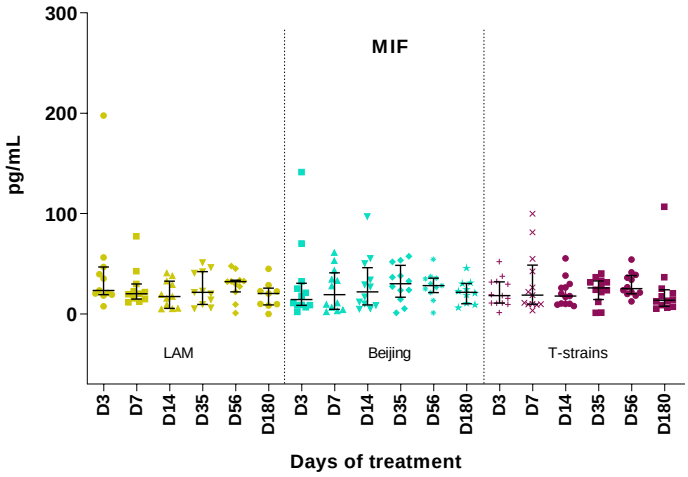
MIF
pg/mL
300
200
100
0
LAM
Beijing
T-strains
D3 D7 D14 D35 D56 D180 D3 D7 D14 D35 D56 D180 D3 D7 D14 D35 D56 D180
Days of treatment

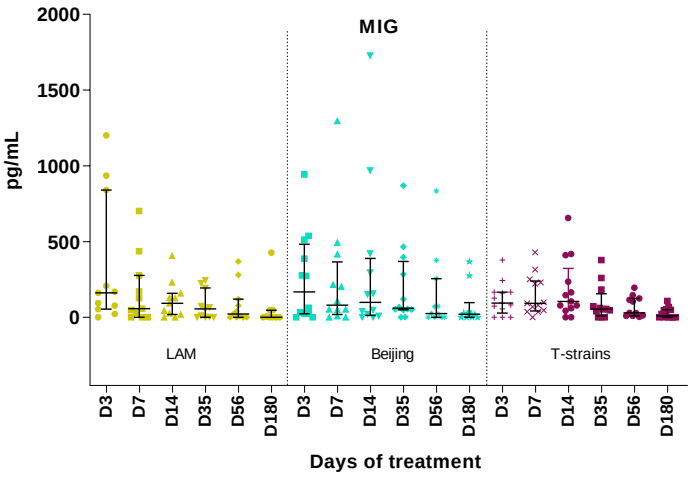
MIG
pg/mL
2000
1500
1000
500
0
LAM
Beijing
T-strains
D3 D7 D14 D35 D56 D180 D3 D7 D14 D35 D56 D180 D3 D7 D14 D35 D56 D180
Days of treatment

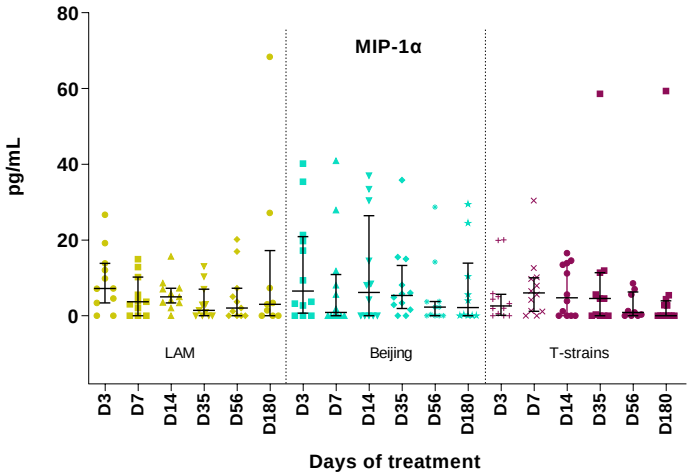
MIP-1α
pg/mL
80
60
40
20
0
LAM
Beijing
T-strains
D3 D7 D14 D35 D56 D180 D3 D7 D14 D35 D56 D180 D3 D7 D14 D35 D56 D180
Days of treatment

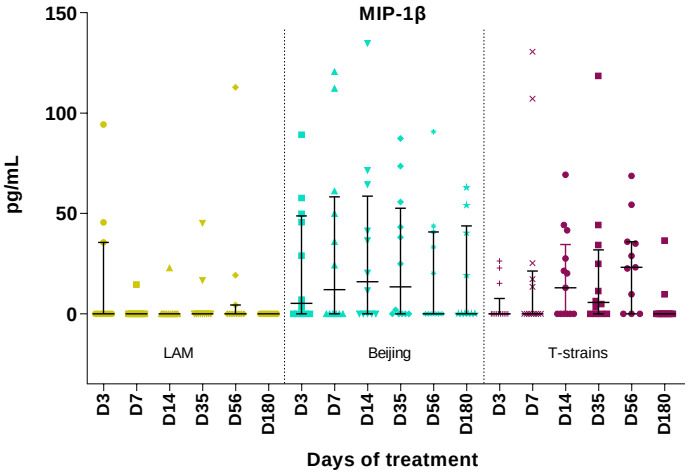
MIP-1β
pg/mL
150
100
50
0
LAM
Beijing
T-strains
D3 D7 D14 D35 D56 D180 D3 D7 D14 D35 D56 D180 D3 D7 D14 D35 D56 D180
Days of treatment

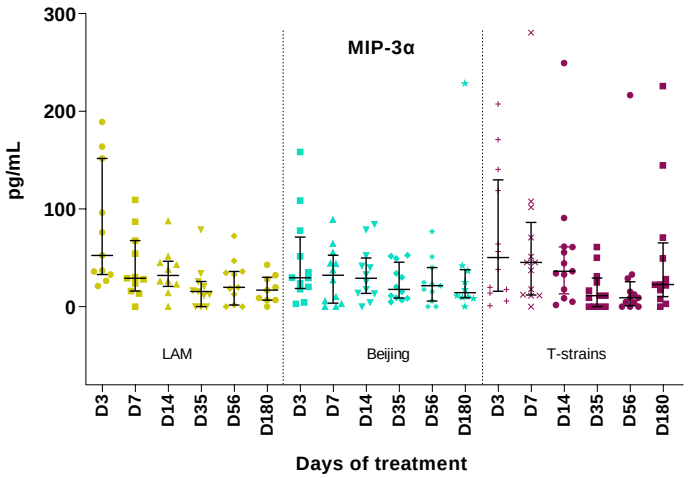
MIP-3α
pg/mL
300
200
100
0
LAM
Beijing
T-strains
D3 D7 D14 D35 D56 D180 D3 D7 D14 D35 D56 D180 D3 D7 D14 D35 D56 D180
Days of treatment

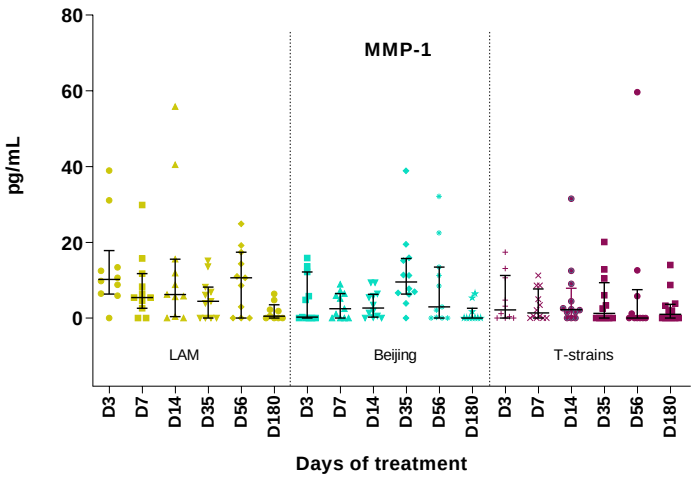
MMP-1
pg/mL
80
60
40
20
0
LAM
Beijing
T-strains
D3 D7 D14 D35 D56 D180 D3 D7 D14 D35 D56 D180 D3 D7 D14 D35 D56 D180
Days of treatment

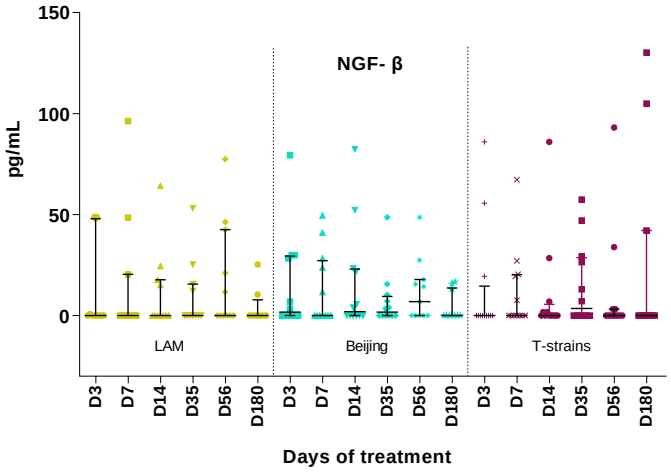
NGF- β
pg/mL
150
100
50
0
LAM
Beijing
T-strains
D3 D7 D14 D35 D56 D180
Days of treatment

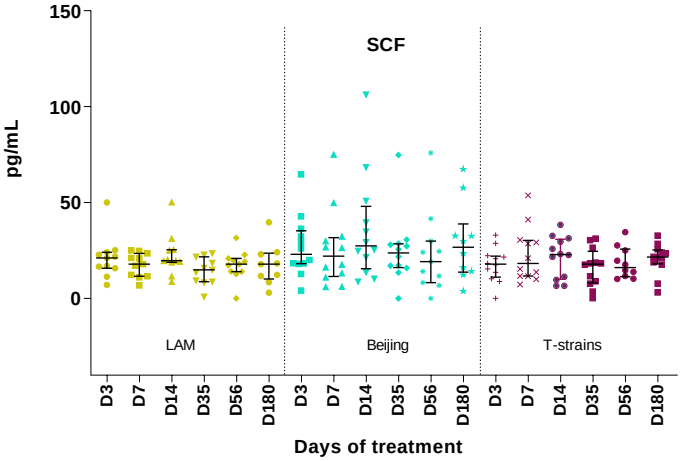
SCF
pg/mL
150
100
50
0
LAM
Beijing
T-strains
D3 D7 D14 D35 D56 D180
Days of treatment

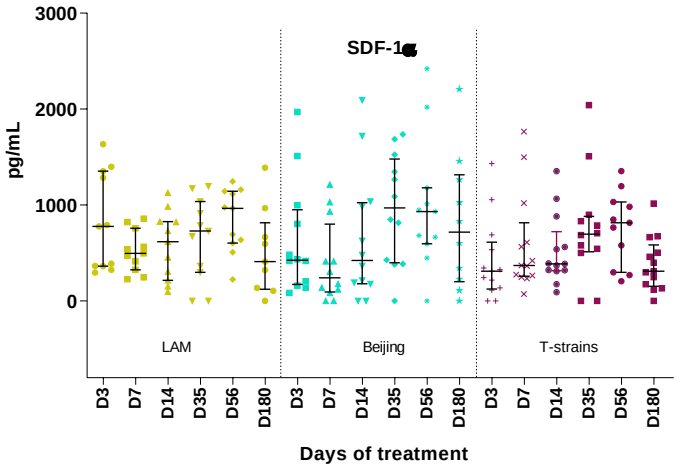
SDF-1α
pg/mL
3000
2000
1000
0
LAM
Beijing
T-strains
D3 D7 D14 D35 D56 D180
Days of treatment

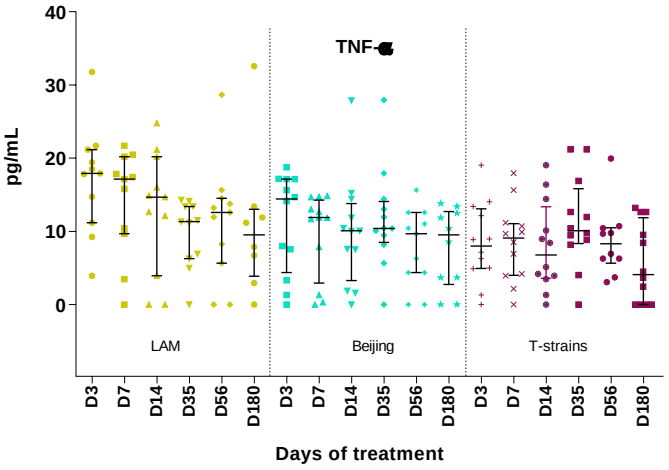
TNF-α
pg/mL
40
30
20
10
0
LAM
Beijing
T-strains
D3 D7 D14 D35 D56 D180
Days of treatment

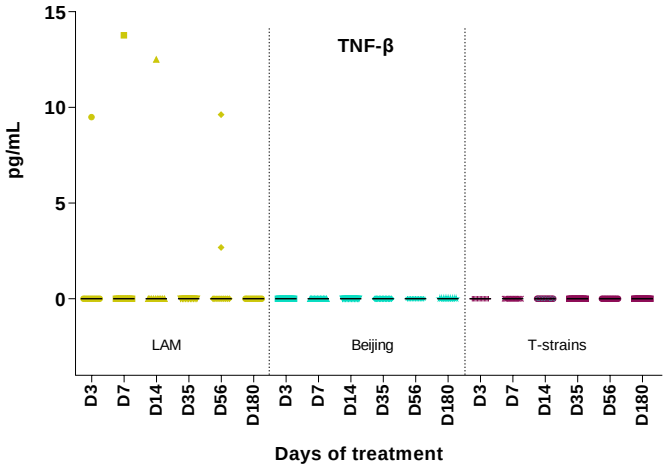
TNF-β
pg/mL
15
10
5
0
LAM
Beijing
T-strains
D3 D7 D14 D35 D56 D180
Days of treatment

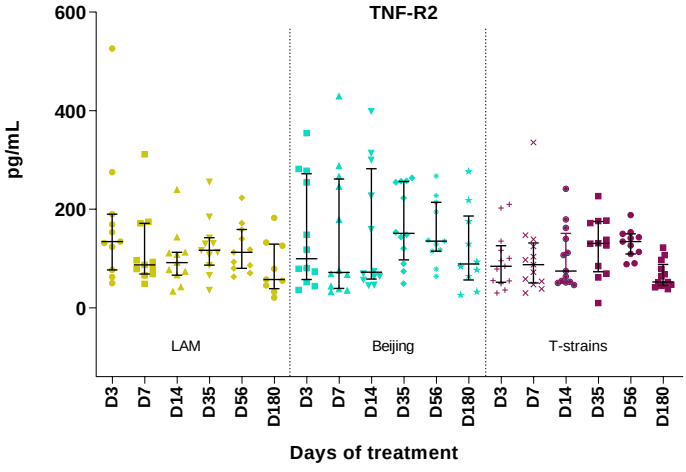
TNF-R2
pg/mL
600
400
200
0
LAM
Beijing
T-strains
D3 D7 D14 D35 D56 D180
Days of treatment

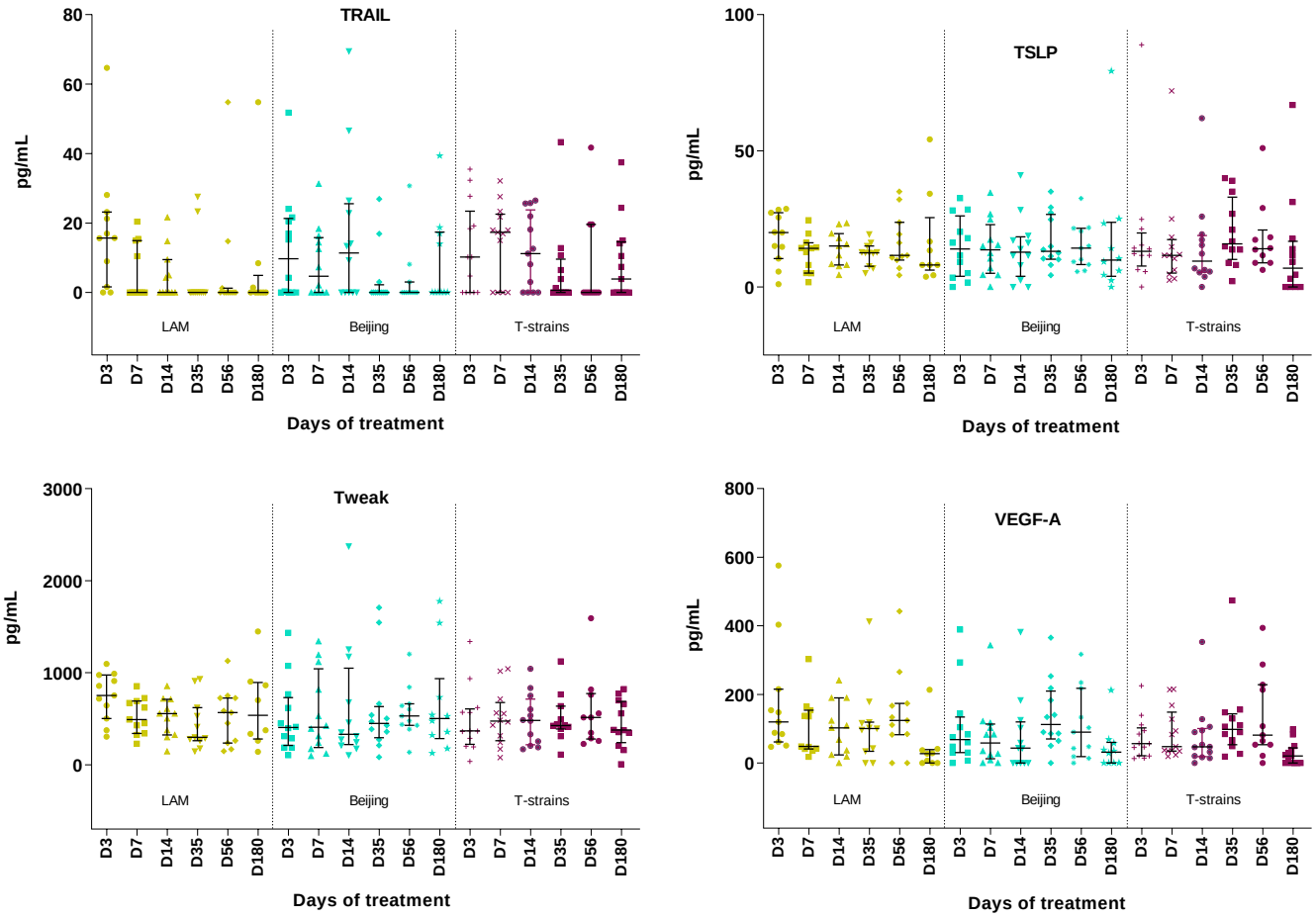

Figure A4: The effect of strain type on cytokine profiles during TB treatment. Lime, mint and purple dots represents samples in the LAM, Beijing and T-strains infected group respectively. The concentrations are expressed in pg/mL and were analysed by the non-parametric Kruskal-wallis test, with significance $P < 0.05$ (corrected by Dunn's multiple comparisons).

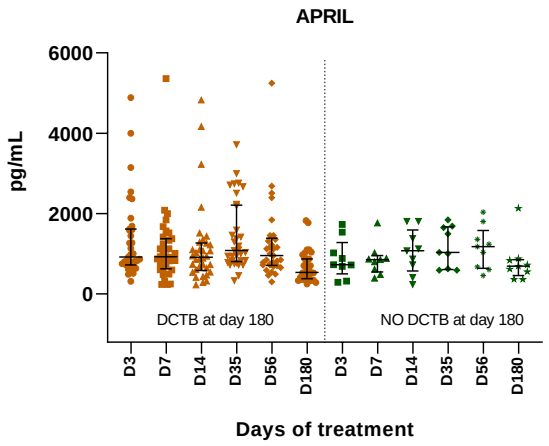
APRIL
pg/mL
6000
4000
2000
0
DCTB at day 180
NO DCTB at day 180
D3 D7 D14 D35 D56 D180 D3 D7 D14 D35 D56 D180
Days of treatment

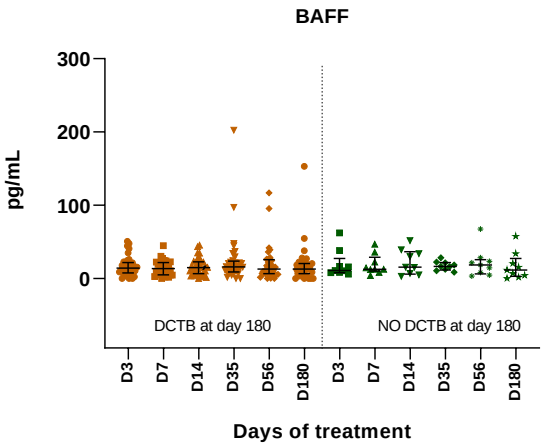
BAFF
pg/mL
300
200
100
0
DCTB at day 180
NO DCTB at day 180
D3 D7 D14 D35 D56 D180 D3 D7 D14 D35 D56 D180
Days of treatment

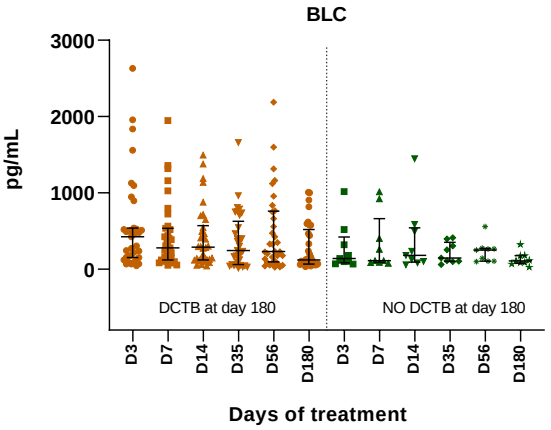
BLC
pg/mL
3000
2000
1000
0
DCTB at day 180
NO DCTB at day 180
D3 D7 D14 D35 D56 D180 D3 D7 D14 D35 D56 D180
Days of treatment

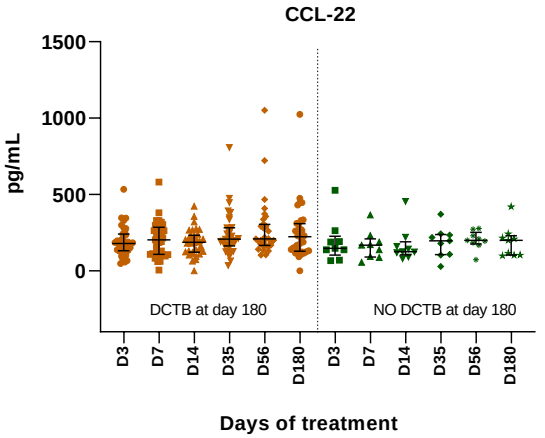
CCL-22
pg/mL
1500
1000
500
0
DCTB at day 180
NO DCTB at day 180
D3 D7 D14 D35 D56 D180 D3 D7 D14 D35 D56 D180
Days of treatment

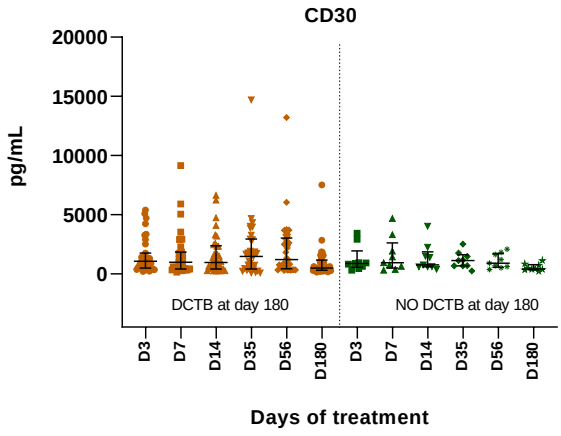
CD30
pg/mL
20000
15000
10000
5000
0
DCTB at day 180
NO DCTB at day 180
D3 D7 D14 D35 D56 D180 D3 D7 D14 D35 D56 D180
Days of treatment

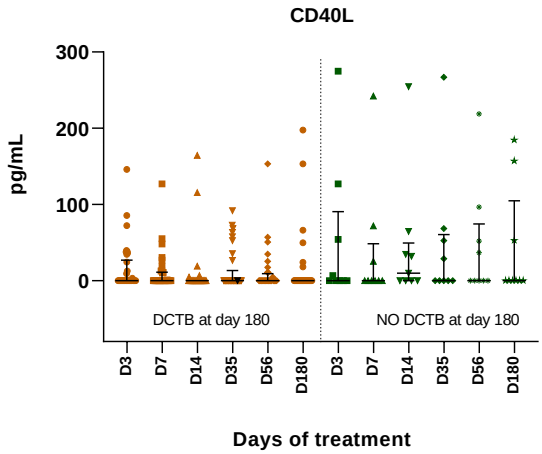
CD40L
pg/mL
300
200
100
0
DCTB at day 180
NO DCTB at day 180
D3 D7 D14 D35 D56 D180 D3 D7 D14 D35 D56 D180
Days of treatment

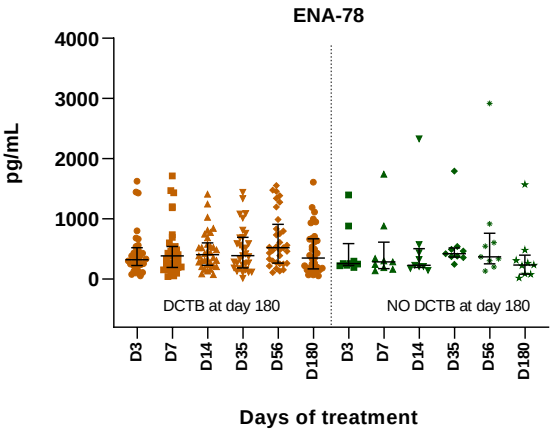
ENA-78
pg/mL
4000
3000
2000
1000
0
DCTB at day 180
NO DCTB at day 180
D3 D7 D14 D35 D56 D180 D3 D7 D14 D35 D56 D180
Days of treatment

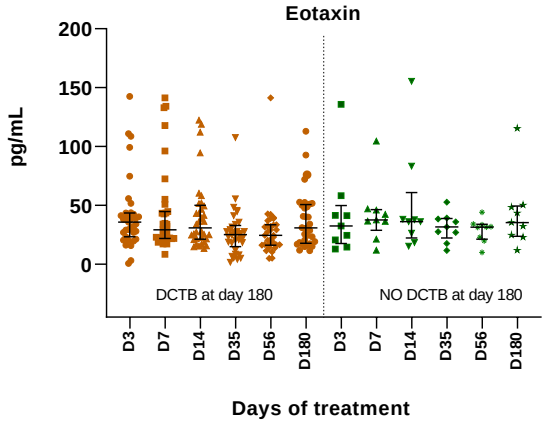
Eotaxin
pg/mL
200
150
100
50
0
DCTB at day 180
NO DCTB at day 180
D3 D7 D14 D35 D56 D180 D3 D7 D14 D35 D56 D180
Days of treatment

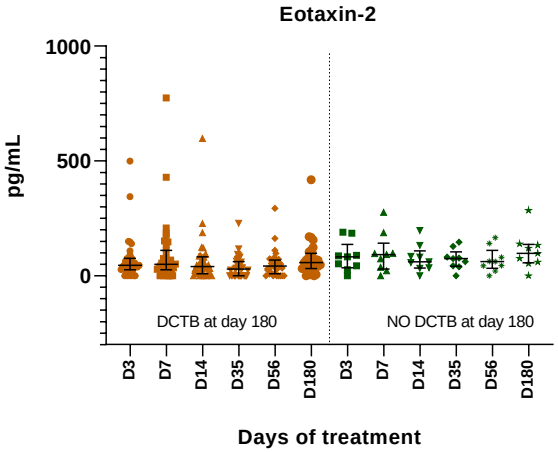
Eotaxin-2
pg/mL
1000
500
0
DCTB at day 180
NO DCTB at day 180
D3 D7 D14 D35 D56 D180 D3 D7 D14 D35 D56 D180
Days of treatment

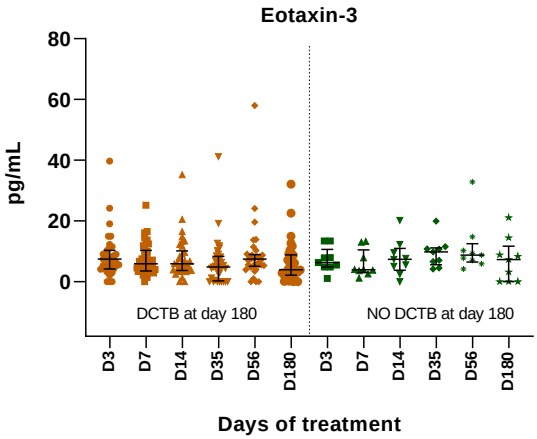
Eotaxin-3
pg/mL
80
60
40
20
0
DCTB at day 180
NO DCTB at day 180
D3 D7 D14 D35 D56 D180 D3 D7 D14 D35 D56 D180
Days of treatment

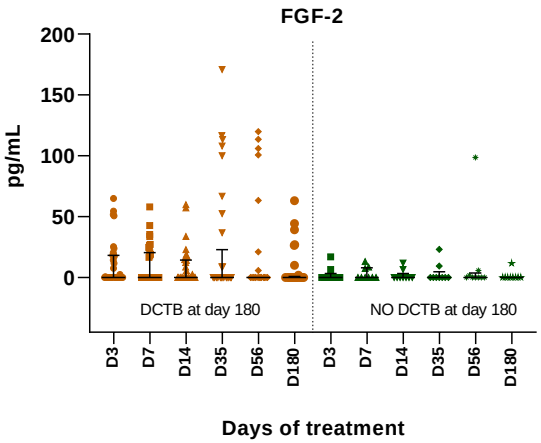
FGF-2
pg/mL
200
150
100
50
0
DCTB at day 180
NO DCTB at day 180
D3 D7 D14 D35 D56 D180 D3 D7 D14 D35 D56 D180
Days of treatment

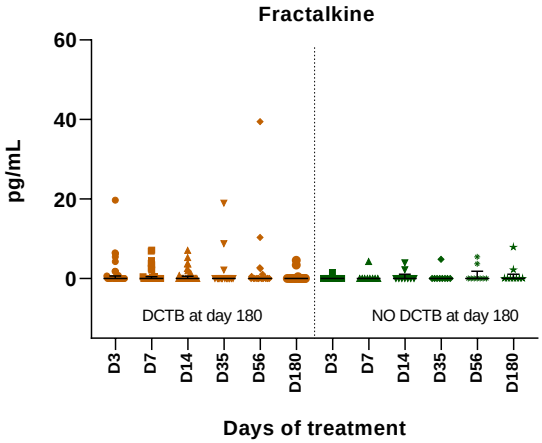
Fractalkine
pg/mL
60
40
20
0
DCTB at day 180
NO DCTB at day 180
D3 D7 D14 D35 D56 D180 D3 D7 D14 D35 D56 D180
Days of treatment

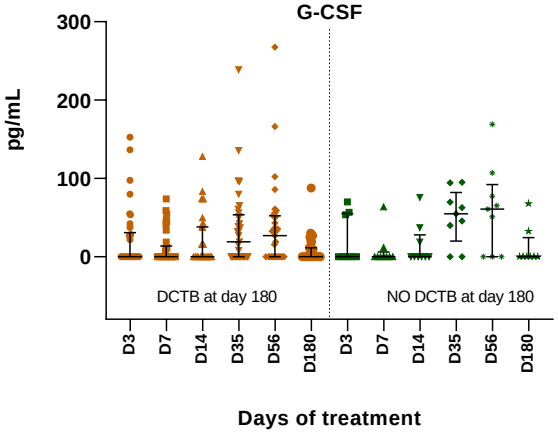
G-CSF
pg/mL
300
200
100
0
DCTB at day 180
NO DCTB at day 180
D3 D7 D14 D35 D56 D180 D3 D7 D14 D35 D56 D180
Days of treatment

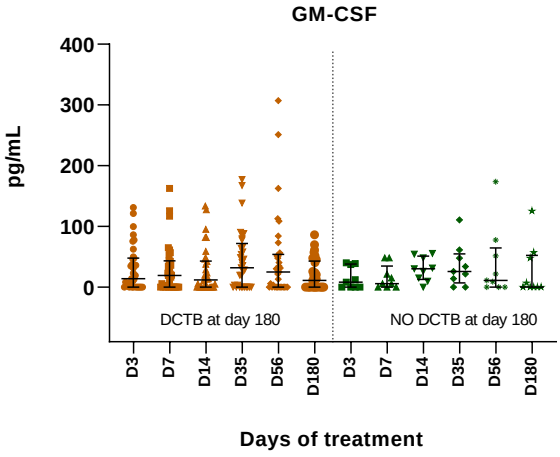
GM-CSF
pg/mL
400
300
200
100
0
DCTB at day 180
NO DCTB at day 180
D3 D7 D14 D35 D56 D180 D3 D7 D14 D35 D56 D180
Days of treatment

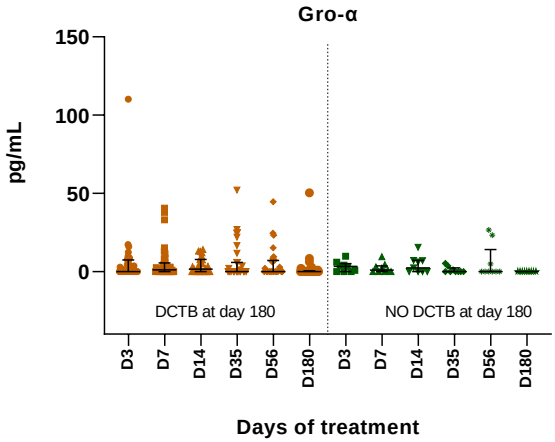
Gro-α
pg/mL
150
100
50
0
DCTB at day 180
NO DCTB at day 180
D3 D7 D14 D35 D56 D180 D3 D7 D14 D35 D56 D180
Days of treatment

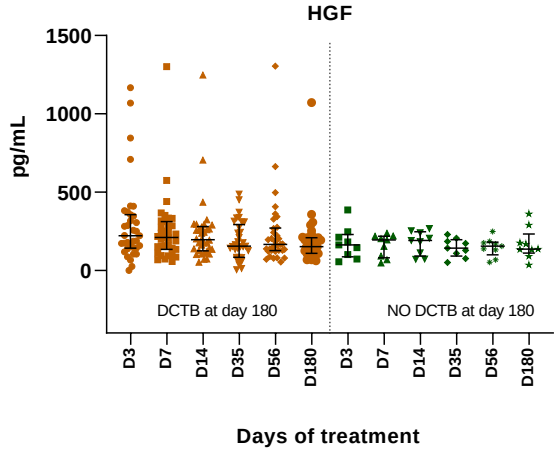
HGF
pg/mL
1500
1000
500
0
DCTB at day 180
NO DCTB at day 180
D3 D7 D14 D35 D56 D180 D3 D7 D14 D35 D56 D180
Days of treatment

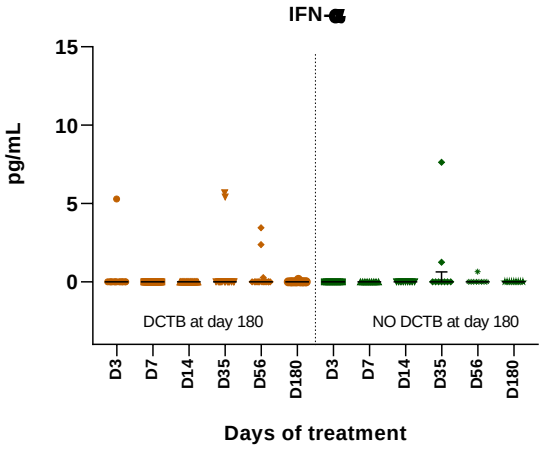
IFN-α
pg/mL
15
10
5
0
DCTB at day 180
NO DCTB at day 180
D3 D7 D14 D35 D56 D180 D3 D7 D14 D35 D56 D180
Days of treatment

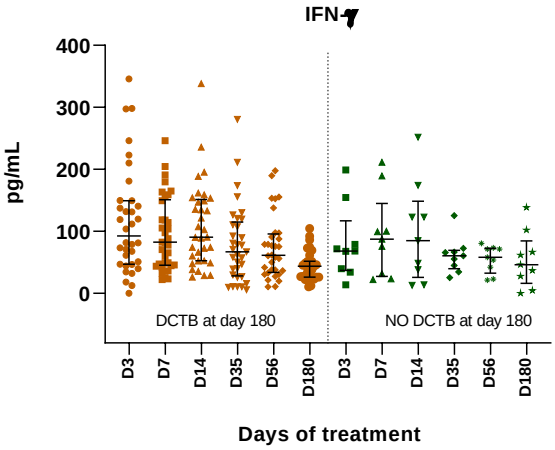
IFN-γ
pg/mL
400
300
200
100
0
DCTB at day 180
NO DCTB at day 180
D3 D7 D14 D35 D56 D180 D3 D7 D14 D35 D56 D180
Days of treatment

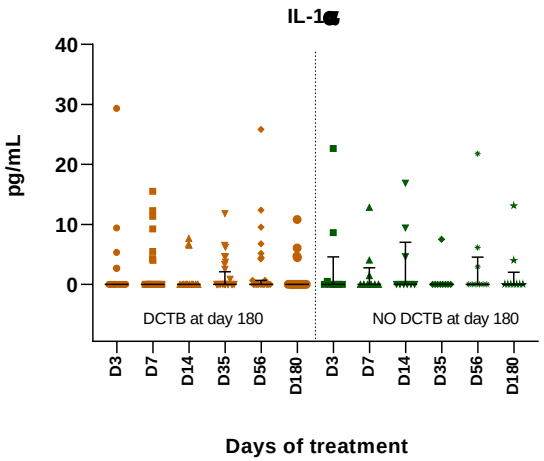
IL-1α
pg/mL
40
30
20
10
0
DCTB at day 180
NO DCTB at day 180
D3 D7 D14 D35 D56 D180 D3 D7 D14 D35 D56 D180
Days of treatment

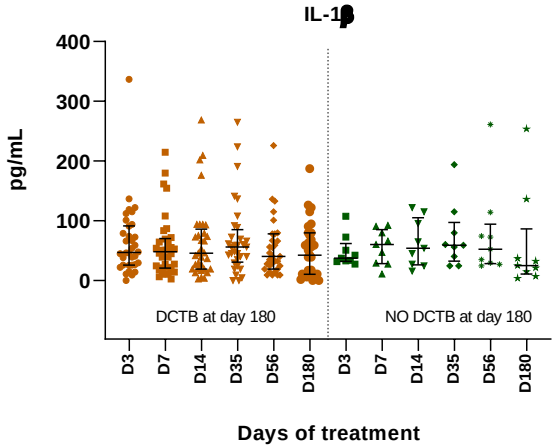
IL-1β
pg/mL
400
300
200
100
0
DCTB at day 180
NO DCTB at day 180
D3 D7 D14 D35 D56 D180 D3 D7 D14 D35 D56 D180
Days of treatment

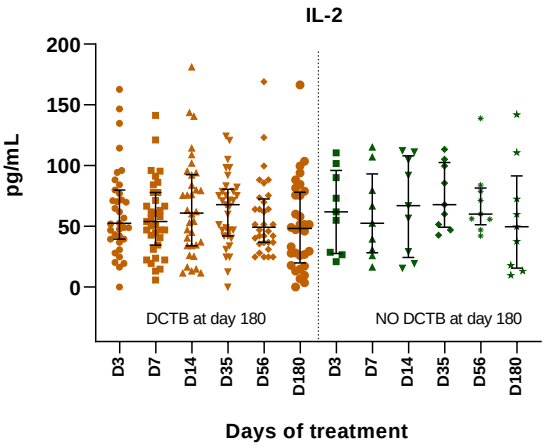
IL-2
pg/mL
200
150
100
50
0
DCTB at day 180
NO DCTB at day 180
D3 D7 D14 D35 D56 D180 D3 D7 D14 D35 D56 D180
Days of treatment

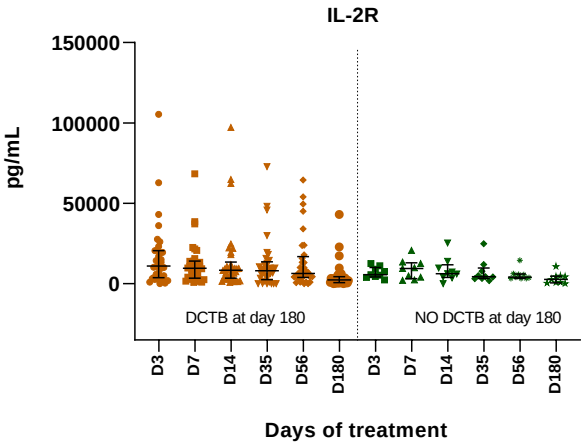
IL-2R
pg/mL
150000
100000
50000
0
DCTB at day 180
NO DCTB at day 180
D3 D7 D14 D35 D56 D180 D3 D7 D14 D35 D56 D180
Days of treatment

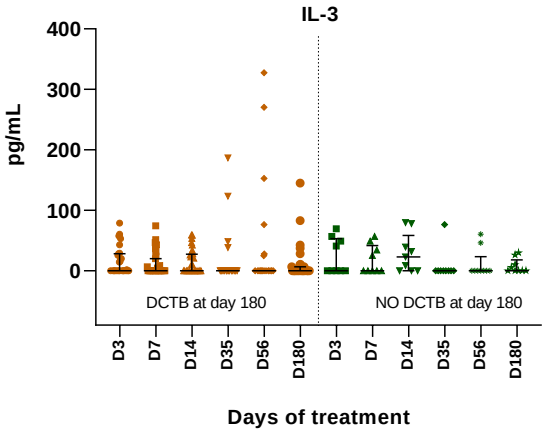
IL-3
pg/mL
400
300
200
100
0
DCTB at day 180
NO DCTB at day 180
D3 D7 D14 D35 D56 D180 D3 D7 D14 D35 D56 D180
Days of treatment

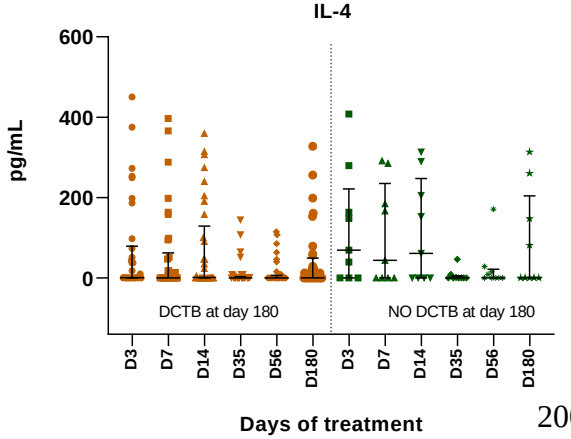
IL-4
pg/mL
600
400
200
0
DCTB at day 180
NO DCTB at day 180
D3 D7 D14 D35 D56 D180 D3 D7 D14 D35 D56 D180
Days of treatment

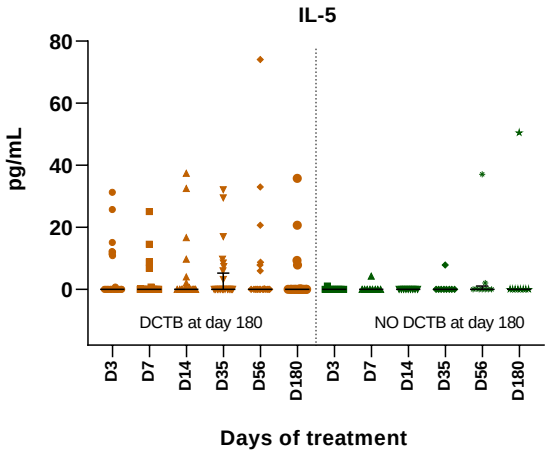
IL-5
pg/mL
80
60
40
20
0
DCTB at day 180
NO DCTB at day 180
D3
D7
D14
D35
D56
D180
Days of treatment

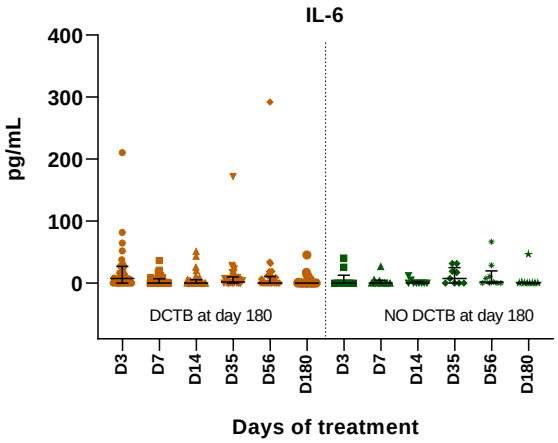
IL-6
pg/mL
400
300
200
100
0
DCTB at day 180
NO DCTB at day 180
D3
D7
D14
D35
D56
D180
Days of treatment

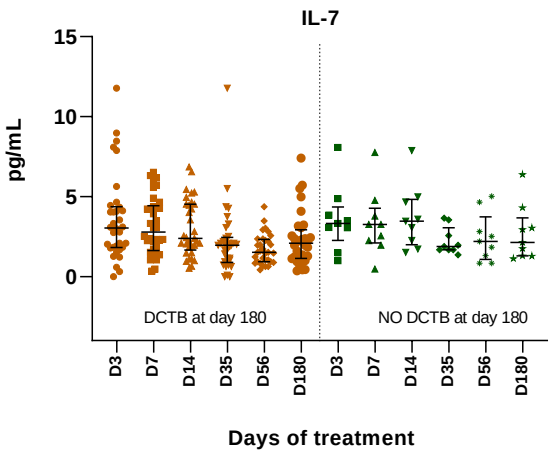
IL-7
pg/mL
15
10
5
0
DCTB at day 180
NO DCTB at day 180
D3
D7
D14
D35
D56
D180
Days of treatment

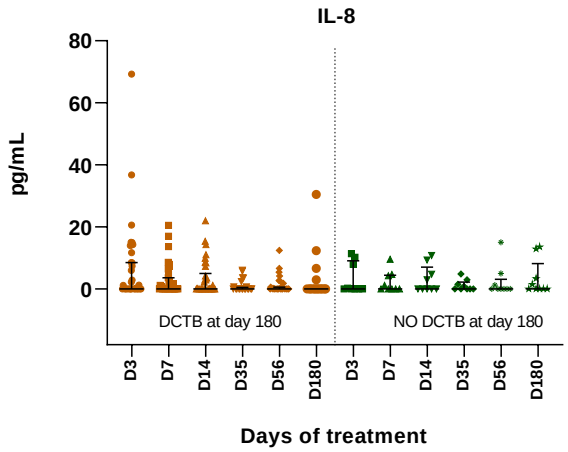
IL-8
pg/mL
80
60
40
20
0
DCTB at day 180
NO DCTB at day 180
D3
D7
D14
D35
D56
D180
Days of treatment

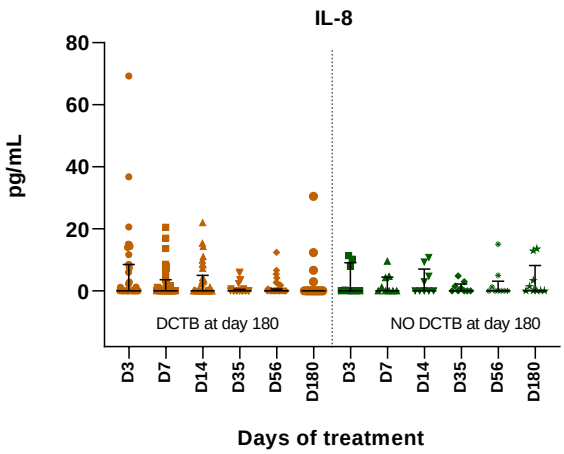
IL-8
pg/mL
80
60
40
20
0
DCTB at day 180
NO DCTB at day 180
D3
D7
D14
D35
D56
D180
Days of treatment

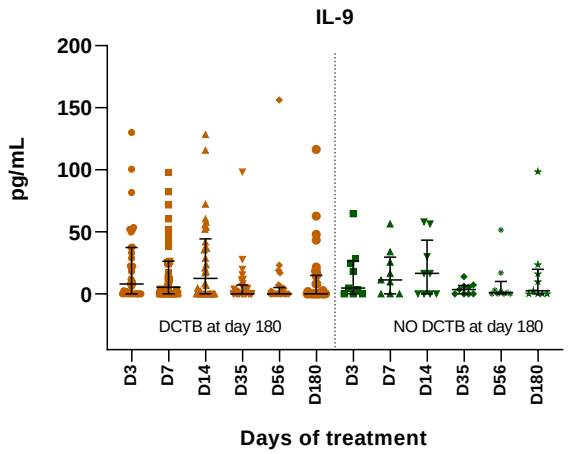
IL-9
pg/mL
200
150
100
50
0
DCTB at day 180
NO DCTB at day 180
D3
D7
D14
D35
D56
D180
Days of treatment

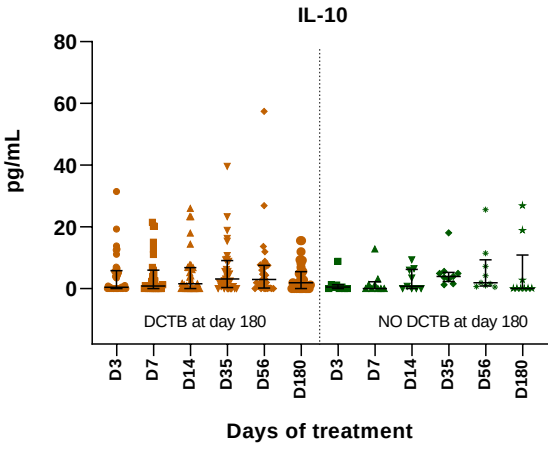
IL-10
pg/mL
80
60
40
20
0
DCTB at day 180
NO DCTB at day 180
D3
D7
D14
D35
D56
D180
Days of treatment

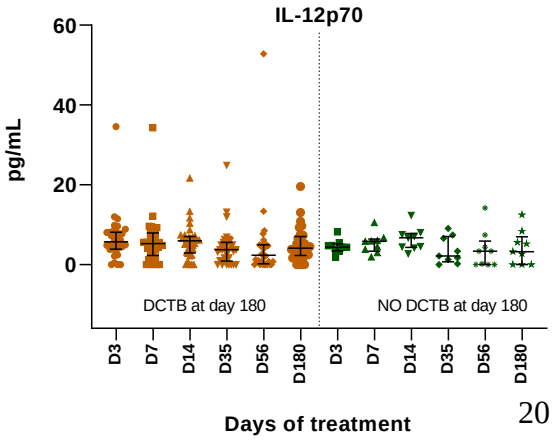
IL-12p70
pg/mL
60
40
20
0
DCTB at day 180
NO DCTB at day 180
D3
D7
D14
D35
D56
D180
Days of treatment

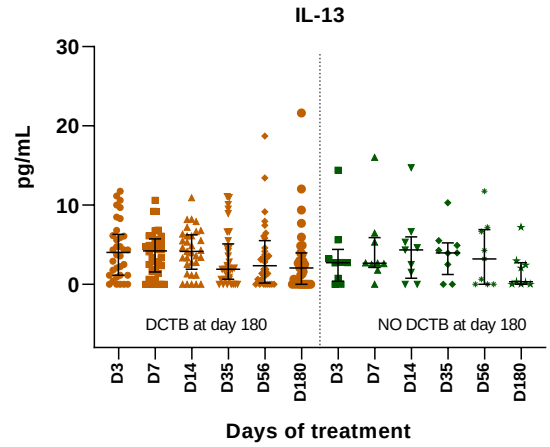
IL-13
pg/mL
30
20
10
0
DCTB at day 180
NO DCTB at day 180
D3
D7
D14
D35
D56
D180
Days of treatment

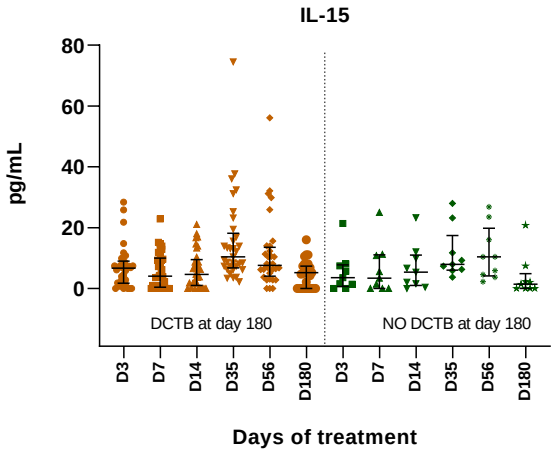
IL-15
pg/mL
80
60
40
20
0
DCTB at day 180
NO DCTB at day 180
D3
D7
D14
D35
D56
D180
Days of treatment

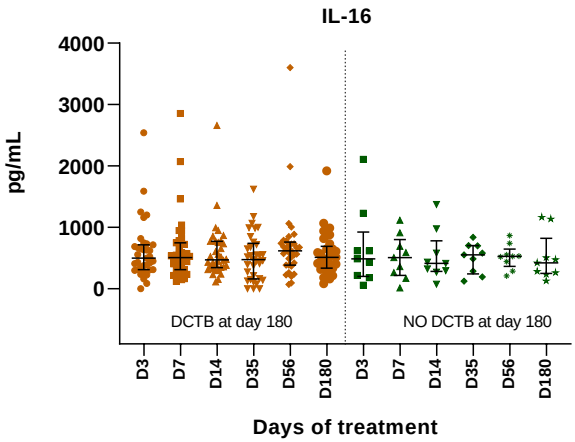
IL-16
pg/mL
4000
3000
2000
1000
0
DCTB at day 180
NO DCTB at day 180
D3
D7
D14
D35
D56
D180
Days of treatment

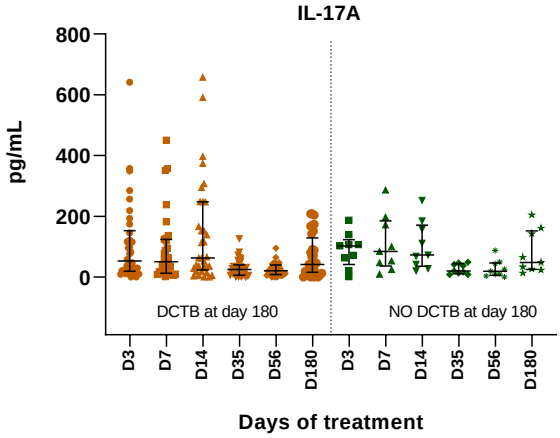
IL-17A
pg/mL
800
600
400
200
0
DCTB at day 180
NO DCTB at day 180
D3
D7
D14
D35
D56
D180
Days of treatment

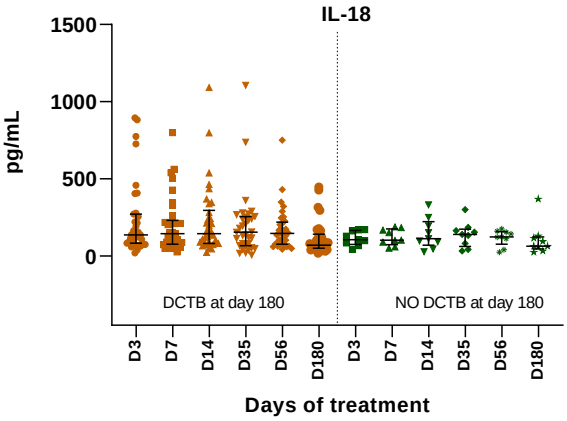
IL-18
pg/mL
1500
1000
500
0
DCTB at day 180
NO DCTB at day 180
D3
D7
D14
D35
D56
D180
Days of treatment

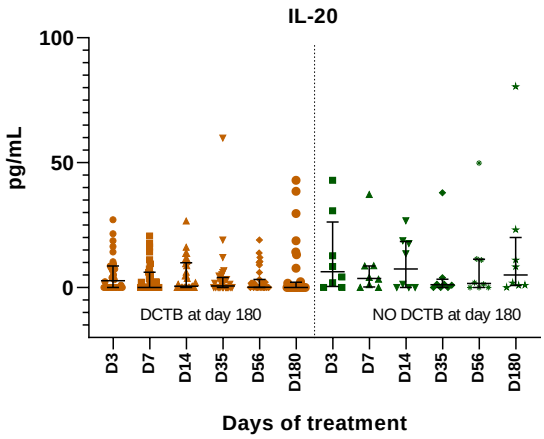
IL-20
pg/mL
100
50
0
DCTB at day 180
NO DCTB at day 180
D3
D7
D14
D35
D56
D180
Days of treatment

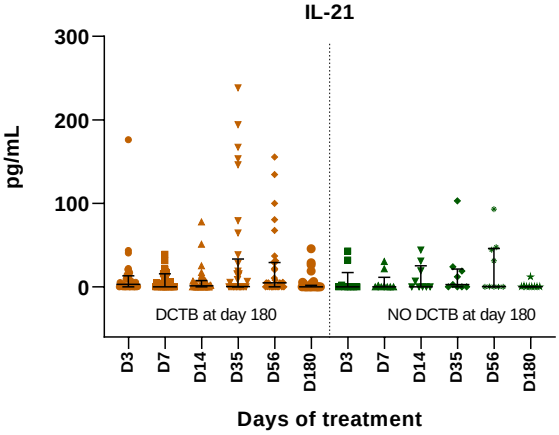
IL-21
pg/mL
300
200
100
0
DCTB at day 180
NO DCTB at day 180
D3
D7
D14
D35
D56
D180
Days of treatment

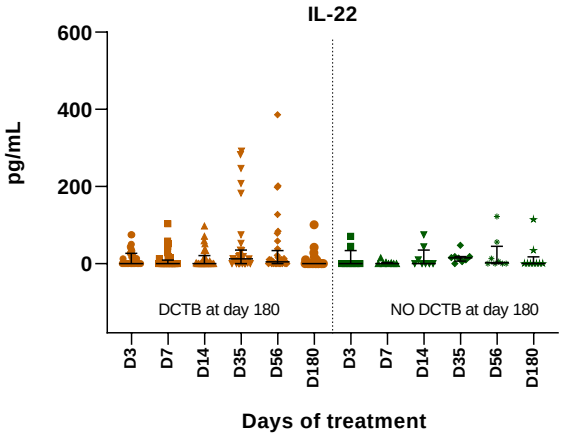
IL-22
pg/mL
600
400
200
0
DCTB at day 180
NO DCTB at day 180
D3
D7
D14
D35
D56
D180
Days of treatment

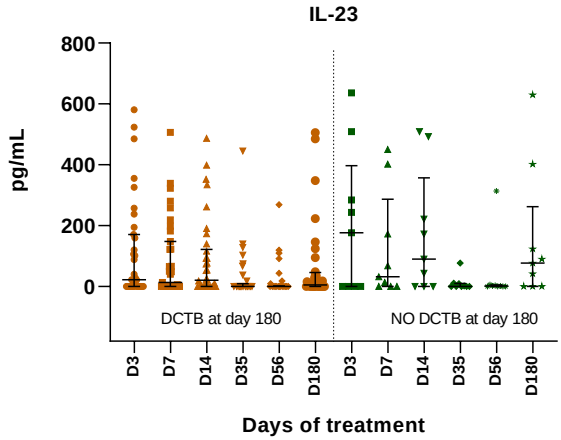
IL-23
pg/mL
800
600
400
200
0
DCTB at day 180
NO DCTB at day 180
D3
D7
D14
D35
D56
D180
Days of treatment

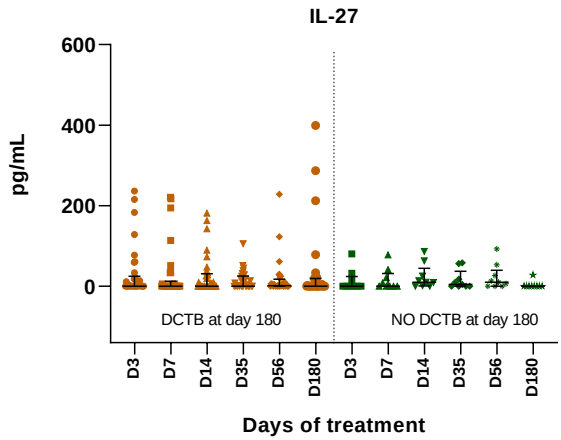
IL-27
pg/mL
600
400
200
0
DCTB at day 180
NO DCTB at day 180
D3
D7
D14
D35
D56
D180
Days of treatment

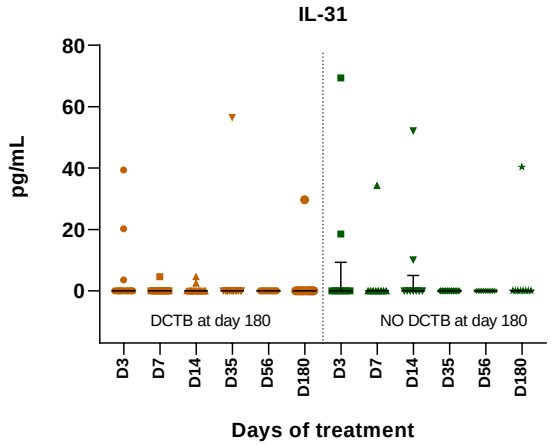
IL-31
pg/mL
80
60
40
20
0
DCTB at day 180
NO DCTB at day 180
D3
D7
D14
D35
D56
D180
Days of treatment

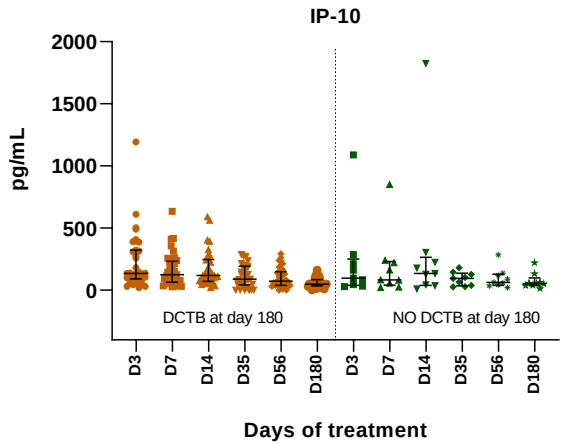
IP-10
pg/mL
2000
1500
1000
500
0
DCTB at day 180
NO DCTB at day 180
D3
D7
D14
D35
D56
D180
Days of treatment

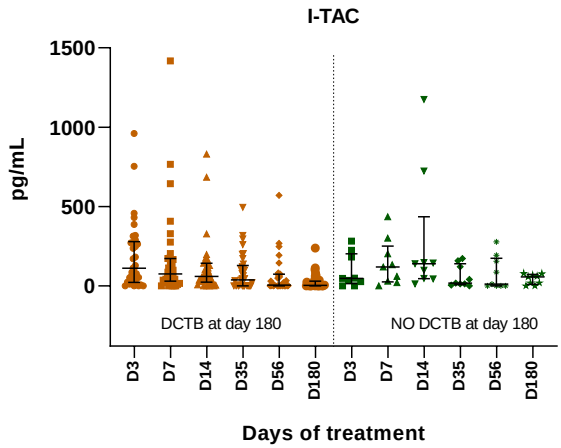
I-TAC
pg/mL
1500
1000
500
0
DCTB at day 180
NO DCTB at day 180
D3
D7
D14
D35
D56
D180
Days of treatment

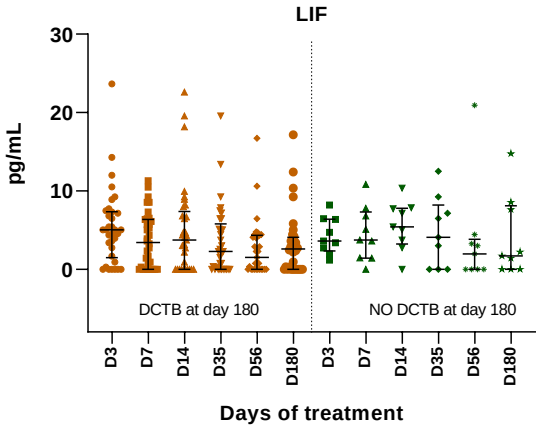
LIF
pg/mL
30
20
10
0
DCTB at day 180
NO DCTB at day 180
D3
D7
D14
D35
D56
D180
Days of treatment

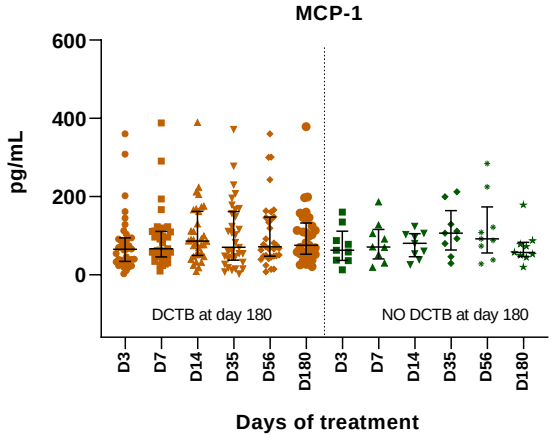
MCP-1
pg/mL
600
400
200
0
DCTB at day 180
NO DCTB at day 180
D3
D7
D14
D35
D56
D180
Days of treatment

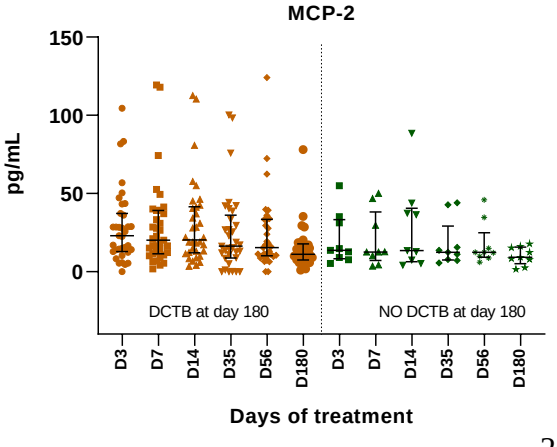
MCP-2
pg/mL
150
100
50
0
DCTB at day 180
NO DCTB at day 180
D3
D7
D14
D35
D56
D180
Days of treatment

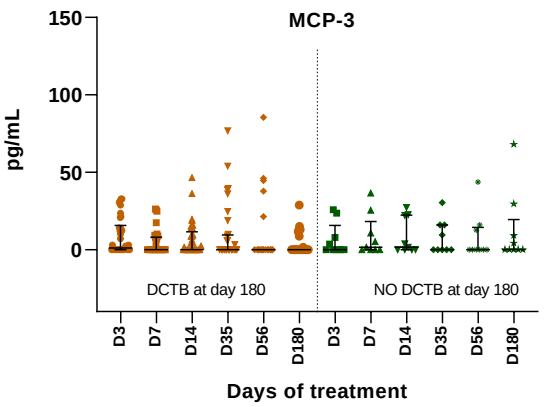
MCP-3
pg/mL
150
100
50
0
DCTB at day 180
NO DCTB at day 180
D3
D7
D14
D35
D56
D180
Days of treatment

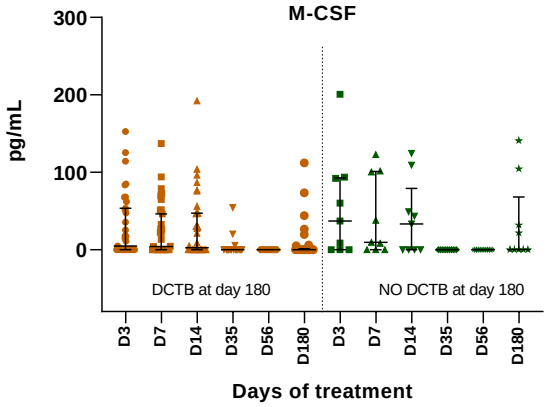
M-CSF
pg/mL
300
200
100
0
DCTB at day 180
NO DCTB at day 180
D3
D7
D14
D35
D56
D180
Days of treatment

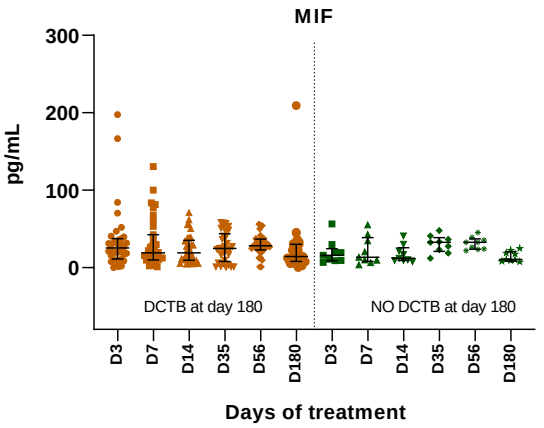
MIF
pg/mL
300
200
100
0
DCTB at day 180
NO DCTB at day 180
D3
D7
D14
D35
D56
D180
Days of treatment

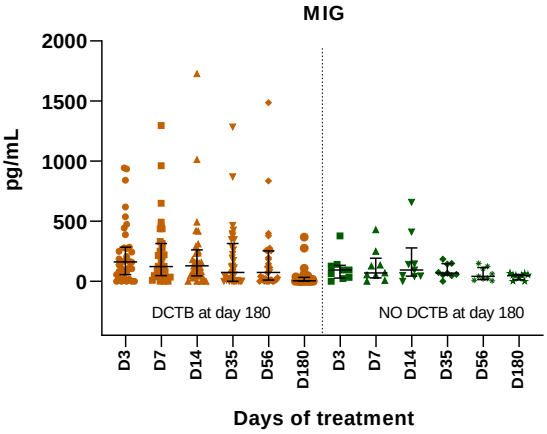
MIG
pg/mL
2000
1500
1000
500
0
DCTB at day 180
NO DCTB at day 180
D3
D7
D14
D35
D56
D180
Days of treatment

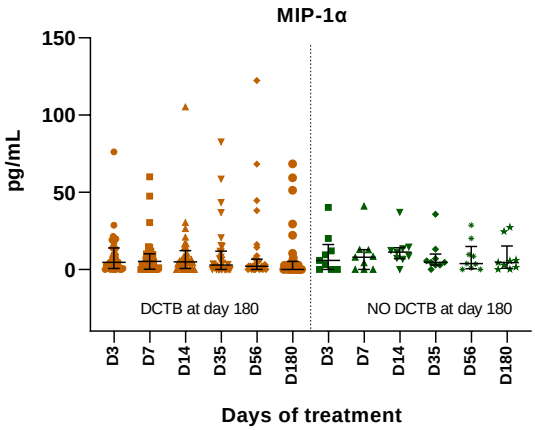
MIP-1α
pg/mL
150
100
50
0
DCTB at day 180
NO DCTB at day 180
D3
D7
D14
D35
D56
D180
Days of treatment

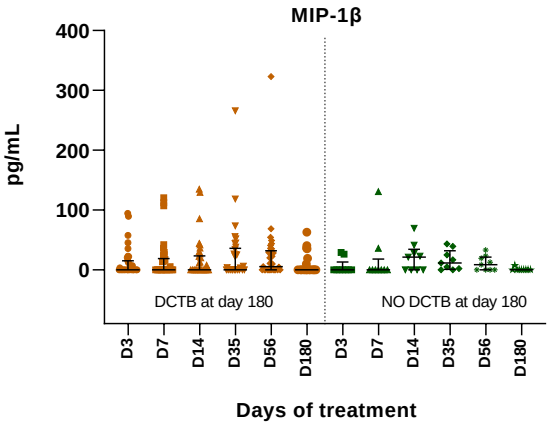
MIP-1β
pg/mL
400
300
200
100
0
DCTB at day 180
NO DCTB at day 180
D3
D7
D14
D35
D56
D180
Days of treatment

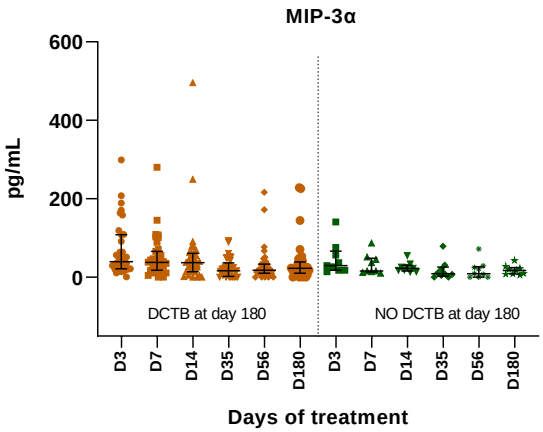
MIP-3α
pg/mL
600
400
200
0
DCTB at day 180
NO DCTB at day 180
D3
D7
D14
D35
D56
D180
Days of treatment

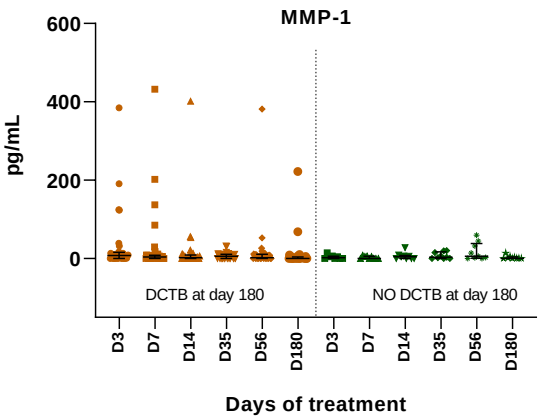
MMP-1
pg/mL
600
400
200
0
DCTB at day 180
NO DCTB at day 180
D3
D7
D14
D35
D56
D180
Days of treatment

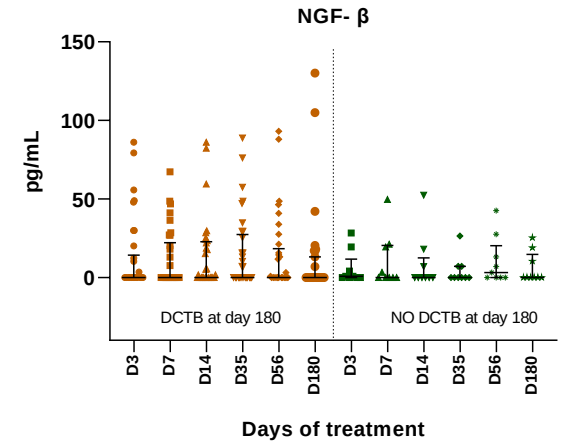
NGF- β
pg/mL
150
100
50
0
DCTB at day 180
NO DCTB at day 180
D3
D7
D14
D35
D56
D180
Days of treatment

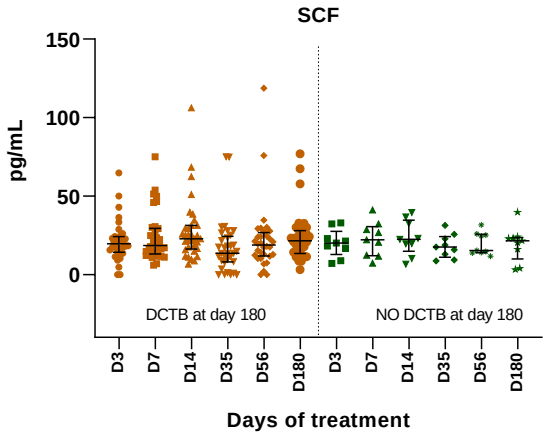
SCF
pg/mL
150
100
50
0
DCTB at day 180
NO DCTB at day 180
D3
D7
D14
D35
D56
D180
Days of treatment

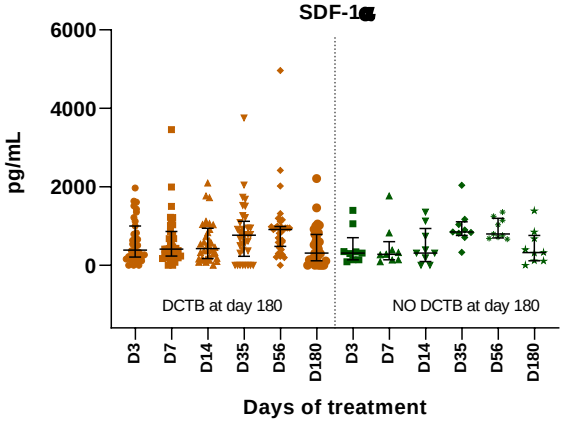
SDF-1α
pg/mL
6000
4000
2000
0
DCTB at day 180
NO DCTB at day 180
D3
D7
D14
D35
D56
D180
Days of treatment

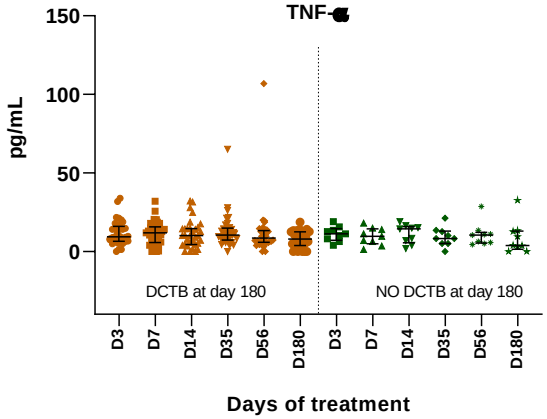
TNF-α
pg/mL
150
100
50
0
DCTB at day 180
NO DCTB at day 180
D3
D7
D14
D35
D56
D180
Days of treatment

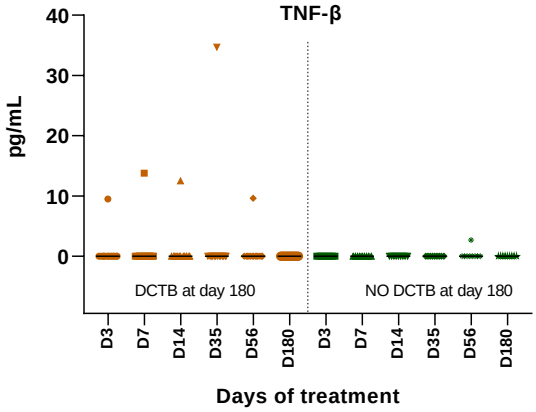
TNF-β
pg/mL
40
30
20
10
0
DCTB at day 180
NO DCTB at day 180
D3
D7
D14
D35
D56
D180
Days of treatment

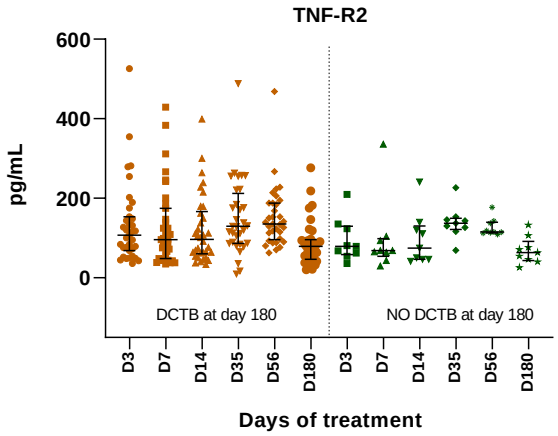
TNF-R2
pg/mL
600
400
200
0
DCTB at day 180
NO DCTB at day 180
D3
D7
D14
D35
D56
D180
Days of treatment

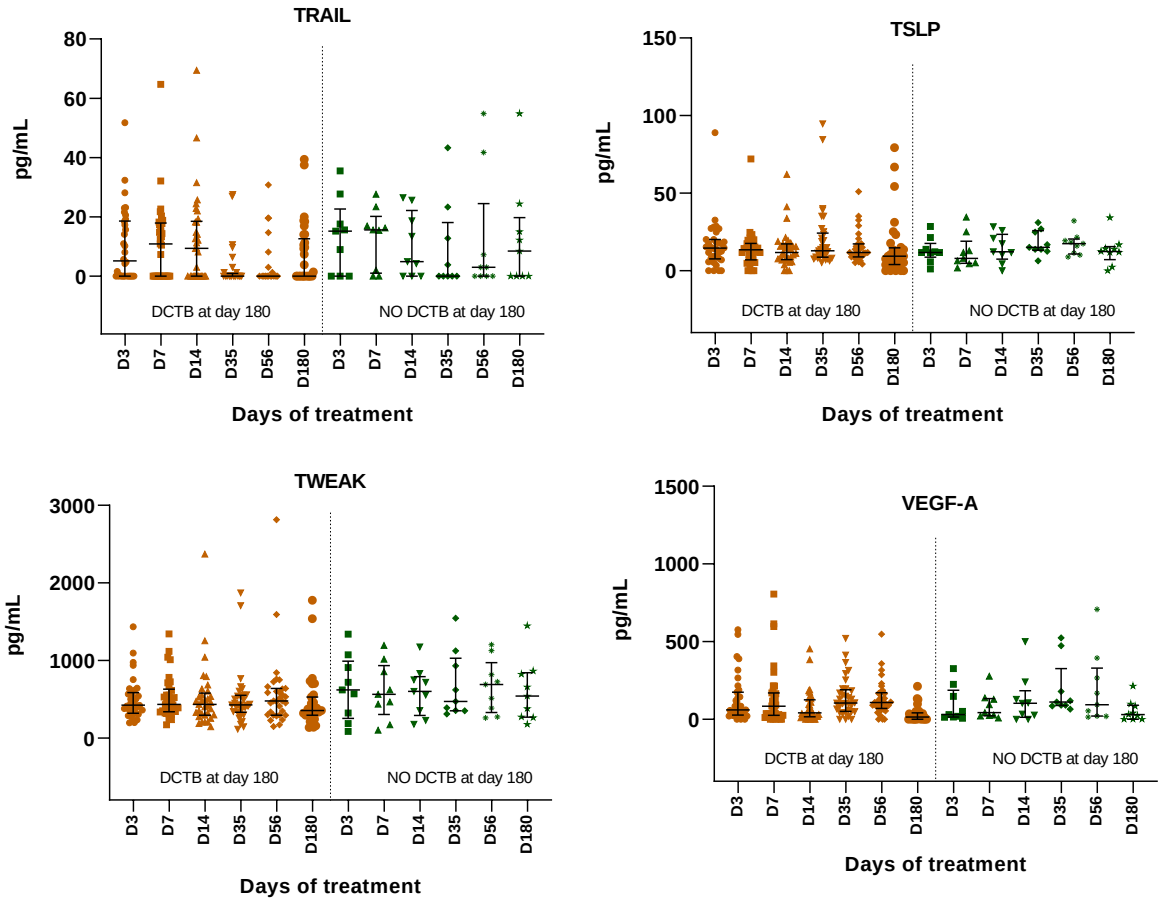

Figure A5. The effect of residual DCTB at the end of treatment. Brown and green dots represents samples of those with residual DCTB at the end of treatment and those without DCTB upon treatment, respectively. The concentrations are expressed in pg/mL and were analysed by the non-parametric Kruskal-wallis test, with significance $P < 0.05$ (corrected by Dunn's multiple comparisons).

APPENDIX B

Revised SNT TB ethics certificate

UNIVERSITY OF THE WITWATERSRAND JOHANNESBURG

R14/49 Dr Z Waja and Professor B Kana

HUMAN RESEARCH ETHICS COMMITTEE (MEDICAL)
CLEARANCE CERTIFICATE NO. M200164

NAME: (Principal Investigator)	Dr Z Waja and Professor B Kana
DEPARTMENT:	Schools of Clinical Medicine (Waja) and Pathology (Kana) Perinatal HIV RU (Waja) & CoE in Biomedical TB Res (Kana) CHBAH (Waja) and NHLS (Kana)
PROJECT TITLE:	Sputum and oral swab collection for novel mycobacteriology testing techniques (SNT study)
DATE CONSIDERED:	Ad hoc
DECISION:	Approved unconditionally
CONDITIONS:	
SUPERVISOR:	Not applicable
APPROVED BY:	Dr CB Penny, Chairperson, HREC (Medical)
DATE OF APPROVAL:	2020/03/18

This clearance certificate is valid for 5 years from date of approval. Extension may be applied for.

DECLARATION OF INVESTIGATORS

To be completed in duplicate and **ONE COPY** returned to the Research Office Secretary on the 3rd Floor, Phillip Tobias Building, Parktown, University of the Witwatersrand, Johannesburg.

I/we fully understand the conditions under which I am/we are authorized to carry out the above-mentioned research and I/we undertake to ensure compliance with these conditions. Should any departure be contemplated, from the research protocol as approved, I/we undertake to submit details to the Committee. **I agree to submit a yearly progress report**. When a funder requires annual re-certification, the application date will be one year after the date when the study was initially reviewed. In this case, the study was initially reviewed in **January** and will therefore reports and re-certification will be due early in the month of **January** each year. Unreported changes to the application may invalidate the clearance given by the HREC (Medical).

Principal Investigator Signature _____ Date _____

PLEASE QUOTE THE CLEARANCE CERTIFICATE NUMBER IN ALL ENQUIRIES

Previous TB ethics certificate

R14/49 Dr Neil Martinson et al

HUMAN RESEARCH ETHICS COMMITTEE (MEDICAL)

CLEARANCE CERTIFICATE NO. M140265

NAME: (Principal Investigator)	Dr Neil Martinson et al
DEPARTMENT:	Perinatal HIV Research Unit Chris Hani Baragwanath Academic Hospital Klersdorp Tshepong Hospital Complex
PROJECT TITLE:	Mycobacterial Biomakers of TB response and success in Adult Patients: A Prospective Cohort version 1.0 dated 27 January 2014
DATE CONSIDERED:	28/02/2014
DECISION:	Approved unconditionally
CONDITIONS:	
SUPERVISOR:	
APPROVED BY:	Professor PE Cleaton-Jones, Chairperson, HREC (Medical)
DATE OF APPROVAL:	05/03/2014

This clearance certificate is valid for 5 years from date of approval. Extension may be applied for.

DECLARATION OF INVESTIGATORS

To be completed in duplicate and **ONE COPY** returned to the Secretary in Room 10004, 10th floor, Senate House, University.

I/we fully understand the conditions under which I am/we are authorized to carry out the above-mentioned research and I/we undertake to ensure compliance with these conditions. Should any departure be contemplated, from the research protocol as approved, I/we undertake to resubmit the application to the Committee. **I agree to submit a yearly progress report.**

Principal Investigator Signature Date

PLEASE QUOTE THE PROTOCOL NUMBER IN ALL ENQUIRIES

Blood collection ethics certificate

UNIVERSITY OF THE WITWATERSRAND JOHANNESBURG

R14/49 Professor CT Tiemessen, et al

HUMAN RESEARCH ETHICS COMMITTEE (MEDICAL)
CLEARANCE CERTIFICATE NO. M190995

NAME: (Principal Investigator)	Professor CT Tiemessen, et al
DEPARTMENT:	National Institute for Communicable Diseases Centre for HIV and Sexually-Transmitted Infections Sandringham
PROJECT TITLE:	HIV-1 positive South African Elite and Long-term Controllers: viral and host targets for functional cure strategies
DATE CONSIDERED:	Ad hoc
DECISION:	Aproved unconditionally
CONDITIONS:	Renewal of M140926
SUPERVISOR:	Not applicable
APPROVED BY:	Dr CB Penny, Chairperson, HREC (Medical)
DATE OF APPROVAL:	2019/10/04

This clearance certificate is valid for 5 years from date of approval. Extension may be applied for.

DECLARATION OF INVESTIGATORS

To be completed in duplicate and **ONE COPY** returned to the Research Office Secretary on the 3rd Floor, Phillip Tobias Building, Parktown, University of the Witwatersrand, Johannesburg.

I/we fully understand the conditions under which I am/we are authorized to carry out the above-mentioned research and I/we undertake to ensure compliance with these conditions. Should any departure be contemplated, from the research protocol as approved, I/we undertake to submit details to the Committee. I **agree to submit a yearly progress report**. When a funder requires annual re-certification, the application date will be one year after the date when the study was initially reviewed. In this case, the study was initially reviewed in **September** and will therefore reports and re-certification will be due early in the month of **September** each year. Unreported changes to the application may invalidate the clearance given by the HREC (Medical).

Principal Investigator Signature — Date: 15 October 2019

PLEASE QUOTE THE CLEARANCE CERTIFICATE NUMBER IN ALL ENQUIRIES

APPENDIX C

Turn-it-in report

turnitin

Digital Receipt

This receipt acknowledges that Turnitin received your paper. Below you will find the receipt information regarding your submission.

The first page of your submissions is displayed below.

Submission author:	Test student
Assignment title:	Draft submission (all, regardless of course/programme)
Submission title:	Itumeleng_Boshielo_PhD Thesis_March_2023_1144115.pdf
File name:	Itumeleng_Boshielo_PhD_Thesis_March_2023_1144115.pdf
File size:	5.54M
Page count:	227
Word count:	70,025
Character count:	380,617
Submission date:	29-Mar-2023 11:49AM (UTC+0200)
Submission ID:	2049857700

Biomarkers to predict Tuberculosis treatment response

Itumeleng Boshielo

1144115

UNIVERSITY OF THE WITWATERSRAND JOHANNESBURG

A thesis submitted to the Faculty of Health Sciences, University of the Witwatersrand, Johannesburg, in fulfilment of the requirements for the degree of Doctor of Philosophy in Medicine.

Johannesburg, 2023

Itumeleng_Boshielo_PhD Thesis_March_2023_1144115.pdf

ORIGINALITY REPORT

4%	1%	5%	0%
SIMILARITY INDEX	INTERNET SOURCES	PUBLICATIONS	STUDENT PAPERS

PRIMARY SOURCES

1	Frédérique Chaucheyras-Durand, Aurélie Ameilbonne, Pauline Auffret, Mickaël Bernard et al. "Supplementation of live yeast based feed additive in early life promotes rumen microbial colonization and fibrolytic potential in lambs", Scientific Reports, 2019 Publication	2%
2	www.frontiersin.org Internet Source	1%
3	"Handbook of Immunosenescence", Springer Science and Business Media LLC, 2019 Publication	1%
4	core.ac.uk Internet Source	1%